The role of the SWI/SNF ATP dependent chromatin remodelling complex in the regulation of the human hair follicle cell proliferation and control of the human cutaneous wound healing

Carl William KELLETT

Submitted for the degree of Doctor of Philosophy

Faculty of Life sciences

University of Bradford

2018

Abstract

Carl William Kellett

The role of the SWI/SNF ATP dependent chromatin remodelling complex in the regulation of the human hair follicle cell proliferation and control of the human cutaneous wound healing

Keywords: Epigenetics, Chromatin Remodelling, SWI/SNF, Wound healing, Hair follicle, Skin, migration, BRG1

Epigenetic regulation of gene expression occurs at a number of levels including covalent DNA and histone modifications, nucleosome positioning and ATP-dependent chromatin remodelling as well as higher order chromatin folding and 3D genome organisation. ATP-dependent chromatin remodelling complexes modulate nucleosome structure, positioning and chromatin de-compaction and are involved in gene activation and repression. SWI/SNF ATP-dependent chromatin remodelling complexes contain either BRG1 or BRM as the core ATPase together with other common and variable subunits. BRG1 is required for terminal epidermal differentiation in mice and humans and for hair follicle stem cell activation during mouse hair follicle regeneration and cutaneous wound healing. However, the role of SWI/SNF complexes in human hair growth and wound healing remain unknown.

Here it is demonstrated that genes encoding SWI/SNF complex subunits are expressed in human hair follicles. It also highlights that siRNA mediated suppression of SWI/SNF complexes in hair follicle culture has no effect on

hair growth, or anagen-catagen transition in the short term, but a significant increase in proliferation of the outer root sheath keratinocytes was seen. The data also documents the expression of several SWI/SNF subunits in human epidermis and that siRNA mediated *SMARCA4* gene suppression in primary human keratinocyte monolayers defined the requirements of BRG1 for wound closure through control of cell migration, but not proliferation.

In summary, this data revealed a diverse SWI/SNF complex subunit composition in human epidermis and hair follicle, and an essential role of the core complex ATPase BRG1 in keratinocyte migration during wound closure and re-epithelisation.

Acknowledgements

I would like to thank my supervisors, Dr Michael Fessing and Dr Natasha Botchkareva for their invaluable support and advice, as well as their patience throughout the research project, without their support and guidance I would never have made it this far.

I would also like to thank my industrial supervisor Dr Ranjit Bhogal, as well as Magda Sawicka and Dr Fei-ling lim, and all the people I have met at Unilever Colworth, for their support. I would also like to thank Unilever and the BBSRC, for giving me this opportunity.

Finally I would like to thank my friends and family, whose unfailing support has helped me through difficult and stressful times, especially my partner who has put up with me throughout this project.

Table of Contents

Abbreviations

ΔNp63	Isomer of p63 not containing terminal transactivation domain
5caC	5'Carboxylcytosine
5fC	5'Formylcytosine
5hmC	5'Hydroxy-methylcytosine
5mC	5'Methylcytosine
ARID	AT-rich interaction domain
ATP	Adenosine-Triphosphate
BAF	BRG1 associated factor
BER	Base excision repair
BM	Basement membrane
BMP	Bone morphogenetic protein
BMPR	Bone morphogenetic protein receptor
BRG1	Brahma related gene 1

BRM	Human brahma homolog
BSA	Bovine serum albumin
C	Cytosine
C/EBP-α/β	CCAAT/enhancer-binding protein-α/β
CD	Cluster of differentiation
cDNA	Complementary DNA
CRC	Chromatin remodelling complex
CTS	Connective tissue sheath
DAPI	4’,6-diamidino-2-phenylindole
DMEM	Dulbecco’s modified eagle medium
DNA	Deoxynucleic acid
DNMT	DNA methyltransferase
DP	Dermal papilla
ECM	Extracellular matrix
EDC	Epidermal differentiation complex

EGF	Epidermal growth factors
EGFR	Epidermal growth factor receptor
FBS	Foetal bovine serum
FGF	Fibroblast growth factors
FGFR	Fibroblast growth factor receptor
Foxn1	Forkhead box protein 1
HaCaT	Aneuploid immortalised keratinocyte cell line
HAT	Histone acetyltransferase
HDAC	Histone deacetylase
HF	Hair follicle
HFSC	Hair follicle stem cell
HG	Hair germ
HS	Hair shaft
IFE	Interfollicluar epidermis
IKKα	Inhibitor of nuclear factor kappa-B kinase subunit alpha

IRS	Inner root sheath
KLF4	Kruppel-like factor 4
Krt	Keratin
Lhx2	LIM/homobox protein 2
LOR	Loricrin
MAPK	Mitogen-activated protein kinase
MMP	Matrix metalloproteinase
mRNA	Messenger RNA
NER	Nucleotide excision repair
NF-κB	Nuclear factor K-light-chain-enhancer of activated B-cells
NICD	Notch Intracellular Domain
ORS	Outer root sheath
PBAF	Polybromo BRG1 associated factor
PBS	Phosphate buffered saline
PCR	Polymerase chain reaction

PFA	Paraformaldehyde
PPAR	Peroxisome proliferator-activated receptor
RNA	Ribonucleic acid
RT	Room temperature
Satb1	Special AT-rich sequence-binding protein 1
SAM	adenosyl-L-methionine
SG	Sebaceous gland
Shh	Sonic hedgehog
siRNA	Short interfering RNA
smad	Mother against decapentaplegic homolog
SMARC	SWI/SNF related, Matrix associated, Actin dependent regulator of chromatin
SWI/SNF	Switch/Sucrose non fermentable
TAp63	Isomer of p63 containing terminal transactivation domain
TCF	Transcription factor

TDG	thymine DNA glycosylase (TDG)
TET	ten-eleven-translocation
TGF-α/β	Transforming growth factor α/β
TNF-α	Tumour necrosis factor α
WNT	Wingless-related MMTV integration site

List of figures

List of tables

1. Introduction

Mammalian skin serves as a barrier between an organism and the external environment, providing protection from environmental hazards such as UV-radiation, micro-organisms, physical trauma and dehydration. The skin also maintains the organism internal temperature, furthermore skin serves as a sensory organ (D'Orazio et al., 2013, Hanel et al., 2016).

Skin is a multi-layered structure, consisting of the outermost epidermis, dermis and sub-cutis. The epidermis is a dynamic self-renewing tissue, primarily made up of keratinocytes as well as melanocytes, Merkel cells and Langerhans cells (Boulais and Misery, 2008, Debeer et al., 2013). The epidermis is also involved in the formation of several epidermal appendages in the skin, including hair follicles, sebaceous and sweat glands and nails (Wang et al., 2016, Lehoczky et al., 2011).

Mammalian hair follicles are skin appendages which are generated as a result of a series of complex ectodermal-mesenchymal interactions (Ahmed et al., 2014, Blanpain and Fuchs, 2009). Almost all human and animal hair follicles are generated during the embryonic stage of development, although in adult mice *de novo* hair follicle generation has been seen after large wound healing (Gay et al., 2013, Rognoni et al., 2016, Zhu et al., 2017).

Like the skin, hair confers several abilities to the host organism, including assisting with thermoregulation, protection from environmental insults, sensory information and enhanced wound healing; although some of these abilities are more obvious in non-human mammals, the quills of a porcupine, whiskers of a cat, or the horn of a rhinoceros for example. The mature hair follicle contains epidermal progenitor and stem cells, which serve not only to replenish and regenerate itself during each cycle,

but also support re-epithelialisation after the cutaneous wounding (Plikus et al., 2015).

Epidermal and hair follicle development and regeneration are controlled by molecular networks of cell signalling pathways, transcription factors and epigenetic regulators. The key components of these networks were characterised in recent decades using genetically modified mice, cultured cells and *ex-vivo* culture of human hair follicles or whole human skin explants (Yang et al., 2014, Philpott et al., 1996, Nakamura et al., 1990). However, most of our knowledge about epidermal and hair follicle biology is based on animal studies; as such it requires further work to define their relevance to humans (Shanks et al., 2009, Arends et al., 2016).

1.1 Epidermal morphogenesis and homeostasis

The epidermis is a self-renewing epithelial tissue, and while keratinocytes make up much of the epidermis there are several additional cell types located within the epidermis, including Langerhans cells which serve an anti-microbial role during infections, Merkel cells which provide touch/pressure sensory information and melanocytes which produce and distribute melanin affecting skin pigmentation and providing protection against UV-B damage (Maricich et al., 2009, Hogan and Burks, 1995, Lewis et al., 2015, Cichorek et al., 2013, Erickson and Echeverri, 2018). Epidermal development takes place during embryogenesis; in mice it begins at embryonic day (E) 9.5 and progresses in a well-timed and predictable way, resulting in a fully formed epidermis by E18.5, while in humans the progression is highly similar but with a longer timeframe, beginning during week 8 and having a fully formed epidermis by week 22/23 (Coolen et al., 2010, Koster and Roop, 2007, Sotiropoulou and Blanpain, 2012).

The adult epidermis is maintained via homeostatic regulation, involving basal layer progenitor cells, which proliferate and undergo terminal differentiation while moving outward in a columnar direction, replenishing the outermost layer (the cornified layer) which is constantly sloughed off.

1.1.1 Epidermal structure and functions

The epidermis is a collection of stratified cells arranged as layers, each demonstrating its own characteristics and functionality. There are four layers in the majority of the skin sites; from deepest to outermost they are; or stratum basale (the basal layer), the stratum spinosum (the spinous layer), the stratum granulosum (the granular layer) and the stratum corneum (the cornified layer), with keratinocytes becoming more differentiated as they progress outward from basal to cornified layers (Horsburgh et al., 2017). There is an additional layer in the particularly thick skinned areas (soles of the feet in humans and foot pads of animals for example) known as the stratum lucidum (the clear layer) which sits between the spinous and granular layer and serves to provide a thick protective layer (Ari et al., 2018, Yousef and Sharma, 2018)

Epidermal keratinocytes become further differentiated as they progress outward, initially losing the ability to proliferate and then a switching of several cytoskeletal gene expression, specifically silencing keratin (also termed cytokeratin, *KRT* or K) 14 and keratin 5, and activating keratin 10 and 1.This is followed by densely packaging these cytoskeletal filaments together and collapsing the cell, creating in a protein envelope (the cornified envelope) around the cell, which is then crosslinked with nearby cells, generating a fully functional and robust barrier system.

This process follows a predictable path and while most mechanisms controlling this process are well understood, especially in mice, some aspects remain elusive. Specifically the non-linear increase in timeframe to obtain a complete functional barrier in human development, as well as the wave like induction of hair follicles in mouse models vs human models and the inherent differences in skin elasticity between mammalian species (de Jong et al., 2017, O'Brien et al., 2019, Orzechowska et al., 2018)

1.1.2 Cellular changes underlying epidermal morphogenesis and homeostasis in murine models

The model of mouse epidermal development is well studied and follows a well-timed and predictable progression, epidermal development occurs during embryogenesis, during the gastrulation stage, the three germ layers form, the outermost of these layers (the ectoderm) will go on to form the epidermis, nervous system, teeth as well as several other tissues. At embryonic day (E) 9.5 the basal epidermal layer is established, keratins 5 and 14 expression is vital to this process (Liu et al., 2013, Lee et al., 2018), this layer maintains its proliferative ability and contains keratinocyte progenitor cells, which will be maintained throughout the host lifetime and will proliferate in order to maintain the mature epidermis. By E14.5 the intermediate layer forms, this is a transient layer only found during epidermal development, its formation is directly associated with the initiation of epithelial stratification, During the early stages of epidermal stratification cells in the intermediate layer maintain a minor proliferative ability, this allows for expansion of the intermediate layer as well as allowing some of the basal cells to continue proliferating symmetrically maintaining the basement membrane accommodating the rapidly expanding embryo, in the late stages of stratification asymmetric basal cell

proliferation reaches up to 70%, at this point the ability to proliferate is lost in intermediate layer cells (Lechler and Fuchs, 2005). By E16.5 the cornified layer begins to form, with full barrier acquisition of the whole epidermis completed by E18.5. It is also worth noting that during epidermal development an additional layer is present at the early stages, the periderm, this is a transient layer which is lost around E14.5. (Koster and Roop, 2007, Blanpain and Fuchs, 2006, Zhu et al., 2014) (This process is summarised in **Fig.1.1**).

Figure 1.1 Summary of epidermal differentiation and homeostasis

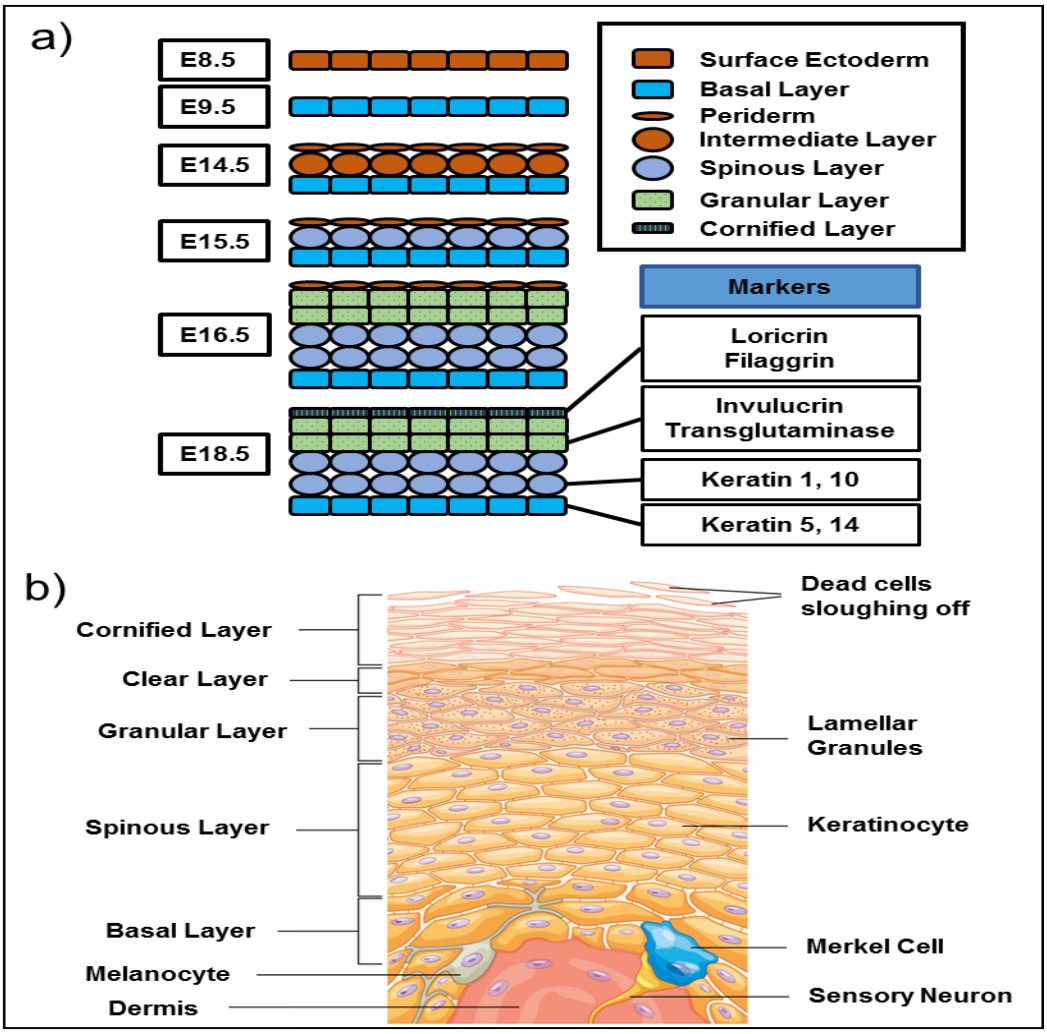

a) Epidermal development in mouse beginning at E8.5, progressing to E18.5, common differentiation markers are shown, b) mature human thick epidermis, highlighting the 5 layers and several additional cell types and processes. Images adapted from (Forni et al., 2012, Natarajan et al., 2014).

1.1.3 Cellular changes underlying epidermal morphogenesis and homeostasis in human models

Human epidermal development occurs in much the same way as with mouse, but with an altered and much longer timeframe, with basal layer initiation occurring at approximately week 8, intermediate layers forming in weeks 9 and 10, the cornified layer beginning to form at the end of week 10, however full barrier acquisition does not occur until a much later stage, approximately week 22 (Coolen et al., 2010). The periderm is also present during human epidermal development, forming at approximately week 5 and being lost at week 22, in humans the periderm undergoes cycles of keratinization and desquamation and produces a waxy substance (the *Vernix caseosa*) which serves to protect the foetus from the amniotic fluid, and later, bacterial assault when leaving the birth canal, while the periderm is lost at week 22 the *vernix caseosa* remains until shortly after birth (Schlessinger and Bhimji, 2018). However despite the longer timeframe the same keratins are present at each stage and serve highly similar functions to their mouse counterparts (Liu et al., 2013, Sotiropoulou and Blanpain, 2012, Zomer and Trentin, 2018).

The basal layer is the lowest layer of the epidermis and serves two primary functions; - firstly, adhesion of the epidermis to the underlying dermis via the basement membrane (BM), this is facilitated by hemi-desmosomes and a variety of additional anchoring filaments, anchoring fibrils and integrins, taken together these form hemi-desmosome (HD)-anchoring filament complexes, which form tight junctions between basal keratinocytes and the BM, this adhesion serves to protect tissues from mechanical forces and shear stressors (Yurchenco, 2011, Jayadev and Sherwood, 2017). Secondly, many cells of the basal layer are capable of proliferation and divide in order to replace the corneocytes lost during normal

shedding; this requires a tightly regulated balancing act to be maintained between proliferation and quiescence, the keratinocyte progenitor cells of the basal layer proliferate asymmetrically to the BM, this produces one basal cell and one suprabasal cell, the basal cell remains in contact with the BM via integrins, which maintains the proliferation environment, while the suprabasal cells no longer receives proliferative signals and instead commit to differentiation, as basal layer divisions continue the suprabasal cell is pushed further outward, continuing to differentiate (Blanpain and Fuchs, 2009, Sotiropoulou and Blanpain, 2012). Cells present in the basal layer express K5 and K14; these are often held as markers of the epidermal progenitor cells.

Once keratinocytes move outward they enter the spinous layer, the first stage in terminal differentiation, once here cells are no longer attached to the BM and lose the ability to proliferate, protein expression also significantly change, with the most notable change being a loss of K5/K14 and the appearance of K1/K10, an abundance of desmosome complexes are also present, resulting in more tight junctions between cells, making the whole epidermis more rigid, as well as maintaining the overall integrity of the epidermis (Simpson et al., 2011, Seltmann et al., 2013).

The granular layer consists of keratinocytes in the late stages of differentiation, keratinocytes in this layer contain large amounts of profilaggrin in keratohyalin granules, profilaggrin is a protein which, when dephosphorylated becomes proteolysed, the created fragments (free filaggrin) are capable of binding to keratin monomers and arranging them into parallel bundles, this bundling causes a collapse of the cell and extensive cross-linking of the keratins together with the cornified envelope proteins (loricrin, involucrin, late cornified envelope protein etc.),

generating an insoluble keratin matrix, which will form the scaffold upon which the cornified envelope will be built (Sandilands et al., 2009, Elias et al., 2014).

The cornified layer is the final product of epidermal differentiation, corneocytes are non-viable cells, having degraded or ejected their nucleus and other 'vital' organelles, the plasma membrane is also lost and replaced with a crosslinked ceramide layer, the cornified envelope, at this point cells are now large and flat. Corneocytes are also very tightly bound to each other, and any intercellular spaces which are present are filled with lipid acting as a hydrophobic matrix, further increasing the inpermeability of the cornified layer (Abdayem et al., 2016). The final result is a robust and functional barrier, capable of withstanding harsh environmental hazards as well as mechanical and microbial stressors and preventing dehydration of the organism.

1.1.4 Key cell signalling pathways controlling epidermal morphogenesis

Epidermal lineage is determined primarily by antagonistic interplay between wingless-related integration site (WNT) signalling and bone morphogenetic protein (BMP) signalling, as well as several other cell signalling molecules. The ectoderm has the potential to differentiate into epithelial or neuronal lineages, WNT signalling is central to an antagonistic signalling system in place to selectively activate either epidermal or neuronal cells lineages (Fuchs, 2007, Davidson et al., 2012, Yoney et al., 2018). Ectodermal cells with high levels of WNT stop responding to fibroblast growth factors (FGFs), this prevents the inhibition of BMP and drives ectodermal cells into the epidermal lineage. However, if the levels of WNT are low, FGF signalling remains unhindered, inhibiting BMP signalling and driving ectodermal cells into a neuronal fate (Fuchs, 2007, Wilson et al., 2001).

On the cell surface WNT ligands bind the frizzled (FZD) receptor and a low-density lipoprotein receptor-related protein 5 or 6 (LRP5/6) to form a larger complex within the cell membrane, this complex recruits intracellular protein dishevelled (DVL) which inhibits the phosphorylation of β-catenin, preventing its degradation in cytoplasm and allowing it to accumulate and translocate to the nucleus where it binds lymphoid enhancer binding factor/transcription factor (LEF-TCF) transcription factors facilitating changes in gene expression (MacDonald and He, 2012).

WNT/β-catenin is also required in neural crest cells, also derived from the ectoderm, in order to generate melanocytes, which provide both pigmentation and protection from UV-B Radiation. A loss of *Wnt1* or *Wnt3a*, in mice, results in a loss of melanoblasts (precursors of mature melanocytes) (Ikeya et al., 1997), later studies also demonstrated that Wnt/β-catenin activation in neural crest cells was sufficient to override lineage selection, resulting in melanocyte fate selection rather than other neuronal lineages (Dorsky et al., 1998, Mort et al., 2015). More recent studies have suggested that WNT signalling may actually inhibit pigmentation, use of ICG-001, a chemical inhibitor of WNT signalling resulted in an increase of pigmentation in human melanoma cells (Kim et al., 2016), which is counter to the previous mouse based studies which supported WNT/β-catenin inhibition has a hypopigmentation effect (Yamaguchi et al., 2009).

Taking these studies into account, it is clear that WNT signalling is vital to epidermal development and regulating skin pigmentation.

BMP ligands bind to BMP receptors (BMPR) on the cell surface, resulting in phosphorylation of SMAD1/5/8 C-termini, allowing for the formation of a trimer of two SMAD1/5/8 proteins and one smad4 protein, SMAD4 facilitates the translocation

of SMAD1/5/8 to the nucleus, activated smads interact with other transcription factors to facilitate a variety of cell specific processes (Xiao et al., 2007, Hill, 2016).

BMPs are vital to the early stages of embryonic development, but they are also required for postnatal development/cell differenation, as demonstrated by their presence in mesoderm and ectoderm tissues. There are several BMP ligands and receptors, which are expressed differently throughout the developing epidermis, BMPR-1A and BMP-7 are only detected in the basal layer, meanwhile BMPR-1B and BMP-6 are absent in basal layer cells, but found in the suprabasal layer (Botchkarev, 2003), this suggests that the role of specific BMPs is to facilitate either proliferation (BMPR-1A and BMP-7) or differentiation (BMPR-1B and BMP-6) in keratinocytes (Botchkarev, 2003, Panchision et al., 2001, Fessing et al., 2010).

Stratification of the epidermis occurs during the formation of the intermediate layer, and is highly dependent upon the mitotic spindle, which regulates the polarity of epidermal cells, with the apical end facing towards the outer, more differentiated cell layers, while all other sides are in contact with adjacent cells, in the basal layer, the basal region interacts with the BM and the extracellular matrix (ECM) therein (Ahringer, 2003, Lazaro-Dieguez et al., 2013)

Keratinocyte polarisation is well studied, but less understood than other simple epithelial polarisation, as mentioned the shift of the mitotic spindle is a key event in stratification, as cells begin proliferating in a ‘stacked’ fashion (Blanpain and Fuchs, 2009). The mechanism by which the mitotic spindle shifts to the apical region is fairly well understood in other species (*Drosophila melanogaster* and *C.elegans*), which has helped to, at least partially, identify the mechanism responsible in

humans and other mammals (Gillies and Cabernard, 2011, Poulson and Lechler, 2010, Lazaro-Dieguez et al., 2013).

PAR-3 is a polarity protein, which marks the apical edge of a cell with the 'polarity landmark', PAR-3 along with two other proteins, insecuteable and LGN, which recruits the mitotic spindle to the apical edge, although this mechanism not fully understood, it is known that a loss of either PAR-3, insecuteable or LGN results in a loss of asymmetrical proliferation, and an increase in symmetrical proliferation (Hao et al., 2010, Ray and Lechler, 2011).

The final stage of epidermal development is to establish the barrier, the cornified layer, a cluster of highly specific genes are required to establish the barrier, these genes are found in a gene rich region of chromosome 1 in humans (chromosome 3 in mice), this region is termed the epidermal differentiation complex (EDC) (Mardaryev et al., 2014, Kypriotou et al., 2012). The EDC encodes many of the structural proteins which make up the cornified envelope; Involucrin, loricrin, and small proline-rich proteins (Sprr). Which become cross-linked by transglutaminases (Tgms), Tgms activity is calcium dependent, as such the formation of the barrier is dependent upon extracellular calcium ions (Ca^{2+}) (Bikle et al., 2012). Elevated extracellular Ca^{2+} increases the amounts of intracellular Ca^{2+}, generating a Ca^{++} gradient increasing from basal to cornified layer, high levels of extracellular Ca^{2+} are detected by the calcium sensing receptor (CaR), a G-protein coupled receptor, which is found more predominantly in suprabasal (spinous and granular layer) cells and when activated by extracellular calcium triggers the mobilisation of E-cadherin to the plasma membrane, facilitating cell-cell adhesion, as such a loss of CaR results in abnormal differentiation and incomplete barrier formation (Tu et al., 2007, Tu et al., 2012, Tharmalingam and Hampson, 2016). It is also worth noting that

when culturing primary keratinocytes *in vitro* the addition of calcium to the media is sufficient to induce differentiation, the mechanism of differentiation is highly similar to the *in vivo* mechanism of differentiation (Bikle et al., 2012).

1.1.4 Key transcription factors controlling epidermal morphogenesis and homeostasis

Mouse studies have identified several transcription factors which play a role in the epidermal differentiation and stratification process (mad/max, c-Myc, AP-1 and AP-2, Klf4, Znf750 to name some), one related transcription factor that is fairly extensively studied is p63 (also known as Trp63), a master regulator of epidermal differentiation and development. p63 is a transcription factor and has been shown to directly regulate the expression of several genes vital to the epidermal differentiation program, including K5 and K14, cellular adhesion molecules P-cadherin and integrin-α3, as well as activating or repressing other transcription factors, including AP-2 and the epigenetic regulators Satb1,Brg1 and Cbx4 (Romano et al., 2007, Romano et al., 2009, Fessing et al., 2011, Mardaryev et al., 2014, Koster and Roop, 2007, Botchkarev et al., 2012, Ihrie and Attardi, 2005, Vanbokhoven et al., 2011). *P63*$^{-/-}$ mice fail to generate a stratified epidermis, they also lack all epidermal appendages, glands, and fail to express K5 or K14. Death occurs shortly after birth due to significant water loss as a result of the barrier defects (Mills et al., 1999, Yang et al., 1999). Heterozygous p63 defects in humans have also been linked to several ectodermal dysplasia syndromes, which are characterised as abnormal development of epidermis, teeth, hair, nails, sweat glands etc. (Koster, 2010).

p63 has two promoter regions and so two distinct isoform groups, the first promoter region generates full length protein containing a N-terminal transactivation domain, a

DNA binding domain and a C-terminal oligomerisation domain, while the alternative promoter results in a p63 protein which is lacking the transactivated N-terminal, but maintains the DNA and C-terminal domains (these isoforms are termed TAp63 and ΔNp63 respectively) (Yang et al., 1998, Soares and Zhou, 2018), these isoforms have shown distinct, but partially overlapping roles in regulation of both epidermal differentiation and stratification. It has been shown that ΔNp63α (a splice variant of ΔNp63) was the most abundantly expressed p63 isoform and is predominantly expressed in the basal layer of the epidermis, while it is almost completely absent in the suprabasal layers (Romano et al., 2012). Specific investigation into ΔNp63α and Tap63 has shown that ΔNp63α has a significant role in regulating epidermal differentiation while Tap63 acts to protect keratinocytes from senescence and repress tumour formation (Koster et al., 2007, Truong et al., 2006, Guo et al., 2009, Romano et al., 2012).

In suprabasal cells P63 has been shown to regulate notch signalling pathway, which is important during keratinocyte differentiation. Notch signalling is activated when Notch ligand expression in the basal cells is activated by forkhead box N1 (foxn1) the Notch ligand protein then binds and activates Notch receptors, a proteolytic cleavage occurs releasing the notch intra-cellular domain (NCID) which is translocated to the nucleus, where it facilitates the binding of transcription factors to target genes, this activation also synergistically effects AP-2 to activate expression of the CCAAT/enhancer-binding protein-α/β (C/EBP-α/β) transcription factors to facilitate the activation of genes required in suprabasal keratinocytes, including K1 and 10, while simultaneously repressing the basal layer specific genes K5 and K14 (Blanpain and Fuchs, 2009, Kolev et al., 2008, Wang et al., 2008). TAp63α also indirectly activates AP-2 during this process. p63 also activates the IKK-α complex which phosphoylates the inhibitor of κB (IκB) inactivating it which inturn activates

Nuclear Factor κB (NF-κB) resulting in the inhibition of proliferation in suprabasal cells and activation of epidermal stratification (Koster and Roop, 2007, Takeda et al., 1999, Koster et al., 2006) .

In addition to p63 several other key transcription factors have been determined to play a vital role regulating the expression of EDC genes (and the acquisition of the epidermal barrier), including; krüpple like factor 4 (klf4), grainyhead like epithelial transactivator (Grhl3/Get1), aryl hydrocarbon receptor nuclear translocator (Arnt), activator protein 1 and 2 (AP-1 and AP-2) (Kypriotou et al., 2012). Diminished or elevated levels of Klf4 is linked to defects in the barrier formation or accelerated barrier formation, respectively, while mutations in Grhl3/Get1 result in barrier defects due to a down-regulation of key genes responsible for lipid metabolism and cell-cell junction formation (Yu et al., 2006b).

The wide array of transcription factors activate the late stage differentiation genes within the EDC, which can only occur after chromatin remodelling complexes establish the specific three dimensional chromatin structure required to facilitate gene activation. p63 has been shown to directly regulate expression of chromatin organisation and remodelling genes Satb1 and BRG1, which are important in this process, loss of either BRG1 or Satb1 leads to defects in epidermal differentiation (Fessing et al., 2011, Mardaryev et al., 2014).

1.2 Hair follicle morphogenesis

The hair follicle is a complex micro-organ which is found in the majority of human skin, with the exceptions of the palms, soles and lips. Hair is one of the defining characteristics of mammals, with almost all mammals being covered with hair;

however, there are some exceptions to this, most fall into the Cetaceans group of aquatic mammals containing dolphins, whales and porpoises, but there are others. Mammalian hair serves a variety of functions, ranging from protection and sensory perception to social interactions and attracting a mate (Stenn and Paus, 2001, Ramos and Miot, 2015). Anatomically speaking the mature hair follicle is made up of several key regions, from the lowest point the bulb, the isthmus and the infundibulum which is continuous with the epidermis. The hair follicle bulb is comprised of the dermal papilla (DP), the matrix and the pre-cortex, the isthmus is the region between the arrector pilus and sebaceous gland, which houses the bulge region, while the infundibulum is the uppermost region, from the sebaceous gland to the epidermis, the hair shaft as well as the connective tissue sheath (CTS) and outer root sheath (ORS) run through three regions, while the inner root sheath runs through the bulb to the isthmus (summarised in **Fig. 1.2a**).

The DP is a tightly packed cluster of specialised fibroblasts which are almost completely surrounded by the HF matrix and pre-cortex, suffice a small region at the base, which is connected to the CTS which serves as a connection point to the circulatory system (Alonso and Fuchs, 2006, Yoshida et al., 2019). The DP is responsible for controlling hair follicle morphogenesis and cycling. It also regulates the size of the overall follicle by controlling the number of matrix cells present within the HF, the DP is the only part of the lower follicle not degraded during cycling due to its role in regulating the signalling pathways required to regenerate the hair follicle (Alonso and Fuchs, 2006, Paus and Cotsarelis, 1999, Driskell et al., 2011, Chi et al., 2010, Gupta et al., 2018). The matrix region is largely made up of undifferentiated cells (also termed transit-amplifying cells), which are capable of a limited amount proliferation before expanding upwards, towards the pre-cortex region of the supra-bulb where they will terminally differentiate either to hair shaft or inner root sheath

(IRS) cell fates (Oshima et al., 2001). The pre-cortex is also interspersed with melanocytes, which produce pigmentation granules ultimately giving the hair shaft its colour (Alonso and Fuchs, 2006, Kauser et al., 2011, Samuelov et al., 2013). The hair shaft itself is made up of terminally differentiated keratinocytes (trichocytes), which arise from the transit-amplifying cells of the matrix, the shaft itself is comprised of three layers; the cuticle, the cortex and the medulla, overall appearance of the hair itself its determined by the pigmentation level and structure of these 3 layers (Miteva and Tosti, 2013).

The isthmus is the middle region, and is relatively devoid of any special features with the exception of the bulge region, the bulge region houses the stem cells of the hair follicle, in mice it is easily identified as a physical bulge of cells located in the outer root sheath between the sebaceous gland and the arrector pili muscle, and is home to several stem cell populations, which give rise to epithelial cells, melanocytes and neural crest-like cells (Yu et al., 2006a, Ito et al., 2005, Yu et al., 2010). However, in humans the bulge regions is less easily identified, as the region does not prominently bulge out, although the stem cell niche is still located between the sebaceous gland and arrector pili muscle. The stem cell niche is vital to hair follicle cycling and regeneration, hair follicle stem cells (HFSCs) are responsible for self-renewal of the follicle, maintaining HF homeostasis, are able to give rise to sebaceous glands and assist in epidermal wound healing (Ito et al., 2005). In adult mice bulge cells have also been shown to be able to generate *de novo* hair follicles in extreme epidermal wound response (Ito et al., 2007), Other than the bulge region, the isthmus contains the anchoring points for the arrector pilus, sebaceous gland and apocrine gland.

The infundibulum is the upper most region of the HF and is contiguous with the epidermis, and so the epidermal cells here are capable of migrating to the epidermis in response to wounding, the infundibulum also contains the connecting points of glandular epidermal accessory appendages (sebaceous and apocrine glands etc.) facilitating secretion (Ramos-e-Silva and Pirmez, 2014).

The IRS is also keratinised, in order to provide a rigid structure and facilitate the overall shape of the HF, the IRS is also made up of 3 layers, from inner-most to outer-most; the IRS cuticle, the Huxley's layer and the Henle's layer, the Huxley and Henle layers contain trichohyalin granules which facilitate cross-linking, providing rigidity (Joshi, 2011, Westgate et al., 2017). The ORS is essentially a pouch of epidermis containing the whole HF, the ORS is a stratified epithelia which is continuous with the epidermis, the ORS serves as an anchoring point for the arrector pili muscle, additionally the ORS is not keratinised below the isthmus (as the IRS is keratinised below this point), the ORS in the isthmus is also the specific location of the bulge region, and the HFSC (Vidal et al., 2005). The CTS is a mesenchymal tissue which surrounds the HF and is dynamically modified during HF cycling, the CTS predominantly contains type I collagen fibres, the distribution and orientation of these fibres is dependent upon HF cycling, the CTS also contributes to maintaining the dermal matrix. (Ito and Sato, 1990, Oh et al., 2012).

1.2.1 Hair follicle structure and functions

The structure and function of the HF is dependent upon its cycling stage, generally when discussing the HF it is assumed to be an anagen stage follicle (unless stated otherwise), this is the period of growth and normal function of the HF. During the anagen phase the HF is growing and elongating, the matrix cells are highly

proliferative, with most of the proliferation occurring at the lowest part of the matrix, below Auber's line, an arbitrary boundary that crosses the widest part of the DP representing the changing matrix cell focus from proliferation (below) and trichocyte differentiation (above) (Alonso and Fuchs, 2006, Driskell et al., 2011). The matrix cells differentiate into both IRS and hair shaft (HS), IRS cells in the lower bulb have already differentiated, losing their proliferative ability, and will continue to move upwards as more IRS cells are added to its base, the IRS is lost at the sebaceous gland entry point, and cells of the IRS are sloughed off and degraded, meanwhile cells becoming HS will move towards the pre-cortex region, between the Auber line and the start of the HS cortex, starting their differentiation as they progress, once at the cortex region the keratinocytes will have fully differentiated into trichocytes (Purba et al., 2016). While most proliferation occurs in the matrix the ORS shows some proliferation intermittently throughout, as the ORS supports growth of the HF the proliferation likely serves to facilitate this, the bulge regions of ORS only proliferate during the early anagen stage, as anagen continues this proliferation ceases and the bulge region enters quiescence, (Purba et al., 2016), the major features of anagen follicles are shown in the expanded section of **Fig 1.2a**.

1.2.2 Cellular changes underlying hair follicle morphogenesis

HF development begins at E14.5 in mice and approximately 9 weeks gestation in human, HF generation involves a series of complex cross-talk events between the epidermis and the underlying mesenchyme. HF initiation begins with a mesenchymal signalling event, the 'first dermal signal' which facilitates the thickening of the epidermis and the formation of the HF placode, once formed the placode signals to dermal cells, which cluster below it forming the specialised dermal cell cluster, this is the 'second dermal signal' (Fu and Hsu, 2013), it is also

worth noting that this initiation process is the same in generating the feather bud or scale placode (Dhouailly, 1973, Olivera-Martinez et al., 2004, Di-Poi and Milinkovitch, 2016). The clustered dermal cells (also termed the dermal condensate) migrates downwards into the dermis, while the epidermal cells proliferate downwards, following and then encompassing the clustered dermal cells which becomes the dermal papilla, this structure is termed the 'hair peg', at this point the DP signals to initiate the formation of the IRS, providing the rigid structure for the HF to continue developing, the ORS begins to surround the IRS as a continuation of the epidermis, and cells between the IRS and DP become matrix cells and begin differentiating to form the hair shaft layers, which will then elongate and protrude through the epidermis (Duverger and Morasso, 2009) This process is summarised in **Fig 1.2b**).

1.2.3 Key cell signalling pathways controlling hair follicle morphogenesis

As follicular development is highly dependent upon the signalling interactions of dermal and epidermal cells, the signalling pathways are highly regulated; however the key signalling mechanisms are highly similar to those seen in epidermal development and homeostasis, as the generation of thickened epidermis and gathering of dermal condensate is seen in the initiation of feathers, scales and hair it is likely that a conserved first dermal signal exists, however it has yet to be identified. To date several conserved signalling pathways have been identified in HF development including; WNT, BMP, sonic hedgehog (SHH), notch and ectodysplasin A1 (EDA).

Of all the conserved signalling pathways the WNT/β-catenin signalling pathway is seen as one of the most vital. As previously mentioned WNT signalling results in

accumulation of cytoplasmic β-catenin, which is translocated to the nucleus where it activates or represses gene expression programmes (MacDonald and He, 2012), and WNT/β-catenin signalling has been identified in both epidermal and mesenchymal development (Andl et al., 2002, Zhang et al., 2008, Fu and Hsu, 2013). Several studies have shown that β-catenin is required to initiate HF development, however the origins of WNT signalling and if WNT/β-catenin alone is the first dermal signal remains to be proven (Rishikaysh et al., 2014).

EDA and its receptor (EDAR) have also been implicated in placode development, although EDA/EDAR mutant mice still developed secondary placodes (including mammary placodes and dental placodes) but failed to generate primary placodes, responsible for guard hairs (Mikkola and Thesleff, 2003). Meanwhile in humans EDA/EDAR mutations lead to hypohidrotic ectodermal displaysia, characterised by malformed teeth, sparse hair coverage and failed development of several exocrine glands, placodes formed also have an irregular or fused borders, suggesting that EDAR is more vital for the development, rather than the initiation of hair placodes. EDAR is regulated by WNT/β-catenin and NF-κB pathways (Durmowicz et al., 2002, Schmidt-Ullrich et al., 2006), and is seen to activate SHH signalling as well as inhibiting BMP (which is known to inhibit placode development), demonstrating a dual function for the EDA/EDAR/NF-κB pathway in the developing placodes (Pummila et al., 2007).

Upon formation of the placode another signalling event recruits dermal fibroblasts to cluster below the placode, formation of this dermal condensate is mediated by fibroblast growth factor (FGF) 20, which is activated by Edar and the Wnt/β-catenin pathway in the newly formed placodes (Huh et al., 2013). Initiation of placodes requires a downregulation of keratinocyte growth factors (KGF) and epidermal

growth factors (EGF), while Kgf and Egf are still present, their receptors are degraded, preventing interaction, although the precise mechanism is as yet unknown (Richardson et al., 2009).

Once the placode and dermal condensate are formed a large increase in keratinocyte proliferation is seen, marking the start of HF organogenesis and the second dermal signal. Eda/Edar/NF-κB signalling drives expansion of the placode downward via activation of Shh, which in turn activates cyclin D1, triggering a rapid proliferation event in epidermal cells (Schmidt-Ullrich and Paus, 2005, Schmidt-Ullrich et al., 2006, Mill et al., 2003). Additionally Shh signalling also has a function in the dermal condensate, through a complex crosstalk between epidermal and mesenchyme cells, Shh based activation of Noggin, drives maturation of the dermal condensate to the DP, which is vital for mouse HF morphogenesis (St-Jacques et al., 1998, Blanpain and Fuchs, 2006, Millar, 2002). Tgf-β2 is also required for the downward proliferation seen in organogenesis; Tgf-β2 activates Snail and Mapk in the expanding epidermal cells, which in turn regulates proliferation and cell adhesion, supporting that loss of Tgf-β2 or Snail result in halted proliferation (Jamora et al., 2005).

The downward expansion of the hair peg and subsequent enveloping of the dermal condensate trigger an increase in proliferation and differentiation of the epithelial cells in the hair peg, this requires a myriad of signalling molecules, as well as precise sequence of events, ensuring that differentiation occurs normally, however only a handful of signalling molecules have been fully investigated, leaving some specific events unknown. The hair peg now begins to form the additional layers which make up the HF; beginning with the IRS, then onto the ORS and hair shaft, central to this is Bmp and Notch signalling cascades (Powell et al., 1998, Rendl et

al., 2008). BMPRIA (the only Bmp receptor currently detected in hair follicles) is required for both IRS and hair shaft differentiation, as such Bmp4 triggers IRS differentiation via activation of BmpRIA, which in turn activates several IRS genes via Gata3 activation as well as up-regulating Bmp levels, creating a feedback loop (Kobielak et al., 2003, Nemer and Nemer, 2003). Hair shaft differentiation is antagonistically regulated by Wnt signalling and BmpRIA, via repeated bouts of inhibition and activation BMPRIA in progenitor cells maintains levels of β-catenin and lef1 at the specific point required for HF keratin expression and hair shaft formation (Kobielak et al., 2003).

Notch signalling has been shown to be involved in numerous cell fate decisions in a variety of cell types, during HF development notch is required to activate proliferation in the DP, in response to epidermal growth factor (Egf) as well as activating transcription of survivin, an apoptosis inhibiting protein, demonstrating that Notch signalling is required for the maintenance of the DP and the hair follicle as a whole (Zhang et al., 2016).

1.2.4 Key transcription factors controlling hair follicle morphogenesis

Control of the gene expression programmes required for HF development is facilitated by a handful of specific transcription factors. As previously stated, p63 $^{-/-}$ mice fail to generate a stratified epithelia and lack all epidermal appendages, including hair, glands and teeth, demonstrating that p63 is vital to the development of hair follicles, however the specific mechanisms of p63 action during HF development remain to be elucidated. Additional mouse based studies into p63 have shown that when ΔNp63α was overexpressed (using a Tet-inducible under the control of *Krt5*), mice showed enlarged HF size and an expanded ORS, as well as

decreased proliferation in matrix cells and failure to differentiate into both hair shaft and IRS, instead the keratinocytes displayed markers of interfollicular epidermis, all down regulated genes are targets of Wnt/β-catenin signalling and so p63 regulates Wnt signalling in order to activate IRS and hair shaft specific genes (Romano et al., 2010).

As well as p63 there are several other key transcription factors, including; Lim/Homobox protein 2 (Lhx2), Forkhead box protein N1 (FoxN1), Snail 1 zinc finger protein (Snail), GATA binding protein 3 (Gata3) and Homeobox protein Hox8 (Msx2). Most are involved in establishing the specific cell differentiation programmes in the cyto-differentiation stage of HF morphogenesis; for example, Gata3 regulates IRS differentiation, while Msx2 and FoxN1 regulate hair shaft differentiation (Ma et al., 2003, Johns et al., 2005), FoxN1 is also required for pigmentation of the shaft as it directly regulates the transfer of pigment from melanocyte to hair shaft cortex (Weiner et al., 2007). Snail is a target of Tgf-β, and serves to regulate cellular adhesion and proliferation in the hair bud, a loss of Snail or Tgf-β stalls HF morphogenesis (Jamora et al., 2005). Lhx2 is crucial in formation and maintenance of the bulge region, during hair follicle morphogenesis Lhx2 is a marker of the hair bud, and its ablation results in cellular disorganisation and transformation into a sebaceous gland (Folgueras et al., 2013).

Figure 1.2 Human hair follicle structure and mouse hair follicle morphogenesis

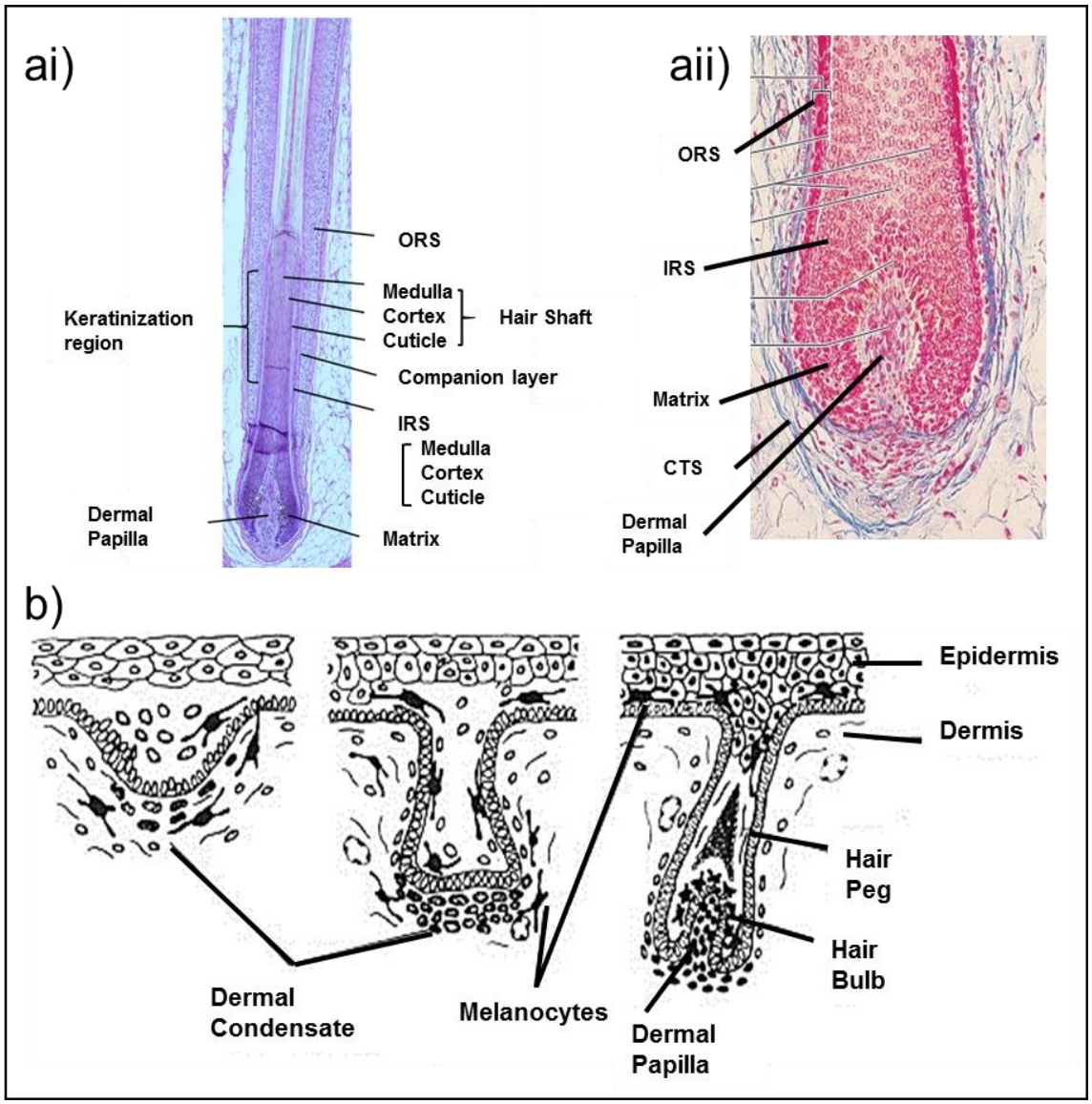

a) Structure of the mature human hair follicle (ai) and expanded bulb region (aii) key features of anagen follicles are highlighted. b) Illustration of murine hair follicle morphogenesis, highlights key structures. Images adapted from (Krause and Foitzik, 2006, Millar, 2002).

1.3 Hair cycling

Postnatally the hair follicle undergoes repeated cycles of growth, shrinkage and rest (anagen, catagen and telogen (respectively), then back to growth (summarised in **Fig. 1.3**). Each cycle can take several years to complete in humans (Schneider et al., 2009, Paus and Cotsarelis, 1999, Alonso and Fuchs, 2006), while it takes approximately three weeks in mice, although the overall process remains highly similar.

1.3.1 Cellular changes during hair cycling

Anagen phase follicles tend to be long and straight, although at an angle to the skin surface, this is to facilitate flattening (as previously described). The length of anagen phase determines the overall length of the hair and is highly dependent on continued proliferation and differentiation of the matrix transit-amplifying cells (Alonso and Fuchs, 2006). Usually the majority of human hairs on the scalp and beard are in the anagen phase (approximately 90%) (Oh et al., 2016).

Anagen-to-Catagen transition has been extensively studied. In young mice this transition can be observed, due to young mice having a synchronised hair cycle up to an age of 12 weeks, humans do not have a synchronised hair cycle making it significantly more difficult to accurately study. Additionally murine anagen-to-catagen occurs in a wave, beginning at the head and travelling down the animal to the tail. However, in humans no such visible wave is seen; with very few human follicles being in catagen (or transitioning to catagen) phase at any given time (Oh et al., 2016).

Catagen phase is when the lower follicle detaches from the dermal papilla and regresses to roughly 1/6th of its original size, through a programmed cell death in the hair bulb, IRS and ORS, hair shaft differentiation also ceases and a ‘club’ forms at the base of the shaft as it migrates towards the upper follicle region (where it anchors in place until shedding), as the majority of the lower follicle has degraded an ‘epidermal stand’ remains, as a means to connect the DP to the upper follicle (Alonso and Fuchs, 2006, Lindner et al., 1997, Sasaki, 2019).

Finally telogen phase is a time of rest, in mice the first telogen phase is short, lasting only a day or two, but subsequent telogen phases last progressively longer (Muller-Rover et al., 2001, Wu et al., 2019a). In humans telogen phase lasts several months, although hair shaft tends to remain attached, but not growing, to the upper, permanent part of the hair follicle, so little visible loss of hair is seen. During this stage the dermal papilla is also retracted towards the bulge region, leaving a short distance between the bulge and dermal papilla, facilitating interactions between the secondary hair gem and the bulge region (Greco et al., 2009, Uccelli et al., 2019).

Telogen-to-Anagen transition occurs with quiescent stem cells being signalled to rapidly proliferate, forming a new bulb, complete with new transit-amplifying cells (Blanpain et al., 2004). The newly formed hair shaft is formed adjacent to the anchored club hair left over from the previous cycle, and will force it to detach and subsequently be shed (also termed exogen), the process is similar to the organogenesis stage of follicular development with Wnt and shh signalling being required for adequate regeneration (Lo Celso et al., 2004, Callahan et al., 2004, Sasaki, 2019).

1.3.2 Key cell signalling pathways controlling hair cycling and regeneration

Generally speaking mouse models have been the cornerstone of hair follicle cycling studies, due to the ease of obtaining samples and the well-defined timeline, although the same (or highly similar) mechanisms are thought to control the human hair cycling. The same cell types and cell cycling transitions occur, however there are several marked inter-species differences, chiefly the timing of cycling transitions, with the anagen phase lasting years in humans, while in mice it is only 2-3 weeks. Additionally, mouse hair cycling is synchronised across the animal up to the age of 12 weeks, while human hair cycling is a mosaic, with individual follicles cycling independently of those around it (Oh et al., 2016) . As such, most information detailed below has been obtained using in mouse models; however the human systems are likely to be similar.

During telogen phase the dermal papilla rests just below the bulge region, telogen-to-anagen transition progresses due to dermal papilla-hair follicle stem cell crosstalk, mediated by Shh, Wnt and Bmp signalling interactions. High levels of Bmp4 maintain bulge cell quiescence by inhibiting *Shh* and *Wnt*; however during telogen-to-anagen transition Noggin inhibits Bmp4, allowing *Shh* and *Wnt* expression to be activated, upregulating β-catenin. β-catenin then accumulates in the hair germ and hair follicle stem cells, overriding quiescence and activating the cells, which proliferate rapidly and become transiently-amplifying daughter cells (Rishikaysh et al., 2014, Greco et al., 2009).

Anagen-to-catagen transition has several molecular markers; however their mechanism of action remains to be fully understood. Fgf5, Egf, Tgfβ family members, p53, and BmpRIA have all been shown to play a role in anagen-to-

catagen transition (Hebert et al., 1994, Andl et al., 2004, Schmidt-Ullrich and Paus, 2005). Egf and its receptor (EgfR) drive catagen by regulating the RAS pathway, which promotes migration, senescence and differentiation (Rishikaysh et al., 2014). The RAS pathway inhibits Shh activity and may also regulate Fgf signalling (Mukhopadhyay et al., 2013).

The onset of telogen is seen as Bmp signalling from the stem cell niche, triggering hair follicle stem cell quiescence, creating a threshold barrier which must be overcome to initiate the next cycle (Hsu et al., 2011, Wang et al., 2017).

1.3.3 Transcription factors regulating hair cycling

The transition from telogen-to-anagen is regulated by NF1C, a nuclear factor which is able to induce shh, Wnt and Lef1, which facilities the accumulation of β-catenin and subsequently overwhelms the Bmp barrier threshold, ending quiescence and driving proliferation as well as inhibiting Tgfβ1 and P21, and so initiating the anagen phase (Naruse et al., 2017, Plasari et al., 2010).

As previously mentioned Sox9 and Lhx2 are required for maintenance of the bulge region while, Lhx2 is required for the initiation of the hair placode, in the mature hair follicle its role differs, it acts to regulate Sox9, Tcf4 and Lgr5 facilitating the switch between maintenance and activation of the hair follicle stem cells (Folgueras et al., 2013). A loss of Lhx2 or Sox9, in mice results in an inability to maintain quiescence of hair follicle stem cells and early entry into anagen phase (Rhee et al., 2006). More recently, Lhx2 has been demonstrated to play a role in wound healing by facilitating proliferation and migration of bulge cells in response to wounding. A loss of Lhx2 results in a reduced rate of wound healing and re-epithelialisation (Mardaryev et al., 2011). Msx2 and Gata3 are also present during the anagen phase and serve a

similar role to the previously described one in hair follicle cyto-differentiation; Msx2 facilitates differentiation of transit-amplifying cells to the hair shaft fate, while gata3 drives differentiation to inner root sheath fate (Ma et al., 2003, Johns et al., 2005).

Nuclear factor of activated T cells C1 (Nfatc1) is another transcription factor involved in regulation of the hair follicle stem cell niche, functionally Nfatc1 overlaps substantially with Lhx2 (Rhee et al., 2006, Horsley et al., 2008). The role of Nfatc1 within bulge cells is to maintain quiescence, a loss of Nfatc1 results in premature transition into anagen phase (Horsley et al., 2008, Keyes et al., 2013). Nfatc1 is only seen in mouse hair follicle stem cell niche. However, increased human hair follicle growth and prolongation of anagen phase has been seen in patients when treated with Cyclosporine A (CSA) (an immunosuppressant) which is a known inhibitor of both human and mouse NFATc1. This increased growth is not a result of the T-cell inactivation as it has been demonstrated in immunocompromised nude mice (Gilhar et al., 1988), but instead due to the inhibitory effect of CSA on secreted frazzled-related protein 1 (SFRP1) in the dermal papilla, SFRP1 has a bi-phasic effect on WNT signalling, high levels of SFPR1 inhibits WNT while low concentrations upregulate WNT, as such CSA inhibits SFRP1, which in turn upregulates WNT signalling to increase hair growth and prolong anagen phase (Zhong et al., 2007, Hawkshaw et al., 2018).

Figure 1.3 Human hair cycle

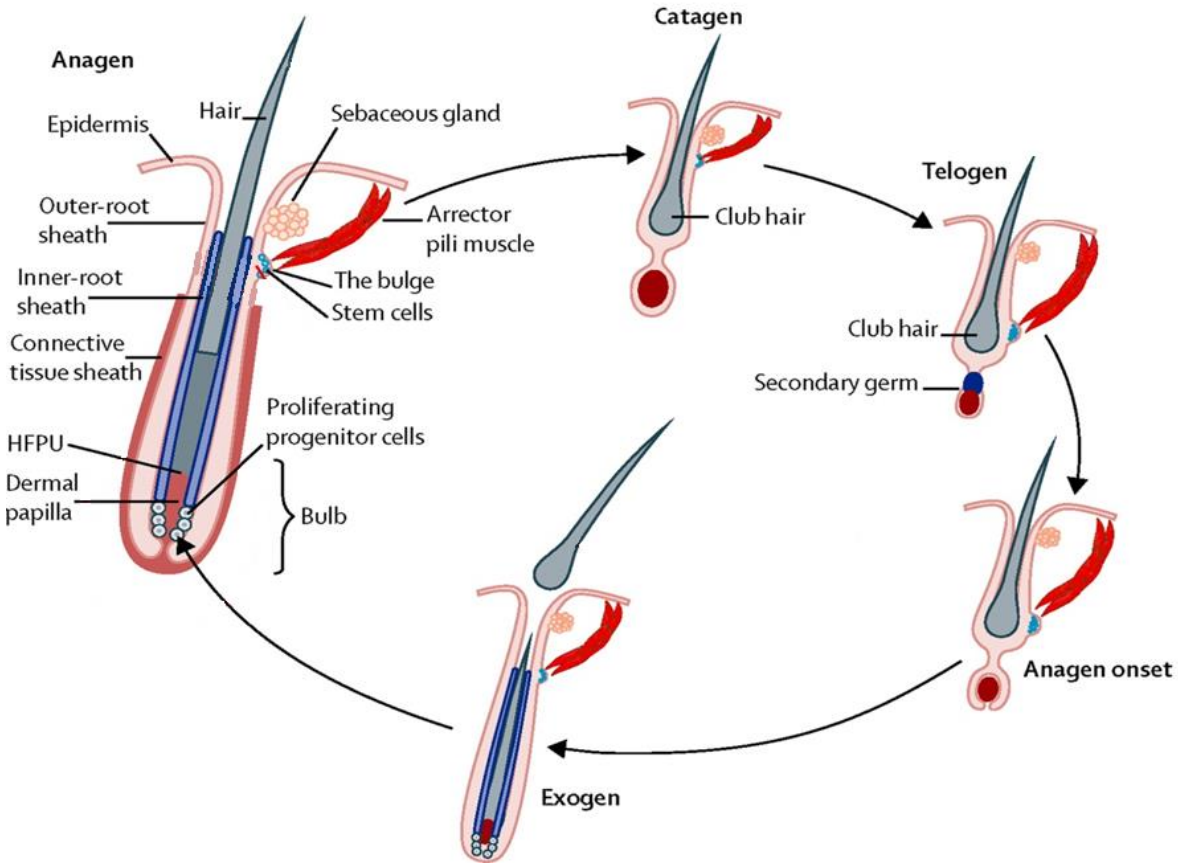

Summary of the human hair cycle, highlighting the major stages. Image adapted from (Paus et al., 2013)

1.4 Epigenetic regulation of epidermal and hair follicle morphogenesis and homeostasis

1.4.1 Epigenetics and chromatin structural organization

Epigenetics is a term first coined in 1942 by Conrad Waddington, originally defined as “The branch of biology which studies the casual interactions between genes and their products which bring their phenotype into being” (Waddington, CH., 1942). This broad statement encompasses all molecular/biochemical pathways that demonstrate the influence on phenotype. Since 1968 a staggering amount of research into epigenetics has taken place, as such the term epigenetics has been redefined to be “the study of gene changes that are mitotically and/or meiotically heritable and that do not entail a change in DNA sequence” (Wu and Morris, 2001). In this way, epigenetics demonstrates how all cells of a host organism share identical genome, yet the observed phenotypes of specific cell/tissues/organs can differ greatly, this is due to the specific gene expression patterns found within progenitor cells and their daughter cells (Fessing, 2014). In its loosest term epigenetics defines processes which affect gene expression; including post-replication DNA modifications, non-coding RNAs, RNA post-translational modifications, histone modifications, nucleosome positioning, ATP-dependent chromatin remodelling and higher order chromatin folding and three dimensional (3D) genome organisation (Jaenisch and Bird, 2003, Bintu et al., 2016, Botchkarev et al., 2012).

Chromatin structure has several tiers of structural organisation from the loose ‘naked’ DNA up to the tightly packaged chromosome seen in cellular metaphase (summarised in Fig 1.4a). Chromatin is also a dynamic structure, capable of rapidly

shifting from the more open states to the more compacted states and back again. DNA is the base form of the physical genome, a sequence of bases connected together by a sugar-phosphate backbone, providing the basic genomic sequence of the host organism. The next tier is the nucleosome, this is the primary unit of chromatin organisation and all additional tiers require nucleosomes. The core nucleosome is a DNA-protein complex consisting of 147 bp of DNA wrapped around a histone octamer. The histone octamer is composed of two copies of each of core histones H2A, H2B, H3 and H4. Core nucleosomes are linked via an additional section of linker DNA, which is 20bp - 60bp long (Luger et al., 1997, Kornberg, 1974, Khorasanizadeh, 2004, Perdigoto et al., 2014). Chromatin in this state is often termed the 10nm fibre or the primary chromatin state; it is also worth noting that there are additional histone variants (H2A.X or H2A.Z for example) which are only seen in selected nucleosomes. Next, these nucleosomes can be compacted, this is due to histone H1 (the linker histone), which binds the linker DNA between nucleosomes to the histones, resulting in a change in the overall structure of the nucleosome chain. When this occurs the linker DNA may also become inaccessible, it is also worth noting that just as with other histones, H1 has several variants, this compacted chromatin state is termed the 30nm fibre or secondary chromatin state (Harshman et al., 2013). These fibres can then be modelled into loops and stacked together anchored to a central chromosome scaffold, this scaffold is not comprised of histone based proteins, but scaffold proteins, topoisomerase IIα (TOPO IIα), condensin and kinesin family member 4 (KIF4), these proteins are thought to form sort of ‘barbers pole’ central to the chromosome axis, although this remains uncertain as little is known about the proteins and their distribution (Poonperm et al., 2015, Samejima et al., 2012). It is worth mentioning that the term ‘chromatin state’ is often utilised to mean either the level of spatial chromatin organisation, as has previously been described, or can refer to the molecular modifications present on

both the DNA or the histones in various regions, the latter has far more conformations as there are any number of applicable modifications that may or may not be present.

3D organisation of chromatin is used to describe the spatio/temporal organisation of chromatin above the 10nm fibre stage within the nucleus, it has been demonstrated that the organisation is not random (Ferrai et al., 2010, Johnston et al., 2019). Originally seen only as heterochromatin and euchromatin, densely packaged inactive or open and transcriptionally active chromatin respectively, it has since been further refined, with heterochromatin being sub divided into constitutive and facultative heterochromatin, constitutive heterochromatin is a long term silencing of regions not required to be transcribed by the cell, while facultative heterochromatin is a more dynamic silencing of genes that may be required during differentiation or stress responses (Maison et al., 2010, Murakami, 2019). Further to this, multiple experiments, using differing techniques, have demonstrated that chromosomes occupy distinct regions of the nucleus, termed chromosome territories (CTs), also the positioning of genes within CTs is not random, but based upon positioning of other genes and nuclear organelles (Naumova and Dekker, 2010, Sanyal et al., 2011, Paulsen et al., 2019). Advancements in this area are due to two techniques, the first involves confocal microscopy based analysis of nuclei stained with fluorescent in situ hybridisation or fluorescent chimeric DNA binding proteins (Kumaran and Spector, 2008, Joffe et al., 2010). Or secondly by utilising Chromosome Conformation Capture (3C) technologies or its derivatives (4C, 5C and hi-C) which involves cross linking chromatin, restriction enzyme digestion, ligation, PCR and sequencing to identify spatially contacting regions (Naumova and Dekker, 2010).

It has been shown that transcriptionally active genes are positioned more closely together within CTs, while inactive genes tend to cluster together in silenced regions closer to the nuclear periphery. A process involving several chromatin architectural proteins (Satb1, Satb2, cohesin and CTCF to name a few) as well as ATP-dependent chromatin remodelling complexes (ISWI, SWI/SNF, NuRD etc.) acting in concert to facilitate the opening of specific genomic regions and manoeuvring the region to within range of specific promoters or enhancers, in order to activate and repress gene expression. A good example of this is the epidermal Differentiation Complex (EDC) locus, a gene dense stretch of DNA encoding several dozen genes required for terminal epidermal differentiation. Studies have shown that the EDC loci is moved during epidermal progenitor cell maturation, taken from an area of gene silencing to an area of transcriptional activation, this remodelling is facilitated by p63, Brg1 and Satb1, as a loss of either results in epidermal differentiation defects (Fessing et al., 2011, Mardaryev et al., 2014).

1.4.2 Covalent DNA modifications

DNA methylation is a modification seen on the DNA of most eukaryotic organisms, however the methylation pattern differs between species or subphylar. For example *Saccharomyces cerevisiae* and the nematode worm *Caenorhabditis elegans* have no DNA methylation, while some fungi only methylate DNA repeats, invertebrates tend to have a mosaic methylation pattern, with regions of extensive methylation interspersed with methylation free zones (Suzuki and Bird, 2008, Liu et al., 2019a, Kvist et al., 2018). The focus here however will specifically be mammalian DNA methylation patterns.

In mammals DNA methylation is a modification resulting in the addition of a methyl group to C5 position of cytosine, giving 5'-methylcytosine (5mC) (shown in Fig 1.4b), this modification occurs most predominantly at CpG dinucleotides (where cytosine is adjacent to guanine), with up to 70% of all CpG sites modified (Jones, 2012, Rivas et al., 2019). One exception however are the short regions (1-2kbp) with high CpG density (termed CpG islands) which remain largely unmethylated. CpG islands are a common feature found at the promoter sites or in the first introns of housekeeping genes (Reik, 2007, Wang and Kadarmideen, 2019). Interesting however is the methylation of the so called CpG island shores, these are located approximately 2kbp from transcriptional start sites (TSS) of CpG island containing gene promoters and are methylated in a differentiation specific manner (Feng et al., 2010).

In mammals maintenance of DNA methylation is carried out by DNA methyltransferase 1 (DNMT1), which is capable of transferring a methyl group from a methyl donor S-adenosyl-L-methionine (SAM) to the cytosine base, during replication methylation status is not transferred to the daughter strand, and so DNA is hemi-methylated, DNMT1 recognises these hemi-methylated sites and restores the methylation state on the newly synthesized strand (Feng et al., 2010, Jimenji et al., 2019). While DNMT1 carries out maintenance, *de novo* methyltransferases 3l, 3a and 3b (DNMT3l and DNMT3a/3b) are responsible for establishing the methylation pattern of cells during embryonic development, and in adult stem cells (Feng et al., 2010), DNMT3l lacks the enzymatic activity, but instead associates with DNMT3a/3b to fulfil its role.

DNA methylation is commonly associated with gene repression, methylated sites inhibit binding of transcription factors, methylated sites may also be targeted by repressive chromatin remodelling complexes, preventing access to the gene (Reik,

2007). However, there are some cases in which DNA methylation may actually result in active gene transcription (Rishi et al., 2010).

DNA methylation has been shown to be vital to survival, mice deficient in DNMTs die either embryonically or shortly after birth. Interestingly, a loss of DNMT1 results in early embryonic death, with lethality occurring at E9.5 (Li et al., 1992, Han et al., 2019), while loss of DNMT3a showed the longest life with death at approximately 4 weeks postnatally (Okano et al., 1999). DNA methylation also plays a vital role in epidermal development, elevated levels of DNMT1 are seen in basal keratinocytes and loss of DNMT1 showed premature differentiation, loss of proliferation and the progenitor state in human basal keratinocytes (Sen et al., 2010). As previously mentioned while 5mC is associated with repression it has been shown to have functions in transcriptional activation, specifically by recruiting CCAAT/enhancer binding protein α (C/EBPα). C/EBPα is an important transcription factor in epidermal differentiation and is predominantly expressed in suprabasal layers, a loss of C/EBPα results in a basal layer hyperplasia, loss of differentiation and increased apoptosis in the suprabasal layer (Oh et al., 2007, Rishi et al., 2010, Marthaler et al., 2017).

Recently, a new DNA modification was found in mammals, or rather a modification of DNA methylation, oxidation of the methyl group in 5'-methylcytosine results in the formation of 5'-hydroxymethylcytosine (5hmC), shortly after its finding the ten-eleven translocation (TET) family of proteins was seen to cause this oxidation to occur. The TET family has 3 members (TET1, TET2 and TET3) and while it was initially seen in TET1, TET2 and TET3 were also confirmed to be able to oxidise 5hmC (Tahiliani et al., 2009, Ito et al., 2010, Ko et al., 2010, Liu et al., 2019b). Interestingly, 5hmC distribution in the genome is distinct from 5mC, and likely demonstrates that 5hmC

has its own functionality, for example 5hmC is seen at elevated levels in mouse embryonic stem cells, which may suggest it has a role in maintaining stem properties (Xu et al., 2011, Wu and Zhang, 2011b), although the primary role of 5hmC is thought to be as an intermediary during DNA demethylation. Currently there are two DNA demethylation mechanisms which have been identified; one possibility is that hemi-hydroxymethylated DNA is not recognised by DNMT1 and so the daughter strand is not re-methylated post replication resulting in a passive replication dependant DNA demethylation (Inoue and Zhang, 2011), another possibility is due to the TET proteins ability to further oxidate 5hmC to form 5'-formylcytosine (5fC), and further still to 5'-carbxycytosine (5caC) (Branco et al., 2012), which may be removed by thymine DNA glycosylase (TDG), which has been shown to activate the base excision repair (BER) pathways to correct thymine to guanine (T:G) mismatch events, interestingly TDG will preferentially bind 5fC over T:G mismatch sites (Branco et al., 2012, Maiti and Drohat, 2011). The BER pathway would then insert an unmethylated cytosine, suggesting this is a likely pathway in rapid demethylation (possible mechanisms are summarised in Fig 1.4c).

1.4.3 Covalent histone modifications

As previously mentioned the nucleosome consists of DNA wrapped around a histone octamer. These histone molecules could be modified in numerous ways. Most often the N-terminal tails are modified, these modifications include acetylation, methylation, phosphorylation, ubiquitination, sumoylation, deamination and several others (Perdigoto et al., 2014). The type of modification and location of said modification will determine the effect on gene transcription, and the chromatin state itself as these modifications are able to alter histone-DNA and histone-histone interactions, and so facilitate access to genes by transcriptional machinery

(Perdigoto et al., 2014, Ikeuchi et al., 2015) (some histone marks are shown in Fig 1.4d). The modifications of the histones are termed histone marks, and each mark correlates with a specific effect, for example H3K4me3 denotes that histone 3, lysine residue 4 is tri-methylated, this is a very common mark and is associated with transcriptional activation (Guenther et al., 2007, Li et al., 2018).

Histone acetylation and methylation are the most well characterised modifications, methylation is associated with both transcriptional activation and repression, while acetylation is more commonly linked with activation, specific enzymes carry out the acetylation or methylation (or any of the other modifications) of histones, these are histone acetyltransferases (HATs) or histone methyltransferases (HMTs), their counterparts are histone deactylases (HDACs) and histone demethylases (HDMTs) which remove the acetyl or methyl group respectively (Qadir and Anwer, 2019).

1.4.3.1 Histone acetylation

Acetylation state of lysine residues on histone tails determines transcriptional effect, by influencing histone-DNA interactions, acetylation of lysine residues is regulated by 2 opposing groups of enzymes, HATs and HDACs. Histone hyper-acetylation is associated with activating gene transcription, while hypo-acetylation is associated with gene repression, due to changes in chromatin compaction and recruitment of bromo-domain containing proteins (Campos and Reinberg, 2009). Specific histone marks are associated with specific transcription responses, interestingly the histone marks seen at a promoter region differ from the marks seen at the gene coding region of active genes, for example, active promoters are enriched with histone marks H3K9ac, H3K18ac and H2B12ac, while H4K12ac and H4k16ac are seen broadly in many gene coding regions (Botchkarev et al., 2012)

Acetylation marks in epidermal development have been associated with promoting proliferation, and inhibiting differentiation, by using HDAC inhibitor triclostatin A (TCA) on primary keratinocytes results in a cell cycle arrest and expression of involucrin (a differentiation marker), loss of both HDAC1 and HDAC2 also results in epidermal stratification failure (Markova et al., 2007, LeBoeuf et al., 2010). Within hair follicle stem cells histone 4 is hypo-acetylated, however after c-Myc mediated release from the stem cell niche, elevated acetylation of histone 4 was seen (Botchkarev et al., 2012, Frye et al., 2007).

1.4.3.2 Histone methylation

Histone methylation is regulated by HMTs and HDMTs; histone methylation differs slightly from acetylation as methylation can be one of three types, mono-, di- or tri-methylation, denoting the number of methyl groups attached to a single amino acid residue. As with acetylation specific methylation marks denote transcriptional activation or repression. Interestingly, histone methylation is associated with both activation and repression, as histone tails can be mono-, di-, or tri- methylated there is a complex relationship between level of the histone methylation and transcriptional response, generally di- or tri-methylated lysine residues result in transcriptional repression, H3K9me2/3, H3K27me3 and H4K20me3 (Wang et al., 2009), while mono-methylated lysine residues are more likely to be associated with activation, with the notable exception of H3K4me3, which is seen at active TSS sites and genes with a paused RNA polymerase II (RNA POL II), meanwhile H3K4me1/2 are found near TSS of active genes and in gene enhancers (Barski et al., 2007, Wang et al., 2009, Botchkarev et al., 2012).

Histone methylation during epidermal development has been investigated in more detail, specifically the marks H3K20me1 and H3K27me3. H3K20me3 are catalysed by setd8-mediated histone methylation and is found at active transcription sites, a loss of Setd8 results in a loss of proliferation and abnormal differentiation of the epidermis (Driskell et al., 2011). Histone mark H3K27me3 is associated with repression, and is found at the TSS of many epidermal genes, to remove this repressive mark and allow epidermal differentiation the Jumonji C domain containing protein D3 (JMJD3) is required; JMJD3 is a demethylase specific to H3K27me3, and a loss of JMJD3 results in failed epidermal differentiation (Sen et al., 2008).

1.4.4 Polycomb repressive complexes

The activity of repressive mark H3K27me3 is mediated by polycomb group proteins (PcGs), this group of proteins is able to block RNA POL II activity by compacting chromatin (Di Croce and Helin, 2013). PcGs form larger complexes, the polycomb repressive complexes (PRCs), there two major families of PRC (PRC1 and PRC2), both act to compact chromatin and repress gene expression, and are vital to development, as well as maintaining stem cell potential (Simon and Kingston, 2009). PRC1 has two major variants, canonical PRC1 is comprised of four core PcGs; RING1, CBX, PCGF and PHC, while non-canonical PRC1 contains only 3 PcGs RING1, PCGF and RYBP (Gao et al., 2012), it is also worth noting that all mammalian PcGs involved in PRCs have multiple homologs (Chen and Dent, 2014). PRC2 contains three PcGs; EZH, EED and SUZ21, it is also likely that additional proteins are incorporated into PRCs (Botchkarev et al., 2012, Plys et al., 2019).

PRC mediated transcriptional repression is proposed to be via one of several mechanisms. Firstly there is PRC2 mediated methylation of H3K27, which is

targeted by Cbx4 (PRC1), and subsequently PRC1 carries out ubiquitination of H2AK119 (H2AK119ub), compacting chromatin and preventing access to gene promoters (Lee et al., 2007, Hammond-Martel et al., 2012). Secondly, PRCs may bind to RNA POL II complexes, preventing elongation and producing short RNA transcripts which are then degraded (Fachinetti et al., 2010). Finally, PRCs act as a chromatin remodelling complex, which are capable of creating 'repressive hubs' or clusters of genes in densely packed chromatin regions (Bantignies and Cavalli, 2011). Each of these possibilities are further explained below.

The PcG protein EZH, a core subunit of PRC2, has two homologs; EZH1 and EZH2, both of which are HMTs which are highly specific to H3K27, EZH1/2 is able to mono-, di- or tri-methylate H3K27 (Yoo and Hennighausen, 2012, Son et al., 2013), however EZH1/2 is unable to carry out its function as a methyltransferase without EED and SUZ12 (Cao and Zhang, 2004, Suh et al., 2019). Several additional proteins have been linked with recruitment of PRC2, for example adipocyte enhancer-binding protein 2 (AEBP2), a zinc-finger binding protein, was shown to bind DNA and recruit PRC2 (Kim et al., 2009). Moreover, the TET proteins may be involved due to their role in modifying 5mC (Wu and Zhang, 2011a), as well as a member of the Jumonji C domain containing protein family, JARID2, is capable of not only enhancing PRC2 recruitment but also in maintaining homeostasis (Son et al., 2013, Li et al., 2010).

The repressive mark H3K27me3 is recognised by Cbx4, a member of the canonical PRC1, this is because H3K27me3 is a recognised by the CHROMO-domain of Cbx4, once bound the RING1/2 protein catalyses the ubiquitination of H2AK119, driving chromatin compaction, which prevents the binding of transcription machinery and ATP-dependent chromatin remodelling complexes, namely SWI/SNF.

(Hammond-Martel et al., 2012, Bantignies and Cavalli, 2011). *In vitro* studies have also demonstrated that H2AK119ub prevents the methylation of H3K4, however H2AK119ub is required to reverse PRC mediated gene silencing, as the H2AK119ub mark is a target of zuotin-related factor 1 (ZRF1), which is able to remove PRC1 from chromatin and activate gene transcription (Richly et al., 2010).

It was previously thought that the repressive capability of PRCs was a result of the H3K27 methylation by PRC2, leading to recruitment of PRC1. However, the discovery of the non-canonical PRC1 called this into question, as H3K27me3 mediated recruitment of PRC1 requires the Cbx PcG, which is not present in the non-canonical PRC1 (Zhen et al., 2014, Bae and Hennighausen, 2014). Additionally, some CpG islands have been shown to be able to recruit both PRC1 and PRC2 by specific mechanisms (Wu et al., 2013, Riising et al., 2014). It has also been demonstrated that a non-canonical PRC1 protein KDM2B facilitates non-canonical PRC1 targeting by binding to CpG rich DNA, specifically involving the zinc-finger domain CXXC. KDM2B was found at the unmethylated CpG islands in mouse embryonic stem cells (mESCs) (Wu et al., 2013). Tet proteins might also have a role in PRC2 recruitment (Wu and Zhang, 2011b) demonstrated that in mouse embryonic stem cells Tet1 and 5hmC were enriched at bivalent gene promoter marked with repressive histone marks H3K4me3 and H3K27me3, and the depletion of Tet1 impaired recruitment of EZH2. Interestingly, it has been shown that the non-canonical PRC1 is able to recruit PRC2 via H2AK119ub. Moreover, AEBP2 and JARID2 associated PRC2 are present in nucleosomes containing the H2AK119ub modification, where they facilitated methylation of H3K27 (Blackledge et al., 2014, Kalb et al., 2014), demonstrating a complex relationship between PRC1 and PCR2 capable of recruiting each other to facilitate transcriptional silencing.

The role of PRC2 in epidermal development has been investigated using mouse models; analysis of the H3K27me3 mark in basal epidermal cells has shown it to be present on several thousand genes associated with neuronal, muscle and hematopoietic cell differentiation. Genes involved in early epidermal differentiation did not contain the H3K27me3 mark; however it was seen at genes controlling late stage differentiation and normally expressed in granular and cornified cells (Ezhkova et al., 2009). EZH2 was highly expressed in the proliferative basal layer, but was down-regulated in differentiated suprabasal cells, knockdown of EZH2 in basal cells resulted in accelerated development of the epidermal barrier, irregular hair follicle formation and upregulation of genes associated with epidermal differentiation, specifically those of the EDC (Ezhkova et al., 2009, Bardot et al., 2013). EZH2 mediated silencing of the epidermal differentiation programme was achieved via preventing binding of AP1, a key transcription factor driving epidermal differentiation. Ablation of either of the other PRC2 subunits (EED or SUZ12) results in a similar phenotype (Conway et al., 2015). Interestingly, the postnatal ablation of any of the PRC2 subunits showed no loss of proliferation in the epidermal progenitor cells (EPCs) in skin, but did show a loss of proliferation in the EPCs of the hair follicle (Dauber et al., 2016). This suggests that PRC2 loss can somehow be mitigated, it is currently thought to be due to the cell niche rather than other intrinsic properties as simultaneous Ezh1 and Ezh2 ablation in cell culture shows equal effects on EPCs regardless of their origin site (Ezhkova et al., 2011, Wassef et al., 2019). Further investigation into the cell micro-environment is required to identify the specific mechanism at work in mitigating the loss of PRC2 in basal layers of epidermis (Botchkarev and Mardaryev, 2016).

CBX4, a component of the canonical PRC1 has also been shown to play a role in epidermal proliferation and differentiation. CBX4 contains a SUMO E3 ligase

activity, which is able to facilitate sumoylation of proteins, including DNMT3a, demonstrating a link between PRC repression and DNA methylation (Li et al., 2007a, Li et al., 2007c, Mohamad Hanif and Shah, 2018). CBX4 is seen to regulate epidermal differentiation in two ways, firstly by preventing senescence in epidermal progenitor cell via PRC mediated repression of the *INK4a* locus, and secondly by promoting differentiation via non PRC mediated mechanisms (Luis et al., 2011). More recently, it has been shown that CBX4 is a direct target of epidermal master regulator p63, the two works in concert to promote epidermal differentiation while repressing non-epidermal lineage genes (Mardaryev et al., 2016).

Figure 1.4 Chromatin structure, DNA modifications and Histone post transcriptional modifications

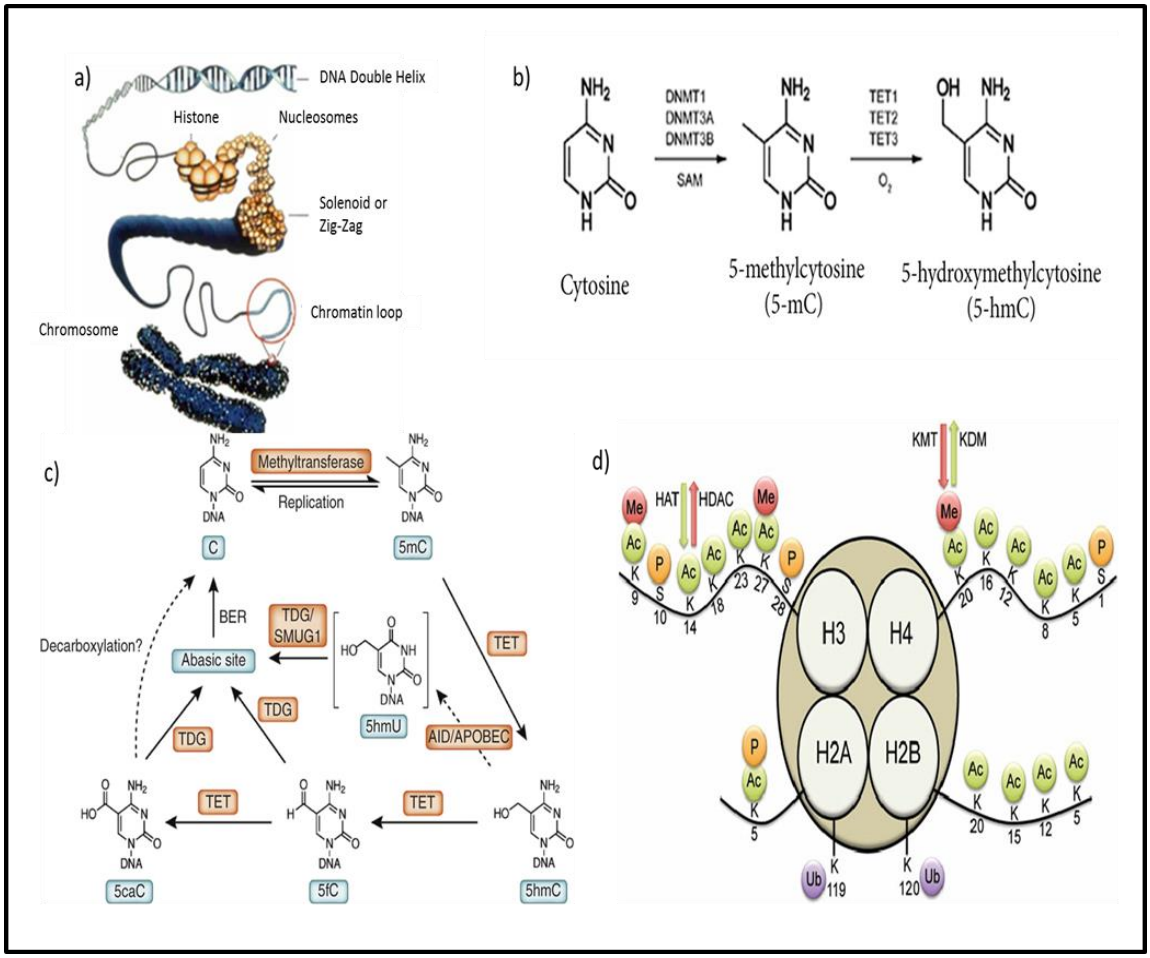

a) Chromatin organisation levels, from the DNA double helix to the metaphase chromosome. b) Schematic of DNA methylation, and subsequent oxidation to generate 5'-hydroxymethylcytosine. c) Proposed mechanisms of demethylation utilising TET family proteins. d) Common histone post-transcriptional modifications. Images adapted from (Luo et al., 2011, (Yang et al., 2013, Song et al., 2012), song et al, 2012, Fortress and Frick, 2015)

1.4.5 ATP-dependent chromatin remodelling

1.4.5.1 Overview of ATP dependent chromatin remodelling

ATP-dependent chromatin remodelling complexes (CRCs) are large multi component complexes at over 1MDa in size and vary in the number of components, all CRCs contain an ATPase subunit which belongs to the superfamily II helicase group (SF2) as well as possessing DExx and HELICc regions separated by a linker region (Bao and Shen, 2007, Barisic et al., 2019). The size of this linker region and additional domains can be used to divide CRCs into four families; SWI/SNF, ISWI, NuRD/Mi-2/CHD and INO80. Members of the SWI/SNF family contain a HSA (helicase SANT associated) and a BROMO region that facilitates the binding to actin or acetylated lysine residues of histone tails respectively. The ISWI family contains a SANT and SLIDE region that are required for histone binding. The NuRD/MI-2/CHD family contains tandem CHROMO domains which is also required for histone binding. Finally, The INO80 family also contains a HSA region similar to that seen in the SWI/SNF family but not the BROMO region, INO80 are also the only family to have larger linker region between the DExx and HELICc regions. While some families are associated more with one specific function, there is no evidence to suggest that each family fulfils a single role, as there are multiple families and sub-families the possibility of synergistic or antagonistic effects between different families exists. CRCs work by weakening the interactions between histones and DNA, an ability derived from the energy obtained through ATP hydrolysis. Disrupting these interactions allows nucleosome switching, sliding or ejection (Saha et al., 2006, Weinhouse et al., 2018). However, the exact mechanism of action undertaken by CRCs is currently unknown, one of the most likely mechanisms is detailed in the ‘loop model’, this involves the generation of a DNA loop caused by the CRC pushing

DNA from the linker section onto the histone core which results in a breaking of histone/DNA bond, this loop then propagates around the histone, resulting in access to the DNA, or the ability to eject, slide or switch the histone, several subunits are thought to be involved in this process, ensuring loop propagation occurs in one direction, or as nucleosome chaperones or facilitating the switch of histone core units (Ludwigsen et al., 2013, Nodelman and Bowman, 2013).

The focus here will be on the SWI/SNF family, specifically the mammalian variant, which is also known as mSWI/SNF or BAF complex (BRG1 Associated Factors or hBRM Associated Factors), and the highly similar PBAF complex (Polybromo BRG1 Associated Factors).

1.4.5.2 SWI/SNF chromatin remodelling complexes and their role in early embryonic development

The SWI/SNF complex was originally discovered in yeast after 2 independent studies into mutations affecting mating type switching and sucrose non-fermenting pathways, *swi* and *snf*. These genes encoded proteins capable of interacting with histones and chromatin, it was later discovered that they were subunits of a much larger multicomponent complex, the complex was named SWI/SNF after the genes leading to its discovery (Sudarsanam and Winston, 2000). The SWI/SNF complex is highly conserved between species; however the exact composition of the complex is changed slightly. The increased genome size and complexity of higher eukaryotes has resulted in expanded gene families rather than single genes encoding different subunits (e.g. *swp73*is present in yeast, while BAF60a, b, and c are the human counter parts).

Later a similar chromatin remodelling complex was discovered in yeast, this remodeller was named RSC (remodelling the structure of chromatin) (Cairns et al., 1994). RSC shares homology with many subunits of SWI/SNF, as well as a similar function in nucleosome remodelling, however RSC is seen at much higher levels than SWI/SNF, suggesting a more vital role (Cairns et al., 1996), It was later discovered that *Sth1* (a subunit of the RSC complex) was required for yeast cell viability.(Treich and Carlson, 1997)

Mammalian SWI/SNF has two variant complexes, BAF and PBAF, which are almost identical in component composition, with very few components being exclusive to one or the other. All components of the BAF and PBAF complex are reported to interact with all or part of the nucleosome; each subunit contains one or more domains which specifically interact with, histones, histone tail residues or DNA, with each subunit providing a specific binding region or enzymatic activity. This multicomponent aspect suggests a vast array of possible functions determined by the specific subunit composition of the BAF/PBAF complexes, which is utilised to facilitate a particular task, rather than single 'all-purpose' complex. Due to the differences in subunit composition there is no single 'BAF complex' but rather a multitude of BAF complexes.

The BAF complex is made up of several core subunits, as well as a number of associated proteins. This has led to disagreements in what makes up the complex, and what should be termed a subunit or associated protein. Here I will mainly discuss subunits, and I will define these as proteins with functionality directly linked to the SWI/SNF complex, or with evolutionally conserved homology within the SWI/SNF complex. Proteins involved in SWI/SNF complex but with common functionality outside of the complex (i.e. β-actin) will be referred to as associated

proteins. Additionally, I will use the term constitutive to define those subunits repeatedly reported to be present in SWI/SNF complexes, while the term facultative will be applied to subunits, which are not reported to be present in all explored SWI/SNF complexes.

The BAF complex is generally considered to be made up of 5 constitutive subunits, and several facultative subunits. The constitutive subunits include an ATPase core, either SMARCA4/BRG1 or SMARCA2/hBRM, which are mutually exclusive in a single complex; the remaining constitutive subunits are ARID1a/BAF250a or BAF250b (mutually exclusive in a single complex) and SMARCC2/BAF170, SMARCC1/BAF155 and INI1/hSNF5/BAF47 (Wang et al., 1996, Lessard et al., 2007). The number of facultative subunits is still being debated (due to different criteria being used to determine subunit or associated protein) currently the total maximum number of subunits found within a BAF complex is 19, and approximately 2-MDa in size of complex (Ronan et al., 2013), any of which may or may not be present depending on the cell/tissue type and developmental stage. The PBAF complex is nearly identical to BAF, with few exceptions, PBAF shares most of the same constitutive subunits (SMARCC2/BAF170, SMARCC1/BAF155 and INI1/hSNF5/BAF47) but does not contain either ARAID1a/BAF250a or ARID1b/BAF250b, instead PBAF contains core subunits ARID2/BAF200 and PBRM/BAF180/polybromo, PBAF also exclusively contains SMARCA4/BRG1 as the ATPase subunit. The facultative subunits are also largely the same, although different isoforms of some subunits have been identified exclusively in PBAF (Yan et al., 2005, Brownlee et al., 2012, Brechalov et al., 2014).

The ATPase subunit of the BAF complex (SMARCA4/BRG1 or SMARCA2/hBRM) contains the DExx and HELICc regions common to all SWI/SNF super-family

members (Lusser and Kadonaga, 2003, Singleton and Wigley, 2002, Clapier et al., 2017). Both also contain the HSA (Helicase SANT associated) region, which serves as a platform for the binding of nuclear actin-related proteins (ARPs), β-actin or actin, this also serves to bind another component BAF53 (Szerlong et al., 2008). BRG1 and hBRM also contain a bromo-domain required for binding acetylated lysine residues; these domains facilitate recognition of the nucleosome target (Haynes et al., 1992, Zeng and Zhou, 2002, Morrison et al., 2017), where acetylated histone tails are generally associated with transcriptionally active sites.

BRG1 and hBRM share approximately 75% homology, however they play non-redundant roles during embryonic development .*Brg1* $^{-/-}$ mouse embryos fail to correctly implant, or terminate at the time of implantation, while *brm* $^{-/-}$ mice are both viable and fertile, with only a few mild changes, namely dysregulation of the fibroblast cell cycle and a larger size compared to the wild type littermates (Bultman et al., 2000, Reyes et al., 1998, Thompson et al., 2015). Other studies have shown that at later stages and in some cell types either BRG1 or BRM can compensate for a loss of the other (Strobeck et al., 2002, Xue et al., 2000, Hoffman et al., 2014, Raab et al., 2017), or even have antagonistic roles (Flowers et al., 2009). These studies support that BRG1 and BRM serve as 'engines' which only drive the remodelling machinery, while the specific accessory components provide specific targeting and functionality.

All variants of BAF or PBAF complex are simply termed BAF or PBAF, however it has been demonstrated previously that BAF complexes can be specific to cell/tissue/stage of development. While there are few validated examples (detailed below and summarised in Fig 1.5), in the future I expect BAF/PBAF complexes will be identified as unique in almost all tissues at one stage or another, which may also prove invaluable to the reprogramming induced pluripotent stem cells.

Embryonic stem cell specific BAF complexes (esBAF) have been described in mouse models, and are shown to regulate pluripotency and maintain cell stemness. esBAF has also been shown to interact directly with pluripotency factors, Oct4, Sox2, Nanog etc. (Ho et al., 2009, Panamarova et al., 2016, Alfert et al., 2019). The composition of esBAF is so far unique and has not been seen elsewhere, esBAF complex contains BRG1, and a homodimer of BAF155, while BRM and BAF170 are not seen in esBAF. Loss of either BRG1, BAF155 or BAF47 at the preimplantation stage result in lethality (Klochendler-Yeivin et al., 2000, Kim et al., 2001, Cabot et al., 2017), supporting their crucial role in cell survival and viability.
BAF45a, BAF53a and BAF60a/b are also seen in esBAF, as well as in other progenitor cell types, suggesting these specific family members are required to maintain the progenitor states (Zhang et al., 2019, Panamarova et al., 2016). While the component composition of esBAF is not unique to either BAF or PBAF complexes, it has also been demonstrated that PBAF is not involved in maintaining the ESC state, as a loss of BAF180 showed no effect on the stemness of ESCs (Wang et al., 2004).

Another tissue specific BAF complex is seen in cardiac progenitor cells, cardiac BAF (cBAF) is not yet fully characterised, however it is known the BAF60c is specifically required (Lickert et al., 2004, Takeuchi and Bruneau, 2009, Sun et al., 2018). Interestingly, cardiac development also requires BAF250b (Lei et al., 2012), which is specific to BAF and not to PBAF, however BAF180, which is specific to PBAF, is also required for cardiac maturation (Wang et al., 2004, Huang et al., 2008). As a result a, loss of either component results in lethal heart defects during murine embryogenesis, supporting that required complexes are stage dependent. A recent study has also shown that BAF60a knockout in embryonic stem cells caused a

redistribution of H3K27me3 marks on chromatin, which may indicate interactions with the PRCs (Alajem et al., 2015).

1.4.5.3 Defects in SWI/SNF complexes in cancer

BAF/PBAF complexes cannot be discussed without talking about their role in cancer, for example BAF47 was originally discovered to have a role in cancer and was later discovered to be a *bona fide* tumour suppressor (Versteege et al., 1998, Biegel et al., 1999), since then the cancer spotlight has been on BAF/PBAF complexes and it estimated that 20% of all human cancers are associated with the mutated BAF/PBAF subunits (Kadoch et al., 2013, Arnaud et al., 2018).

Almost all BAF/PBAF subunits and associated proteins are linked to cancer, which is unsurprising when you consider the role of the BAF/PBAF complexes in regulating cellular processes including; chromatin organisation, control of gene transcription, DNA repair pathways and cell cycle control. This has led to the BAF/PBAF complexes becoming the focus for the development of new anticancer drugs (Farnaby et al., 2019).

Tumours associated with a loss of BAF/PBAF complex subunit mutations often result in specific tumour types dependent upon which subunit is mutated. For example a biallelic loss of BAF47 results in rhabdoid tumours (Eaton et al., 2011), while BRG1 mutations are associated with small cell carcinoma, hypercalcaemic type (SCCOHT) (Jelinic et al., 2014).

There are several excellent reviews on BAF/PBAF complex association with cancer (Hohmann and Vakoc, 2014, Helming et al., 2014, Shain and Pollack, 2013).

1.4.5.4 SWI/SNF complexes and epidermal and hair follicle biology

The role of BRG1 during epidermal development is well established, a systemic loss of BRG1 results in lethality at the peri-implantation stage (discussed previously), epidermal specific ablation of Brg1 in mice revealed its crucial role in limb and epidermal barrier development (Indra et al., 2005). This study demonstrated that Brg1 is required to facilitate terminal differentiation of keratinocytes and adequate barrier formation, but not for maintaining proliferation or early stages of keratinocyte differentiation. A later study demonstrated that BRG1 is a direct target of p63, and is required to relocate the EDC from the nuclear periphery into the more transcriptionally favourable nuclear interior, which facilitates transcriptional activation of the EDC, giving rise to fully differentiated corneocytes and adequate barrier formation (Mardaryev et al., 2014). It has also been shown that BAF and p63 co-regulate over 200 genes specific to the epidermal lineage and their co-expression is mutually required to maintain an open chromatin landscape enabling epidermal differentiation (Bao et al., 2015).

ACTL6a/BAF53a has also been implicated in epidermal development by modulating the BAF complex activity, preventing its binding to the KLF4, as well as other keratinocyte specific gene promoter regions, preventing their activation, maintaining the epidermal progenitor state and preventing premature keratinocyte differentiation (Bao et al., 2013). It was also demonstrated that epidermis specific knockout of BAF53a abolished the epidermal progenitor state, resulting in terminal differentiation and tissue loss. The activity of BAF53a was also demonstrated to be directly due to its interaction with BAF complexes and in turn the KLF4 transcription factor (Bao et al., 2013). This data also supports that BAF subunits have a regulatory role over the

complex itself, and do not simply act as targeting molecules, which may also suggest the role of some subunits is entirely to regulate the complex itself.

BRG1 has also been shown to effect hair follicle homeostasis. Hair follicle stem cells are located in the bulge region and are utilised in both epidermal wound healing and regeneration of the hair follicle during hair cycling. It has been demonstrated that Brg1 is indispensable to the maintenance of the murine hair follicle stem cell reservoir, as well as facilitating their activation during anagen induction and the cutaneous wound healing response (Xiong et al., 2013). This effect is part of a reciprocal feedback loop between Brg1 and Shh, by which Shh signalling activates Brg1 via Gli1 transcription factor, to regenerate the follicle during cycling, while Brg1 helps to recruits NF-κB to activate *Shh* gene transcription to maintain hair matrix cell proliferation. The murine hair follicles stem cell specific Brg1 ablation results in an inhibition in hair matrix cell proliferation and differentiation as well as the gradual loss of the hair follicle stem cell reservoir (Xiong et al., 2013).

Figure 1.5 Chromatin remodelling complexes and cell specific SWI/SNF complexes

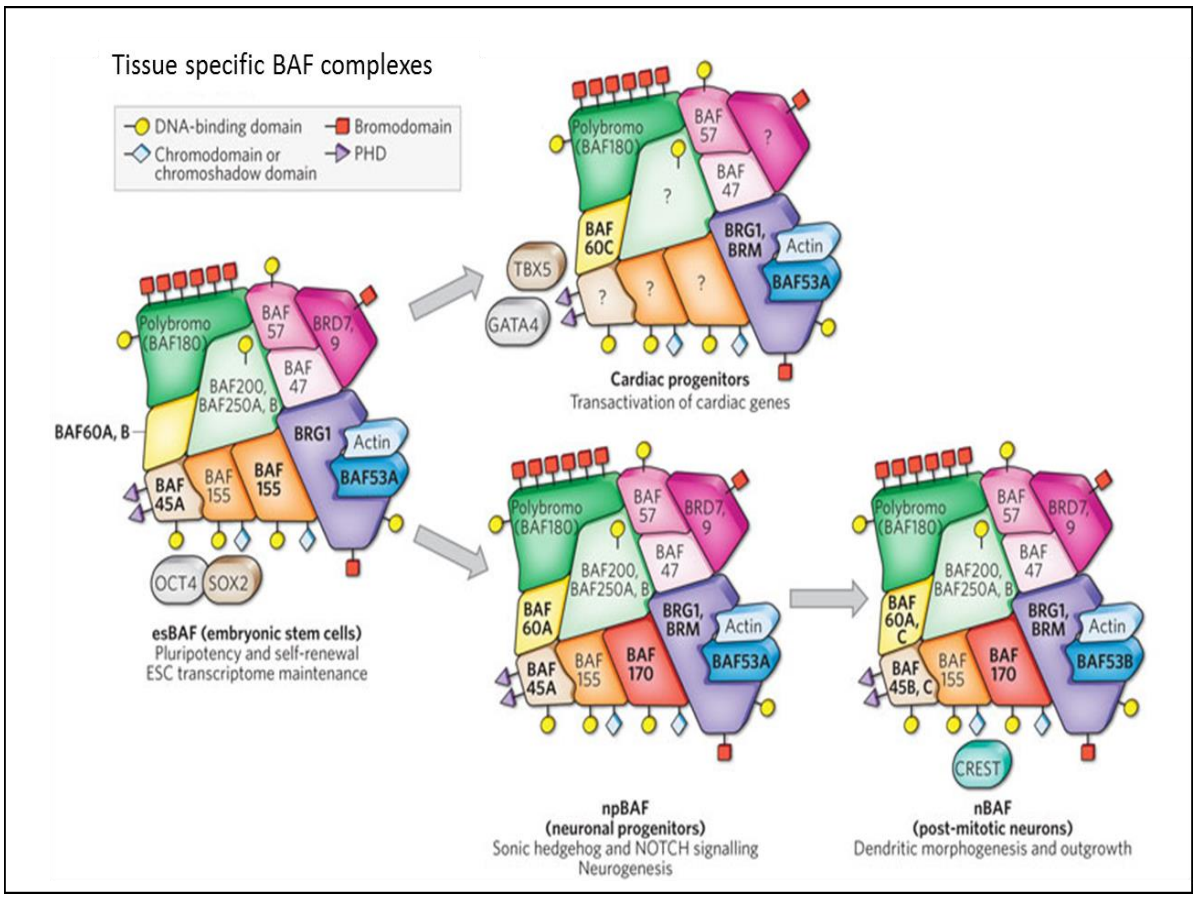

Examples of cell type specific BAF/PBAF complexes, as well as some of the signalling pathways involved with their regulation. (Image adapted from Ho and Crabtree, 2010)

1.5 Epidermal regeneration during skin wound healing

A cutaneous wound is a break in the epidermis and underlying dermis; this could be any kind of lesion, burn or tear in the skin, resulting in a loss of its integrity and disruption of the underlying structure and function. This loss in the protective barrier must be corrected rapidly to ensure homeostasis is resumed, a healed wound is one in which connective tissue have been restored and re-epithelialisation has occurred (Rittie, 2016).

One of the key issues in epidermal wound healing research is that clinically a wound is any rupture in the skins continuity, as such minor lesions replicated in the lab may not recapitulate the large scale lacerations which could fully penetrate the flesh and muscle beneath, however a base understanding of the mechanisms involved will hopefully translate into improvements in all clinical applications in cutaneous wound healing.

1.5.1 Skin wound healing process overview

Wound healing is usually divided into three phases; inflammation, proliferation and remodelling. These are not linear events however, they overlap over time until the wound is healed (shown in Fig 1.6a) (Reinke and Sorg, 2012). My primarily focus will be on wound closure and re-epithelisation.

1.5.1.1 Keratinocyte proliferation, migration and differentiation during skin wound healing

Skin wound healing process is highly dependent upon the size, location and depth of the wound, all of which can drastically affect the time taken to reach the

proliferation phase, as well as the length of time the proliferation phase continues for (Shaw and Martin, 2009). Within mammalian species wound healing relies primarily upon the activation, migration and differentiation of inter-follicular epidermal keratinocytes and HF stem cells (Plikus et al., 2012).

Re-epithelisation of a wound by keratinocytes is carried out by a combination of migration and proliferation of keratinocytes in close proximity to the wound edge (Martin, 1997, Shaw and Martin, 2009). Basal keratinocytes at the edge of the wound proliferate and move as a collective 'sheet' across a provisional 'wound healing matrix' prepared during the inflammation stage. In order for the keratinocytes to migrate a series of modifications must take place. These modifications begin with modifying their cell-cell/cell-matrix attachments, loosening the tight bonds holding them in place (Nguyen et al., 2000). Then the formation of actin rich lamella protrusions which are required for 'crawling' (Mitchison and Cramer, 1996), as well as the upregulation of proteolytic enzymes, metalloproteinases (MMPs) which specifically degrade type-IV collagen found in the basement membrane allowing cells to detach and migrate and facilitates penetration of the interface between scab and viable tissue (Pilcher et al., 1999). Migrating keratinocytes secrete laminin V to facilitate regeneration of the basement membrane. At the forefront of the migrating wound 'tongue' keratinocytes continue to proliferate, these cells are hypertrophic and produce similar actin rich lamella protrusions to maintain migratory directionality (Coulombe, 1997). Additionally, during migration new cytoskeletal filaments are expressed, namely K6, K16 and K17, while differentiation-associated keratins (K1/K10) are down-regulated (Wawersik et al., 2001, Myers et al., 2007). However, the expression of these keratins require proper regulation as the overexpression of K16 results in epidermal lesions (Coulombe et al., 1995). As a wound is a three dimensional structure the

migrating keratinocytes are converging on a single point in the centre, furthest from any healthy tissue, when migrating keratinocytes meet contact inhibition occurs, halting the progress and establishing a new basement membrane, keratinocytes then begin to differentiate, shutting down the K6, K16 and K17 expression and re-establishing normal differentiation and stratification pathways, beginning at the wound edge and gradually encroaching on the centre of the wound (Broughton et al., 2006, Li et al., 2007b).

Migration of keratinocytes is regulated by a series of transcription factors, which are seen to be upregulated at the wound edge. These factors include AP-1 components, c-JUN and c-FOS. A loss of c-JUN has previously been shown to delay wound healing in mice, and a loss of Nuclear hormone receptor co-activator (NRC), a co-activator of c-JUN and c-FOS results in development of chronic wounds (Mahajan et al., 2004, Schafer and Werner, 2007).

1.5.1.2 Epidermal and hair follicle stem cell activation

It is well established that wounds in regions with an abundance of hair follicles heal faster than regions lacking hair follicles (Stojadinovic et al., 2011). Mice wounded during anagen phase of the hair cycle heal faster than in telogen phase (Ansell et al., 2011). This is due to skin injury activating the IFE and HF stem cells, which subsequently migrate to the epidermal wound and assist in regeneration (Carrasco et al., 2015, Lewis, 2013).

The HF stem cell regions is humans is colloquially termed the bulge region (discussed previously), the structure of the HF in this region facilitates a dual function for the $CD200^{+}$ stem cells found here. The ORS where the bulge is located is continuous with both the base of the hair follicle and the IFE, allowing the stem

cells to migrate to either, regenerating the HF or to supply epidermal stem cells in response to wounding (shown in Fig 1.6b) (Cotsarelis, 2006). Generally these stem cells maintain a high proliferative potential but are usually quiescent and can remain dormant for extended periods (several months) only being activated when required for HF or wound regeneration (Lavker and Sun, 2000, Wong and Reiter, 2011). An absence of all hair follicles has been shown to have no effect on epidermal integrity or homeostasis; however it is detrimental to wound healing (Weyandt et al., 2009, Waters et al., 2007).

A previous study indicated that transplantation of HF stem cells may serve a role in managing chronic wounds; mice which have undergone bulge cell transplantation can repopulate epidermis, sebaceous gland and epithelial layers of the HF itself (Oshima et al., 2001). However more recent studies have countered this, demonstrating that the recruitment of hair follicle stem cells to the wound was not required for adequate wound healing (Driskell et al., 2015).

IFE and HF stem cells have previously been shown to maintain open chromatin states at genes unrelated to their lineage, suggesting they reserve the potential to transition to a close lineage if required (Bock et al., 2012). Moreover, genome wide methylation studies have demonstrated that many adult progenitor cells have distinct methylation patterns required to maintain their stem cell like properties, and a change of this methylation pattern is associated with lineage differentiation (Botchkarev et al., 2012). It has been shown that epigenetic regulator changes expression at the wound edge change drastically compared with normal healthy epidermis. Ezh2 and Eed, members of PRC2, are drastically down regulated in wounded mouse epidermis, while the histone demethylase Jmjd3 is upregulated, this results in fewer H3K27me3 histone modifications, specifically at the *c-Myc* and

Egfr genes, indicating that a loss of PCR2 mediated repressive histone modifications are required for wound healing (Shaw and Martin, 2009, De Santa et al., 2007).

De novo hair follicle neo-genesis has also been observed in cases of wound healing. It was shown that the bulge derived stem cells in mice are not the progenitors of the new hair follicle placodes (Ito et al., 2007). It has also been shown that IFE stem cells are unipotent, only giving rise to the epidermis (Plikus et al., 2015). However, this has only been tested *in vitro* and with small wounds, responses to large scale wounds, or wounds on larger mammals, have yet to be tested.

Figure 1.6 Epidermal wound healing

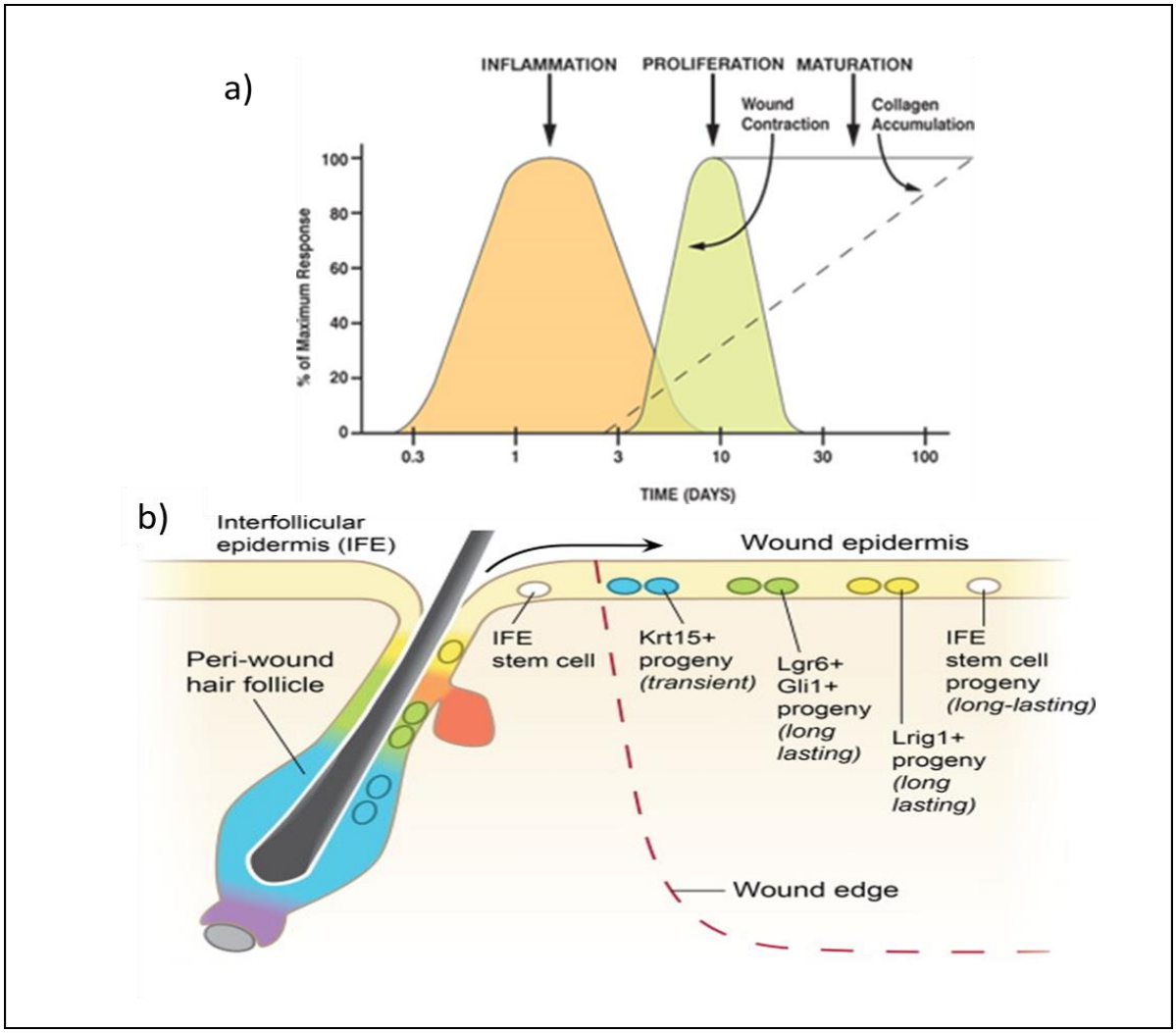

a) Phases of wound healing. b) Contribution of HF stem cells to epidermal healing, markers and key signalling pathways are noted. (Images adapted from Polimeni et al., 2006 and Brownell et al., 2011)

Research Aims

- Determine expression of SWI/SNF chromatin remodelling complex specific subunits composition in human epidermis and hair follicle.

It has previously been demonstrated that SWI/SNF complexes with a specific composition of subunit proteins is capable of regulating cell specific differentiation, with that in mind aim one is to determine if there is a specific SWI/SNF complex at work within human epidermis and hair follicles. Beginning with determining which ATPase subunit is most prevalent, as BRG1 and BRM are mutually exclusive, then to determine if BAF or PBAF complexes are present within the same systems, and if so then determining if there is a specific role for each variant.

- Determine the role (if any) of SWI/SNF complexes in control of human hair growth.

A previous study has linked BRG1, a central subunit of the SWI/SNF complex, with maintaining the hair follicle stem cell reservoir in mice, building on that aim two is to determine if SWI/SNF complexes play a role in regulating human hair follicle growth. This will be investigated by using a siRNA inhibitor to suppress key components of the SWI/SNF complex, and measuring the total growth after transfection, additionally any effect on the rate of anagen-catagen transition between groups will also be investigated.

- Identify the role of SWI/SNF chromatin remodelling complexes in epidermal keratinocyte migration during cutaneous wound healing.

As previously discussed SWI/SNF complexes have a defined role in terminal differentiation of the epidermis, however, there a potential role for SWI/SNF complexes in cutaneous wound healing has not yet been investigated. As such, aim three is to determine if SWI/SNF complexes have a role in cellular migration, proliferation, apoptosis or other associated processes during cutaneous wound healing. The siRNA mediated suppression technique will also be used along with an *ex-vivo* wound healing model to determine any effect the complex has.

2. Materials and Methods

Table 2.1 Donor information

Sample Type	Age/Sex of the donor	Location of sample	Experimental usage
Full thickness Skin	64 Female	Facelift	Ex vivo wounding and IF staining
Full thickness Skin	67 Female	Facelift	Ex vivo wounding and IF staining
Full thickness Skin	69 Female	Facelift	Ex vivo wounding and IF staining
Full thickness Skin	62 Female	Facelift	Keratinocyte isolation and Scratch assay
Full thickness Skin	57 Female	Facelift	Keratinocyte isolation and Scratch assay
Full thickness Skin	65 Female	Facelift	Keratinocyte isolation and Scratch assay
Full thickness Skin	63 Female	Facelift	Keratinocyte isolation and Scratch assay
Follicular Extraction Unit	39 Male	Occipital scalp	RNA isolation and Staining

Follicular Extraction Unit	69 Male	Occipital scalp	RNA isolation and Staining
Follicular Extraction Unit	48 Male	Occipital scalp	RNA isolation and Staining
Follicular Extraction Unit	65 Male	Occipital scalp	RNA isolation and Staining
Follicular Extraction Unit	45 Male	Occipital scalp	RNA isolation and Staining
Follicular Extraction Unit	62 Male	Occipital scalp	RNA isolation and Staining
Follicular Extraction Unit	54 Male	Occipital scalp	SMARCA4 siRNA transfection
Follicular Extraction Unit	35 Male	Occipital scalp	SMARCA4 siRNA transfection
Follicular Extraction Unit	68 Male	Occipital scalp	SMARCA4 siRNA transfection
Follicular Extraction Unit	52 Male	Occipital scalp	SMARCA4 siRNA transfection siRNA
Follicular Extraction Unit	57 Male	Occipital scalp	SMARCC1 /SMARCC2 siRNA transfection

Follicular Extraction Unit	65 Male	Occipital scalp	SMARCC1 /SMARCC2 siRNA transfection
Follicular Extraction Unit	68 Male	Occipital scalp	SMARCC1 /SMARCC2 siRNA transfection
Follicular Extraction Unit	46 Male	Occipital scalp	SMARCC1 /SMARCC2 siRNA transfection
Purchased keratinocytes	Neonatal Male	Foreskin	Scratch assay
Purchased keratinocytes	Neonatal Male	Foreskin	Scratch assay
Purchased keratinocytes	29 Female	Breast	Scratch assay and Transcriptomics
Purchased keratinocytes	29 Female	Breast	Scratch assay and Transcriptomics
Purchased keratinocytes	29 Female	Breast	Scratch assay and Transcriptomics

2.1 Human tissue procurement

All human tissue samples were obtained either as full thickness skin from cosmetic/elective surgery procedures through our ethical tissue department at the University of Bradford, or the excess from follicular unit extraction (FUE) techniques used during hair transplant surgery, directly from the Farjo hair institute (Manchester). A full list of donors/samples can be found in **table 2.1**.

2.1.1 Human tissue preparation

Full thickness human skin tissue samples were either; used directly for *Ex vivo* wounding experiments (described in 2.3.2), or embedded in OCT (optimal cutting temperature compound) and snap frozen using liquid nitrogen, and stored at -80°C until required

FUEs were manually dissected and trimmed of surrounding tissue, and cut at the isthmus/infundibulum boundary with a scalpel blade and either; placed into hair follicle culture media (Williams-E media (Gibco) with 2 mmol/L L-glutamine (Glutamax®), hydrocortisone 10ng/ml, insulin 10 µg/ml, penicillin 100 U/ml, streptomycin 100 µg/ml (hereafter termed HF media)), for transfection experiments (described in 2.2), embedded in OCT and frozen at -80°C, or placed in TRI reagent (Zymo Research #R2050-1-200).

2.2 siRNA mediated transfection of isolated hair follicles

Isolated hair follicles were incubated overnight (at 37°C 5%Co_2) in HF media to assess growth; those which showed evidence of continued growth, defined as new growth beyond the original cut at the isthmus/infundibulum boundary (Langan et al.,

2015), were selected for transfection experiments, hair follicles which showed no growth were excluded.

Transfection was carried out using Accell siRNA, targeting either *SMARCA4* (Dharmacon #E-010431-00-0005), *SMARCC1* (Dharmacon #E-010813-00-0005), *SMARCC2* (Dharmacon #E-010812-00-0005), or non-targeting control (Dharmacon #D-001910-10-05), as directed by the manufacturer's directions. Briefly this involves diluting the siRNA in serum free Williams E media (Gibco # 12551032) supplemented with Hydrocortisone 10ng/ml (w/v) (Sigma-Aldrich #H6909), L-glutamine 10µl/ml (v/v) (ThermoFisher #25030081) and insulin 1µl/ml (v/v) (hereafter referred to as HF2 media). Creating a 1µM final concentration, hair follicles were then grown in siRNA/HF media for 3 days, the media was then changed for HF media for a further 3 days (6 days total). Follicles where then either snap frozen in OCT using liquid nitrogen, and stored at 80°C or placed in TRI reagent until required.

2.3 Partial thickness *Ex Vivo* wound healing model

2.3.1 Twin scalpel laceration tool

A modified scalpel tool was used to create a linear incision (rather than a punch biopsy which is generally used) as a model for the wound (Stojadinovic and Tomic-Canic, 2013), this tool is simply two clean scalpel blades/handles attached securely together (as shown in **figure 2.1**). This tool creates a uniform dual line incision along the length of the tissue and provides a more reproducible partial thickness wounding model.

2.3.2 Partial thickness *Ex vivo* wounding model

Full thickness non-hairy skin samples were obtained from female donors (60's) (refer to **table 2.1**) who had undergone facelift surgery. The sample was then placed in a 50ml falcon tube containing 1x PBS and gently vortexed; this was repeated up to 3 times (to clear any remaining blood from the sample). The skin was then removed from the tube and placed, epidermis down, in a sterile P100 dish containing 5ml 1x PBS and the excess fat trimmed using forceps or scissors, once trimmed the skin was washed again (as previously described). The skin was then placed, dermis down, in a sterile P100 dish containing 5ml, then, using forceps to pin the skin in place, a dual straight line incision was cut into the skin (ensuring that the blades did not cut clean through the epidermis and dermis, but only the dermis) using the twin scalpel blade tool described in 2.3.1, this incision was then removed using scissors or forceps. The skin was then cut into appropriate sizes (~10mm^2) and placed into 24mm transwell inserts, which were then placed into 6 well multiwall plates which contained 2ml of complete DMEM media (Dulbecco's modified eagle media (DMEM) supplemented with sterile 10% FBS, 25nM HEPES, 100 unit/ml penicillin & 100ug/ml streptomycin, 2mM L-glutamine and 100mM sodium pyruvate (all supplied from Gibco), after inserting the transwell inserts to the multiwell plate and additional 1.2ml of DMEM was added to the transwell insert (siRNA transfection solutions (Described in 2.3.3) were added directly to the wound area at this point) and the lid placed on the plate. The wounds were then placed in an incubator (37°C/5%CO_2), and media replaced every 2 days.

Wounds were left for 1, 3, 5 or 7 days, at which point the samples were imaged using a GXCAM-9 camera and GX7 imaging software (GT Vision Ltd) on a Nikon

SMZ1000 steromicroscope, then embedded in OCT, snap frozen in liquid nitrogen and stored at -80°c until needed.

Figure 2.1: Making the twin blade tool

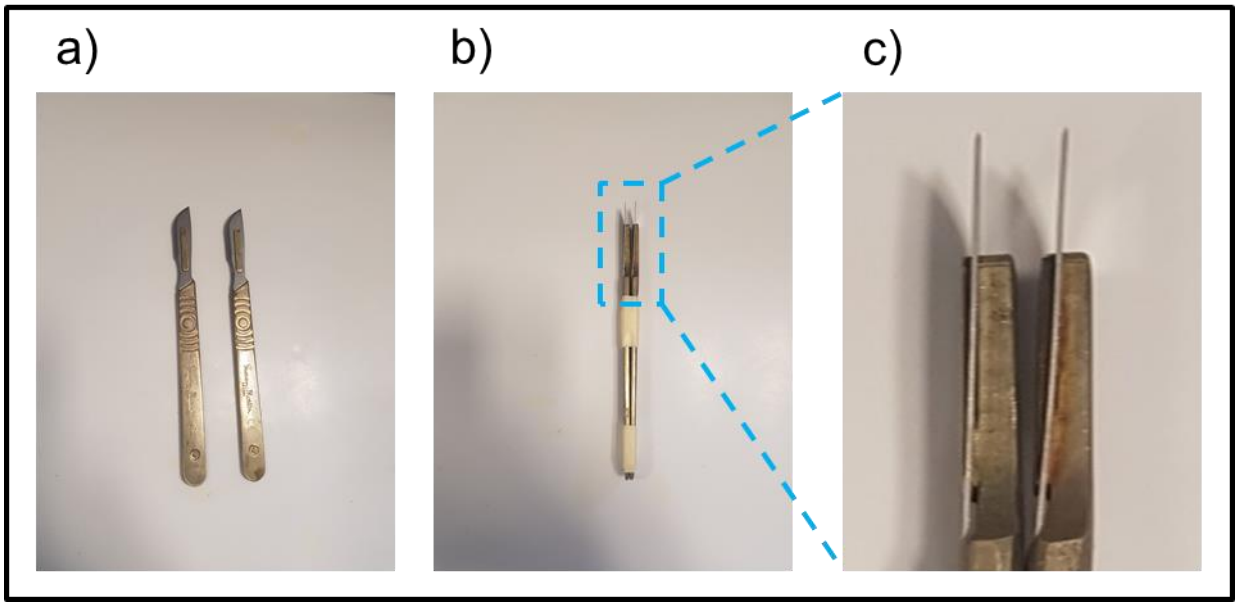

Figure 2.1, a simple twin blade cutting tool created from two scalpel blades taped together to give a uniform dual laceration in the tissue

2.3.3 Transfection of partial thickness *ex-vivo* wounds using lipofectamine™ RNAiMAX

Small interfering RNAs (siRNAs) were used for transient transfection, human SMARTpool: ON-TARGETplus siRNAs directed against *SMARCA4* and a non-targeting control were purchased (Dharmacon L-010431-00-0005 and D-001810-10-05, respectively).

Lipofectamine RNAiMAX/siRNA complexes were prepared as described in the manufacturer's protocol, with the exception that 50 pmol final concentration was used rather than the suggested 25 pmol (preliminary experiments determined that 25 pmol was insufficient). Briefly, this protocol involved preparing the lipofectamine complex, the siRNA complex and then combining them. 250µl of final transfection solution was then added to each well and incubated for 48 hours (37°C/5%CO_2), and media replaced every 2 days.

Transfected partial thickness *ex-vivo* wounds were left for 3, 5 or 7 days at which point the samples were imaged using a GXCAM-9 camera and GX7 imaging software (GT Vision Ltd) on a Nikon SMZ1000 steromicroscope, then embedded in OCT, snap frozen in liquid nitrogen and stored at -80°c until needed.

2.4 Cell culture

2.4.1 Sample preparation

Primary human keratinocytes (PHEKs) were obtained from either full thickness skin donations, or purchased from PromoCell (C-12001 and C-12003), refer to **table 2.1**.

2.4.1.1 Primary isolation of human keratinocytes

The tissue was washed and trimmed as described in 2.3.2 (stopping before the lacerations were made). After trimming the tissue it was submerged in a falcon tube containing 5ml dispase solution (1U/ml) and incubated at 4°C overnight. After incubation the tissue and dispase solution were transferred to a sterile P100 dish and the epidermis separated from the dermis (this was done using forceps to hold the dermis and epidermis and peel them apart). Then the separated epidermis was placed into a falcon tube containing 5ml 1x Trypsin/EDTA (Gibco 25300054) (the separated dermis can be used for isolation of dermal fibroblasts or discarded) and incubated at 37°C for 30 mins, briefly mixing/vortexing every 5 minutes. The trypsin was then neutralised using trypsin neutralising solution (PromoCell #C-41100), the solution was then passed through a 70µm cell strainer into a fresh falcon tube and centrifuged at 180*g* for 5 mins to give a pellet, the pellet was then resuspended in 10ml of complete keratinocyte growth medium 2 (KGM2 (PromoCell #C-20011) supplemented with Bovine Pituitary Extract 0.004 ml/ml, Epidermal Growth Factor (recombinant human) 0.125 ng/ml, Insulin (recombinant human) 5 µg/ml, Hydrocortisone 0.33 µg/ml, Epinephrine 0.39 µg/ml, Transferrin (recombinant human) 10 µg/ml, CaCl2 0.06 mM) and placed in a T75 flask (Corning 430641 and

placed in an incubator (37°C/5%CO_2) ready for use. Media was replaced every 2 days.

2.4.1.2 Purchased primary human keratinocytes

Purchased cells had undergone quality controls and were delivered in cryosolution ready for resuspension. Resuspension of cryopreserved samples was performed by adding 14ml of complete KGM2 media to a T75 flask, then warming the cryopreserved cells in the 37°C water bath (constantly swirling the tube of cells while warming), once fully thawed the cells were added to the 14ml KGM2 media and placed in an incubator (37°C/5% CO_2), media was replaced every 2 days until cells were required.

2.4.2 Splitting cells

Once cultured cells reached <70% confluency they were split, this involved washing cells in 5ml sterile Dulbecco's phosphate buffered saline (DPBS) (Gibco), then adding 3ml of 0.05% trypsin-EDTA solution (Gibco), detached cells were transferred to a 15ml falcon tube containing 3ml trypsin neutralising solution (Gibco). The combined mix was then centrifuged at 200 rcf for 5 mins, the supernatant was removed and the pellet resuspended in 10ml of complete KGM2 media cells were either split at a 1:4 ratio in a new T75 flask containing 12.5ml of complete KGM2 media, or counted and seeded at 3.1 X 10^5 in 6 well plates, with 2ml of complete KGM2 media as required. Passaged cells were returned to the incubator at 37°C/5% CO_2 and media replaced every 2 days.

PHEKs were seeded at 1.2 x 10^5 and cultured in 6 well plates, with 2ml of complete KGM2 media, for transfection, immuno-fluorescent analysis, qRT-PCR analysis and

scratch migration assay experiments. PHEK cells were grown to 60% confluency prior initiating any experiments.

2.4.3 Transfection of cultured cells using lipofectamine™ RNAiMAX

Small interfering RNAs (siRNAs) were used for transient transfection of primary keratinocyte cells (PHEKs), human SMARTpool: ON-TARGETplus siRNAs directed against *SMARCA4* and a non-targeting control were purchased (Dharmacon L-010431-00-0005 and D-001810-10-05, respectively).

Lipofectamine RNAiMAX/siRNA complexes were prepared as described in the manufacturer's protocol, with the exception that 50 pmol final concentration was used rather than the suggested 25 pmol. Briefly, this protocol involved preparing the lipofectamine complex, the siRNA complex and then combining them. 250µl of final transfection solution was then added to each well and incubated for 48 hours, after incubation cells were used for either Immuno-fluorescent analysis, qRT-PCR analysis or scratch mediated wounding assay experiments.

2.7.4 Fluorescent immunocytochemistry

PHEKs were grown in 6 well plates containing sterile 16 X 16mm glass coverslips (Menzel Gläser) and 2ml complete KGM2, cells were seeded at $1.2x10^5$/ml and grown to 60% confluency, then transfected using siRNA (as described in 2.4.3). Media was aspirated from the well and 2ml of 4% paraformaldehyde (v/v) added to each well for 10 mins, paraformaldehyde was then removed and wells were washed with 1xPBS 3 times for 2 mins each. 200µl of primary blocking solution (consisting of 1% bovine serum albumin (BSA) (w/v), 0.01% Triton X-100 (v/v), 0.2% saponin (w/v), in 1x PBS) was added to each coverslip and left to incubate for 10 mins.

Primary antibody (detailed in table 2.1) were combined with primary blocking solution, 300µl of primary antibody mix was then added to each well, plates were then sealed with parafilm and incubated overnight at 4°C.
After incubation primary antibody was removed and wells were washed 3 times with 1xPBS for 5 mins each. Secondary antibodies prepared in 1%BSA/PBS and 200µl was then added to each well, plates were sealed with parafilm and incubated at 37°C for 1 hour, after incubation wells were washed 3 times at 2 mins each with 1xPBS. Vectashield antifade mounting medium with DAPI (Vector Laboratories H-1200) was applied to clean slides; the coverslips were carefully removed from wells using forceps and placed face-down onto the vectashield slides, slides were allowed to dry before sealing with clear nail polish. Slides were stored at +4°C until viewed.

Immuno-fluorescent analysis was carried out as described 2.7.3.

2.4.5 Scratch mediated cell migration assay

Preliminary experiments were carried our without the addition of Mitomycin C, all final experiments were with Mitomycin C treatment.

6 well plates containing siRNA transfected cells, at >85% confluency, were further cultured for 2 hours in 2ml KGM2 10µg/ml mitomycin C. after mitomycin C treatment wells were washed 3 times using 2ml of sterile 1xPBS, after washing 2ml of 1x PBS was added to the wells. Using a sterilised ruler and 1000µl disposable pipette tip, a single vertical scratch was made in each well (Liang et al., 2007). Wells were washed again with 1xPBS and 2ml complete KGM2 media added, wells were then imaged at 1, 24 and 48 hours post scratching, total RNA was also isolated at 1, 24 and 48 hours post scratching.

2.4.6 Scratch mediated cell migration closure rate

Scratch assay wells were observed and imaged using a Nikon TS100 inverted microscope and Act-2u (Excel Technologies) imaging software and Nikon su41 camera. Images taken at 10x (minimum 3 images per well). Analysis of images carried out using ImageJ software, an accurate scale was set and 30 measurements taken per image, statistical analysis carried out using Prism v.6, Mann-Whitney U Test, significance set as P=<0.05.

2.5 RNA extraction and cDNA synthesis

2.5.1 RNA isolation

Total RNA was isolated from either isolated hair follicles (from FUEs or full thickness skin) or PHEK cell culture. Hair follicles were collected in 300µl of TRI reagent and mechanically homogenised using a mortar and pestle homogeniser (ThermoFisher #11522443). Cell culture isolates did not require homogenisation and were simply lysed in TRI reagent.

RNA isolation was carried out using the ZymoBIOMICS RNA miniprep kit (Zymo Research #R2001, following the manufacturer's protocol. In summary this involved adding an equal volume of absolute ethanol to the TRI reagent/tissue homogenate (ThermoFisher #10517694) and mixing thoroughly. This mix was then transferred to a Zymo-Spin^{TM} column and centrifuged (all centrifugations were done at 13,000 x *g* and flow through discarded unless stated otherwise); 400µl RNA wash buffer was then added centrifuged for 1 min. The additional DNase digestion step was performed by adding the DNase mix (5µl DNase I and 75µl DNA digestion buffer) directly to the column membrane and incubated at RT for 15mins. After incubation

400µl of RNA prewash buffer was added and centrifuged, followed by 700µl RNA wash buffer and centrifuged for 2 mins, centrifuged again (to ensure all liquid has passed from the membrane tube to the collection tube), the collection tube was then discarded and a clean RNase free collection tube added to the column. To elute RNA 30µl of nuclease free water was added directly to the membrane and centrifuged, the membrane column was then discarded.

RNA concentration and purity measured using an Implen P330 nonophotometer, any samples not falling within >1.8 to <2.0 280/260 and 230/260 wavelength absorption were rejected, RNA was then stored at -80°C until required.

2.5.2 cDNA synthesis

cDNA synthesis was performed using the qPCRBIO cDNA synthesis kit (PCR Biosystems #PB30.11-02) following the manufacturer's protocol. Briefly, this used 100ng of isolated total RNA (obtained as described in 2.5.1), which was added to 4µl of 5x cDNA synthesis mix and 1µl of RTase and brought up to a total volume of 20µl using PCR grade nuclease free water. cDNA was then synthesised using an Eppendorf® Mastercycler® Nexus thermal cycler (Eppendorf #EP6331000025) and Incubated at 42°C for 30 minutes, then 85°C for 10 minutes. Synthesised cDNA was then stored at -20°C until required.

2.6 RT-qPCR

The qPCR mastermix was prepared as follows:-

Reagent	Volume
qPCRBIO SyGreen mix Hi-ROX (PCR Biosystems #PB20.12-01)	5µl
Primer mix (forward and reverse) 5µM	2µl
cDNA	0.5µl
Nuclease free water	2.5µl

qPCR mastermixes were loaded into 96 well plates and centrifuged at 4000rpm for 5 mins.

qPCR carried out using a StepOnePlus real time PCR machine from applied Biosystems, and programmed using the StepOne software v2.1, 'FAST' functions, programme was set to 95°C for 2 minutes, then 40 cycles of 95°C for 10 seconds, 30 seconds of the required annealing temp (table 2.1) and 72°C for 30 secs, finally after cycling a final elongation of 72°C for 5 mins. For all genes of interest RT-qPCR was performed in triplicate, melt curve analysis was carried out to ensure the validity of target amplification. Delta CT values were collated and relative expression levels of target genes generated with GAPDH used as housekeeping. cDNA synthesised from total human reference RNA (Clontech #636690) was used as a positive control,

total RNA was used as a negative control, finally all primers pairs were created to cross an intron/exon boundary on either the forward or reverse (**table 2.2**).

Table 2.2 List of primers used in qRT-PCR

Gene	Sequence	Annealing temp
SMARCA4/BRG1	FW: AACAACCTGAACGGCATCCT RV: CCAGTTGGACAGCGTTGAGA	63
SMARCA2/BRM	FW: GAGCCCGAGTTTAGGAAGAGG RV: CAGTCAGTAGAGTAATGCTTGC	63
PBRM1/BAF180	FW: AGCCATCACCTTTGCTGGAA RV: LCTTTGGGGTAGACTGTGGGG	63
ARID1a/BAF250a	FW: CGGGGATGTATTCTCCTAGCC RV: TGGCCGCTTGTAATTCTGCT	62
ARID1b/BAF250b	FW: GAAATATGAGCAGCATGACCCC RV: AAACTGCCTTGCCTGCTTTG	62
ARID2/BAF200	FW: CACCACAGCAGAGGGTCG RV: TTCGCGAATCCGCCTAAAGT	62
SMARCC1/BAF155	FW: AAATGAACAGGGATGGCGGA RV: GAGGTAGATGTTGGGTCTGGTC	63

SMARCC2/BAF170	FW: ATGACCGACCTGGATGAACAG RV: GGGAATGATGATGTGGTGGGT	63
SMARCB1/INI5/BAF47	FW: GGACCAGTTTGAGTGGGACA RV: GGTTCTCGCTGAAGGCGTAG	63
K16	FW: TATTCTTCCCGCGAGGTCTT RV: GTGGTAGAGGCAGCTCAGTT	63
K17	FW: ATCCTGCTGGATGTGAAGACG RV: GGTGGTCACCGGTTCTTTCTT	62
GAPDH	FW: TTGAGGTCAATGAAGGGGTC RV: GAAGGTGAAGGTGGGAGTC	62
RUNX1	FW: CTGCCCATCGCTTTCAAGGT RV: GCCGAGTAGTTTTCATCATTGCC	62
CXCR2	FW: CCTGTCTTACTTTTCCGAAGGAC RV: TTGCTGTATTGTTGCCCATGT	62
CXCL3	FW: CGCCCAAACCGAAGTCATAG RV: GCTCCCCTTGTTCAGTATCTTTT	62

MMP7	FW: GAGTGAGCTACAGTGGGAACA RV: CTATGACGCGGGAGTTTAACAT	62
SERPINA3	FW: TGCCAGCGCACTCTTCATC RV: TGTCGTTCAGGTTATAGTCCCTC	62
KRT80	FW: CCTCCCTAATTGGCAAGGTG RV: AGATGCCCGAGGTCGAAGAT	62
WNT4	FW: GTACGCCATCTCTTCGGCAG RV:GCGATGTTGTCAGAGCATCCT	62
KLF4	FW:CCCACATGAAGCGACTTCCC RV:CAGGTCCAGGAGATCGTTGAA	62
SNAI1	FW:TCGGAAGCCTAACTACAGCGA RV:AGATGAGCATTGGCAGCGAG	62
CDK1	FW:AAACTACAGGTCAAGTGGTAGCC RV:TCCTGCATAAGCACATCCTGA	62

All primers were designed by myself using primer BLAST (Ye et al., 2012) and purchased from Sigma-Aldrich

2.7 Fluorescent Immunohistochemistry

2.6.1 Sample preparation

Embedded skin and hair follicle samples were cut using the cryostat microme HM550 (Thermofisher) set to -33°C for hairy skin or -30°C for hair follicles, sections were cut at a thickness of 8µm and collected onto adhesive SuperFrost Plus slides (VWR international, Cat, No: 631-0447) and stored at -80^{o} until needed.

2.7.2 Immuno-fluorescence staining procedure

Prepared slides were selected from the freezer and allowed to air dry for 10 min at room temperature (RT), once dry samples were then encircled with a PAP pen (Vector Labs H-4000). The tissue was fixed using 4% paraformaldehyde/PBS (v/v) for 10 mins at RT in a coplin jar. Slides were then washed 3 times for 5 mins each in 1x PBS. 100µl of primary blocking solution (consisting of 1% bovine serum albumin (BSA) (w/v), 0.01% Triton X-100 (v/v), 0.2% saponin (w/v), in 1x PBS) was then added to each section and left to incubate for 1 hour. Primary antibodies were prepared using primary blocking solution (as detailed in table 2.3) and 100µl of primary antibody mix added to each section, slides were then incubated overnight at +4°C in a humidified chamber.

After incubation slides were washed in 1xPBS 3 times for 5 mins. The secondary antibody was prepared using 1% BSA/PBS, and 100µl of the secondary antibody mix was then added to each section and incubated at 37°C for 1 hour, after incubation slides were washed again (3x 5 mins) in 1xPBS. Sections were mounted using Vectashield antifade mounting medium with DAPI (Vector Laboratories H-

1200) and coverslips added before sealing using clear nail polish. Slides were then stored at +4°C until needed.

To ensure the validity, a control experiment was carried out for each secondary antibody, where no primary antibody was added to sections. All primary antibodies were validated by knockout studies by the manufacturer.

Table 2.2: Antibody table

Primary Antibody	**Dilution**	**Origin**
Mouse Anti-BRG1	1:50	Santa Cruz (sc-17796)
Rabbit Anti-BRM	1:400	Abcam (ab15587)
Rabbit Anti-BAF155	1:400	Santa Cruz (sc-10756)
Rabbit Anti-Ini1 (BAF47)	1:400	Santa Cruz (sc-13055)
Rabbit Anti-Ki67	1:100	Abcam (ab15580)
Rabbit Anti active caspase 3	1:100	Abcam (ab2302)
Secondary Antibody	**Dilution**	**Origin**
Donkey anti-rabbit Alexa-Fluor 555	1:200	Life Technologies (A31572)
Goat Anti-mouse Alexa-Fluor 555	1:200	Life Technologies (A11001)

2.7.3 Fluorescence microscopy

Immunofluorescence staining was observed and imaged using a Nikon Eclipse 50i, fluorescent microscope, and image analysis software (image pro express 9.1, Media Cybernetics), using an Qimaging EXI aqua camera.

2.7.4 Pair wise comparison of signal intensity of fluorescence images using ImageJ

A semi-quantitative technique allowing for a comparison of signal intensity between cells/regions of an image was utilised with various immunofluorescence stained slides (McCloy et al., 2014). This technique involves measuring the intensity of target signal from cells/regions and subtracting the background value to give a corrected total cell fluorescence (CTCF) value, using the following calculation:-
CTCF = integrated intensity – (area of cell or region X mean fluorescence of background)

2.7.5 Haematoxylin and Alkaline phosphatase staining

Solutions were prepared immediately before carrying out alkaline phosphatase (AP) staining.

Solution A: 30mM Tris base, 7mM TrisHCL, 100mM NaCl in 1x PBS

Solution B: 4M sodium Natrite, 4mM new Fuchsin

Solution C: 600mM of Naphthol dissolved in DiMethylformamide

AP staining was carried out as previously described (Lewis et al., 2014, Sharov et al., 2006). First prepared slides were selected from the freezer and left to air dry for 10 mins at RT; slides were then fixed in acetone at -20°C for 10 mins. Slides were then washed for 3 mins in 1x PBS. While slides were being washed solution A and B were mixed in a Coplin jar, solution C was then added, generating the AP solution. Once washed slides were placed in the AP solution for 15 mins, then washed again in 1x PBS for 5 mins. Haematoxylin was then added to each slide for approximately 60 seconds; the slides were then placed in an empty coplin jar and washed under cold running water for 5 mins. Slides were then sealed with mounting medium and sealed with clear nail polish.

2.7.6 Brightfield microscopy

Slides were visualised and imaged using a Nikon Eclispe 50i microscope and image analysis software (image pro express 9.1, Media Cybernetics) using a moticam 5+ camera

2.7.7 Analysis of SWI/SNF subunit protein levels in ex vivo wounds

Fluorescent images of 3, 5, and 7 days post wounding skin were stained for BRG1. The relative expression levels of BRG1 were obtained and compared between the wound associated cells and the distal epidermis using the semi-quantitative technique described in 2.7.4. Mann-Whitney U test was used to determine any possible significance as the data was non parametric.

2.7.8 Analysis of efficient *ex vivo* wound healing

Brightfield images of the *ex vivo* wounds were processed and analysed using ImageJ software (NIH), the wound edges were measured for both length and area, from the start of the wound to the leading edge of the epithelial tongue. The mean length and area were generated from 3 donors, at 2 different time points (3, and 5 days) and compared between control siRNA treated or SMARCA4 siRNA treated wound tissue. Students T-test was performed to identify any significance.

2.7.9 Analysis of proliferation and apoptosis in ex vivo wounds

Fluorescent images of day 3, 5 and 7 post wounding skin were stained for Ki67 (a proliferation marker) and analysed using ImageJ software, counting the total number of cells and the total number of Ki67 strongly positive cells. Three time points from each donor and treatment group (*SMARCA4* or control) were analysed. Mean percentage of Ki67 positive cells were obtained and Students T-test used to compare any possible significance.

The same was carried out for active caspase 3 (an apoptosis marker).

2.7.10 Analysis of proliferation and apoptosis in Hair follicles

Fluorescent images of cryosectioned hair follicles were stained for Ki-67 (a proliferation marker) and analysed using ImageJ software, counting the total number of cells in the outer root sheath or the matrix region and the total number of Ki-67 strongly positive cells in the same regions. At least 12 follicles from each donor and treatment group (*SMARCA4*, SMARCC1/*SMARCC2* or control) were analysed.

Mean percentage of Ki-67 positive cells were obtained and Students T-test used to compare any possible significance.

The same was carried out for active caspase 3 (an apoptosis marker).

2.8 Microarray data

2.8.1. Sample preparation

RNA samples were obtained from siRNA transfected primary human epidermal keratinocytes (as described in 2.4.3) and frozen at -80°C until needed.

All reagents utilised were provide as part of the Agilent One-Color RNA spike-in kit (5188-5282) of the Agilent Hybridisation Kit (5188-5242)

2.8.1. Colour spike in

The one-colour spike mix stock was heated to 37°C, vortexed and briefly centrifuged, and diluted as per manufacturer's directions. Next the labelling reaction was prepared as directed in **Table 2.3**; the mix was then heated to 65°C for 10 mins, then immediately chilled on ice for 5 mins, and finally mixed with cDNA master mix (detailed in **Table 2.4**). the combined colour spike and cRNA master mix was then incubated at 40°C for 2 hours, then 65°C for 15 mins and then chilled on ice for 5 mins; the chilled samples were then added to 60ul of transcription master mix (detailed in **Table 2.5**) and incubated at 40°C for 2 hours. Samples were stored at -80°C until needed or used immediately for cRNA purification.

2.8.2. cRNA purification

cRNA was purified using the Qiagen RNeasy mini kit (Qiagen #74104).

20µl of nuclease free water was added to each cRNA sample (bringing final volume to 100µl), 350µl of buffer RLT was then added and mixed by pipetting/vortexing. Once mixed 250µl of molecular biology grade 100% ethanol was added and mixed by pipetting, the whole volume (700µl) was then transferred to an RNeasy mini column and collection tube and centrifuged at 13,000 rpm for 30 secs. The flow through and collection tube was discarded and the mini column placed into a new collection tube. 500µl RPE buffer was then added and the samples spun again for 30 secs at 13,000 rpm, the flow through was discarded and this step repeated. The samples were then spun for 1 min at 13,000 rpm (to ensure all liquid was removed), the collection tube was then discarded and the mini column transferred to a clean 1.5ml collection tube with a lid. 25µl of nuclease free water was added (to elute the cRNA) and incubated for 1 min before being spun at 13,000 rpm for 30 secs. The mini column was discarded and the eluted cRNA kept in the dark. Quantification was then completed using a nanodrop 1000 spectrophotometer, a spike in efficiency formula ($\frac{concentration\ of\ Cy3}{Concentration\ of\ cRNA}$ X 1000 = pmol Cy3 per µg cRNA) was applied and any samples scoring less than 1 (the efficiency threshold) were excluded. Samples were stored at -80°C or used directly for hybridisation.

2.8.3. Hybridisation

Hybridisation mix was prepared as detailed in **Table 2.6**, and gently mixed, samples were then incubated for 30 mins at 60°C to fragment RNA, then immediately chilled on ice for 1 min. 25µl of 2x GEx Hybridization Buffer HI-RPM was added to stop the

fragmentation reaction and carefully mixed by pipetting (avoiding introducing bubbles), the samples were then centrifuged at 13,000 rpm for 1 min and placed on ice while the hybridisation chamber was prepared.

A gasket slide was loaded into the Agilent sureHyb chamber base and aligned as directed by the manufacturer, and 40µl of hybridisation sample was added to each gasket section. The array was slowly placed over the gasket slide and the Agilent SureHyb chamber was sandwiched and sealed as directed by the manufacturer. The chamber was then placed in a rotisserie hybridisation oven at 65°C for 17 hours.

After hybridisation slides were washed with GE wash buffer (provided in the kit) for 1 min at room temp, then washed again with GE wash buffer for 1 min at 37°C, and finally in acetonitrile (room temp) for 10 secs.

2.8.4. Scanning and analysis

Hybridised slides were scanned using an Agilent microarray scanner; features were extracted using the Agilent feature extraction software.

Features were then analysed using GeneSpring GX software (Agilent), and analysis confirmed using Galaxy open source bioinformatics platform.

Differential expression of genes was obtained and analysed using DAVID GO term enrichment analysis.

Table 2.3 Labelling reaction

Component	Volume (per reaction)
Nuclease free water	Make up to 8.3ul total volume
Spike-mix 3rd dilution (made per manufacturer's direction)	2.0µl
T7 promoter primer	1.2µl
RNA volume	200ng total

Table 2.4 cDNA master mix

Component	Volume (Per reaction)
5x First strand buffer	4µl
0.1M DTT	2µl
10mM dNTP mix	1µl
MMLV-RT	1µl
RNaseOUT	0.5µl
Final volume	8.5µl

Must be added in order

Table 2.5 Transcription master mix

component	Volume (Per reaction)
Nuclease free water	15.3µl
4x Transcription buffer	20µl
0.1M DTT	6µl
50% PEG	6.4µl
RNaseOUT	0.5µl
Inorganic pyrophosphatase	0.6µl
T7 RNA polymerase	0.8µl
Cyanine 3-CTP	2.4µl
Total volume	60µl

Table 2.6 Hybridisation mix

Component	Volume (per reaction)
Cyanine 3-labeled cRNA	600ng
Nuclease free water	Make cRNA volume up to 19µl
10x blocking agent	5µl
25x fragmentation buffer	1µl
Total volume	25µl

3. Results

3.1 SWI/SNF complexes modulates the balance between cell proliferation and differentiation in the human hair follicle.

3.1.1 Cell-type specific composition of SWI/SNF complexes in different human hair follicle compartments.

SWI/SNF chromatin remodelling complexes contain either BRG1 or BRM as the core ATPase (Kadoch et al., 2016, Kadoch and Crabtree, 2015). To determine the potential roles of these ATPases in human hair follicle biology, first the expression level of the SWI/SNF core subunits were analysed on the mRNA and protein level in the whole hair follicles.

RT-qPCR analysis of the total mRNA isolated from whole hair follicles indicated a much higher expression level of BRG1 in comparison to BRM (**Fig 3.1a**). Furthermore, immuno-fluorescent analysis showed that both BRG1 and BRM proteins are expressed in the hair follicle, although, with slightly different expression patterns (**Fig 3.1b and c**). High level of BRG1 expression was observed in the bulb region as well as the inner and outer root sheaths, but undetectable in the dermal papilla and connective tissue sheath, while BRM protein was present in the dermal papilla and connective tissue sheath.

Next, The expression of additional SWI/SNF subunits: *SMARCB1*/BAF47, *SMARCC1*/BAF155, and *SMARCC2*/BAF170 were investigated. These subunits are required for complex stability, preventing protein degradation as well as providing molecular scaffolding for additional subunits to incorporate into the SWI/SNF complex (DelBove et al., 2011) .

SMARCB1/BAF47 has a lower mRNA expression level than *SMARCC1*/BAF155 and *SMARCC2*/BAF170, as well as a vastly different protein expression pattern to *SMARCC1*. Interestingly, BAF47 protein is expressed in the pre-cortex region of the hair bulb and not the matrix, as is seen with other subunits, including BAF155, which has a similar expression pattern to BRG1 (**Figures 3.1b, 3.2c**).

Human SWI/SNF complexes have 2 common variants, BAF and PBAF, each containing unique subunits in addition to the common ones (Hodges et al., 2016, Yan et al., 2005). I further analysed the presence of these subunits to determine if one or both SWI/SNF complex types are present in the human hair follicle cells.

Expression of both BAF and PBAF complex specific subunits were detected at the mRNA level (**Fig 3.3**).

In summary these data indicate specific expression patterns for specific SWI/SNF subunits and the presence of both BAF and PBAF variants in human hair follicles, which could suggest different roles for specific SWI/SNF complexes within hair follicle cell sub-populations. As BRG1 was established as the abundant ATPase core subunit and knowing that both BAF and PBAF complexes are present within the hair follicle supressing BRG1 would effectively suppress both BAF and PBAF variants of SWI/SNF complex in human hair follicles.

Figure 3.1 Expression of the SWI/SNF ATPase subunits in the human hair follicle

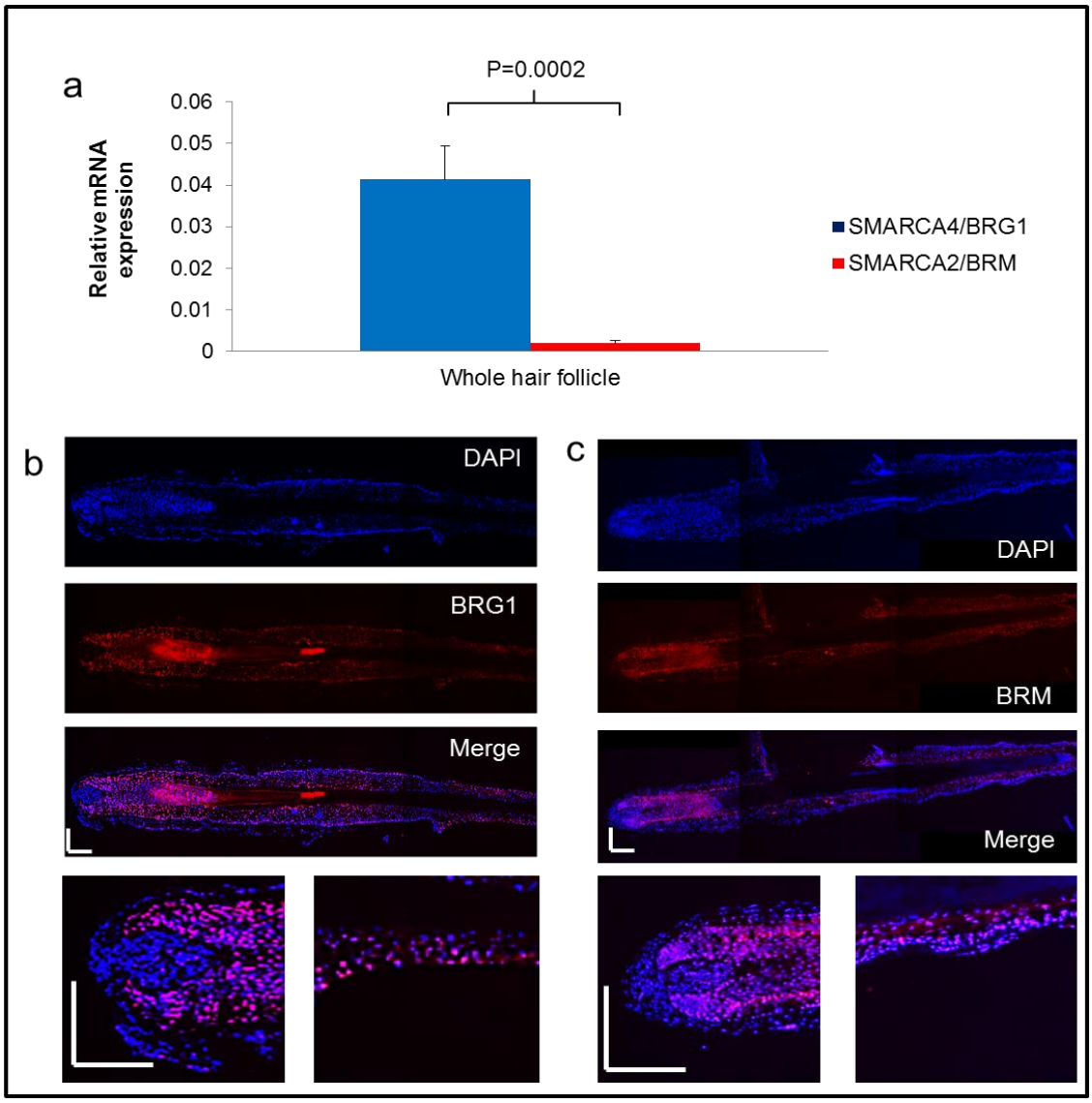

(a) RT-qPCR analysis of *SMARCA4*/BRG1 and *SMARCA2*/BRM expression using RNA isolated from the whole hair follicle normalised to *GAPDH*. >5 follicles per donor, 6 donors per gene, and 3 replicates per gene, Mean mRNA expression and ± standard deviation are shown, p=0.0002, Student's T-Test. Immunostaining of (b) BRG1 protein, and (c) BRM protein expression in human hair follicles counterstained with DAPI, representative of 6 male donors between the age of 39 and 69, mean age 54. Images taken at 100x magnification and stitched, expanded images at 200x magnification, Scale bars = 100µm.

Figure 3.2 Expression of SWI/SNF core subunits in human hair follicles

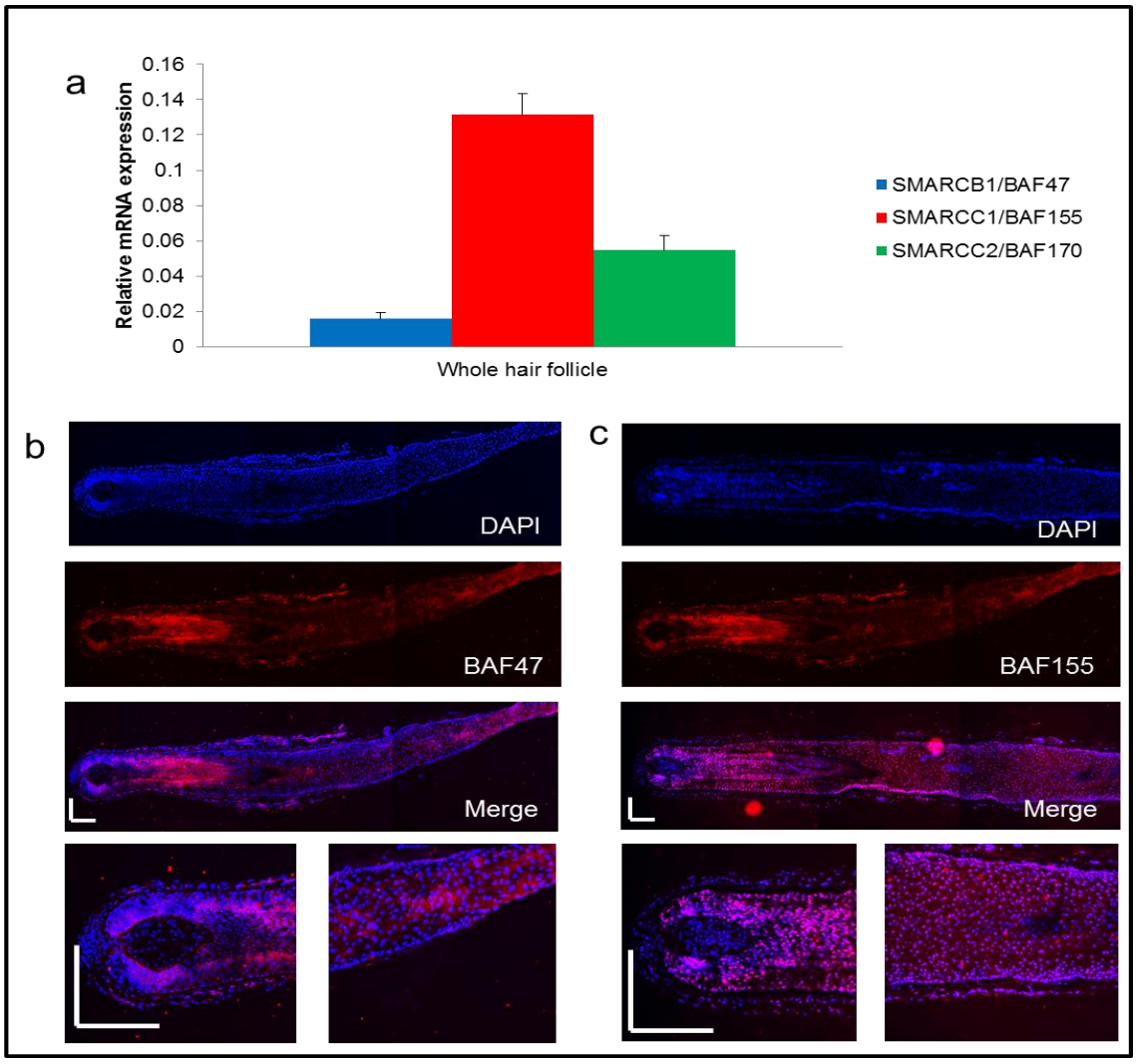

(a) RT-qPCR analysis of *SMARCB1*/BAF47, *SMARCC1*/BAF155 and *SMARCC2*/BAF170 expression using RNA isolated from the whole hair follicle normalised to *GAPDH*. >5 follicles per donor, 6 donors per gene, and 3 replicates per gene, Mean mRNA expression and standard deviation are shown, Student's T-Test. Immunostaining of (b) BAF47 protein, and (c) BAF155 protein expression in human hair follicles, representative of 6 male donors between the age of 39 and 69, mean age 54. Images taken at 100x magnification and stitched, expanded images at 200x magnification, Scale bars = 100µm.

Figure 3.3 Expression of the mRNA encoding BAF and PBAF specific subunits in human hair follicles

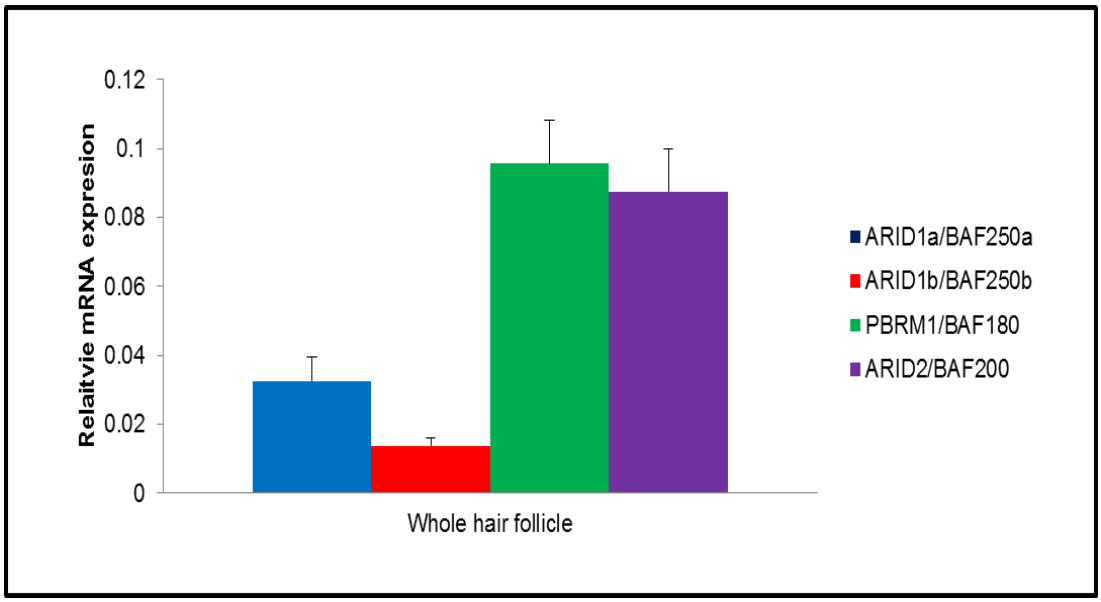

RT-qPCR analysis of *ARID1a*/BAF250a, *ARID1b*/BAF250b, *and PBRM*/BAF180 and *ARID2*/BAF200 expression using RNA isolated from the whole hair follicle normalised to *GAPDH*. >5 follicles per donor, 6 donors per gene, and 3 replicates per gene, Mean mRNA expression and ± standard deviation are shown.

3.1.2 SWI/SNF complexes control the cell proliferation in the outer root sheath, but not in hair matrix and are not essential for the short term sustaining of the human hair growth.

As this data revealed that BRG1, but not BRM is predominantly expressed in the human hair follicle epithelium (**Fig. 3.1a**) it was selected as a suppression target to reveal the role of the SWI/SNF complex in the control of cell proliferation, differentiation and hair growth in the human hair follicle. The Accell siRNA technology was selected as to facilitate the suppression of *SMARCA4*/BRG1, The initial penetration tests indicated that it would serve as to efficiently deliver siRNA to the deeper parts of the whole hair follicles (**Fig 3.4a**).

Treatment of human hair follicles in an *ex vivo* culture with *SMARCA4*/BRG1 siRNA resulted in significant reduction of BRG1 protein within 3 days (**Fig 3.4b-d**). The amount of hair growth of the *ex vivo* culture after the siRNA mediated BRG1 suppression. This data indicated no significant changes in the hair shaft growth or anagen-catagen transition between control and BRG1 knockdown follicles (**Fig. 3.5**), suggesting that BRG1 is not required for sustaining anagen or for promoting hair growth, at least in short term *ex vivo* hair follicle culture.

To determine, if BRG1 suppression could potentially lead to the longer term changes in the human hair growth, the analysis of cellular proliferation using immuno-fluorescent staining of the hair follicles with Ki-67 antibodies after treatment with the control or SMARCA4 siRNA. Surprisingly This analysis revealed a significant increase in the outer root sheath cell proliferation, while no significant changes in hair matrix cell proliferation has been observed (**Fig. 3.6**).

To further validate that these findings reflect the functional significance of SWI/SNF complex in control of the outer root sheath cell proliferation, the same analyses were repeated after using the Accell siRNA mediated suppression of *SMARCC1*/BAF155 and *SMACC2*/BAF170. Studies using mouse models have previously demonstrated that loss of BAF155 and BAF170 results in a loss of SWI/SNF functionality. My analyses shown that siRNA mediated depletion of BAF155 and BAF170 (**Fig. 3.7**) does not affect hair growth in short term hair follicle culture ex vivo, and leads to the significant increase in the outer root sheath, but not hair matrix cell proliferation (**Fig 3.8, 3.9**).

In summary, these data demonstrated that in the human hair follicle during the anagen phase of hair cycle SWI/SNF complex controls the cellular proliferation in the outer root sheath, but is not essential for the anagen sustaining and hair shaft growth, at least in the short term.

Figure 3.4 Effective siRNA mediated suppression of BRG1 in the human hair follicle culture ex vivo

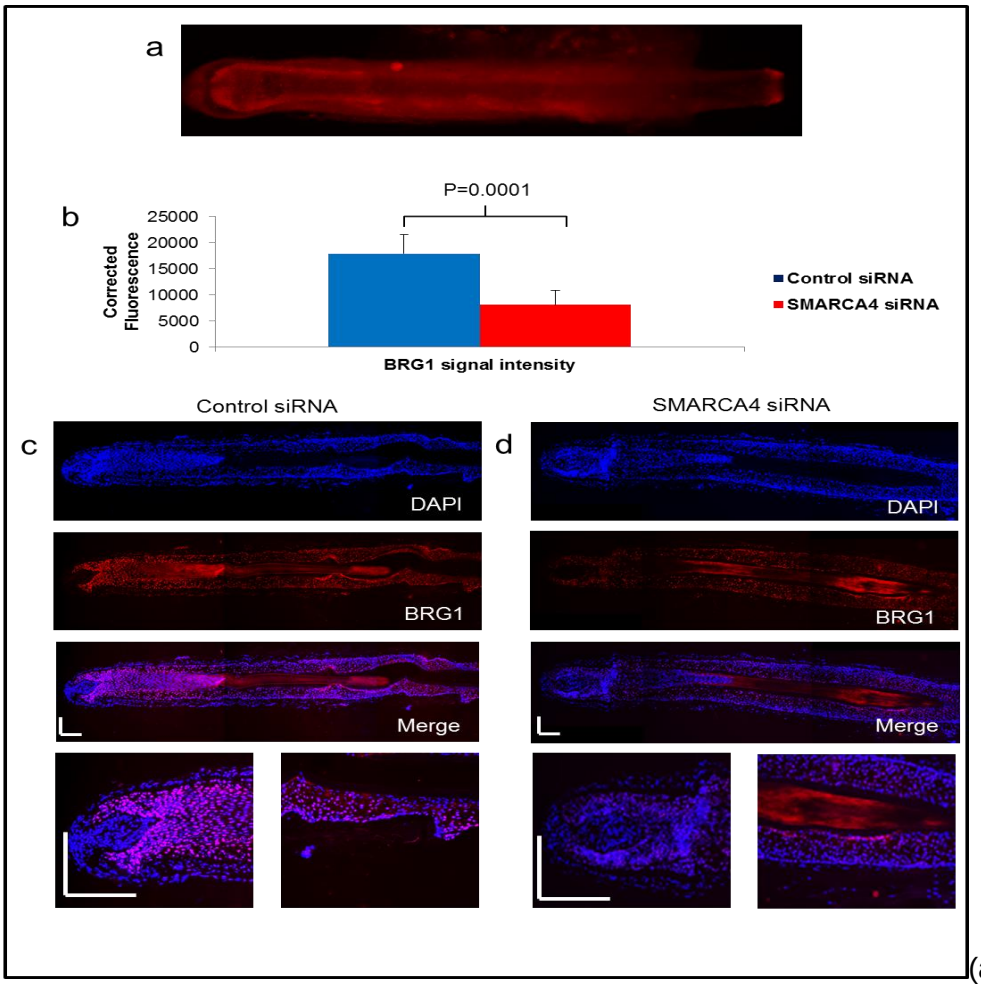

(a)

Validation of the Accell siRNA technology using the Accell human control siRNA kit – red, Demonstrates an efficient penetration and delivery of siRNA into difficult to transfect tissues. b) Relative corrected fluorescence comparing BRG1 protein signal intensity between control and BRG1 knockdown follicles. >5 follicles per donor, 4 donors per group (Control/Treated), and 20 measurements per follicle. Mean signal intensity and ± standard deviation are shown. Mann-Whitney U test. Immunostaining of of BRG1 protein expression in human hair follicles treated with (c) control siRNA or (d) *SMARCA4* siRNA, representative of 4 male donors between the age of 35 and 68, mean age 55. Images taken at 100x magnification and stitched, expanded images at 200x magnification, Scale bars = 100µm.

Figure 3.5 Suppression of BRG1 in human hair follicles has no effect on short term growth, or anagen-catagen transition

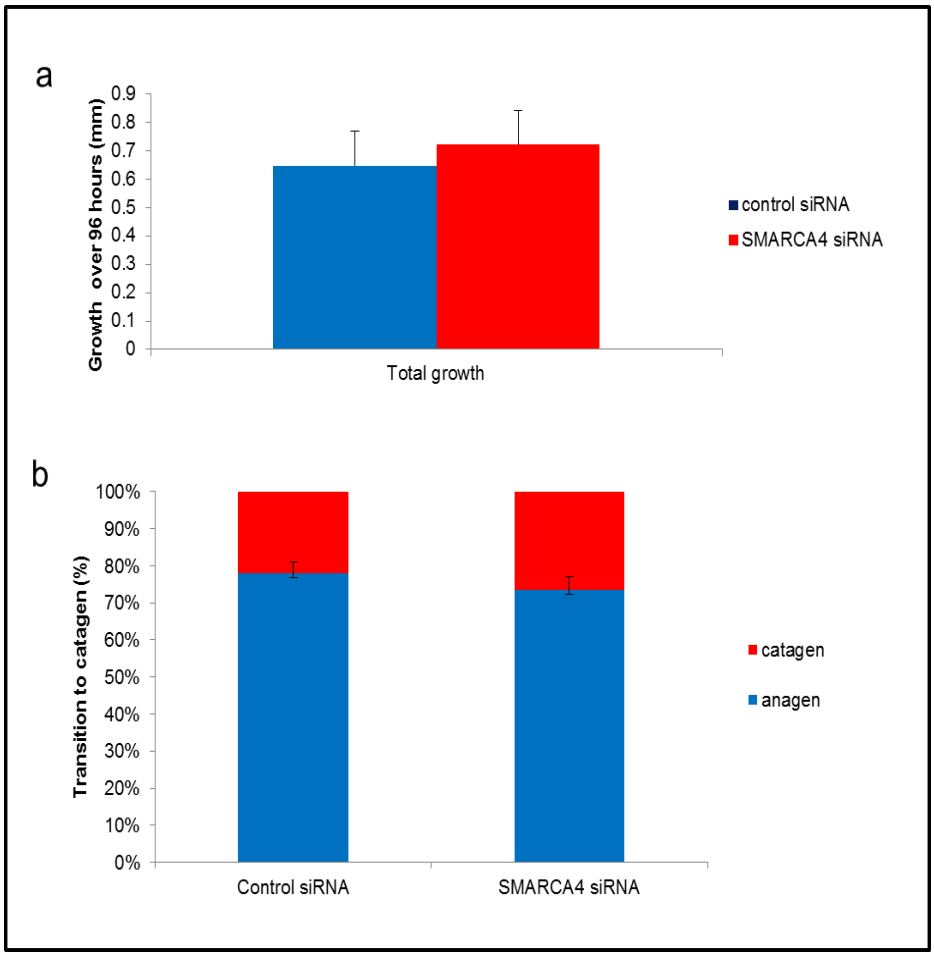

(a) Average hair follicle growth over 96 hours post transfection with either control siRNA or *SMARCA4* siRNA treated hair follicles. >12 follicles per donor, 4 donors per group (Control/Treated), Mean total growth and ± standard deviation are shown, Student's T-Test. b) number of follicles which transitioned into Catagen phase during the experiment. >12 follicles per donor, 4 donors per group (treated/control), Mean percentage of anagen-catagen transitions and standard deviation are shown, Student's T-Test, representative of 4 male donors between the age of 35 and 68, mean age 55

Figure 3.6 Suppression of BRG1 in human hair follicles increases proliferation in the ORS but not the matrix region

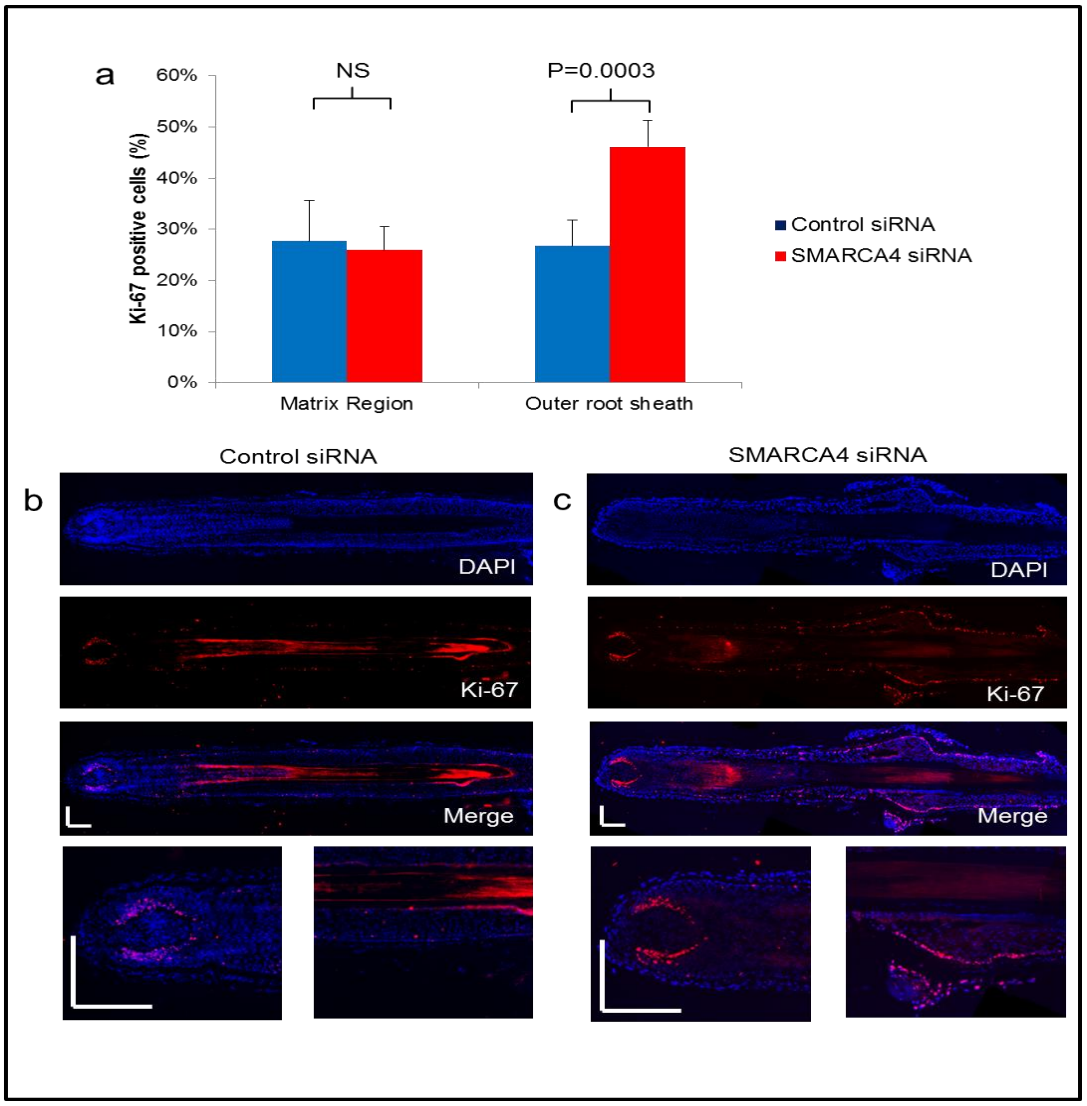

(a) Percentage of Ki-67 positive cells (positive cells/total cells in region) in matrix region and the outer root sheath; comparing control siRNA and *SMARCA4* siRNA treated hair follicles. >12 follicles per donor, 4 donors per group (Control/Treated), Mean Ki-67 positive percentage (%) and ± standard deviation are shown, Student's T-Test. Immunostaining of Ki-67 protein expression in human hair follicles treated with (b) control siRNA or (c) SMARCA4 siRNA, representative of 4 male donors between the age of 35 and 68, mean age 55. Images taken at 100x magnification and stitched, expanded images at 200x magnification, Scale bars = 100µm.

Figure 3.7 Effective siRNA mediated suppression of BAF155 and BAF170 in the human hair follicle culture ex vivo.

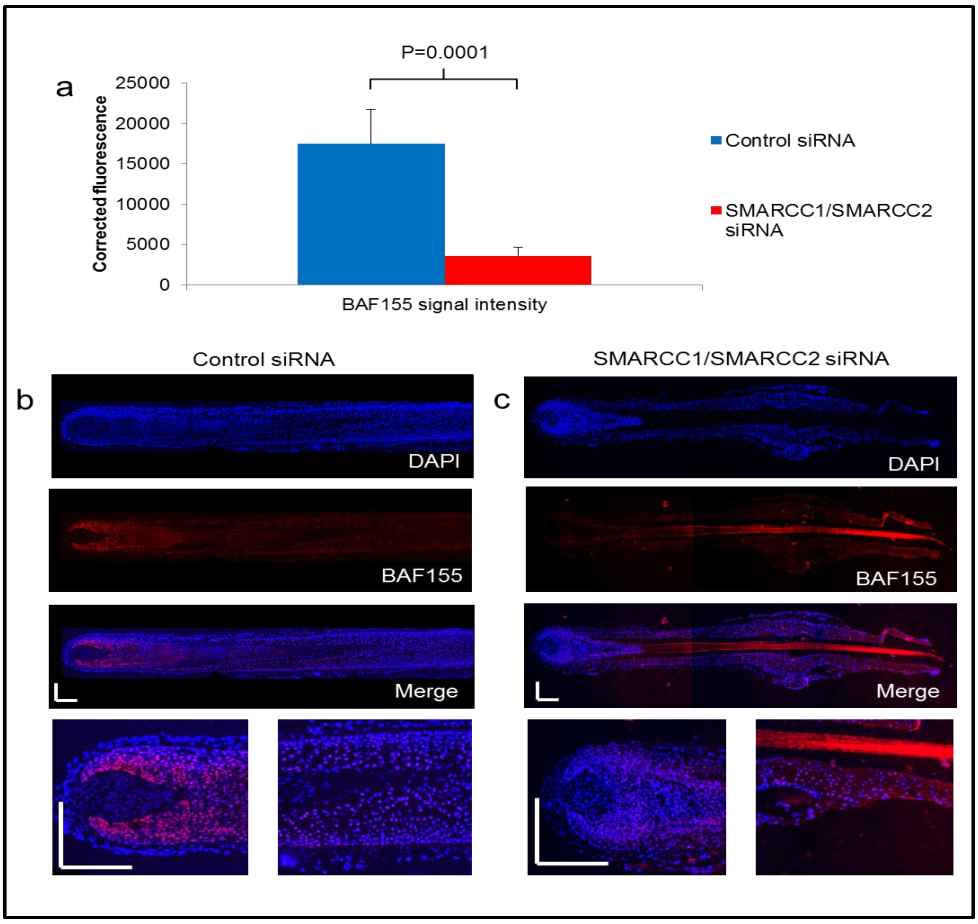

(a) Relative corrected fluorescence comparing BAF155 protein signal in control siRNA treated and SMARCC1/SMARCC2 siRNA treated human hair follicles. >12 follicles per donor, 4 donors per group (Control/Treated), and 20 measurements per follicle, Mean corrected fluorescence value and ± standard deviation is shown, Mann-Whitney U Test. Immunostaining of BAF155 protein expression in human hair follicles treated with (b) control siRNA or (c) SMARCC1/SMARCC2 siRNA (c), representative of 4 male donors between the age of 46 and 65, mean age 56. Images taken at 100x magnification and stitched, expanded images at 200x magnification, Scale bars = 100µm.

Figure 3.8 Suppression of BRG1 in human hair follicles has no effect on short term growth, or anagen Catagen transition

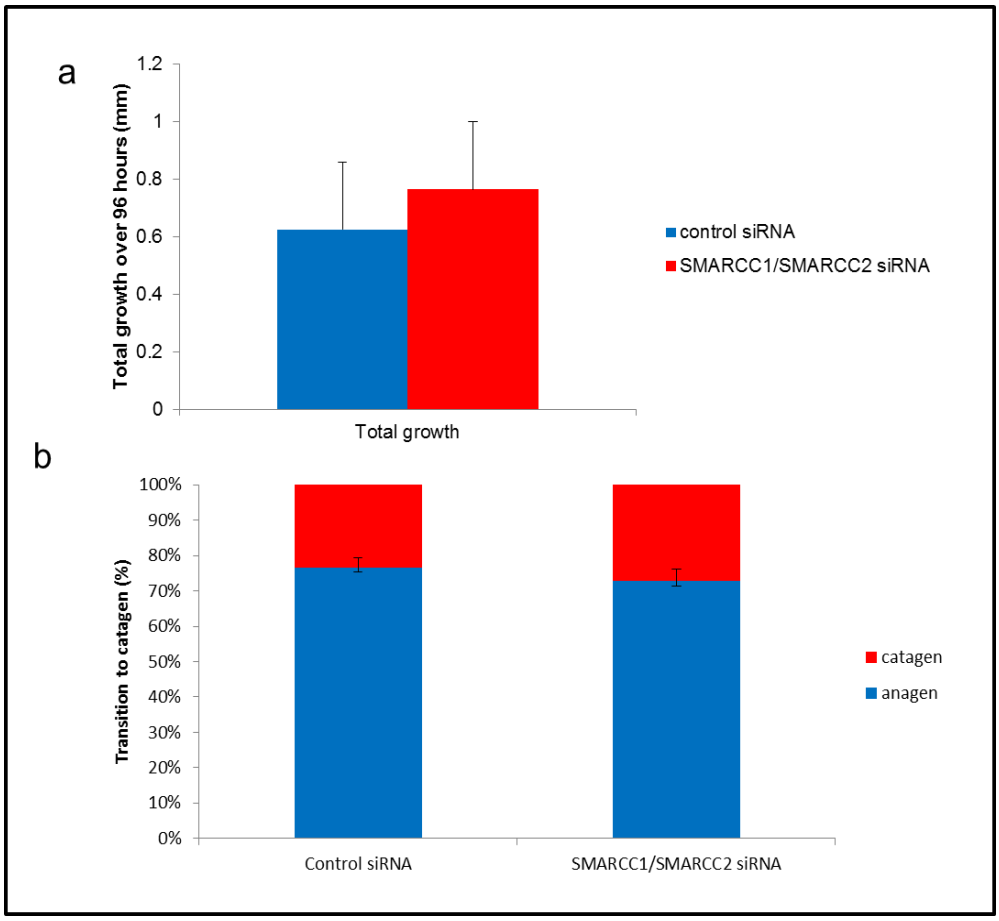

(a) Average hair follicle growth over 96 hours post transfection with either control siRNA or *SMARCC1/SMARCC2* siRNA treated hair follicles. >12 follicles per donor, 4 donors per group (Control/Treated), Mean total growth and ± standard deviation are shown, Student's T-Test. b) number of follicles which transitioned into Catagen phase during the experiment. >12 follicles per donor, 4 donors per group (treated/control), Mean percentage of anagen-catagen transitions and standard deviation are shown, Student's T-Test, representative of 4 male donors between the age of 46 and 65, mean age 56.

Figure 3.9 Suppression of BAF155 and BAF170 in human hair follicles mimics the effects seen in BRG1 suppression

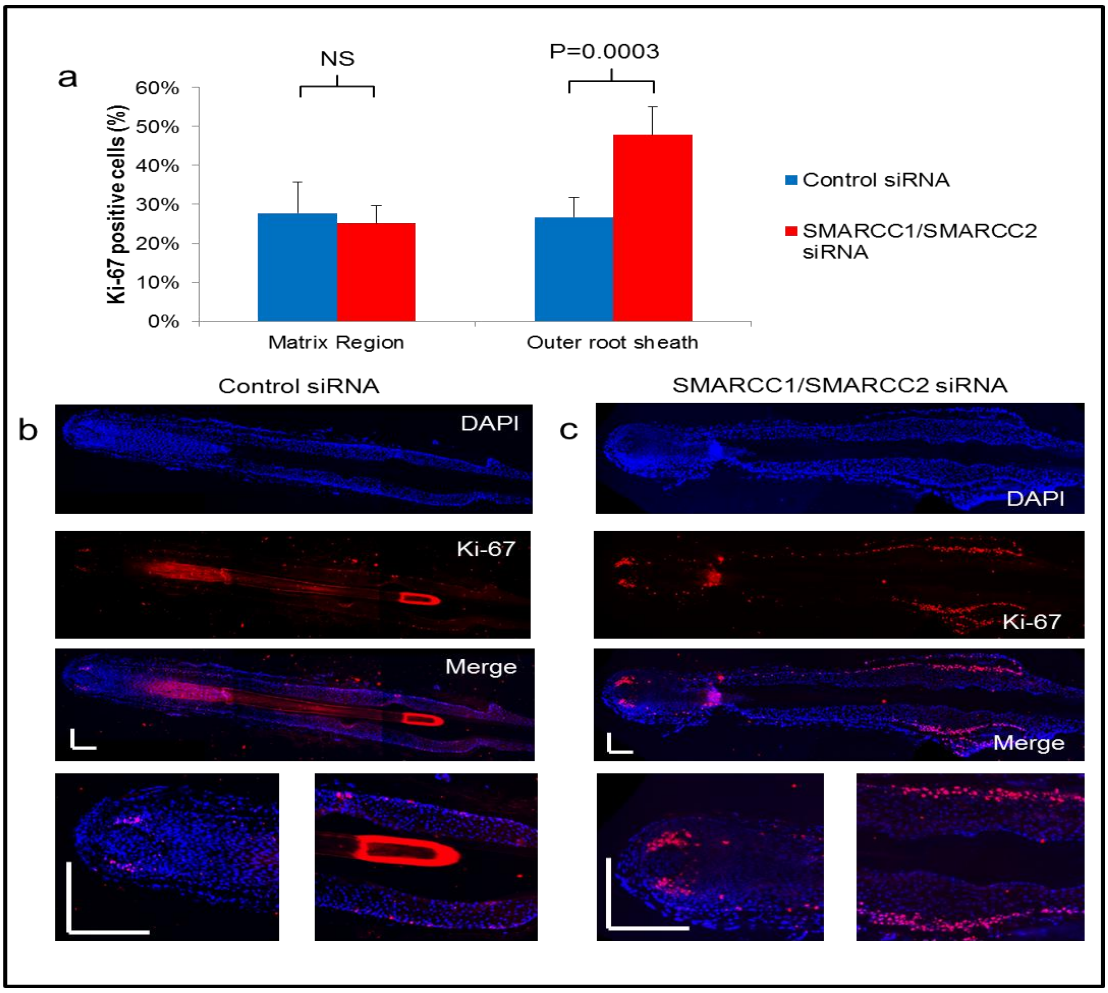

(a) Percentage of Ki-67 positive cells (positive cells/total cells in region) in matrix region and the outer root sheath; comparing control siRNA and *SMARCC1/SMARCC2* siRNA treated hair follicles. >12 follicles per donor, 4 donors per group (Control/Treated), Mean Ki-67 positive percentage (%) and ± standard deviation are shown, Student's T-Test. Immunostaining of Ki-67 protein expression in human hair follicles treated with (b) control siRNA or (c) *SMARCC1/SMARCC2* siRNA, representative of 4 male donors between the age of 46 and 65, mean age 56. Images taken at 100x magnification and stitched, expanded images at 200x magnification, Scale bars = 100µm.

3.2 BRG1 controls the epithelial cell migration during cutaneous wound healing

3.2.1 Both SWI/SNF ATPases BRG1 and BRM are expressed in the human epidermis

Several studies have previously demonstrated that *SMARCA4*/BRG1 plays a crucial role in epidermal development by controlling late epidermal keratinocyte differentiation and barrier formation in both mice (Indra et al., 2005, Mardaryev et al., 2014) and humans (Bao et al., 2013, Bao et al., 2015). However, the role of *SMARCA4*/BRG1 in human keratinocyte proliferation and migration during cutaneous wound healing remains unknown. To provide potential insight about the role of SWI/SNF complexes in human cutaneous wound healing the expression of SWI/SNF subunits in the epidermis was determined using immuno-fluorescence techniques combined with a semi-quantitative fluorescence intensity measuring technique, this technique allows for an active comparison of the target protein at specific sites between two groups, however it does not give a precise level of activity of the target protein, only a quantification of the fluorescent signal intensity. This analysis revealed the similar expression pattern of both BRG1 and BRM throughout the epidermis; however BRG1 appears more prominently than BRM, especially in the supra-basal epidermis (**Fig. 3.10**).

Figure 3.10 Both BRG1 and BRM are expressed in human epidermis.

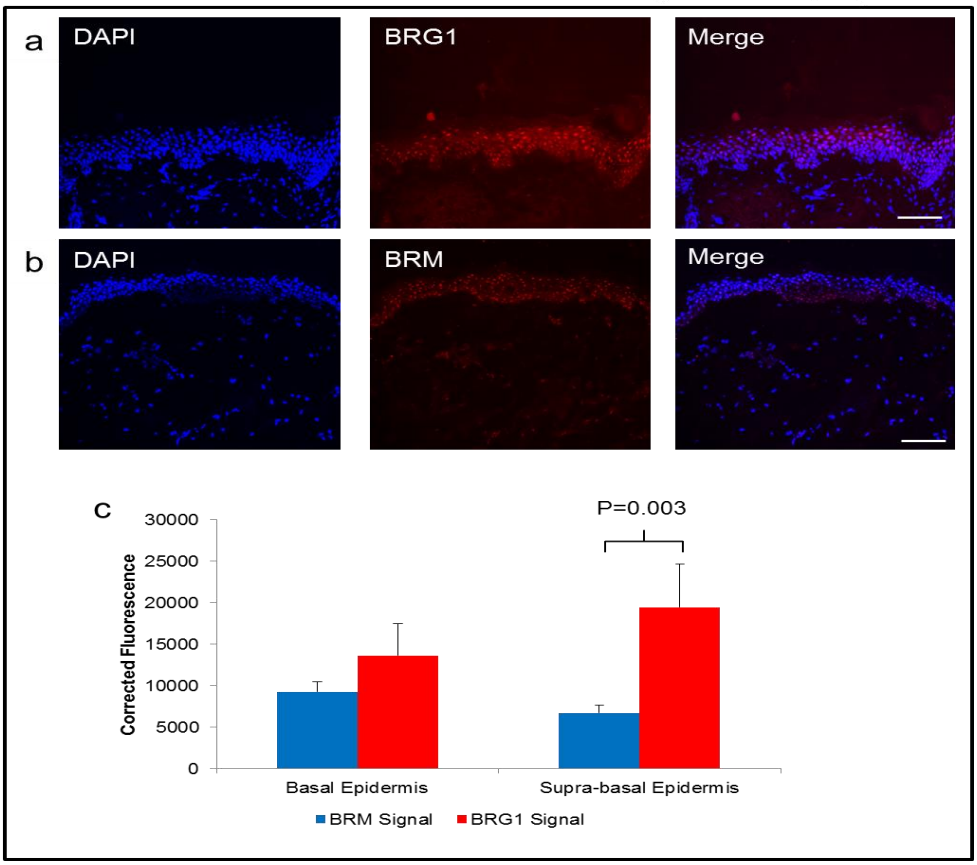

Immunostaining for SWI/SNF ATPase subunits (a) BRG1 and (b) BRM in human epidermis. Representative images of 3 female donors aged between 64 and 69. Images taken at 100x magnification, scale bar = 100µm. c) Relative corrected fluorescence comparing BRG1 and BRM protein signal in the basal and supra basal epidermis of a single donor. 3 donors, 20 measurements per region, Mean corrected fluorescence value and ± standard deviation is shown, Mann-Whitney U Test.

3.2.2 BRG1 expression is upregulated in the hyper-proliferative and migrating epithelia of the skin wounds.

As the previous data highlighted an abundance of BRG1 protein in the epidermis, the next step was to investigate the expression of BRG1 in *ex vivo* wounded skin using immunostaining, followed by the semi-quantitative measurement of the fluorescent signals. This analysis revealed that at day 3 of wounding a significant upregulation of BRG1 expression in the hyper-proliferative and migrating wound epithelia in comparison to the distant unaffected epidermis (**Fig. 3.11**).

3.2.3 BRG1 regulates wound closure rate, but does not affect epithelial cell proliferation and apoptosis in the *ex vivo* wounded full thickness skin.

By incorporating an siRNA mediated knockdown of *SMARCA4*/BRG1 (as described previously) with the human *ex vivo* wound healing model, a significant knockdown of BRG1 protein was observed after the 48 hour siRNA treatment (**Fig 3.12a,b**).

Further analysis of the wound indicated a delay in wound healing was occurring, while healing was still occurring, the rate of wound closure was delayed (**Fig 3.12c**). Haematoxylin staining of both control and BRG1 knockdown wounds at 3 and 5 days post wounding revealed the average length of hyper-proliferative and migrating epithelia was significantly decreased, while the average thickness of the epidermis was increased (**Fig 3.13**).

In order to determine the specific mechanism underpinning this delay, markers for proliferation and apoptosis (Ki-67 and active caspase 3) were analysed using immunostaining. However, no difference was seen with either marker (**fig 3.14** and **3.15**). These data indicate that BRG1 plays a role within wound healing by modulating migration pathways, but not proliferation or apoptosis pathways.

Figure 3.11 BRG1 protein expression is significantly upregulated in hyper-proliferative and migrating wound epithelia.

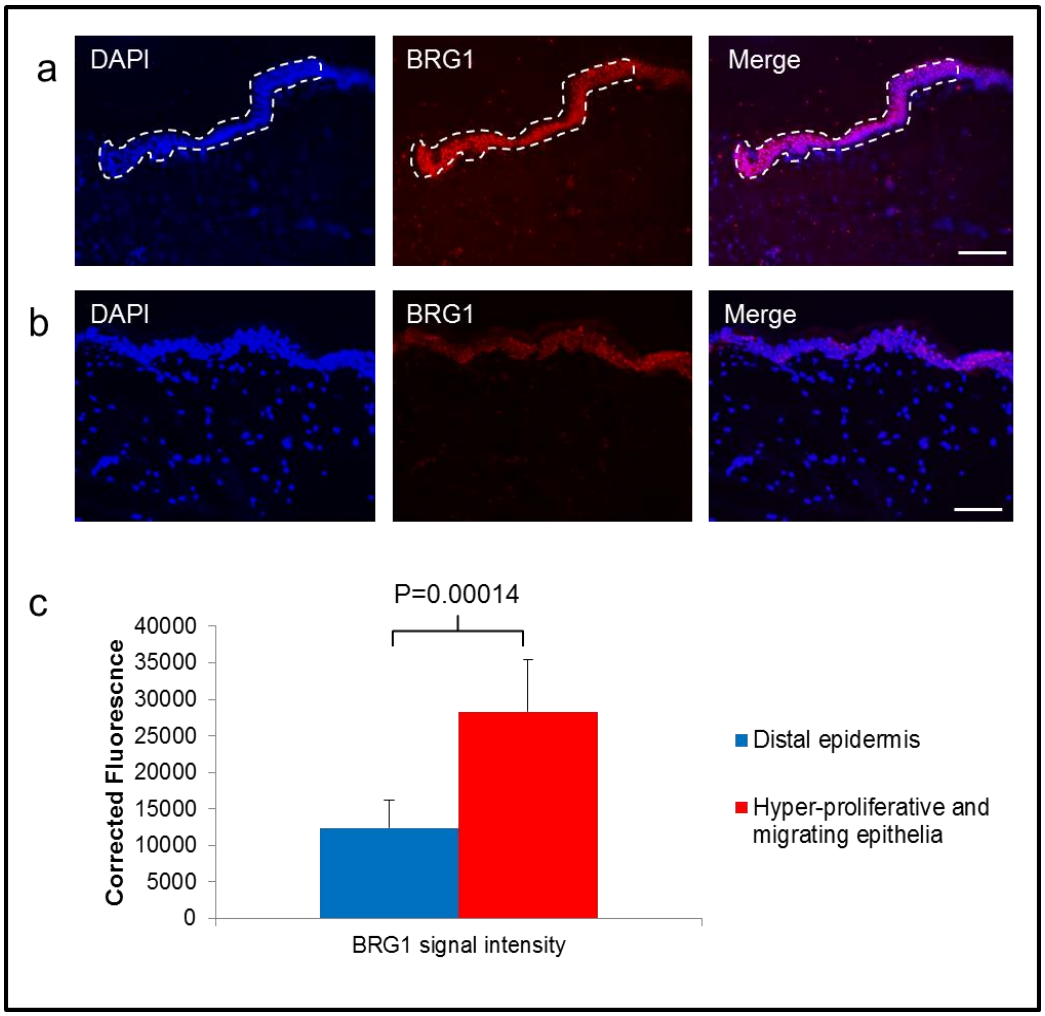

Immunostaining of BRG1 in (a) human *ex vivo* wound edge and (b) distal unaffected epidermis. Dashed line denotes hyper-proliferating and migrating wound epithelia, scale bars = 100µl. c) Relative corrected fluorescence comparing BRG1 signal in the hyper-proliferative and migrating epithelia and distal unwounded epidermis of a single donor at 3 days post wounding. 3 donors, 20 measurements per region, Mean corrected fluorescence value and ± standard deviation is shown, Mann-Whitney U Test.

Figure 3.12 BRG1 suppression significantly delays the rate of wound healing in ex vivo wounds.

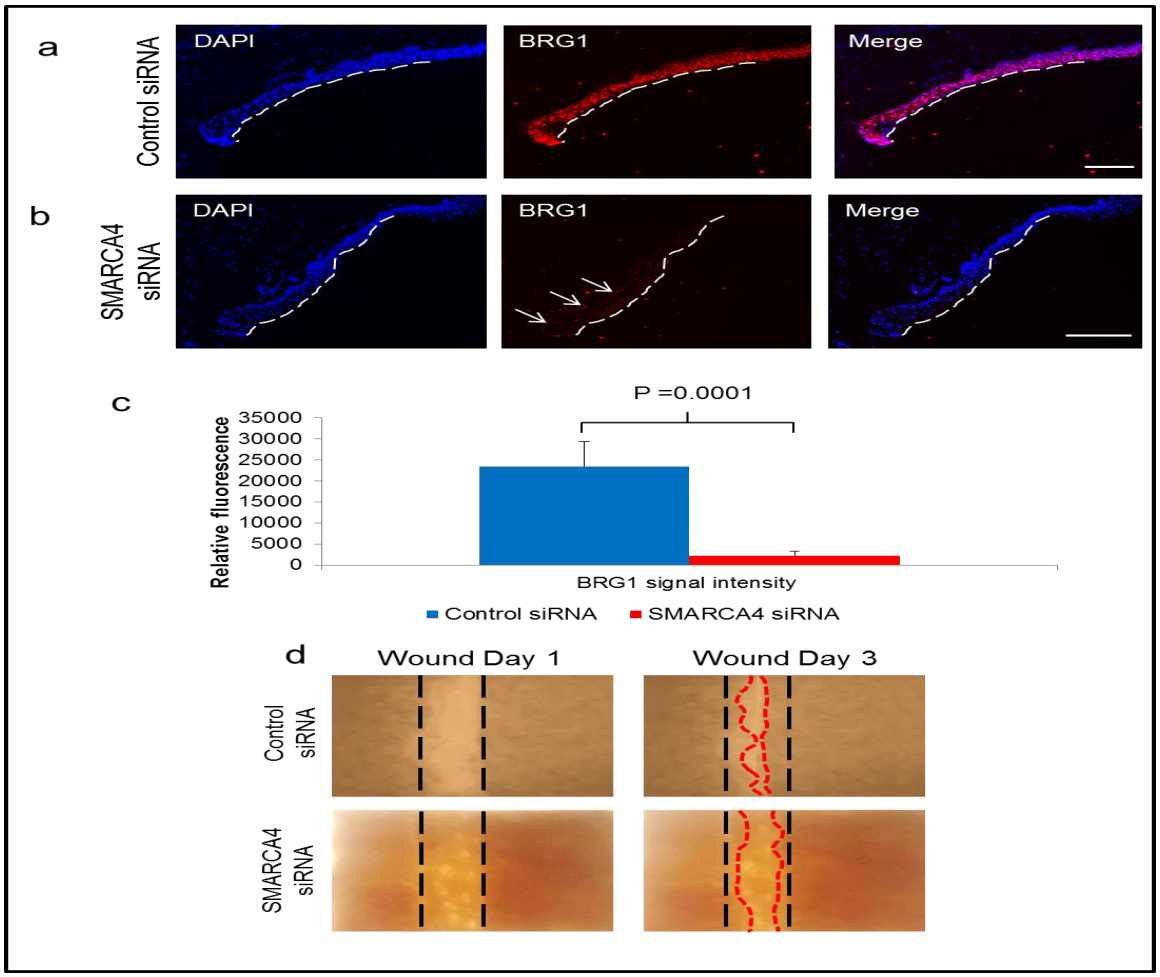

Immunostaining of BRG1 in human *ex vivo* day 3 wounds treated with (a) control siRNA or (b) SMARCA4 siRNA. Dashed line denotes base of the wound edge, arrows highlight positive BRG1 cells, scale bars = 100µl. c) Relative corrected fluorescence comparing BRG1 signal in the hyper-proliferative and migrating epithelia between control and SMARCA4 siRNA treated wounds of a single donor at 3 days post wounding. 3 donors, 20 measurements per region, Mean corrected fluorescence value and ± standard deviation is shown, Mann-Whitney U Test. d) Representative stereomicroscope images of partial thickness *ex vivo* wounds treated with control siRNA or SMARCA4 at 1 and 3 days post wounding. Black dashed line indicates initial wound, red dashed line denotes closing wound edge.

Figure 3.13 BRG1 suppression significantly reduces the length of wound edge during cutaneous wound healing

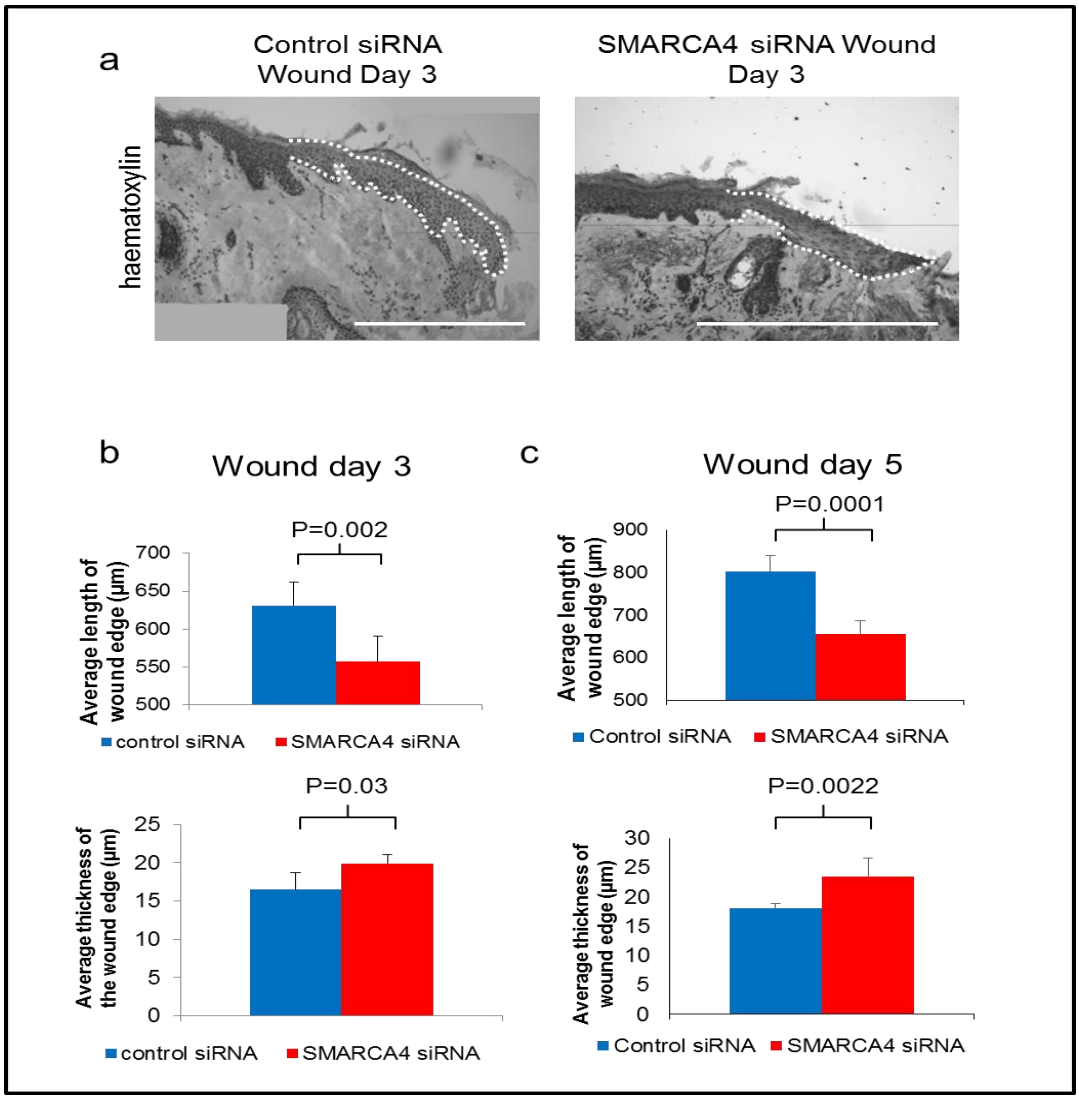

Haematoxylin staining of human ex vivo wounds day 3 treated with either non-targeting control siRNA or SMARCA4 siRNA. White dotted line indicates the hyper-proliferative and migrating epithelia. Comparison of wound characteristics between non-targeting siRNA and SMARCA4 siRNA highlighting differences in total wound length and wound thickness at 3 days post wounding (b) or 5 days post wounding (c). 3 donors, 20 measurements per region, Mean length or thickness and ± standard deviation is shown, scale bar = 500µm, Student's T-Test.

Figure 3.14 BRG1 suppression has no effect on proliferation in the hyper-proliferating and migrating epithelia.

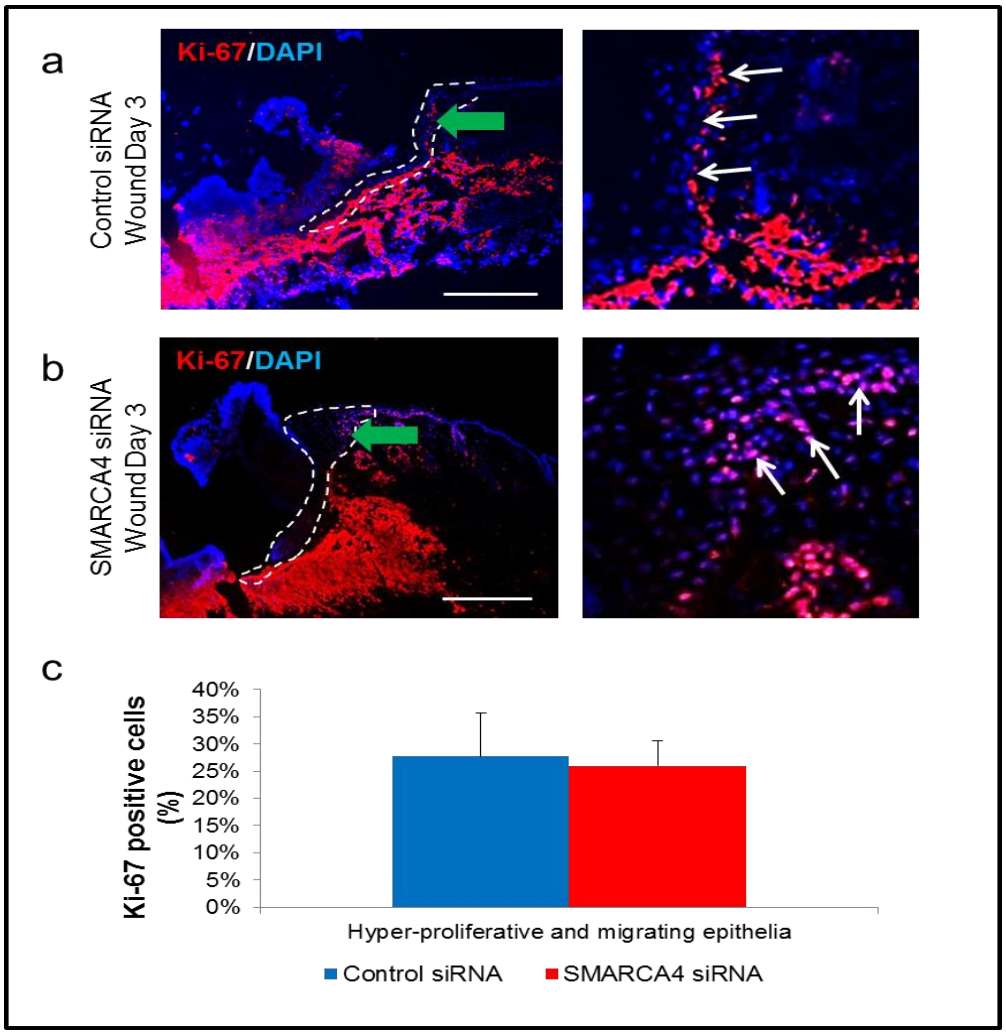

Immunostaining of Ki-67 protein in human epidermal wound tissue 3 days post wounding treated with either control siRNA (a), or SMARCA4 siRNA (b). Wounds created in tissue from the same donor. White dashed line indicates the wound edge. Green arrow indicates area of higher magnification, white arrowheads indicate positive cells. n=3 donors, scale bar = 200µm. c) Percentage of Ki-67 positive cells (positive cells/total cells in region) in wound edge, comparing control siRNA and SMARCA4 siRNA treated *ex vivo* wounds. 3 donors, 3 images per wound, Mean Ki-67 positive percentage (%) and ± standard deviation are shown, Student's T-Test.

Figure 3.15 BRG1 suppression has no effect on apoptosis in the hyper-proliferating and migrating epithelia.

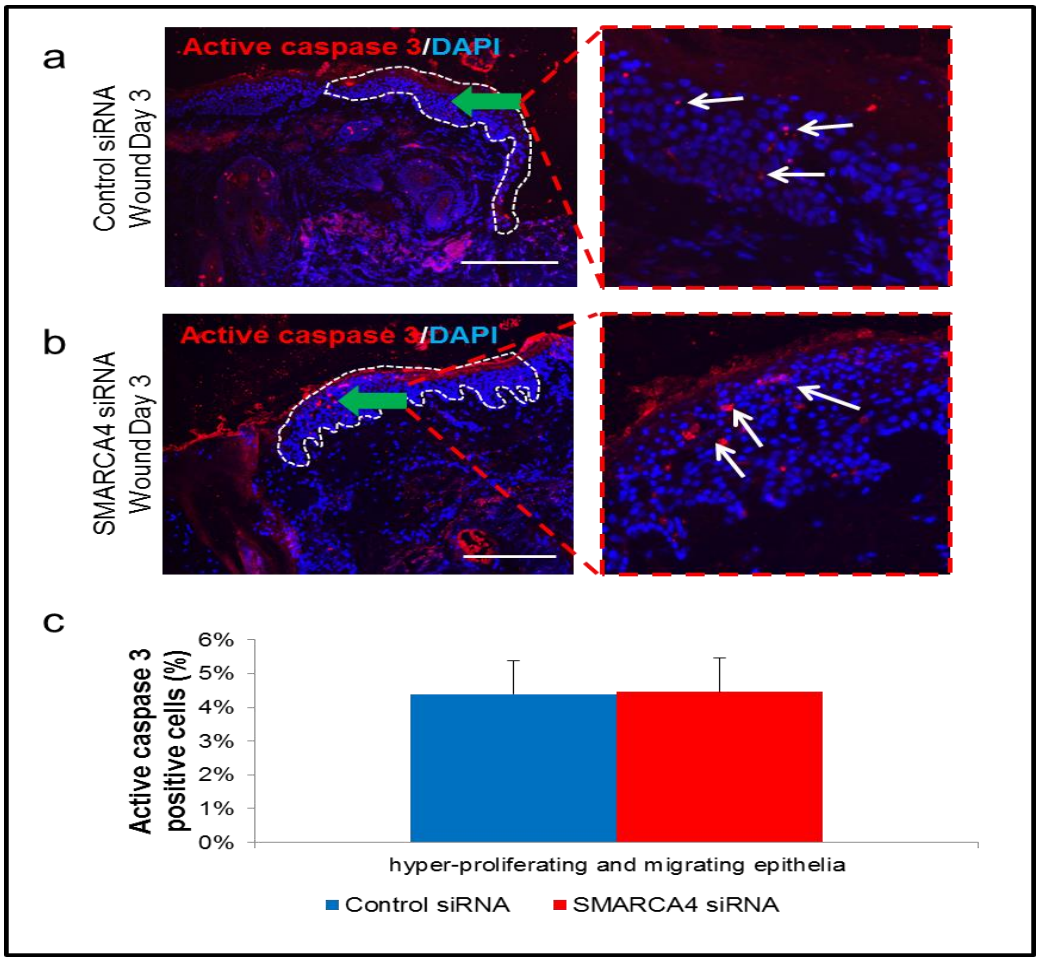

Immunostaining of Active caspase 3 protein in human epidermal wound tissue 3 days post wounding treated with either control siRNA (a), or SMARCA4 siRNA (b). Wounds created in tissue from the same donor. White dashed line indicates the wound edge. Green arrow indicates area of higher magnification, white arrowheads indicate positive cells. n=3 donors, scale bar = 200µm. c) Percentage of Active caspase 3 positive cells (positive cells/total cells in region) in wound edge, comparing control siRNA and SMARCA4 siRNA treated *ex vivo* wounds. 3 donors, 3 images per wound, Mean Active caspase positive percentage (%) and ± standard deviation are shown, Student's T-Test.

The delay in wound healing demonstrated in Figure 3.12 -3.13 combined with the lack of changes to proliferation and apoptosis seen in Figure 3.14 & 3.15, indicates that wound associated migration is regulated by BRG1 while proliferation and apoptosis is not, resulting in a shorter, but thicker wound edge in SMARCA4 siRNA transfected wounds.

3.2.4 BRG1 controls primary human epidermal keratinocyte migration, but does not affect their proliferation and apoptosis after scratch wounding ex vivo.

Taken together, the data from Figures 3.12 - 3.15 indicates a clear role for SMARCA4/BRG1 and the SWI/SNF complex in regulating migration during wound healing. However, due to the inherent limitations with partial thickness ex vivo wound healing models, further investigation would be increasingly problematic, as such the investigation was moved to a cultured keratinocyte monolayer model, this would grant a greater reproducibility as well as a wider array of downstream applications which could help to elucidate the specific mechanisms by which SWI/SNF regulates wound associated migration. Before beginning any new investigations it was first determined if the previously observed effects of BRG1 suppression were accurately recapitulated in the cell culture model. To do primary human epidermal keratinocytes (PHEKs) were transfected using the same siRNA and Lipofectamine delivery method utilised for the ex vivo wounds (described in 2.3.3 and 2.4.3). As previously seen in *ex vivo*, an efficient suppression of BRG1 was achievable, and validated mRNA level and with immunostaining for BRG1 protein (**Fig 3.16**). A more efficient knockdown was seen with cell culture than *ex vivo* transfection, suggesting that any effects seen may be exaggerated in comparison to the *ex vivo* model we used previously.

A scratch wound assay was used to uncover the specific mechanisms involved in BRG1 regulation of migration, this technique is a relatively quick and simple method to determine the wound response and migratory capabilities of cultured cell monolayers (Liang et al., 2007).

Immunostaining for proliferation and apoptosis (using Ki-67 and active caspase 3, respectively) was also carried out, revealing no significant change in either parameter when comparing control and SMARCA4 siRNA transfected PHEKs (**Fig 3.17**), while a total percentage of PHEKs were positive for active caspase 3 in comparison to the *ex vivo* model, it is likely that this is simply an artefact of using a cell culture model over an *ex vivo* model.

As it has been shown that BRG1 suppression has no effect on proliferation or apoptosis, but only migration PHEKs were also treated with Mitomycin C, which alkylates DNA preventing replication, prior to scratching.

PHEKs were transfected with either control or SMARCA4 siRNA for 48 hours, then Mitomycin C for 2 hours, and then the scratch wound was inflicted, images and RNA were collected at 1 hours, 24 hours, and 48 hours post scratching (scheme of experiments is highlighted in **Fig 3.18**).

While no significant differences were observed at 24 hours, a significant delay in migration was observed at 48 hours (**Fig 3.15**), supporting the data seen in *ex vivo* wounds.

Figure 3.16 Effective suppression of BRG1 in PHEKs after siRNA mediated suppression

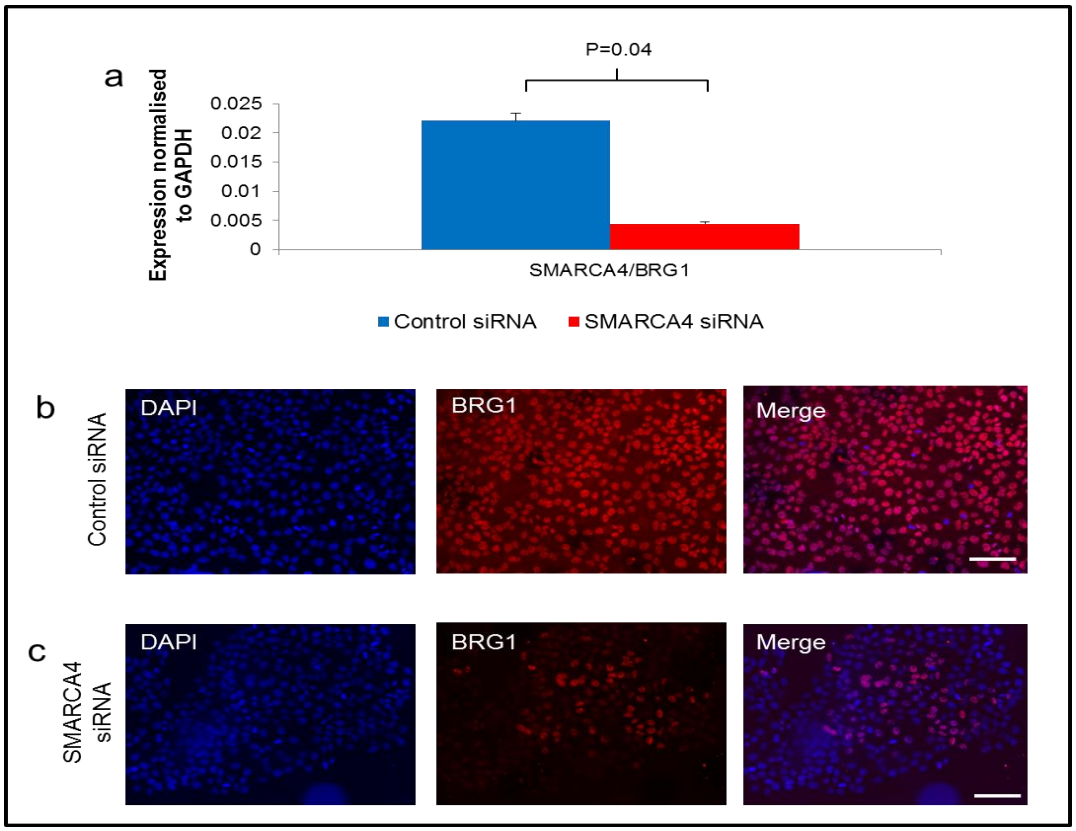

a) RT-qPCR analysis of BRG1 expression using RNA isolated from PHEKs transfected with either; control siRNA or SMARCA4 siRNA for 48 hours, mean expression normalised to GAPDH and ± standard deviation. 9 donors, 3 wells per group (control/treated) 3 replicates per gene. Student's T-test. Immunostaining for BRG1 protein in PHEKs transfected with either control siRNA (b) or SMARCA4 siRNA (c). 200x magnification, scale bar = 50µm.

Figure 3.17 BRG1 suppression has no effect on proliferation or apoptosis on cultured PHEK monolayers

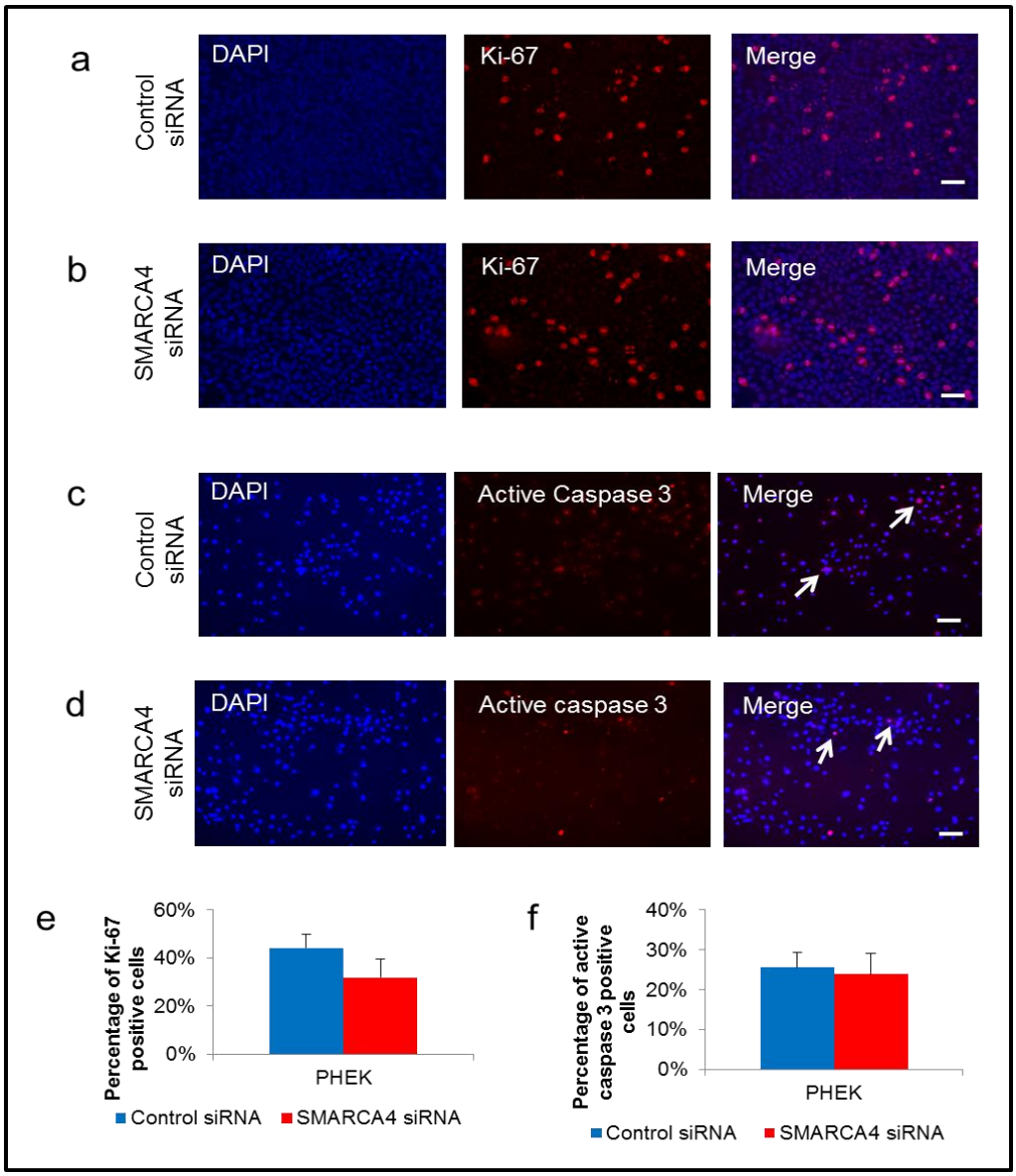

Immunostaining for Ki-67 protein in cultured PHEKs transfected with either; control siRNA (a) or SMARCA4 siRNA (b). Immunostaining for active caspase 3 protein in cultured PHEKs transfected with either; control siRNA (c) or SMARCA4 siRNA (d), white arrowheads indicate positive cells. Comparison of either; Ki-67 positive cells (e) or active caspase 3 cells in both control and SMARCA4 siRNA transfected PHEKs. 9 donors, 3 wells per group, 3 measurements per well. Scale bar=50µm. Mean positive cells ± standard deviation. Student's T-Test.

Figure 3.18 BRG1 suppression significantly delays migration in scratch wound assay at 48 hours

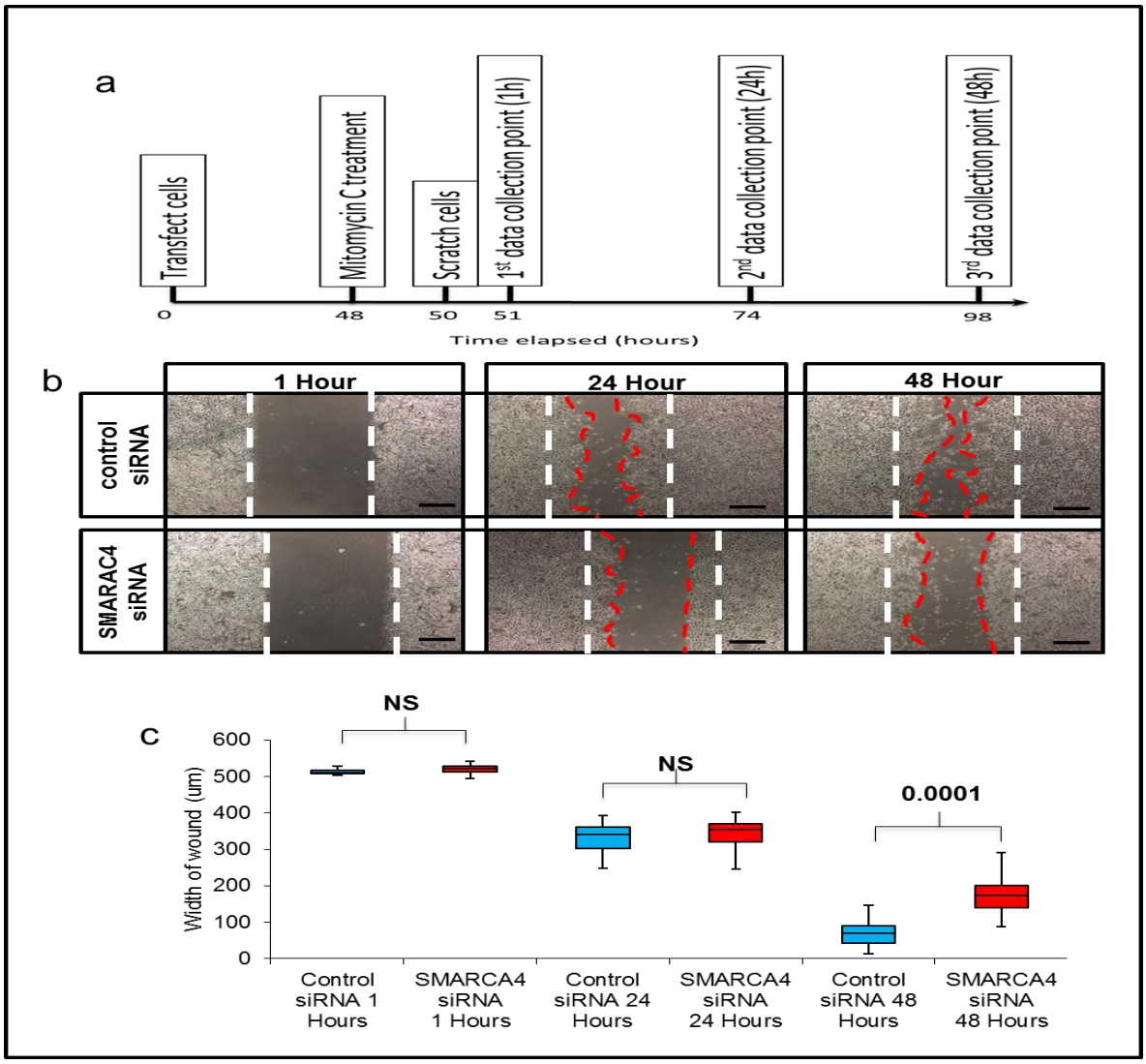

a) Scheme of experiment. b) Representative images of the keratinocyte migration after scratching in either control or SMARCA4 siRNA cells, at 1, 24 and 48 hours post scratching. White dashed line denotes original scratch width; red dashed line denotes the edge of migrating keratinocytes. Scale bar =200µm c) box-whisker plots measuring width of wound comparing control siRNA and SMARCA4 siRNA at 1, 24 and 48 hours. 2nd, 3rd quartiles, median, maximum and minimum values shown. 7 Donors, 3 wells per group, 20 measurements per well, Mann-Whitney U test.

3.3 BRG1 controls epidermal keratinocyte migration during cutaneous wound healing by regulating the expression of the genes involved in the key wound response pathways.

To further define the molecular pathways controlled by BRG1 in the human epidermal keratinocytes during the wound healing microarray transcriptome profiling analysis was performed using RNA isolated from the cells transfected with control or SMARCA4 siRNA followed by scratch wounding (scheme of experiment shown in **Fig 3.19a**). First, the differences in gene expression were determined between the control siRNA treated cells collected in 1 and 24 hours after scratch wounding, reflecting immediate and intermediate wound response, this provided a baseline of gene expression changes taking place in response to scratch wounding response.

This analysis highlighted a series of gene expression changes due scratch wounding, in total 5493 significant (1.8 fold up or down) expression changes were seen, 2266 upregulated and 3227 downregulated. Go term enrichment returned several common terms linked with wound healing. Cell migration and response to wounding GO terms were enriched in upregulated gene expression changes, while cell-cell adhesion, regulation of cell cycle and epidermis development GO terms were enriched in downregulated gene expression changes (**Fig 3.19 and Supplementary data 7.3**). in addition to GO terms matching wound healing, several specific gene expression changes were seen which matches previously reported data (Klein et al., 2017, Sass et al., 2017) (**Fig 3.19 and Supplementary data 7.3**), indicating the technique effectively recapitulates wound healing.

Once the baseline of wound healing response was established, the effect of BRG1 suppression on gene expression in cultured keratinocytes was investigated,

comparing SMARCA4 siRNA treated cells collected in 1 hour after scratch wounding, with the control siRNA treated cells collected in 1 hour after scratch wounding.

This analysis showed a significant gene expression change in 7418 genes in total, with 546 upregulated targets and 6872 downregulated, supporting the previous studies that state BRG1 acts as a transcription activator (Kadoch and Crabtree, 2015). Interestingly several GO terms involving wound healing response, cell migration and cytoskeletal organisation were enriched in the downregulated gene expression changes, indicated that BRG1 is required for adequate wound healing responses in keratinocytes (**Fig 3.20**), in the immediate short term as the wound is inflicted.

To further determine effects of BRG1 suppression on keratinocytes a comparison of the comparing SMARCA4 siRNA treated cells collected in 24 hour after scratch wounding, with the SAMRCA4 siRNA treated cells collected in 1 hour after scratch wounding.

This analysis showed a significant gene expression change in 3147 genes, with a roughly equal distribution between up and down regulated genes (1394 genes and 1753, respectively). Of the 1394 upregulated genes only 53 were upregulated in BRG1 suppressed keratinocytes at both 1 hour and 24 hours after scratching, while 512 genes (of 1753) were downregulated in both 1 hour and 24 hours after scratching, demonstrating that these changes are a result of the loss of BRG1, and not a result of the scratch based wound (**Fig 3.21**). Enrichment of GO terms for the upregulated genes indicates that BRG1 is required to repress mast cell identity, while enrichment of GO terms in downregulated genes are involved in migration and

cytoskeletal organisation (**Fig 3.21 and Supplementary data 7.1 and 7.2**). Additionally when BRG1 is down regulated GO term enrichment also highlights embryo implantation and epidermal differentiation terms, which is constant with previous data on the effects of BRG1 knockdown (Mardaryev et al., 2014, Reyes et al., 1998, Bultman et al., 2000, Bao et al., 2013), validating the analysis.

To determine the wound healing specific pathways which are affected by the loss of BRG1, the expression changes of genes upregulated in control siRNA cells collected at 24 hours after scratching, were compared with genes which were downregulated in SMARCA4 siRNA treated cells collected at 24 hours after scratching. A total of 2266 targets were upregulated in the control siRNA treated cells at 24 hour after scratching, while 2724 targets were downregulated in SMARCA4 siRNA treated cells at 24 hours after scratching, with 918 of those genes overlapping (**fig 3.22**). Demonstrating that approximately 40% of the genes required for wound healing are regulated (either directly or indirectly) by BRG1, or the SWI/SNF complex. Enrichment of GO terms for these shared genes highlighted several terms linked with wound healing pathways, for instance migration, wound healing, inflammation and epithelial to mesenchymal transition pathways (**fig 3.22 and supplementary data 7.1, 7.2 and 7.3**), all of which support the significant delays observed in the scratch mediated wound assays previously observed.

Several key wound healing genes were also significantly differentially expressed with the loss of BRG1; the loss of these targets was validated using qRT-PCR (**fig 3.23**). The expression of multiple *KRT* genes were shown to be regulated by BRG1, to further determine if these played a role in later wound healing qRT-PCR analysis of *KRT16,* and *KRT17* (stress keratins) was carried out comparing control siRNA treated PHEKs and SMARCA4 siRNA treated PHEKs collected in 48 hours after

scratching. Interestingly, a failure to induce *KRT16/17* was seen in the BRG1 knockdown group. The expression of *KRT16/17* is highly similar between control and BRG1 knockdown groups in control group; however at 48 hours a significant induction of *KRT16/17* was seen in the control group meanwhile the expression remained unchanged in the BRG1 knockdown group (**Fig 3.24a, 3.25a**). K16 and K17, were also investigated using *ex vivo* wound model, which validated the significant decrease in levels of K16/K17 in the BRG1 knockdown group compared with the control group (**Fig 3.24, 3.25).**

Taken together these data indicate that BRG1 is vital to promote an adequate wound response, by modulating the migratory capacity of keratinocytes.

Figure 3.19 Scratch mediated wound healing using control siRNA treated keratinocytes shows strong similarity to normal wound healing/scratch wound assay GO enrichment terms

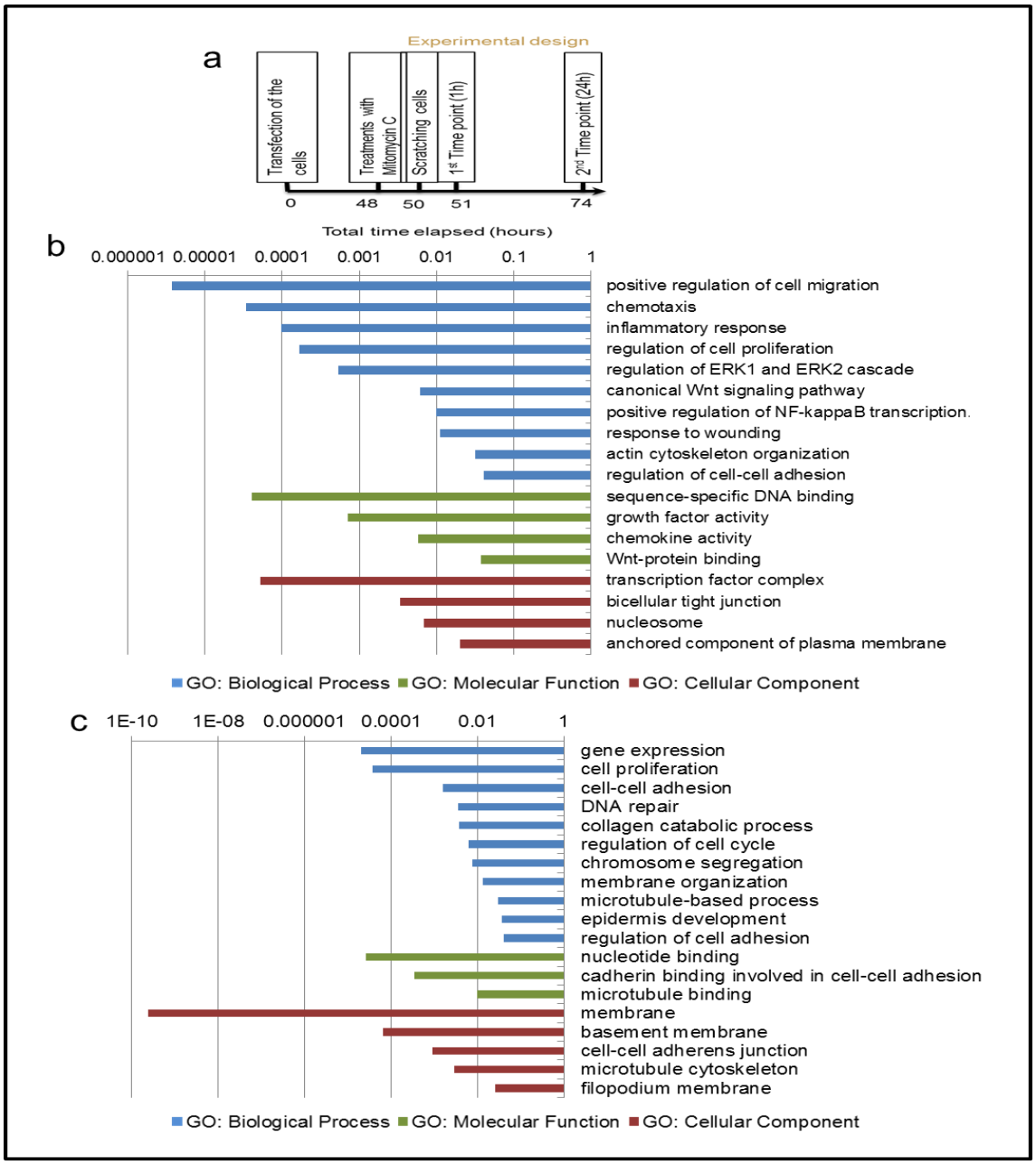

a) Scheme of experiment. Selected wound healing GO terms of the upregulated gene expression changes (b) and downregulated gene expression changes (c), using DAVID bioinformatic resources. Bars represent the log10 p-values of each category. n= 3 female donors aged 29 and 32.

Figure 3.20 BRG1 suppression shows an immediate enrichment of wound healing GO terms in downregulated gene expression changes

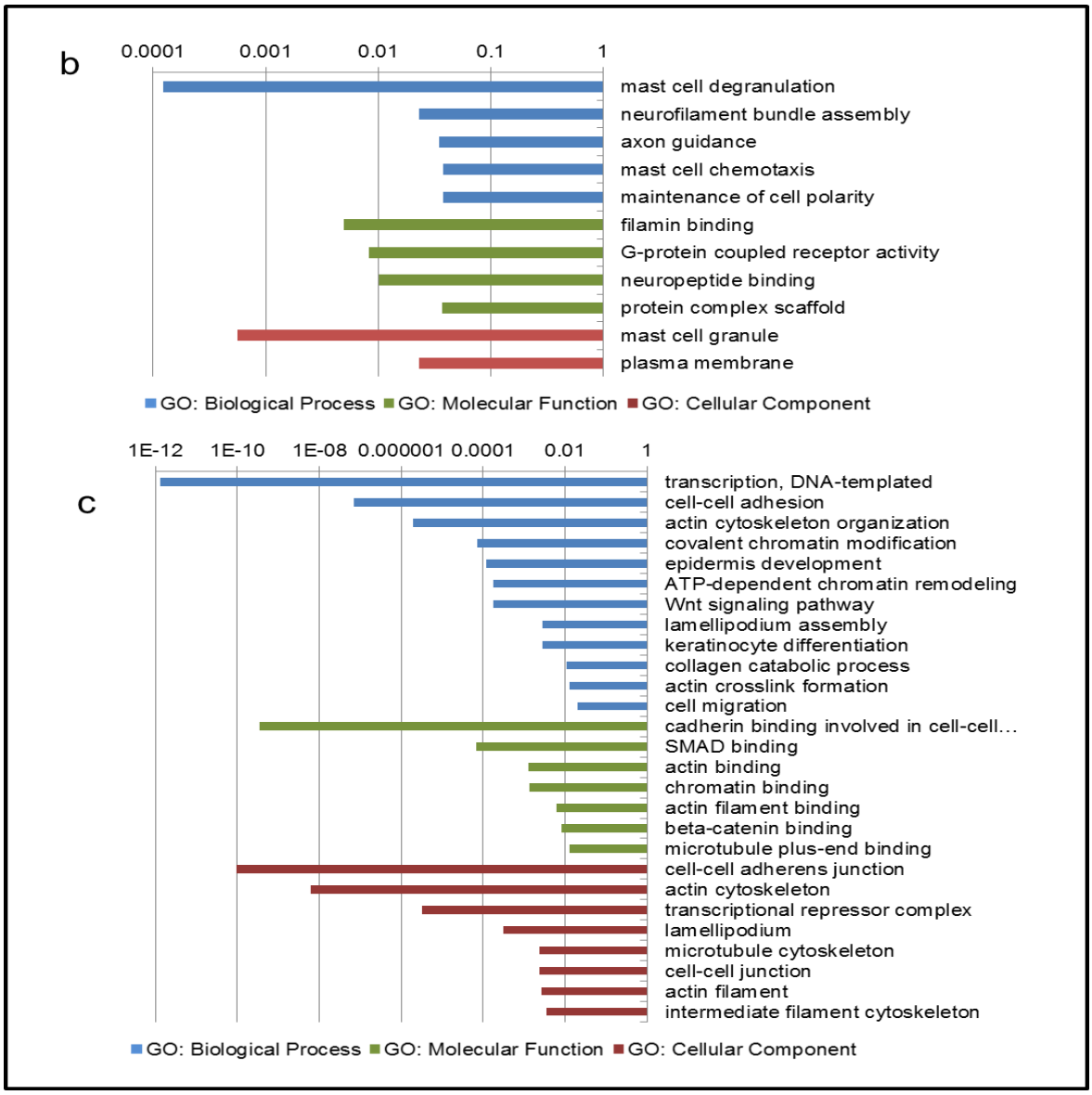

Selected wound healing GO terms of the upregulated gene expression changes (a) and downregulated gene expression changes (b), using DAVID bioinformatic resources. Bars represent the log10 p-values of each category. n= 3 female donors aged 29 and 32.

Figure 3.21 BRG1 regulates several key pathways required for normal wound associated migration

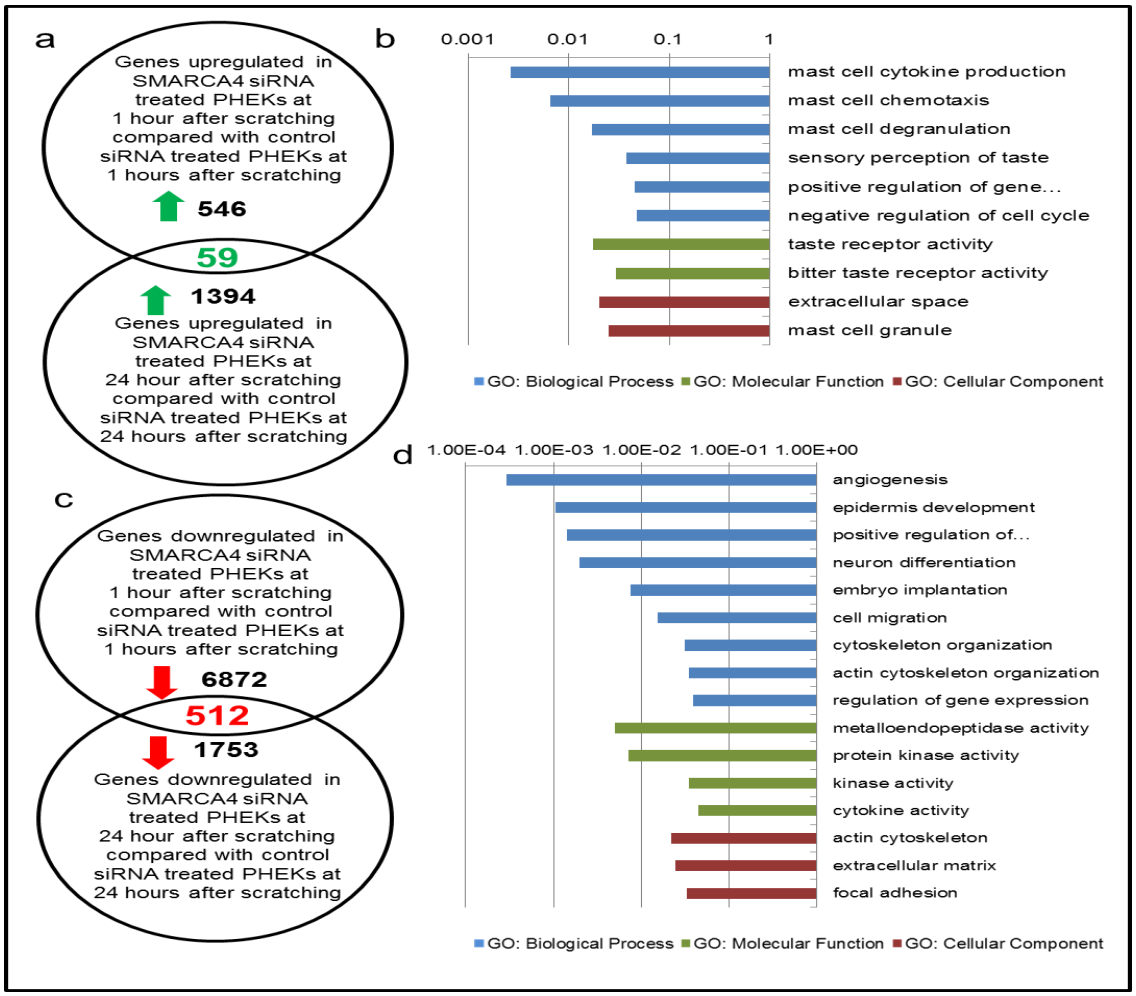

a) Venn diagram indicating the total number of genes upregulated due to BRG1 suppression at either; 1 hour or 24 hour after scratching, the overlap are genes upregulated in at both 1 and 24 hours after scratching. b) GO term enrichment of the 59 shared genes identified in (a) using DAVID bioinformatic resources. The bars represent the log10 p-values of each category. c) Venn diagram indicating the total number of genes downregulated due to BRG1 suppression at either 1 hour or 24 hour after scratching, the overlap are genes downregulated in at both 1 and 24 hours after scratching. d) selected GO term enrichment of the 512 shared genes identified in (c) using DAVID bioinformatic resources. The bars represent the log10 p-values of each category. n= 3 female donors aged 29 and 32.

Figure 3.22 BRG1 controls expression of up to 40% of the genes required for wound associated migration

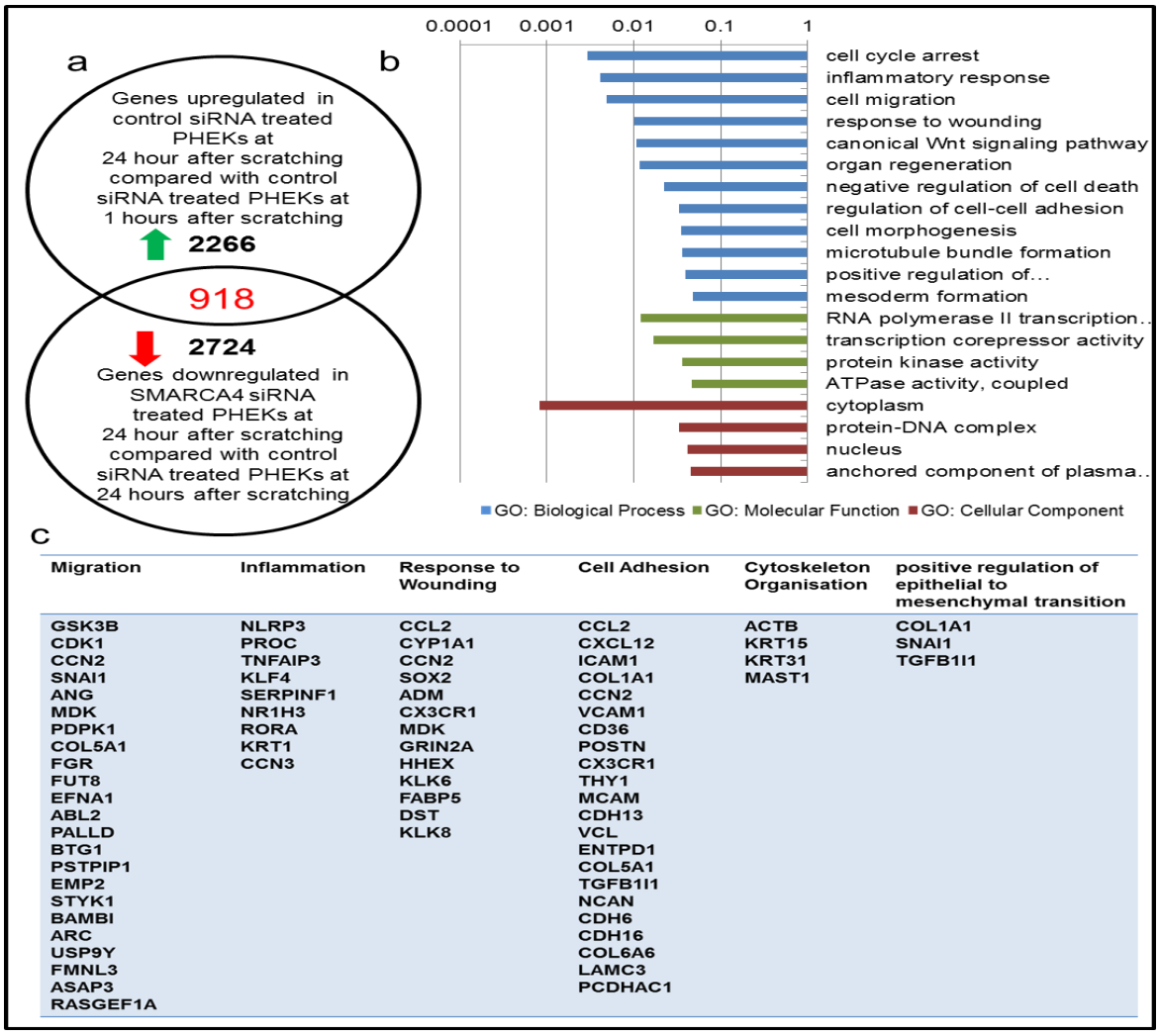

c

Migration	Inflammation	Response to Wounding	Cell Adhesion	Cytoskeleton Organisation	positive regulation of epithelial to mesenchymal transition
GSK3B	NLRP3	CCL2	CCL2	ACTB	COL1A1
CDK1	PROC	CYP1A1	CXCL12	KRT15	SNAI1
CCN2	TNFAIP3	CCN2	ICAM1	KRT31	TGFB1I1
SNAI1	KLF4	SOX2	COL1A1	MAST1	
ANG	SERPINF1	ADM	CCN2		
MDK	NR1H3	CX3CR1	VCAM1		
PDPK1	RORA	MDK	CD36		
COL5A1	KRT1	GRIN2A	POSTN		
FGR	CCN3	HHEX	CX3CR1		
FUT8		KLK6	THY1		
EFNA1		FABP5	MCAM		
ABL2		DST	CDH13		
PALLD		KLK8	VCL		
BTG1			ENTPD1		
PSTPIP1			COL5A1		
EMP2			TGFB1I1		
STYK1			NCAN		
BAMBI			CDH6		
ARC			CDH16		
USP9Y			COL6A6		
FMNL3			LAMC3		
ASAP3			PCDHAC1		
RASGEF1A					

a) Venn diagram indicating the total number of genes upregulated in control siRNA PHEKs at 24 hours after scratching, compared with number of genes downregulated in SMARCA4 siRNA at 24 hours after scratching, the overlap are genes upregulated in at 24 hours after scratching in control cells, but downregulated at 24 hours after scratching in BRG1 suppressed cells. b) GO term enrichment of the 918 shared genes identified in (a) using DAVID bioinformatic resources. The bars represent the log10 p-values of each category. n= 3 female donors aged 29 and 32. c) key genes regulated by BRG1 during wound associated migration

Figure 3.23 BRG1 suppression delays migration by regulating specific wound healing associated genes

a

GENE	Fold change in control siRNA treated cells at 24 hours after scratching	Fold change in SMARCA4 siRNA treated cells at 24 hours after scratching
SMARCA4	+1.1	-9.31
CXCL3	+16.06	-2.63
CXCR2	+2.1	-2.93
MMP7	+1.9	-3.48
SERPINA3	+4.74	-2.39
KRT80	+5.04	-1.81
WNT4	+2.87	-3.41
KLF4	+2.54	-2.01
SNAI1	+2.96	-1.86
CDK1	+2.13	-1.84

b

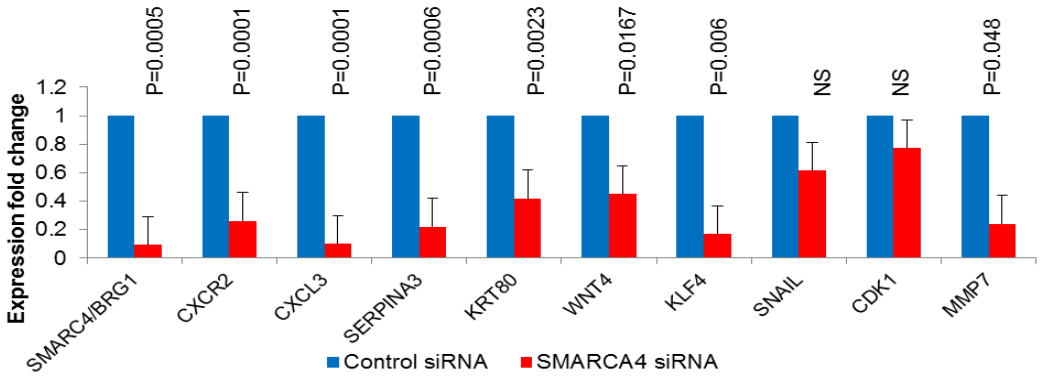

a) Fold change, as seen in microarray, of several wound healing and migration associated genes control siRNA treated PHEKs at 24 hours after scratching and SMARCA4 siRNA treated PHEKs at 24 hours after scratching. b) RT-qPCR validation of selected genes. Fold change shown, n= 3 female donors aged 29 and 32, Student's T-Test.

Figure 3.24 BRG1 regulates migration by inducing an upregulation of stress keratin K16

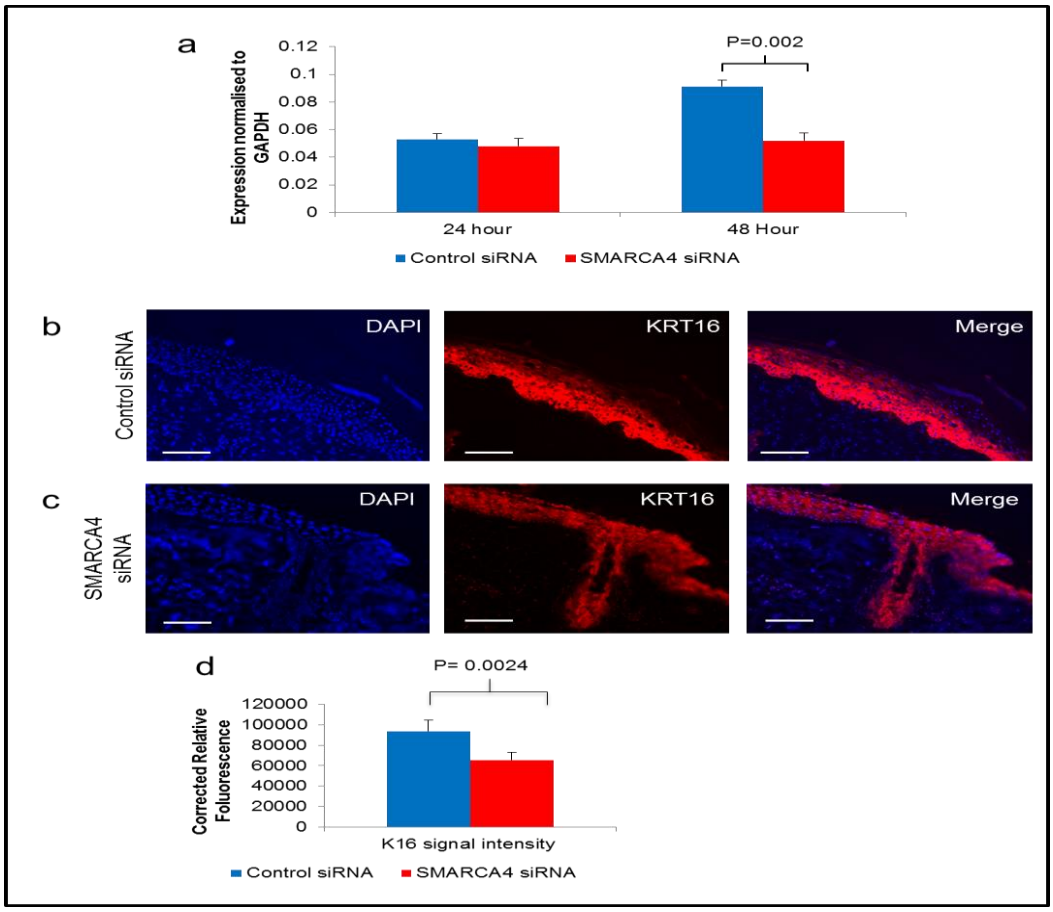

a) RT-qPCR analysis of K16 expression at 24 and 48 hours post scratching using RNA isolated from PHEKs transfected with either; control siRNA or SMARCA4 siRNA, mean expression normalised to GAPDH and ± standard deviation. 3 donors, 3 wells per group (control/treated), 3 replicates per gene, Student's T-test. Immunostaining of K16 protein in human epidermal wound tissue 3 days post wounding treated with either control siRNA (b), or SMARCA4 siRNA (c). Wounds created in tissue from the same donor, scale bar = 100µm. d) Relative fluorescence comparing K16 protein signal intensity between control and BRG1 knockdown wounds. n=3 female donors per group (Control/Treated), and 20 measurements per wound. Mean signal intensity and ± standard deviation are shown. Mann-Whitney U test.

Figure 3.25 BRG1 regulates migration by inducing an upregulation of stress keratin K16

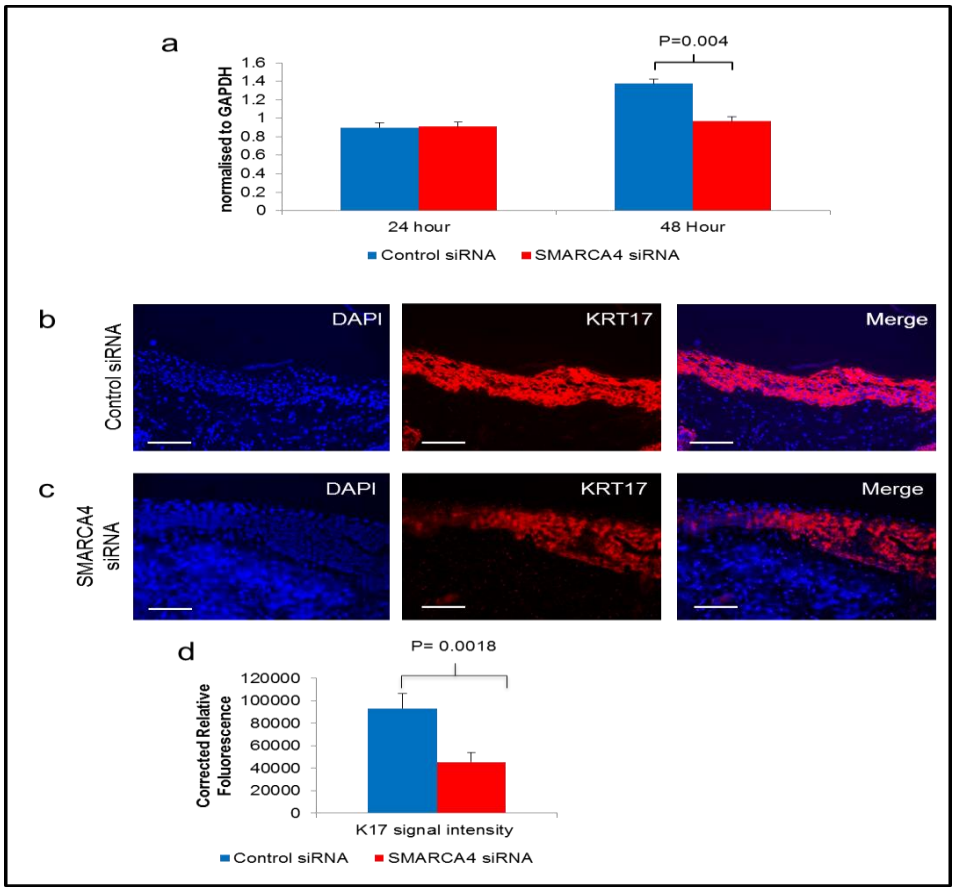

a) RT-qPCR analysis of K16 expression at 24 and 48 hours post scratching using RNA isolated from PHEKs transfected with either; control siRNA or SMARCA4 siRNA, mean expression normalised to GAPDH and ± standard deviation. 3 donors, 3 wells per group (control/treated), 3 replicates per gene, Student's T-test. Immunostaining of K16 protein in human epidermal wound tissue 3 days post wounding treated with either control siRNA (b), or SMARCA4 siRNA (c). Wounds created in tissue from the same donor, scale bar = 100µm. d) Relative fluorescence comparing K16 protein signal intensity between control and BRG1 knockdown wounds. n=3 female donors per group (Control/Treated), and 20 measurements per wound. Mean signal intensity and ± standard deviation are shown. Mann-Whitney U test.

4. Discussion

4.1 Diverse SWI/SNF chromatin remodelling complexes are present in the human hair follicle

To explore the potential role of the SWI/SNF chromatin remodelling complexes in the control of human hair growth the expression of genes encoding the SWI/SNF complex subunit in the whole isolated hair follicles were analysed using RT-qPCR and Immuno-fluorescent technology.

These findings indicated that *SMARCA4* mRNA is expressed at a much higher level than *SMARCA2* mRNA in the majority of the whole hair follicle cells. Immuno-fluorescent analysis also indicated slightly differing expression patterns for BRG1 and BRM in the hair follicle; with both BRG1 and BRM being found in matrix and pre-cortex of the hair follicle bulb, and the inner and outer root sheaths of the of the hair follicle, with almost no BRG1 expression detected in the dermal papilla and connective tissue sheath. Meanwhile, BRM expression was found all cells of the hair follicle, including the dermal papilla and connective tissue sheath.

Previous studies have demonstrated that SWI/SNF complexes with different subunit composition perform different functions, or driving differentiation, depending on the cell type and the differentiation state in mice (Kadoch et al., 2016, Kadoch and Crabtree, 2015). The differences observed could suggest that BRG1 containing SWI/SNF complexes are required mostly for the cell proliferation and differentiation of keratinocyte lineages; while BRM containing complexes might be required for maintaining cellular identity within mesenchymal lineages.

To further uncover the diverse SWI/SNF complex subunit compositions in the human hair follicle, the expression of the core subunits *SMARCC2*, *SMARCC1 a*nd

SMARCB1 in the whole hair follicles was also investigated. These subunits are reported to be present in all the SWI/SNF complexes in postnatal organisms (Euskirchen et al., 2012). Interestingly, these data showed that *SMARCC2* and *SMARCB1* were expressed at comparable levels in whole hair follicles, while *SMARCC1* mRNA was much more abundant. BAF155/BAF170 have been shown to form both homodimers and heterodimers, it is known that in mouse embryonic stem cells Baf155 is forms a homodimer and Baf170 is not expressed (Ho et al., 2009). This data suggests BAF155 might form homodimers in several human hair follicle cell sub-populations, potentially to maintain HF stem cells. However as individual cell populations were not investigated and so this has yet to be validated.

It has also been shown that BAF155 specifically is required to bind to BAF47, via the SWIRM and RPT1 domain interaction of BAF155 and BAF47 respectively (Yan et al., 2017). However, the immuno-fluorescent analysis indicates BAF47 and BAF155 are expressed in different cell sub-populations (shown in **Fig 3.2**), This contradicts the previously reported findings which stated that both BAF155 and BAF47 are required to provide full functionality to the SWI/SNF complexes (Phelan et al., 1999, Yan et al., 2017, Nakayama et al., 2017) in almost all tested tissues as well as several human cancers, it may also indicate that BAF47 has (as yet unknown) functionality beyond a SWI/SNF complex subunit in some human cell populations.

The potential role for SWI/SNF complexes in regulating/maintaining hair follicle cycle, as mouse models have demonstrated a role for Brg1 during telogen to angen shift, BRG1 in humans could maintain anagen, so a loss of BRG1 could push hair follicles into catagen phase earlier than normal, however this was not the case as no significant change was seen between control and BRG1 knockdown follicles. There is a possibility of masking occurring during these experiments, as insulin is a

prominent growth factor. To counter this, a second experiment could have been carried out without insulin to determine if insulin was masking any potential role of BRG1 in maintaining anagen phase, or alternatively a known catagen inducer (INFγ for instance) could be used to force catagen and investigate any possible differences between control and BRG1 knockdown follicles. Unfortunately due to time constraints this was not pursued.

Two families of the SWI/SNF complexes are present in mammals, termed BAF and PBAF (Kadoch and Crabtree, 2015, Kadoch et al., 2016). The presence of both BAF and PBAF complex specific subunits were seen in whole human hair follicles (*ARID1a*, *ARID1b* and *ARID2*, *PBRM*, respectively (Hodges et al., 2016)). Previous studies have indicated that the two complexes have different biological functions, as the complexes are evolutionarily conserved and their ancestral homologs have been shown to play different roles in both yeast and *drosophila* (Hodges et al., 2016, Dechassa et al., 2008, Molnar et al., 2006, Rendina et al., 2010). However, in mammals there are fewer specific examples of specific BAF or PBAF functions, as the BAF and PBAF complexes are assembled combinatorially, and they are likely assembled/disassembled transiently as need arises (Hodges et al., 2016, Wu et al., 2009). Interestingly, there is some evidence indicating that PBAF complexes are required for maintaining genetic integrity during mitosis (Bajpai et al., 2010). Most other evidence of different roles for the specific BAF or PBAF complexes is found in cancer studies. Mutations in the SWI/SNF complex subunits are commonly found in cancers, with up to 20% of all cancers containing such mutations, and many of the subunits being tumour suppressors (Hodges et al., 2016, Arnaud et al., 2018, McBride et al., 2018).

While little evidence of different roles for the BAF and PBAF complexes has been confirmed, there is evidence of different roles of the SWI/SNF complex based on the composition of subunits. The diversity in the SWI/SNF complex composition observed in human hair follicles might also reflect that the composition changes are required during specific cell state transitions. Such a requirement has been demonstrated in the process of murine neuronal progenitor differentiation; where *Actl6a*/Baf53a and *Phf10*/Baf45a SWI/SNF subunits (found in the neuronal progenitor cells) being lost and their expression swapped with *Actl6b*/Baf53b, *Dpf1*/Baf45b and *Dpf3*/Baf45c subunits in the differentiated neurons (Lessard et al., 2007). It was later demonstrated that microRNAs miR-9/9* and miR-124 facilitate this conversion by suppressing Baf53a expression during neuronal differentiation (Yoo et al., 2009). However, currently no similar mechanism has been described in regulation of human hair follicle cell sub-populations.

4.2 SWI/SNF complexes play a role in maintaining cell proliferation balance in the outer root sheath of the human hair follicles

To identify the potential role of the SWI/SNF complexes in the human hair follicle biology, BRG1, or BAF155 and BAF170 gene expression in whole hair follicles was suppressed using Accell siRNA technology. While an efficient suppression of either BRG1 or BAF155 and BAF170 was achieved no change in growth or anagen-catagen transition was observed within the short term (6 days total culture time) in the *ex vivo* follicle culture (**Fig 3.5, Fig 3.8**). As previous experiments showed a higher expression level of these subunits in the matrix/pre-cortex of hair follicle bulbs, it was hypothesised that a loss of SWI/SNF would affect the proliferation

and/or differentiation of cells in these hair follicle compartments. However, analysis revealed no change occurred in the matrix/pre-cortex cell proliferation. However, unexpectedly, a significant increase in cell proliferation was seen in the outer root sheath, in many cases (approximately 60%) this was also accompanied by the swelling of the highly proliferative cell population (visible in **Fig 3.6c, 3.7c, 3.9c**). Currently, there are two possibilities that are most likely explaining these observations. First, the SWI/SNF complex might be required to restrict the epithelial stem cell proliferation in the outer root sheath during anagen. Interestingly, in mice Brg1 is required for the hair follicle stem cell activation and proliferation during anagen induction, and Brg1 deficiency leads to the inhibition of the anagen progression and stem cell pool depletion (Xiong et al., 2013). These observations, in comparison to the previously reported findings in mice, could reflect the distinct roles for Brg1 in control of stem cell activation and proliferation during telogen-anagen transition and control of the balance in proliferation in the outer root sheath during anagen. The second possibility is that SWI/SNF maintains the cell type specific expression programme of outer root sheath keratinocytes, and when BRG1 is lost the expression programme is changed leading to the changes in cell identity and resulting in the increased proliferation of the altered cells. The second hypothesis is also somewhat supported by the GO term enrichment analysis of the BRG1 suppressed PHEKs (**Figs 3.21, 3.22 and supplementary data**), where the enrichment of several GO terms associated with keratinocyte differentiation, as well as other cell lineage identity are affected. Moreover, several keratins are downregulated when BRG1 is suppressed, namely *KRT15* and *KRT19* which are hair follicle specific keratins (**Fig 3.23**). There are multiple previous reports demonstrating the role of SWI/SNF in maintaining or orchestrating differentiation of multiple cell lineages (Fessing et al., 2011, Toto et al., 2016, Lessard et al., 2007). Taken together it is likely the latter of the two options is correct, However, further

studies using laser capture microdissection techniques to isolate the cells and determine any lineage specific changes in gene expression programmes using RT-qPCR and or microarray transcriptome profiling technologies will be required.

Throughout this investigation a number of insurmountable differences are encountered when comparing these data to previous studies involving mice. As mentioned there has been much more work carried out using mice, due to the ability to investigate developmentally, as well as a well understood hair cycling system, not to mention the ability to generate transgenic species to fully ablate expression of genes. All of these differences give multiple areas of investigation which cannot be mimicked using human studies. As previously mentioned in mouse models Brg1 has been linked to maintaining the stem cell reservoir of the bulge region, however this is only during telogen to anagen transition, with current technology this cannot be examined using a human model, roughly 5% of human hair follicles are in telogen phase, there is no way to accurately identify and extract them in order to perform hair cycle transition experiments. Additionally the hair cycle 'wave' that occurs in mice allows for precisely timed experiments which can be maintaining *in vivo* allowing for a long term investigation to take place, using human models hair follicles must be cultured *ex vivo* giving a finite time frame which can be observed, this method also removes the hair follicle from its micro-environment and results in a great amount of stress inflicted upon the follicle, before an investigation can even take place, potentially masking results with stress responses or (as previously mentioned) masking effects of the growth media which provides an abundance of growth factors and hormones. As such a true comparison of human and mouse hair follicle models cannot be carried out without accepting the limitations in place, retreating to the old adage "all models are wrong, but some models are useful", a

direct comparison usually cannot be made, but should be used to guide further investigation.

In summary, a diverse expression pattern of the SWI/SNF complex subunit encoding genes in human hair follicles suggests an important function of the SWI/SNF complex in control of the hair follicle activity. The suppression of BRG1, and co-suppression of BAF155 and BAF170 expression in *ex vivo* culture hair follicles using specific siRNA highlighted a distinct role for SWI/SNF complexes in the outer root sheath cells of hair follicles, however a specific molecular mechanism has to be identified in the future studies.

4.3 The SWI/SNF complex modulates epidermal keratinocyte migration during cutaneous wound healing

Previous studies have demonstrated that the BRG1 is required for normal epidermal development in both mice (Indra et al., 2005, Mardaryev et al., 2014) and humans (Bao et al., 2013); however its specific role in epidermal wound healing was previously unexplored. Using Immuno-fluorescence the expression of both BRG1 and BRM ATPases was determined in human epidermis. Both BRG1 and BRM is expressed throughout the epidermis. However BRG1 was more abundant throughout the epidermis, especially in the supra-basal layer, which would support previous studies highlighting the role of BRG1 in terminal epidermal differentiation (Bao et al., 2013).

Epidermal progenitor cell differentiation drives the epidermal self-renewal throughout the whole life of the organism, and BRG1 containing SWI/SNF complexes have been shown to be essential for this process (Bao et al., 2013, Indra et al., 2005,

Mardaryev et al., 2014). Moreover, these cells could also proliferate and migrate to the site of the skin injury for the wound re-epithelialisation. It has been shown that BRG1 is more abundant in the hyper-proliferative and migrating epithelia (HPE) of the wounds (**Fig 3.11**), suggesting that BRG1 is involved in the control of the wound re-epithelisation process. Building on this it was demonstrated that the suppression of the BRG1 expression leads to the significant delay in wound healing without effect on the cell proliferation or apoptosis at the wound edge (**Fig 3.12-3.15**). While previous studies have demonstrated that Brg1 is required for hair follicle stem cell proliferation as we as facilitating their contribution to the cutaneous wound healing in mice (Xiong et al., 2013). No studies have investigated the role of BRG1 in epidermal keratinocytes activation during cutaneous wound re-epithelialisation has not been reported prior to this investigation.

To further investigate the role of BRG1 in wound healing migration a cell culture based scratch mediated wound healing assay using primary human epidermal keratinocytes (PHEKs) was utilised (Liang et al., 2007). Once again the suppression of BRG1 in these cells had no effect on proliferation or apoptosis (**Fig 3.17**) but a significant delay in migration was observed. As proliferation and apoptosis were unchanged by BRG1 suppression, BRG1 must regulate keratinocyte migration, resulting in a delay to wound closure when BRG1 is suppressed.

Microarray transcriptome profiling and the GO term enrichment analysis of BRG1 suppressed keratinocytes highlighted multiple terms linked with cell migration (**Fig 3.22c and supplementary data)**, such as cell migration, and cytoskeleton organisation, indicating that BRG1 regulates transcriptional wound response controlling cell migration. Additionally, GO term enrichment linked terms were associated with angiogenesis, epidermis development, and embryo implantation; all

of which have previously been linked to BRG1 functions (Lan et al., 2017, Bultman et al., 2000, Mardaryev et al., 2014).

Further analysis of the microarray data indicates that BRG1 is a negative regulator of mast cell identity, as when BRG1 was suppressed many of the up-regulated genes were enriched for GO terms linked with mast cell chemotaxis and degranulation (**Fig 3.19b, 3.20b and supplementary data**). This has previously been alluded to in mouse T-cells (Wurster and Pazin, 2008), but no direct evidence was given. However, mast cell lineage has been shown to be regulated by a specific microphthalmia-associated transcription factor (MITF) isoform (Shahlaee et al., 2007), and BRG1 has been shown in several studies to interact directly with various MITF isoforms (Ondrusova et al., 2013, Saladi et al., 2013, Mehta et al., 2015, Laurette et al., 2015), suggesting that this is the likely case with mast cells. However, this was not the focus of this work, so there has been no validation of this interaction.

GO term enrichment of control siRNA treated PHEK scratch mediated wound samples shows significant enrichment of multiple terms involved in wound response (**Fig 3.19b,c and supplementary data**), including cell migration, cell-cell adhesion, cytoskeleton organisation, response to wounding, and several known wound response pathways (ERK, WNT, and NF κB). Several key wound healing transcription factors (including *ZEB1*, *SNAI1*, and *GRHL3*) were up-regulated as expected (Medici et al., 2008, Lamouille et al., 2014, Klein et al., 2017), indicating an accurate recapitulation of the wound healing process.

After determining that the control group was an accurate facsimile for normal wound healing, the investigation of the BRG1 specific changes could take place. By

comparing the differences in expression seen in BRG1 suppressed PHEKs and control siRNA treated PHEKs at 24 hours post scratching, the significant gene changes would be due to the loss of BRG1. Focusing on the genes which are up-regulated in control cells (which are similar to those seen in other wound healing studies) but down-regulated in BRG1 suppressed cells, a selection of genes involved in migration, which are also regulated by BRG1, would be highlighted. A total of 2266 genes were up-regulated in control wound response at 24 hours post scratch, while 2724 genes were downregulated in BRG1 suppressed scratch mediated wound cells collected at 24 hours after scratching, of these genes 918 were overlapped, indicating that BRG1 is responsible for regulating approximately 40% of the genes involved in keratinocyte migration (**Fig 3.22a**). Several key genes were in this list, including *SNAI1, WNT4, KLF4* and *SOX2*; however *ZEB1* and *GRHL3* (prominent genes involved in epithelial-mesenchymal transition) expression were not affected by the loss of BRG1.

To fully determine the changes occurring due to the loss of BRG1 chromatin immuno-precipitation and sequencing or assay for transposase-accessible chromatin using sequencing (ChIP-seq or ATAC-seq, respectively) would be needed, this would determine direct vs indirect targets as well as the binding sites of transcription factors or histone marks and the 'chromatin landscape', which would fully elucidate the changes occurring due to the suppression of BRG1 during keratinocyte migration.

These findings suggest that BRG1 is required for migration, and epidermal-mesenchymal transition (EMT), although not via *ZEB1* or *GRHL3* pathways. This data indicates that BRG1 is required for expression of *SNAI1* (also termed *SNAIL*), which inhibits E-cadherin expression (Batlle et al., 2000, Cano et al., 2000), a

hallmark of EMT. As *SNAI1* is an inhibitor of E-cadherin (*CDH1*) there should have been an increase in E-cadherin in BRG1 suppressed samples in 24 hours after scratching. However this was not the case, this is likely due to additional genes which regulate E-cadherin suppression, such as *ZEB1* and *ZEB2* (Andersen et al., 2005), which were expressed at a higher level in BRG1 suppressed samples in 24 hours after scratching (**Fig 3.23a**).

Other key genes/pathways highlighted from the microarray analysis are in the WNT pathway. β-catenin independent Wnts, Wnt4, Wnt5a and Wnt11, have been seen to support wound healing in mouse models (Fathke et al., 2006). A more recent paper has highlighted a role of human WNT4 in increasing wound healing rate in second degree burns in rats (Zhang et al., 2015), this study utilised human umbilical cord mesenchymal stem cell derived exosomes (hucMSC-ex), which contain high levels of WNT4. This study showed that injection of the hucMSC-ex into the wound site increased the wound healing rate. Consistent with this observation, this investigation showed an increase in *WNT4* in control siRNA treated cells at 24 hours after scratching, but a decrease in *WNT4* in BRG1 suppressed cells at 24 hours after scratching, suggesting that WNT4 does play a role in keratinocyte migration (**Fig 3.23**).

Additionally, several enriched GO terms indicate BRG1 regulates cytoskeletal formation/organisation, normal epidermal wound healing response relies on a switching of cytokeratin (*KRT*) genes to direct the formation of the cytoskeleton for mobility, most notable of these is the activation of *KRT6*, *KRT16* and *KRT17* (Wawersik et al., 2001, Mazzalupo et al., 2003, Wong and Coulombe, 2003). These keratins are required for normal wound induced cell migration, where they act through reducing desmosome stability and inter-cellular contacts in keratinocytes

controlled by the protein kinase C alpha (PKCα) localization near the cellular membrane (Loschke et al., 2016). In control siRNA treated cells at 48 hours after scratching *KRT16* and *KRT17* showed a significant increase in expression, however in BRG1 suppressed cells in 48 hours after scratching the expression of *KRT16* and *KRT17* showed no induction of expression (**Fig 3.24a, 3.25a**). The gene encoding PKCα (*PRKCA*) is also down regulated in BRG1 suppressed cells, there is also a significant decrease in the levels of K16/K17 protein in BRG1 knockdown day 3 wounds, further supporting the role of BRG1 in regulating a number of KRTs, and not only those required in terminal epidermal differentiation as has been previously reported (Indra et al., 2005, Mardaryev et al., 2014, Bao et al., 2013).

Taken together, these data indicate a specific role for BRG1 in modulating specific EMT pathways through regulation of SNAI1 expression. BRG1 also regulates the formation and organisation of the cytoskeleton which is vital to wound healing migration. However these data are primarily obtained from a keratinocyte based 2D migration model, as such it cannot truly explain the effects occurring during *in vivo* wound healing.

5. Conclusions

Multiple variations of the SWI/SNF complex are present in the different human hair follicle cells.

SWI/SNF complex controls the balance of cell proliferation in the human hair follicle outer root sheath.

BRG1 is upregulated in the hyper-proliferating and migrating epithelia in the cutaneous wound.

SWI/SNF complex controls epidermal keratinocyte migration without effecting their proliferation and apoptosis during the skin wound healing.

BRG1 acts predominantly as a transcription co-activator in the human epidermal keratinocytes during the skin wound healing.

BRG1 controls the changes in transcription programmes associated with the epithelial cell cytoskeletal remodelling and skin mobility, but not cell adhesion during the skin wound healing.

6. Future Studies

6.1 Determining the role of SWI/SNF in regulating proliferation of the outer root sheath cells in whole human hair follicles

This work highlighted a potential role for SWI/SNF in regulating proliferation, or possibly differentiation, in the outer root sheath of hair follicles. Using laser capture microdissection (LCM) to isolate the cells which showed a drastic increase in proliferation after BRG1 suppression and comparing them with control outer root sheath cells, using microarray transcriptome analysis or similar, would elucidate if they are losing their stem like properties or differentiating into something other than ORS keratinocytes as suggested. There has been some investigation into Brg1s role in murine hair follicle cycling, however this does not match with the current data seen in humans, but with current technologies human hair follicle cycling cannot be accurately observed to determine if the roles are similar.

6.2 Determining direct or indirect targets of BRG1 suppression during keratinocyte migration.

While many migration, inflammation and wound healing associated genes are shown to be regulated by BRG1, the question remains as to whether they are direct or indirect targets. Chromatin immuno-precipitation combined sequencing (ChIP-seq), would adequately determine direct or indirect targets. This same technique could also be used to elucidate specific SWI/SNF complex composition with in sub population of hair follicle cells.

6.3 further investigate the role of BRG1 on cytoskeletal elements and immune cells.

Multiple GO terms and associated genes identified with microarray transcriptome analysis indicate that BRG1 regulates cytoskeletal elements and various cytokines. As fibroblasts are both required for wound healing and able to migrate more freely than keratinocytes, an investigation in to the role of BRG1 within fibroblast migration would determine if the effect is truly due to an effect on cytoskeletal formation/synthesis, or if its unique to the keratinocytes undergoing EMT. Additionally this work has highlighted a potential role for BRG1 and SWI/SNF in regulating inflammation, an integral part to wound healing, which could suggest BRG1 has a much larger role in wound healing than modulation of keratinocyte migration.

6.4 Overexpression of BRG1 in keratinocyte migration

As these data all point to a loss of BRG1 resulting in a delay to keratinocyte migration, it can be assumed that the overexpression of BRG1 would have the opposite effect, speeding up keratinocyte migration, and so speeding up wound healing. However, given the abundance of data implicating BRG1 and the rest of the SWI/SNF complex in cancer, specifically in skin cancer/melanoma, it would be more effective to identify the mechanism at work and determine if there are safer pathways which can be exploited to obtain the same result.

The first step would be to use a plasmid/viral vector to overexpress BRG1 in a cell culture model, and determine if it does have the desired effect of speeding up keratinocyte migration.

6.5 Recovery of phenotype using BRM.

As previously stated, SWI/SNF has 2 mutually exclusive ATPase subunits, BRG1 and BRM, as this study focused on BRG1 there is a possibility that BRM could be used to recover the negative effects. Alternatively a double knockdown of BRG1 and BRM may further excaudate the effect resulting in a more prominent delay, or potentially a full inhibition, of keratinocyte migration. A new chemical inhibitor has recently been developed, which is reportedly highly specific for SWI/SNF ATPase subunits and capable of inhibiting their function (Wu et al., 2019b).

By combining these future studies a clear picture of the specific mechanisms at work could be obtained, which would determine if BRG1 could be exploited to enhance/speed up keratinocyte migration in a clinical aspect. As stated there is currently a strong link to SWI/SNF errors and cancer, which would need to be fully addressed before attempting to exploit BRG1 in an *in vivo* setting. While this may be a pipe dream, completion of these suggested future studies would go a long way towards determining if it will ever be feasible.

7. Bibliography

ABDAYEM, R., FORMANEK, F., MINONDO, A. M., POTTER, A. & HAFTEK, M. 2016. Cell surface glycans in the human stratum corneum: distribution and depth -related changes. *Exp Dermatol*.

AHMED, M. I., ALAM, M., EMELIANOV, V. U., POTERLOWICZ, K., PATEL, A., SHAROV, A. A., MARDARYEV, A. N. & BOTCHKAREVA, N. V. 2014. MicroRNA-214 controls skin and hair follicle development by modulating the activity of the Wnt pathway. *J Cell Biol,* 207**,** 549-67.

AHRINGER, J. 2003. Control of cell polarity and mitotic spindle positioning in animal cells. *Curr Opin Cell Biol,* 15**,** 73-81.

ALAJEM, A., BIRAN, A., HARIKUMAR, A., SAILAJA, B. S., AARONSON, Y., LIVYATAN, I., NISSIM-RAFINIA, M., SOMMER, A. G., MOSTOSLAVSKY, G., GERBASI, V. R., GOLDEN, D. E., DATTA, A., SZE, S. K. & MESHORER, E. 2015. Differential Association of Chromatin Proteins Identifies BAF60a/SMARCD1 as a Regulator of Embryonic Stem Cell Differentiation. *Cell Rep,* 10**,** 2019-31.

ALFERT, A., MORENO, N. & KERL, K. 2019. The BAF complex in development and disease. *Epigenetics Chromatin,* 12**,** 19.

ALONSO, L. & FUCHS, E. 2006. The hair cycle. *J Cell Sci,* 119**,** 391-3.

ANDERSEN, H., MEJLVANG, J., MAHMOOD, S., GROMOVA, I., GROMOV, P., LUKANIDIN, E., KRIAJEVSKA, M., MELLON, J. K. & TULCHINSKY, E. 2005. Immediate and delayed effects of E-cadherin inhibition on gene regulation and cell motility in human epidermoid carcinoma cells. *Mol Cell Biol,* 25**,** 9138-50.

ANDL, T., AHN, K., KAIRO, A., CHU, E. Y., WINE-LEE, L., REDDY, S. T., CROFT, N. J., CEBRA-THOMAS, J. A., METZGER, D., CHAMBON, P., LYONS, K. M., MISHINA, Y., SEYKORA, J. T., CRENSHAW, E. B., 3RD & MILLAR, S. E. 2004. Epithelial Bmpr1a regulates differentiation and proliferation in postnatal hair follicles and is essential for tooth development. *Development,* 131**,** 2257-68.

ANDL, T., REDDY, S. T., GADDAPARA, T. & MILLAR, S. E. 2002. WNT signals are required for the initiation of hair follicle development. *Dev Cell,* 2**,** 643-53.

ANSELL, D. M., KLOEPPER, J. E., THOMASON, H. A., PAUS, R. & HARDMAN, M. J. 2011. Exploring the "hair growth-wound healing connection": anagen phase promotes wound re-epithelialization. *J Invest Dermatol,* 131**,** 518-28.

ARENDS, M. J., WHITE, E. S. & WHITELAW, C. B. 2016. Animal and cellular models of human disease. *J Pathol,* 238**,** 137-40.

ARI, H. H., KURU, N., USLU, S. & OZDEMIR, O. 2018. Morphological and Histological Study on the Foot Pads of the Anatolian Bobcat (Lynx lynx). *Anat Rec (Hoboken),* 301**,** 932-938.

ARNAUD, O., LE LOARER, F. & TIRODE, F. 2018. BAFfling pathologies: Alterations of BAF complexes in cancer. *Cancer Lett,* 419**,** 266-279.

BAE, W. K. & HENNIGHAUSEN, L. 2014. Canonical and non-canonical roles of the histone methyltransferase EZH2 in mammary development and cancer. *Mol Cell Endocrinol,* 382**,** 593-7.

BAJPAI, R., CHEN, D. A., RADA-IGLESIAS, A., ZHANG, J., XIONG, Y., HELMS, J., CHANG, C. P., ZHAO, Y., SWIGUT, T. & WYSOCKA, J. 2010. CHD7 cooperates with PBAF to control multipotent neural crest formation. *Nature,* 463**,** 958-62.

BANTIGNIES, F. & CAVALLI, G. 2011. Polycomb group proteins: repression in 3D. *Trends Genet,* 27**,** 454-64.

BAO, X., RUBIN, A. J., QU, K., ZHANG, J., GIRESI, P. G., CHANG, H. Y. & KHAVARI, P. A. 2015. A novel ATAC-seq approach reveals lineage-specific reinforcement of the open chromatin landscape via cooperation between BAF and p63. *Genome Biol,* 16**,** 284.

BAO, X., TANG, J., LOPEZ-PAJARES, V., TAO, S., QU, K., CRABTREE, G. R. & KHAVARI, P. A. 2013. ACTL6a enforces the epidermal progenitor state by suppressing SWI/SNF-dependent induction of KLF4. *Cell Stem Cell,* 12**,** 193-203.

BAO, Y. & SHEN, X. 2007. SnapShot: chromatin remodeling complexes. *Cell,* 129**,** 632.

BARDOT, E. S., VALDES, V. J., ZHANG, J., PERDIGOTO, C. N., NICOLIS, S., HEARN, S. A., SILVA, J. M. & EZHKOVA, E. 2013. Polycomb subunits Ezh1 and Ezh2 regulate the Merkel cell differentiation program in skin stem cells. *EMBO J,* 32**,** 1990-2000.

BARISIC, D., STADLER, M. B., IURLARO, M. & SCHUBELER, D. 2019. Mammalian ISWI and SWI/SNF selectively mediate binding of distinct transcription factors. *Nature,* 569**,** 136-140.

BARSKI, A., CUDDAPAH, S., CUI, K., ROH, T. Y., SCHONES, D. E., WANG, Z., WEI, G., CHEPELEV, I. & ZHAO, K. 2007. High-resolution profiling of histone methylations in the human genome. *Cell,* 129**,** 823-37.

BATLLE, E., SANCHO, E., FRANCI, C., DOMINGUEZ, D., MONFAR, M., BAULIDA, J. & GARCIA DE HERREROS, A. 2000. The transcription factor snail is a repressor of E-cadherin gene expression in epithelial tumour cells. *Nat Cell Biol,* 2**,** 84-9.

BIEGEL, J. A., ZHOU, J. Y., RORKE, L. B., STENSTROM, C., WAINWRIGHT, L. M. & FOGELGREN, B. 1999. Germ-line and acquired mutations of INI1 in atypical teratoid and rhabdoid tumors. *Cancer Res,* 59**,** 74-9.

BIKLE, D. D., XIE, Z. & TU, C. L. 2012. Calcium regulation of keratinocyte differentiation. *Expert Rev Endocrinol Metab,* 7**,** 461-472.

BINTU, L., YONG, J., ANTEBI, Y. E., MCCUE, K., KAZUKI, Y., UNO, N., OSHIMURA, M. & ELOWITZ, M. B. 2016. Dynamics of epigenetic regulation at the single-cell level. *Science,* 351**,** 720-4.

BLACKLEDGE, N. P., FARCAS, A. M., KONDO, T., KING, H. W., MCGOURAN, J. F., HANSSEN, L. L., ITO, S., COOPER, S., KONDO, K., KOSEKI, Y., ISHIKURA, T., LONG, H. K., SHEAHAN, T. W., BROCKDORFF, N., KESSLER, B. M., KOSEKI, H. & KLOSE, R. J. 2014. Variant PRC1 complex-dependent H2A ubiquitylation drives PRC2 recruitment and polycomb domain formation. *Cell,* 157**,** 1445-59.

BLANPAIN, C. & FUCHS, E. 2006. Epidermal stem cells of the skin. *Annu Rev Cell Dev Biol,* 22**,** 339-73.

BLANPAIN, C. & FUCHS, E. 2009. Epidermal homeostasis: a balancing act of stem cells in the skin. *Nat Rev Mol Cell Biol,* 10**,** 207-17.

BLANPAIN, C., LOWRY, W. E., GEOGHEGAN, A., POLAK, L. & FUCHS, E. 2004. Self-renewal, multipotency, and the existence of two cell populations within an epithelial stem cell niche. *Cell,* 118**,** 635-48.

BOCK, C., BEERMAN, I., LIEN, W. H., SMITH, Z. D., GU, H. C., BOYLE, P., GNIRKE, A., FUCHS, E., ROSSI, D. J. & MEISSNER, A. 2012. DNA Methylation Dynamics during In Vivo Differentiation of Blood and Skin Stem Cells. *Molecular Cell,* 47**,** 633-647.

BOTCHKAREV, V. A. 2003. Bone morphogenetic proteins and their antagonists in skin and hair follicle biology. *J Invest Dermatol,* 120**,** 36-47.

BOTCHKAREV, V. A., GDULA, M. R., MARDARYEV, A. N., SHAROV, A. A. & FESSING, M. Y. 2012. Epigenetic regulation of gene expression in keratinocytes. *J Invest Dermatol,* 132**,** 2505-21.

BOTCHKAREV, V. A. & MARDARYEV, A. N. 2016. Repressing the Keratinocyte Genome: How the Polycomb Complex Subunits Operate in Concert to Control Skin and Hair Follicle Development. *J Invest Dermatol,* 136**,** 1538-40.

BOULAIS, N. & MISERY, L. 2008. The epidermis: a sensory tissue. *Eur J Dermatol,* 18**,** 119-27.

BRANCO, M. R., FICZ, G. & REIK, W. 2012. Uncovering the role of 5-hydroxymethylcytosine in the epigenome. *Nat Rev Genet,* 13**,** 7-13.

BRECHALOV, A. V., GEORGIEVA, S. G. & SOSHNIKOVA, N. V. 2014. Mammalian cells contain two functionally distinct PBAF complexes incorporating different isoforms of PHF10 signature subunit. *Cell Cycle,* 13**,** 1970-1979.

BROUGHTON, G., 2ND, JANIS, J. E. & ATTINGER, C. E. 2006. The basic science of wound healing. *Plast Reconstr Surg,* 117**,** 12S-34S.

BROWNLEE, P. M., CHAMBERS, A. L., OLIVER, A. W. & DOWNS, J. A. 2012. Cancer and the bromodomains of BAF180. *Biochem Soc Trans,* 40**,** 364-9.

BULTMAN, S., GEBUHR, T., YEE, D., LA MANTIA, C., NICHOLSON, J., GILLIAM, A., RANDAZZO, F., METZGER, D., CHAMBON, P., CRABTREE, G. & MAGNUSON, T. 2000. A Brg1 null mutation in the mouse reveals functional differences among mammalian SWI/SNF complexes. *Mol Cell,* 6**,** 1287-95.

CABOT, B., TSENG, Y. C., CRODIAN, J. S. & CABOT, R. 2017. Differential expression of key subunits of SWI/SNF chromatin remodeling complexes in porcine embryos derived in vitro or in vivo. *Mol Reprod Dev,* 84**,** 1238-1249.

CAIRNS, B. R., KIM, Y. J., SAYRE, M. H., LAURENT, B. C. & KORNBERG, R. D. 1994. A multisubunit complex containing the SWI1/ADR6, SWI2/SNF2, SWI3, SNF5, and SNF6 gene products isolated from yeast. *Proc Natl Acad Sci U S A,* 91**,** 1950-4.

CAIRNS, B. R., LORCH, Y., LI, Y., ZHANG, M., LACOMIS, L., ERDJUMENT-BROMAGE, H., TEMPST, P., DU, J., LAURENT, B. & KORNBERG, R. D. 1996. RSC, an essential, abundant chromatin-remodeling complex. *Cell,* 87**,** 1249-60.

CALLAHAN, C. A., OFSTAD, T., HORNG, L., WANG, J. K., ZHEN, H. H., COULOMBE, P. A. & ORO, A. E. 2004. MIM/BEG4, a Sonic hedgehog-responsive gene that potentiates Gli-dependent transcription. *Genes Dev,* 18**,** 2724-9.

CAMPOS, E. I. & REINBERG, D. 2009. Histones: Annotating Chromatin. *Annual Review of Genetics,* 43**,** 559-599.

CANO, A., PEREZ-MORENO, M. A., RODRIGO, I., LOCASCIO, A., BLANCO, M. J., DEL BARRIO, M. G., PORTILLO, F. & NIETO, M. A. 2000. The transcription factor snail controls epithelial-mesenchymal transitions by repressing E-cadherin expression. *Nat Cell Biol,* 2**,** 76-83.

CAO, R. & ZHANG, Y. 2004. SUZ12 is required for both the histone methyltransferase activity and the silencing function of the EED-EZH2 complex. *Mol Cell,* 15**,** 57-67.

CARRASCO, E., CALVO, M. I., BLAZQUEZ-CASTRO, A., VECCHIO, D., ZAMARRON, A., DE ALMEIDA, I. J., STOCKERT, J. C., HAMBLIN, M. R., JUARRANZ, A. & ESPADA, J. 2015. Photoactivation of ROS Production In Situ Transiently Activates Cell Proliferation in Mouse Skin and in the Hair Follicle Stem Cell Niche Promoting Hair Growth and Wound Healing. *J Invest Dermatol,* 135**,** 2611-22.

CHEN, T. & DENT, S. Y. 2014. Chromatin modifiers and remodellers: regulators of cellular differentiation. *Nat Rev Genet,* 15**,** 93-106.

CHI, W. Y., ENSHELL-SEIJFFERS, D. & MORGAN, B. A. 2010. De novo production of dermal papilla cells during the anagen phase of the hair cycle. *J Invest Dermatol,* 130**,** 2664-6.

CICHOREK, M., WACHULSKA, M., STASIEWICZ, A. & TYMINSKA, A. 2013. Skin melanocytes: biology and development. *Postepy Dermatol Alergol,* 30**,** 30-41.

CLAPIER, C. R., IWASA, J., CAIRNS, B. R. & PETERSON, C. L. 2017. Mechanisms of action and regulation of ATP-dependent chromatin-remodelling complexes. *Nat Rev Mol Cell Biol,* 18**,** 407-422.

CONWAY, E., HEALY, E. & BRACKEN, A. P. 2015. PRC2 mediated H3K27 methylations in cellular identity and cancer. *Curr Opin Cell Biol,* 37**,** 42-8.

COOLEN, N. A., SCHOUTEN, K. C., MIDDELKOOP, E. & ULRICH, M. M. 2010. Comparison between human fetal and adult skin. *Arch Dermatol Res,* 302**,** 47-55.

COTSARELIS, G. 2006. Epithelial stem cells: a folliculocentric view. *J Invest Dermatol,* 126**,** 1459-68.

COULOMBE, P. A. 1997. Towards a molecular definition of keratinocyte activation after acute injury to stratified epithelia. *Biochem Biophys Res Commun,* 236**,** 231-8.

COULOMBE, P. A., BRAVO, N. S., PALADINI, R. D., NGUYEN, D. & TAKAHASHI, K. 1995. Overexpression of human keratin 16 produces a distinct skin phenotype in transgenic mouse skin. *Biochem Cell Biol,* 73**,** 611-8.

D'ORAZIO, J., JARRETT, S., AMARO-ORTIZ, A. & SCOTT, T. 2013. UV radiation and the skin. *Int J Mol Sci,* 14**,** 12222-48.

DAUBER, K. L., PERDIGOTO, C. N., VALDES, V. J., SANTORIELLO, F. J., COHEN, I. & EZHKOVA, E. 2016. Dissecting the Roles of Polycomb Repressive Complex 2 Subunits in the Control of Skin Development. *J Invest Dermatol,* 136**,** 1647-55.

DAVIDSON, K. C., ADAMS, A. M., GOODSON, J. M., MCDONALD, C. E., POTTER, J. C., BERNDT, J. D., BIECHELE, T. L., TAYLOR, R. J. & MOON, R. T. 2012. Wnt/beta-catenin signaling promotes differentiation, not self-renewal, of human embryonic stem cells and is repressed by Oct4. *Proc Natl Acad Sci U S A,* 109**,** 4485-90.

DE JONG, L. W., VIDAL, J. S., FORSBERG, L. E., ZIJDENBOS, A. P., HAIGHT, T., ALZHEIMER'S DISEASE NEUROIMAGING, I., SIGURDSSON, S., GUDNASON, V., VAN BUCHEM, M. A. & LAUNER, L. J. 2017. Allometric scaling of brain regions to intra-cranial volume: An epidemiological MRI study. *Hum Brain Mapp,* 38**,** 151-164.

DE SANTA, F., TOTARO, M. G., PROSPERINI, E., NOTARBARTOLO, S., TESTA, G. & NATOLI, G. 2007. The histone H3 lysine-27 demethylase Jmjd3 links inflammation to inhibition of polycomb-mediated gene silencing. *Cell,* 130**,** 1083-94.

DEBEER, S., LE LUDUEC, J. B., KAISERLIAN, D., LAURENT, P., NICOLAS, J. F., DUBOIS, B. & KANITAKIS, J. 2013. Comparative histology and immunohistochemistry of porcine versus human skin. *Eur J Dermatol,* 23**,** 456-66.

DECHASSA, M. L., ZHANG, B., HOROWITZ-SCHERER, R., PERSINGER, J., WOODCOCK, C. L., PETERSON, C. L. & BARTHOLOMEW, B. 2008. Architecture of the SWI/SNF-nucleosome complex. *Mol Cell Biol,* 28**,** 6010-21.

DELBOVE, J., ROSSON, G., STROBECK, M., CHEN, J., ARCHER, T. K., WANG, W., KNUDSEN, E. S. & WEISSMAN, B. E. 2011. Identification of a core member of the SWI/SNF complex, BAF155/SMARCC1, as a human tumor suppressor gene. *Epigenetics,* 6**,** 1444-53.

DHOUAILLY, D. 1973. Dermo-epidermal interactions between birds and mammals: differentiation of cutaneous appendages. *J Embryol Exp Morphol,* 30**,** 587-603.

DI-POI, N. & MILINKOVITCH, M. C. 2016. The anatomical placode in reptile scale morphogenesis indicates shared ancestry among skin appendages in amniotes. *Sci Adv,* 2**,** e1600708.

DI CROCE, L. & HELIN, K. 2013. Transcriptional regulation by Polycomb group proteins. *Nat Struct Mol Biol,* 20**,** 1147-55.

DORSKY, R. I., MOON, R. T. & RAIBLE, D. W. 1998. Control of neural crest cell fate by the Wnt signalling pathway. *Nature,* 396**,** 370-3.

DRISKELL, I., OEZTUERK-WINDER, F., HUMPHREYS, P. & FRYE, M. 2015. Genetically induced cell death in bulge stem cells reveals their redundancy for hair and epidermal regeneration. *Stem Cells,* 33**,** 988-98.

DRISKELL, R. R., CLAVEL, C., RENDL, M. & WATT, F. M. 2011. Hair follicle dermal papilla cells at a glance. *J Cell Sci,* 124**,** 1179-82.

DURMOWICZ, M. C., CUI, C. Y. & SCHLESSINGER, D. 2002. The EDA gene is a target of, but does not regulate Wnt signaling. *Gene,* 285**,** 203-11.

DUVERGER, O. & MORASSO, M. I. 2009. Epidermal patterning and induction of different hair types during mouse embryonic development. *Birth Defects Res C Embryo Today,* 87**,** 263-72.

EATON, K. W., TOOKE, L. S., WAINWRIGHT, L. M., JUDKINS, A. R. & BIEGEL, J. A. 2011. Spectrum of SMARCB1/INI1 mutations in familial and sporadic rhabdoid tumors. *Pediatr Blood Cancer,* 56**,** 7-15.

ELIAS, P. M., GRUBER, R., CRUMRINE, D., MENON, G., WILLIAMS, M. L., WAKEFIELD, J. S., HOLLERAN, W. M. & UCHIDA, Y. 2014. Formation and functions of the corneocyte lipid envelope (CLE). *Biochim Biophys Acta,* 1841**,** 314-8.

ERICKSON, J. R. & ECHEVERRI, K. 2018. Learning from regeneration research organisms: The circuitous road to scar free wound healing. *Dev Biol,* 433**,** 144-154.

EUSKIRCHEN, G., AUERBACH, R. K. & SNYDER, M. 2012. SWI/SNF chromatin-remodeling factors: multiscale analyses and diverse functions. *J Biol Chem,* 287**,** 30897-905.

EZHKOVA, E., LIEN, W. H., STOKES, N., PASOLLI, H. A., SILVA, J. M. & FUCHS, E. 2011. EZH1 and EZH2 cogovern histone H3K27 trimethylation and are essential for hair follicle homeostasis and wound repair. *Genes Dev,* 25**,** 485-98.

EZHKOVA, E., PASOLLI, H. A., PARKER, J. S., STOKES, N., SU, I. H., HANNON, G., TARAKHOVSKY, A. & FUCHS, E. 2009. Ezh2 orchestrates gene expression for the stepwise differentiation of tissue-specific stem cells. *Cell,* 136**,** 1122-35.

FACHINETTI, D., BERMEJO, R., COCITO, A., MINARDI, S., KATOU, Y., KANOH, Y., SHIRAHIGE, K., AZVOLINSKY, A., ZAKIAN, V. A. & FOIANI, M. 2010. Replication termination at eukaryotic chromosomes is mediated by Top2 and occurs at genomic loci containing pausing elements. *Mol Cell,* 39**,** 595-605.

FARNABY, W., KOEGL, M., ROY, M. J., WHITWORTH, C., DIERS, E., TRAINOR, N., ZOLLMAN, D., STEURER, S., KAROLYI-OEZGUER, J., RIEDMUELLER, C., GMASCHITZ, T., WACHTER, J., DANK, C., GALANT, M., SHARPS, B., RUMPEL, K., TRAXLER, E., GERSTBERGER, T., SCHNITZER, R., PETERMANN, O., GREB, P., WEINSTABL, H., BADER, G., ZOEPHEL, A., WEISS-PUXBAUM, A., EHRENHOFER-WOLFER, K., WOHRLE, S., BOEHMELT, G., RINNENTHAL, J., ARNHOF, H., WIECHENS, N., WU, M. Y., OWEN-HUGHES, T., ETTMAYER, P., PEARSON, M., MCCONNELL, D. B. & CIULLI, A. 2019. BAF

complex vulnerabilities in cancer demonstrated via structure-based PROTAC design. *Nat Chem Biol,* 15**,** 672-680.

FATHKE, C., WILSON, L., SHAH, K., KIM, B., HOCKING, A., MOON, R. & ISIK, F. 2006. Wnt signaling induces epithelial differentiation during cutaneous wound healing. *BMC Cell Biol,* 7**,** 4.

FENG, S., JACOBSEN, S. E. & REIK, W. 2010. Epigenetic reprogramming in plant and animal development. *Science,* 330**,** 622-7.

FERRAI, C., DE CASTRO, I. J., LAVITAS, L., CHOTALIA, M. & POMBO, A. 2010. Gene positioning. *Cold Spring Harb Perspect Biol,* 2**,** a000588.

FESSING, M. Y. 2014. Gene regulation at a distance: higher-order chromatin folding and the coordinated control of gene transcription at the epidermal differentiation complex locus. *J Invest Dermatol,* 134**,** 2307-10.

FESSING, M. Y., ATOYAN, R., SHANDER, B., MARDARYEV, A. N., BOTCHKAREV, V. V., JR., POTERLOWICZ, K., PENG, Y., EFIMOVA, T. & BOTCHKAREV, V. A. 2010. BMP signaling induces cell-type-specific changes in gene expression programs of human keratinocytes and fibroblasts. *J Invest Dermatol,* 130**,** 398-404.

FESSING, M. Y., MARDARYEV, A. N., GDULA, M. R., SHAROV, A. A., SHAROVA, T. Y., RAPISARDA, V., GORDON, K. B., SMORODCHENKO, A. D., POTERLOWICZ, K., FERONE, G., KOHWI, Y., MISSERO, C., KOHWI-SHIGEMATSU, T. & BOTCHKAREV, V. A. 2011. p63 regulates Satb1 to control tissue-specific chromatin remodeling during development of the epidermis. *J Cell Biol,* 194**,** 825-39.

FLOWERS, S., NAGL, N. G., JR., BECK, G. R., JR. & MORAN, E. 2009. Antagonistic roles for BRM and BRG1 SWI/SNF complexes in differentiation. *J Biol Chem,* 284**,** 10067-75.

FOLGUERAS, A. R., GUO, X., PASOLLI, H. A., STOKES, N., POLAK, L., ZHENG, D. & FUCHS, E. 2013. Architectural niche organization by LHX2 is linked to hair follicle stem cell function. *Cell Stem Cell,* 13**,** 314-27.

FORNI, M. F., TROMBETTA-LIMA, M. & SOGAYAR, M. C. 2012. Stem cells in embryonic skin development. *Biol Res,* 45**,** 215-22.

FRYE, M., FISHER, A. G. & WATT, F. M. 2007. Epidermal stem cells are defined by global histone modifications that are altered by Myc-induced differentiation. *PLoS One,* 2**,** e763.

FU, J. & HSU, W. 2013. Epidermal Wnt controls hair follicle induction by orchestrating dynamic signaling crosstalk between the epidermis and dermis. *J Invest Dermatol,* 133**,** 890-8.

FUCHS, E. 2007. Scratching the surface of skin development. *Nature,* 445**,** 834-42.

GAO, Z., ZHANG, J., BONASIO, R., STRINO, F., SAWAI, A., PARISI, F., KLUGER, Y. & REINBERG, D. 2012. PCGF homologs, CBX proteins, and RYBP define functionally distinct PRC1 family complexes. *Mol Cell,* 45**,** 344-56.

GAY, D., KWON, O., ZHANG, Z., SPATA, M., PLIKUS, M. V., HOLLER, P. D., ITO, M., YANG, Z., TREFFEISEN, E., KIM, C. D., NACE, A., ZHANG, X., BARATONO, S., WANG, F., ORNITZ, D. M., MILLAR, S. E. & COTSARELIS, G. 2013. Fgf9 from dermal gammadelta T cells induces hair follicle neogenesis after wounding. *Nat Med,* 19**,** 916-23.

GILHAR, A., PILLAR, T. & ETZIONI, A. 1988. The effect of topical cyclosporin on the immediate shedding of human scalp hair grafted onto nude mice. *Br J Dermatol,* 119**,** 767-70.

GILLIES, T. E. & CABERNARD, C. 2011. Cell division orientation in animals. *Curr Biol,* 21**,** R599-609.

GRECO, V., CHEN, T., RENDL, M., SCHOBER, M., PASOLLI, H. A., STOKES, N., DELA CRUZ-RACELIS, J. & FUCHS, E. 2009. A two-step mechanism for stem cell activation during hair regeneration. *Cell Stem Cell,* 4**,** 155-69.

GUENTHER, M. G., LEVINE, S. S., BOYER, L. A., JAENISCH, R. & YOUNG, R. A. 2007. A chromatin landmark and transcription initiation at most promoters in human cells. *Cell,* 130**,** 77-88.

GUO, X., KEYES, W. M., PAPAZOGLU, C., ZUBER, J., LI, W., LOWE, S. W., VOGEL, H. & MILLS, A. A. 2009. TAp63 induces senescence and suppresses tumorigenesis in vivo. *Nat Cell Biol,* 11**,** 1451-7.

GUPTA, A. C., CHAWLA, S., HEGDE, A., SINGH, D., BANDYOPADHYAY, B., LAKSHMANAN, C. C., KALSI, G. & GHOSH, S. 2018. Establishment of an in vitro organoid model of dermal papilla of human hair follicle. *J Cell Physiol,* 233**,** 9015-9030.

HAMMOND-MARTEL, I., YU, H. & AFFAR EL, B. 2012. Roles of ubiquitin signaling in transcription regulation. *Cell Signal,* 24**,** 410-21.

HAN, C., CUI, C., XING, X., LU, Z., ZHANG, J., LIU, J. & ZHANG, Y. 2019. Functions of intrinsic disorder in proteins involved in DNA demethylation during pre-implantation embryonic development. *Int J Biol Macromol,* 136**,** 962-979.

HANEL, K. H., PFAFF, C. M., CORNELISSEN, C., AMANN, P. M., MARQUARDT, Y., CZAJA, K., KIM, A., LUSCHER, B. & BARON, J. M. 2016. Control of the Physical and Antimicrobial Skin Barrier by an IL-31-IL-1 Signaling Network. *J Immunol,* 196**,** 3233-44.

HAO, Y., DU, Q., CHEN, X., ZHENG, Z., BALSBAUGH, J. L., MAITRA, S., SHABANOWITZ, J., HUNT, D. F. & MACARA, I. G. 2010. Par3 controls epithelial spindle orientation by aPKC-mediated phosphorylation of apical Pins. *Curr Biol,* 20**,** 1809-18.

HARSHMAN, S. W., CHEN, M. M., BRANSON, O. E., JACOB, N. K., JOHNSON, A. J., BYRD, J. C. & FREITAS, M. A. 2013. Isolation and analysis of linker histones across cellular compartments. *J Proteomics,* 91**,** 595-604.

HAWKSHAW, N. J., HARDMAN, J. A., HASLAM, I. S., SHAHMALAK, A., GILHAR, A., LIM, X. & PAUS, R. 2018. Identifying novel strategies for treating human hair loss disorders: Cyclosporine A suppresses the Wnt inhibitor, SFRP1, in the dermal papilla of human scalp hair follicles. *PLoS Biol,* 16**,** e2003705.

HAYNES, S. R., DOLLARD, C., WINSTON, F., BECK, S., TROWSDALE, J. & DAWID, I. B. 1992. The bromodomain: a conserved sequence found in human, Drosophila and yeast proteins. *Nucleic Acids Res,* 20**,** 2603.

HEBERT, J. M., ROSENQUIST, T., GOTZ, J. & MARTIN, G. R. 1994. FGF5 as a regulator of the hair growth cycle: evidence from targeted and spontaneous mutations. *Cell,* 78**,** 1017-25.

HELMING, K. C., WANG, X. & ROBERTS, C. W. 2014. Vulnerabilities of mutant SWI/SNF complexes in cancer. *Cancer Cell,* 26**,** 309-17.

HILL, C. S. 2016. Transcriptional Control by the SMADs. *Cold Spring Harb Perspect Biol,* 8.

HO, L., JOTHI, R., RONAN, J. L., CUI, K., ZHAO, K. & CRABTREE, G. R. 2009. An embryonic stem cell chromatin remodeling complex, esBAF, is an essential component of the core pluripotency transcriptional network. *Proc Natl Acad Sci U S A,* 106**,** 5187-91.

HODGES, C., KIRKLAND, J. G. & CRABTREE, G. R. 2016. The Many Roles of BAF (mSWI/SNF) and PBAF Complexes in Cancer. *Cold Spring Harb Perspect Med,* 6.

HOFFMAN, G. R., RAHAL, R., BUXTON, F., XIANG, K., MCALLISTER, G., FRIAS, E., BAGDASARIAN, L., HUBER, J., LINDEMAN, A., CHEN, D., ROMERO, R., RAMADAN, N., PHADKE, T., HAAS, K., JASKELIOFF, M., WILSON, B. G., MEYER, M. J., SAENZ-VASH, V., ZHAI, H., MYER, V. E., PORTER, J. A., KEEN, N., MCLAUGHLIN, M. E., MICKANIN, C., ROBERTS, C. W., STEGMEIER, F. & JAGANI, Z. 2014. Functional epigenetics approach identifies BRM/SMARCA2 as a critical synthetic lethal target in BRG1-deficient cancers. *Proc Natl Acad Sci U S A,* 111**,** 3128-33.

HOGAN, A. D. & BURKS, A. W. 1995. Epidermal Langerhans' cells and their function in the skin immune system. *Ann Allergy Asthma Immunol,* 75**,** 5-10; quiz 10-2.

HOHMANN, A. F. & VAKOC, C. R. 2014. A rationale to target the SWI/SNF complex for cancer therapy. *Trends Genet,* 30**,** 356-63.

HORSBURGH, S., FULLARD, N., ROGER, M., DEGNAN, A., TODRYK, S., PRZYBORSKI, S. & O'REILLY, S. 2017. MicroRNAs in the skin: role in development, homoeostasis and regeneration. *Clin Sci (Lond),* 131**,** 1923-1940.

HORSLEY, V., ALIPRANTIS, A. O., POLAK, L., GLIMCHER, L. H. & FUCHS, E. 2008. NFATc1 balances quiescence and proliferation of skin stem cells. *Cell,* 132**,** 299-310.

HSU, Y. C., PASOLLI, H. A. & FUCHS, E. 2011. Dynamics between stem cells, niche, and progeny in the hair follicle. *Cell,* 144**,** 92-105.

HUANG, X., GAO, X., DIAZ-TRELLES, R., RUIZ-LOZANO, P. & WANG, Z. 2008. Coronary development is regulated by ATP-dependent SWI/SNF chromatin remodeling component BAF180. *Dev Biol,* 319**,** 258-66.

HUH, S. H., NARHI, K., LINDFORS, P. H., HAARA, O., YANG, L., ORNITZ, D. M. & MIKKOLA, M. L. 2013. Fgf20 governs formation of primary and secondary dermal condensations in developing hair follicles. *Genes Dev,* 27**,** 450-8.

IHRIE, R. A. & ATTARDI, L. D. 2005. A new Perp in the lineup: linking p63 and desmosomal adhesion. *Cell Cycle,* 4**,** 873-6.

IKEUCHI, M., IWASE, A. & SUGIMOTO, K. 2015. Control of plant cell differentiation by histone modification and DNA methylation. *Current Opinion in Plant Biology,* 28**,** 60-67.

IKEYA, M., LEE, S. M., JOHNSON, J. E., MCMAHON, A. P. & TAKADA, S. 1997. Wnt signalling required for expansion of neural crest and CNS progenitors. *Nature,* 389**,** 966-70.

INDRA, A. K., DUPE, V., BORNERT, J. M., MESSADDEQ, N., YANIV, M., MARK, M., CHAMBON, P. & METZGER, D. 2005. Temporally controlled targeted somatic mutagenesis in embryonic surface ectoderm and fetal epidermal keratinocytes unveils two distinct developmental functions of BRG1 in limb morphogenesis and skin barrier formation. *Development,* 132**,** 4533-44.

INOUE, A. & ZHANG, Y. 2011. Replication-dependent loss of 5-hydroxymethylcytosine in mouse preimplantation embryos. *Science,* 334**,** 194.

ITO, M., LIU, Y., YANG, Z., NGUYEN, J., LIANG, F., MORRIS, R. J. & COTSARELIS, G. 2005. Stem cells in the hair follicle bulge contribute to wound repair but not to homeostasis of the epidermis. *Nat Med,* 11**,** 1351-4.

ITO, M. & SATO, Y. 1990. Dynamic ultrastructural changes of the connective tissue sheath of human hair follicles during hair cycle. *Arch Dermatol Res,* 282**,** 434-41.

ITO, M., YANG, Z., ANDL, T., CUI, C., KIM, N., MILLAR, S. E. & COTSARELIS, G. 2007. Wnt-dependent de novo hair follicle regeneration in adult mouse skin after wounding. *Nature,* 447**,** 316-20.

ITO, S., D'ALESSIO, A. C., TARANOVA, O. V., HONG, K., SOWERS, L. C. & ZHANG, Y. 2010. Role of Tet proteins in 5mC to 5hmC conversion, ES-cell self-renewal and inner cell mass specification. *Nature,* 466**,** 1129-33.

JAENISCH, R. & BIRD, A. 2003. Epigenetic regulation of gene expression: how the genome integrates intrinsic and environmental signals. *Nat Genet,* 33 Suppl**,** 245-54.

JAMORA, C., LEE, P., KOCIENIEWSKI, P., AZHAR, M., HOSOKAWA, R., CHAI, Y. & FUCHS, E. 2005. A signaling pathway involving TGF-beta2 and snail in hair follicle morphogenesis. *PLoS Biol,* 3**,** e11.

JAYADEV, R. & SHERWOOD, D. R. 2017. Basement membranes. *Curr Biol,* 27**,** R207-R211.

JELINIC, P., MUELLER, J. J., OLVERA, N., DAO, F., SCOTT, S. N., SHAH, R., GAO, J., SCHULTZ, N., GONEN, M., SOSLOW, R. A., BERGER, M. F. & LEVINE, D. A. 2014. Recurrent SMARCA4 mutations in small cell carcinoma of the ovary. *Nat Genet,* 46**,** 424-6.

JIMENJI, T., MATSUMURA, R., KORI, S. & ARITA, K. 2019. Structure of PCNA in complex with DNMT1 PIP box reveals the basis for the molecular mechanism of the interaction. *Biochem Biophys Res Commun*.

JOFFE, B., LEONHARDT, H. & SOLOVEI, I. 2010. Differentiation and large scale spatial organization of the genome. *Curr Opin Genet Dev,* 20**,** 562-9.

JOHNS, S. A., SOULLIER, S., RASHBASS, P. & CUNLIFFE, V. T. 2005. Foxn1 is required for tissue assembly and desmosomal cadherin expression in the hair shaft. *Dev Dyn,* 232**,** 1062-8.

JOHNSTON, M., NIKOLIC, A., NINKOVIC, N., GUILHAMON, P., CAVALLI, F., SEAMAN, S., ZEMP, F., LEE, J., ABDELKAREEM, A., ELLESTAD, K., MURISON, A., KUSHIDA, M., COUTINHO, F., MA, Y., MUNGALL, A., MOORE, R., MARRA, M., TAYLOR, M., DIRKS, P., PUGH, T., MORRISSY, S., ST CROIX, B., MAHONEY, D., LUPIEN, M. & GALLO, M. 2019. High-resolution structural genomics reveals new therapeutic vulnerabilities in glioblastoma. *Genome Res*.

JONES, P. A. 2012. Functions of DNA methylation: islands, start sites, gene bodies and beyond. *Nat Rev Genet,* 13**,** 484-92.

JOSHI, R. S. 2011. The Inner Root Sheath and the Men Associated with it Eponymically. *Int J Trichology,* 3**,** 57-62.

KADOCH, C., COPELAND, R. A. & KEILHACK, H. 2016. PRC2 and SWI/SNF Chromatin Remodeling Complexes in Health and Disease. *Biochemistry,* 55**,** 1600-14.

KADOCH, C. & CRABTREE, G. R. 2015. Mammalian SWI/SNF chromatin remodeling complexes and cancer: Mechanistic insights gained from human genomics. *Sci Adv,* 1**,** e1500447.

KADOCH, C., HARGREAVES, D. C., HODGES, C., ELIAS, L., HO, L., RANISH, J. & CRABTREE, G. R. 2013. Proteomic and bioinformatic analysis of mammalian SWI/SNF complexes identifies extensive roles in human malignancy. *Nat Genet,* 45**,** 592-601.

KALB, R., LATWIEL, S., BAYMAZ, H. I., JANSEN, P. W., MULLER, C. W., VERMEULEN, M. & MULLER, J. 2014. Histone H2A monoubiquitination promotes histone H3 methylation in Polycomb repression. *Nat Struct Mol Biol,* 21**,** 569-71.

KAUSER, S., WESTGATE, G. E., GREEN, M. R. & TOBIN, D. J. 2011. Human hair follicle and epidermal melanocytes exhibit striking differences in their aging profile which involves catalase. *J Invest Dermatol,* 131**,** 979-82.

KEYES, B. E., SEGAL, J. P., HELLER, E., LIEN, W. H., CHANG, C. Y., GUO, X. Y., ORISTIAN, D. S., ZHENG, D. Y. & FUCHS, E. 2013. Nfatc1 orchestrates aging in hair follicle stem cells. *Proceedings of the National Academy of Sciences of the United States of America,* 110**,** E4950-E4959.

KHORASANIZADEH, S. 2004. The nucleosome: from genomic organization to genomic regulation. *Cell,* 116**,** 259-72.

KIM, H., KANG, K. & KIM, J. 2009. AEBP2 as a potential targeting protein for Polycomb Repression Complex PRC2. *Nucleic Acids Res,* 37**,** 2940-50.

KIM, J. K., HUH, S. O., CHOI, H., LEE, K. S., SHIN, D., LEE, C., NAM, J. S., KIM, H., CHUNG, H., LEE, H. W., PARK, S. D. & SEONG, R. H. 2001. Srg3, a mouse homolog of yeast SWI3, is essential for early embryogenesis and involved in brain development. *Mol Cell Biol,* 21**,** 7787-95.

KIM, K. I., JEONG, D. S., JUNG, E. C., LEE, J. H., KIM, C. D. & YOON, T. J. 2016. Wnt/beta-catenin signaling inhibitor ICG-001 enhances pigmentation of cultured melanoma cells. *J Dermatol Sci*.

KLEIN, R. H., LIN, Z., HOPKIN, A. S., GORDON, W., TSOI, L. C., LIANG, Y., GUDJONSSON, J. E. & ANDERSEN, B. 2017. GRHL3 binding and enhancers rearrange as epidermal keratinocytes transition between functional states. *PLoS Genet,* 13**,** e1006745.

KLOCHENDLER-YEIVIN, A., FIETTE, L., BARRA, J., MUCHARDT, C., BABINET, C. & YANIV, M. 2000. The murine SNF5/INI1 chromatin remodeling factor is essential for embryonic development and tumor suppression. *EMBO Rep,* 1**,** 500-6.

KO, M., HUANG, Y., JANKOWSKA, A. M., PAPE, U. J., TAHILIANI, M., BANDUKWALA, H. S., AN, J., LAMPERTI, E. D., KOH, K. P., GANETZKY, R., LIU, X. S., ARAVIND, L., AGARWAL, S., MACIEJEWSKI, J. P. & RAO, A. 2010. Impaired hydroxylation of 5-methylcytosine in myeloid cancers with mutant TET2. *Nature,* 468**,** 839-43.

KOBIELAK, K., PASOLLI, H. A., ALONSO, L., POLAK, L. & FUCHS, E. 2003. Defining BMP functions in the hair follicle by conditional ablation of BMP receptor IA. *J Cell Biol,* 163**,** 609-23.

KOLEV, V., MANDINOVA, A., GUINEA-VINIEGRA, J., HU, B., LEFORT, K., LAMBERTINI, C., NEEL, V., DUMMER, R., WAGNER, E. F. & DOTTO, G. P. 2008. EGFR signalling as a negative regulator of Notch1 gene transcription and function in proliferating keratinocytes and cancer. *Nat Cell Biol,* 10**,** 902-11.

KORNBERG, R. D. 1974. Chromatin structure: a repeating unit of histones and DNA. *Science,* 184**,** 868-71.

KOSTER, M. I. 2010. p63 in skin development and ectodermal dysplasias. *J Invest Dermatol,* 130**,** 2352-8.

KOSTER, M. I., DAI, D., MARINARI, B., SANO, Y., COSTANZO, A., KARIN, M. & ROOP, D. R. 2007. p63 induces key target genes required for epidermal morphogenesis. *Proc Natl Acad Sci U S A,* 104**,** 3255-60.

KOSTER, M. I., KIM, S., HUANG, J., WILLIAMS, T. & ROOP, D. R. 2006. TAp63alpha induces AP-2gamma as an early event in epidermal morphogenesis. *Dev Biol,* 289**,** 253-61.

KOSTER, M. I. & ROOP, D. R. 2007. Mechanisms regulating epithelial stratification. *Annu Rev Cell Dev Biol,* 23**,** 93-113.

KRAUSE, K. & FOITZIK, K. 2006. Biology of the hair follicle: the basics. *Semin Cutan Med Surg,* 25**,** 2-10.

KUMARAN, R. I. & SPECTOR, D. L. 2008. A genetic locus targeted to the nuclear periphery in living cells maintains its transcriptional competence. *J Cell Biol,* 180**,** 51-65.

KVIST, J., GONCALVES ATHANASIO, C., SHAMS SOLARI, O., BROWN, J. B., COLBOURNE, J. K., PFRENDER, M. E. & MIRBAHAI, L. 2018. Pattern of DNA Methylation in Daphnia: Evolutionary Perspective. *Genome Biol Evol,* 10**,** 1988-2007.

KYPRIOTOU, M., HUBER, M. & HOHL, D. 2012. The human epidermal differentiation complex: cornified envelope precursors, S100 proteins and the 'fused genes' family. *Exp Dermatol,* 21**,** 643-9.

LAMOUILLE, S., XU, J. & DERYNCK, R. 2014. Molecular mechanisms of epithelial-mesenchymal transition. *Nat Rev Mol Cell Biol,* 15**,** 178-96.

LAN, J., LI, H., LUO, X., HU, J. & WANG, G. 2017. BRG1 promotes VEGF-A expression and angiogenesis in human colorectal cancer cells. *Exp Cell Res,* 360**,** 236-242.

LANGAN, E. A., PHILPOTT, M. P., KLOEPPER, J. E. & PAUS, R. 2015. Human hair follicle organ culture: theory, application and perspectives. *Exp Dermatol,* 24**,** 903-11.

LAURETTE, P., STRUB, T., KOLUDROVIC, D., KEIME, C., LE GRAS, S., SEBERG, H., VAN OTTERLOO, E., IMRICHOVA, H., SIDDAWAY, R., AERTS, S., CORNELL, R. A., MENGUS, G. & DAVIDSON, I. 2015. Transcription factor MITF and remodeller BRG1 define chromatin organisation at regulatory elements in melanoma cells. *Elife,* 4.

LAVKER, R. M. & SUN, T. T. 2000. Epidermal stem cells: properties, markers, and location. *Proc Natl Acad Sci U S A,* 97**,** 13473-5.

LAZARO-DIEGUEZ, F., COHEN, D., FERNANDEZ, D., HODGSON, L., VAN IJZENDOORN, S. C. & MUSCH, A. 2013. Par1b links lumen polarity with LGN-NuMA positioning for distinct epithelial cell division phenotypes. *J Cell Biol,* 203**,** 251-64.

LEBOEUF, M., TERRELL, A., TRIVEDI, S., SINHA, S., EPSTEIN, J. A., OLSON, E. N., MORRISEY, E. E. & MILLAR, S. E. 2010. Hdac1 and Hdac2 act redundantly to control p63 and p53 functions in epidermal progenitor cells. *Dev Cell,* 19**,** 807-18.

LECHLER, T. & FUCHS, E. 2005. Asymmetric cell divisions promote stratification and differentiation of mammalian skin. *Nature,* 437**,** 275-80.

LEE, J., BSCKE, R., TANG, P. C., HARTMAN, B. H., HELLER, S. & KOEHLER, K. R. 2018. Hair Follicle Development in Mouse Pluripotent Stem Cell-Derived Skin Organoids. *Cell Rep,* 22**,** 242-254.

LEE, M. G., VILLA, R., TROJER, P., NORMAN, J., YAN, K. P., REINBERG, D., DI CROCE, L. & SHIEKHATTAR, R. 2007. Demethylation of H3K27 regulates polycomb recruitment and H2A ubiquitination. *Science,* 318**,** 447-50.

LEHOCZKY, J. A., ROBERT, B. & TABIN, C. J. 2011. Mouse digit tip regeneration is mediated by fate-restricted progenitor cells. *Proc Natl Acad Sci U S A,* 108**,** 20609-14.

LEI, I., GAO, X., SHAM, M. H. & WANG, Z. 2012. SWI/SNF protein component BAF250a regulates cardiac progenitor cell differentiation by modulating chromatin accessibility during second heart field development. *J Biol Chem,* 287**,** 24255-62.

LESSARD, J., WU, J. I., RANISH, J. A., WAN, M., WINSLOW, M. M., STAAHL, B. T., WU, H., AEBERSOLD, R., GRAEF, I. A. & CRABTREE, G. R. 2007. An essential switch in subunit composition of a chromatin remodeling complex during neural development. *Neuron,* 55**,** 201-15.

LEWIS, C. J. 2013. Stem cell application in acute burn care and reconstruction. *J Wound Care,* 22**,** 7-8, 10, 12-6.

LEWIS, C. J., MARDARYEV, A. N., POTERLOWICZ, K., SHAROVA, T. Y., AZIZ, A., SHARPE, D. T., BOTCHKAREVA, N. V. & SHAROV, A. A. 2014. Bone morphogenetic protein signaling suppresses wound-induced skin repair by inhibiting keratinocyte proliferation and migration. *J Invest Dermatol,* 134**,** 827-837.

LEWIS, J. M., BURGLER, C. D., FREUDZON, M., GOLUBETS, K., GIBSON, J. F., FILLER, R. B. & GIRARDI, M. 2015. Langerhans Cells Facilitate UVB-Induced Epidermal Carcinogenesis. *J Invest Dermatol,* 135**,** 2824-33.

LI, B., ZHOU, J., LIU, P., HU, J., JIN, H., SHIMONO, Y., TAKAHASHI, M. & XU, G. 2007a. Polycomb protein Cbx4 promotes SUMO modification of de novo DNA methyltransferase Dnmt3a. *Biochem J,* 405**,** 369-78.

LI, E., BESTOR, T. H. & JAENISCH, R. 1992. Targeted mutation of the DNA methyltransferase gene results in embryonic lethality. *Cell,* 69**,** 915-26.

LI, G., MARGUERON, R., KU, M., CHAMBON, P., BERNSTEIN, B. E. & REINBERG, D. 2010. Jarid2 and PRC2, partners in regulating gene expression. *Genes Dev,* 24**,** 368-80.

LI, J., CHEN, J. & KIRSNER, R. 2007b. Pathophysiology of acute wound healing. *Clin Dermatol,* 25**,** 9-18.

LI, S., SHEN, L. & CHEN, K. N. 2018. Association between H3K4 methylation and cancer prognosis: A meta-analysis. *Thorac Cancer,* 9**,** 794-799.

LI, Y. Q., ZHOU, P. Z., ZHENG, X. D., WALSH, C. P. & XU, G. L. 2007c. Association of Dnmt3a and thymine DNA glycosylase links DNA methylation with base-excision repair. *Nucleic Acids Res,* 35**,** 390-400.

LIANG, C. C., PARK, A. Y. & GUAN, J. L. 2007. In vitro scratch assay: a convenient and inexpensive method for analysis of cell migration in vitro. *Nat Protoc,* 2**,** 329-33.

LICKERT, H., TAKEUCHI, J. K., VON BOTH, I., WALLS, J. R., MCAULIFFE, F., ADAMSON, S. L., HENKELMAN, R. M., WRANA, J. L., ROSSANT, J. & BRUNEAU, B. G. 2004. Baf60c is essential for function of BAF chromatin remodelling complexes in heart development. *Nature,* 432**,** 107-12.

LINDNER, G., BOTCHKAREV, V. A., BOTCHKAREVA, N. V., LING, G., VAN DER VEEN, C. & PAUS, R. 1997. Analysis of apoptosis during hair follicle regression (catagen). *Am J Pathol,* 151**,** 1601-17.

LIU, S., AAGEAARD, A., BECHSGAARD, J. & BILDE, T. 2019a. DNA Methylation Patterns in the Social Spider, Stegodyphus dumicola. *Genes (Basel),* 10.

LIU, S., ZHANG, H. & DUAN, E. 2013. Epidermal development in mammals: key regulators, signals from beneath, and stem cells. *Int J Mol Sci,* 14**,** 10869-95.

LIU, Y., XU, S., ZU, T., LI, F., SANG, S., LIU, C., AN, Y., MI, B., ORGILL, D. P., MURPHY, G. F. & LIAN, C. G. 2019b. Reversal of TET-mediated 5-hmC loss in hypoxic fibroblasts by ascorbic acid. *Lab Invest*.

LO CELSO, C., PROWSE, D. M. & WATT, F. M. 2004. Transient activation of beta-catenin signalling in adult mouse epidermis is sufficient to induce new hair follicles but continuous activation is required to maintain hair follicle tumours. *Development,* 131**,** 1787-99.

LOSCHKE, F., HOMBERG, M. & MAGIN, T. M. 2016. Keratin Isotypes Control Desmosome Stability and Dynamics through PKCalpha. *J Invest Dermatol,* 136**,** 202-13.

LUDWIGSEN, J., KLINKER, H. & MUELLER-PLANITZ, F. 2013. No need for a power stroke in ISWI-mediated nucleosome sliding. *EMBO Rep,* 14**,** 1092-7.

LUGER, K., MADER, A. W., RICHMOND, R. K., SARGENT, D. F. & RICHMOND, T. J. 1997. Crystal structure of the nucleosome core particle at 2.8 A resolution. *Nature,* 389**,** 251-60.

LUIS, N. M., MOREY, L., MEJETTA, S., PASCUAL, G., JANICH, P., KUEBLER, B., COZUTTO, L., ROMA, G., NASCIMENTO, E., FRYE, M., DI CROCE, L. & BENITAH, S. A. 2011. Regulation of human epidermal stem cell proliferation and senescence requires polycomb- dependent and -independent functions of Cbx4. *Cell Stem Cell,* 9**,** 233-46.

LUSSER, A. & KADONAGA, J. T. 2003. Chromatin remodeling by ATP-dependent molecular machines. *Bioessays,* 25**,** 1192-200.

MA, L., LIU, J., WU, T., PLIKUS, M., JIANG, T. X., BI, Q., LIU, Y. H., MULLER-ROVER, S., PETERS, H., SUNDBERG, J. P., MAXSON, R., MAAS, R. L. & CHUONG, C. M. 2003. 'Cyclic

alopecia' in Msx2 mutants: defects in hair cycling and hair shaft differentiation. *Development,* 130**,** 379-89.

MACDONALD, B. T. & HE, X. 2012. Frizzled and LRP5/6 receptors for Wnt/beta-catenin signaling. *Cold Spring Harb Perspect Biol,* 4.

MAHAJAN, M. A., DAS, S., ZHU, H., TOMIC-CANIC, M. & SAMUELS, H. H. 2004. The nuclear hormone receptor coactivator NRC is a pleiotropic modulator affecting growth, development, apoptosis, reproduction, and wound repair. *Mol Cell Biol,* 24**,** 4994-5004.

MAISON, C., QUIVY, J. P., PROBST, A. V. & ALMOUZNI, G. 2010. Heterochromatin at mouse pericentromeres: a model for de novo heterochromatin formation and duplication during replication. *Cold Spring Harb Symp Quant Biol,* 75**,** 155-65.

MAITI, A. & DROHAT, A. C. 2011. Thymine DNA glycosylase can rapidly excise 5-formylcytosine and 5-carboxylcytosine: potential implications for active demethylation of CpG sites. *J Biol Chem,* 286**,** 35334-8.

MARDARYEV, A. N., GDULA, M. R., YARKER, J. L., EMELIANOV, V. U., POTERLOWICZ, K., SHAROV, A. A., SHAROVA, T. Y., SCARPA, J. A., JOFFE, B., SOLOVEI, I., CHAMBON, P., BOTCHKAREV, V. A. & FESSING, M. Y. 2014. p63 and Brg1 control developmentally regulated higher-order chromatin remodelling at the epidermal differentiation complex locus in epidermal progenitor cells. *Development,* 141**,** 101-11.

MARDARYEV, A. N., LIU, B., RAPISARDA, V., POTERLOWICZ, K., MALASHCHUK, I., RUDOLF, J., SHAROV, A. A., JAHODA, C. A., FESSING, M. Y., BENITAH, S. A., XU, G. L. & BOTCHKAREV, V. A. 2016. Cbx4 maintains the epithelial lineage identity and cell proliferation in the developing stratified epithelium. *J Cell Biol,* 212**,** 77-89.

MARDARYEV, A. N., MEIER, N., POTERLOWICZ, K., SHAROV, A. A., SHAROVA, T. Y., AHMED, M. I., RAPISARDA, V., LEWIS, C., FESSING, M. Y., RUENGER, T. M., BHAWAN, J., WERNER, S., PAUS, R. & BOTCHKAREV, V. A. 2011. Lhx2 differentially regulates Sox9, Tcf4 and Lgr5 in hair follicle stem cells to promote epidermal regeneration after injury. *Development,* 138**,** 4843-52.

MARICICH, S. M., WELLNITZ, S. A., NELSON, A. M., LESNIAK, D. R., GERLING, G. J., LUMPKIN, E. A. & ZOGHBI, H. Y. 2009. Merkel cells are essential for light-touch responses. *Science,* 324**,** 1580-2.

MARKOVA, N. G., KARAMAN-JURUKOVSKA, N., PINKAS-SARAFOVA, A., MAREKOV, L. N. & SIMON, M. 2007. Inhibition of histone deacetylation promotes abnormal epidermal differentiation and specifically suppresses the expression of the late differentiation marker profilaggrin. *Journal of Investigative Dermatology,* 127**,** 1126-1139.

MARTHALER, A. M., PODGORSKA, M., FELD, P., FINGERLE, A., KNERR-RUPP, K., GRASSER, F., SMOLA, H., ROEMER, K., EBERT, E., KIM, Y. J., BOHLE, R. M., MULLER, C. S. L., REICHRATH, J., VOGT, T., MALEJCZYK, M., MAJEWSKI, S. & SMOLA, S. 2017. Identification of C/EBPalpha as a novel target of the HPV8 E6 protein regulating miR-203 in human keratinocytes. *PLoS Pathog,* 13**,** e1006406.

MARTIN, P. 1997. Wound healing--aiming for perfect skin regeneration. *Science,* 276**,** 75-81.

MAZZALUPO, S., WONG, P., MARTIN, P. & COULOMBE, P. A. 2003. Role for keratins 6 and 17 during wound closure in embryonic mouse skin. *Dev Dyn,* 226**,** 356-65.

MCBRIDE, M. J., PULICE, J. L., BEIRD, H. C., INGRAM, D. R., D'AVINO, A. R., SHERN, J. F., CHARVILLE, G. W., HORNICK, J. L., NAKAYAMA, R. T., GARCIA-RIVERA, E. M., ARAUJO, D. M., WANG, W. L., TSAI, J. W., YEAGLEY, M., WAGNER, A. J., FUTREAL, P. A., KHAN, J., LAZAR, A. J. & KADOCH, C. 2018. The SS18-SSX Fusion Oncoprotein Hijacks BAF Complex Targeting and Function to Drive Synovial Sarcoma. *Cancer Cell,* 33**,** 1128-1141 e7.

MCCLOY, R. A., ROGERS, S., CALDON, C. E., LORCA, T., CASTRO, A. & BURGESS, A. 2014. Partial inhibition of Cdk1 in G 2 phase overrides the SAC and decouples mitotic events. *Cell Cycle,* 13**,** 1400-12.

MEDICI, D., HAY, E. D. & OLSEN, B. R. 2008. Snail and Slug promote epithelial-mesenchymal transition through beta-catenin-T-cell factor-4-dependent expression of transforming growth factor-beta3. *Mol Biol Cell,* 19**,** 4875-87.

MEHTA, G., KUMARASAMY, S., WU, J., WALSH, A., LIU, L., WILLIAMS, K., JOE, B. & DE LA SERNA, I. L. 2015. MITF interacts with the SWI/SNF subunit, BRG1, to promote GATA4 expression in cardiac hypertrophy. *J Mol Cell Cardiol,* 88**,** 101-10.

MIKKOLA, M. L. & THESLEFF, I. 2003. Ectodysplasin signaling in development. *Cytokine Growth Factor Rev,* 14**,** 211-24.

MILL, P., MO, R., FU, H., GRACHTCHOUK, M., KIM, P. C., DLUGOSZ, A. A. & HUI, C. C. 2003. Sonic hedgehog-dependent activation of Gli2 is essential for embryonic hair follicle development. *Genes Dev,* 17**,** 282-94.

MILLAR, S. E. 2002. Molecular mechanisms regulating hair follicle development. *J Invest Dermatol,* 118**,** 216-25.

MILLS, A. A., ZHENG, B., WANG, X. J., VOGEL, H., ROOP, D. R. & BRADLEY, A. 1999. p63 is a p53 homologue required for limb and epidermal morphogenesis. *Nature,* 398**,** 708-13.

MITCHISON, T. J. & CRAMER, L. P. 1996. Actin-based cell motility and cell locomotion. *Cell,* 84**,** 371-9.

MITEVA, M. & TOSTI, A. 2013. Dermatoscopy of hair shaft disorders. *J Am Acad Dermatol,* 68**,** 473-81.

MOHAMAD HANIF, E. A. & SHAH, S. A. 2018. Overview on Epigenetic Re-programming: A Potential Therapeutic Intervention in Triple Negative Breast Cancers. *Asian Pac J Cancer Prev,* 19**,** 3341-3351.

MOLNAR, C., LOPEZ-VAREA, A., HERNANDEZ, R. & DE CELIS, J. F. 2006. A gain-of-function screen identifying genes required for vein formation in the Drosophila melanogaster wing. *Genetics,* 174**,** 1635-59.

MORRISON, E. A., SANCHEZ, J. C., RONAN, J. L., FARRELL, D. P., VARZAVAND, K., JOHNSON, J. K., GU, B. X., CRABTREE, G. R. & MUSSELMAN, C. A. 2017. DNA binding drives the association of BRG1/hBRM bromodomains with nucleosomes. *Nat Commun,* 8**,** 16080.

MORT, R. L., JACKSON, I. J. & PATTON, E. E. 2015. The melanocyte lineage in development and disease. *Development,* 142**,** 1387.

MUKHOPADHYAY, A., KRISHNASWAMI, S. R., COWING-ZITRON, C., HUNG, N. J., REILLY-RHOTEN, H., BURNS, J. & YU, B. D. 2013. Negative regulation of Shh levels by Kras and Fgfr2 during hair follicle development. *Dev Biol,* 373**,** 373-82.

MULLER-ROVER, S., HANDJISKI, B., VAN DER VEEN, C., EICHMULLER, S., FOITZIK, K., MCKAY, I. A., STENN, K. S. & PAUS, R. 2001. A comprehensive guide for the accurate classification of murine hair follicles in distinct hair cycle stages. *J Invest Dermatol,* 117**,** 3-15.

MURAKAMI, Y. 2019. Phosphorylation of repressive histone code readers by casein kinase 2 plays diverse roles in heterochromatin regulation. *J Biochem,* 166**,** 3-6.

MYERS, S. R., LEIGH, I. M. & NAVSARIA, H. 2007. Epidermal repair results from activation of follicular and epidermal progenitor keratinocytes mediated by a growth factor cascade. *Wound Repair Regen,* 15**,** 693-701.

NAKAMURA, M., RIKIMARU, T., YANO, T., MOORE, K. G., PULA, P. J., SCHOFIELD, B. H. & DANNENBERG, A. M., JR. 1990. Full-thickness human skin explants for testing the toxicity of topically applied chemicals. *J Invest Dermatol,* 95**,** 325-32.

NAKAYAMA, R. T., PULICE, J. L., VALENCIA, A. M., MCBRIDE, M. J., MCKENZIE, Z. M., GILLESPIE, M. A., KU, W. L., TENG, M., CUI, K., WILLIAMS, R. T., CASSEL, S. H., QING, H., WIDMER, C. J., DEMETRI, G. D., IRIZARRY, R. A., ZHAO, K., RANISH, J. A. &

KADOCH, C. 2017. SMARCB1 is required for widespread BAF complex-mediated activation of enhancers and bivalent promoters. *Nat Genet,* 49**,** 1613-1623.

NARUSE, T., AOKI, M., FUJIMOTO, N., ARASE, S., OURA, H., UEDA, Y. & IKEDA, A. 2017. Novel ALK5 inhibitor TP0427736 reduces TGF-betainduced growth inhibition in human outer root sheath cells and elongates anagen phase in mouse hair follicles. *Pharmacol Rep,* 69**,** 485-491.

NATARAJAN, V. T., GANJU, P., RAMKUMAR, A., GROVER, R. & GOKHALE, R. S. 2014. Multifaceted pathways protect human skin from UV radiation. *Nat Chem Biol,* 10**,** 542-51.

NAUMOVA, N. & DEKKER, J. 2010. Integrating one-dimensional and three-dimensional maps of genomes. *J Cell Sci,* 123**,** 1979-88.

NEMER, G. & NEMER, M. 2003. Transcriptional activation of BMP-4 and regulation of mammalian organogenesis by GATA-4 and -6. *Dev Biol,* 254**,** 131-48.

NGUYEN, B. P., GIL, S. G. & CARTER, W. G. 2000. Deposition of laminin 5 by keratinocytes regulates integrin adhesion and signaling. *J Biol Chem,* 275**,** 31896-907.

NODELMAN, I. M. & BOWMAN, G. D. 2013. Nucleosome sliding by Chd1 does not require rigid coupling between DNA-binding and ATPase domains. *EMBO Rep,* 14**,** 1098-103.

O'BRIEN, M. E., CHANDRA, D., WILSON, R. C., KAROLESKI, C. M., FUHRMAN, C. R., LEADER, J. K., PU, J., ZHANG, Y., MORRIS, A., NOURAIE, S., BON, J., URBAN, Z. & SCIURBA, F. C. 2019. Loss of skin elasticity is associated with pulmonary emphysema, biomarkers of inflammation, and matrix metalloproteinase activity in smokers. *Respir Res,* 20**,** 128.

OH, J. K., KWON, O. S., KIM, M. H., JO, S. J., HAN, J. H., KIM, K. H., EUN, H. C. & CHUNG, J. H. 2012. Connective tissue sheath of hair follicle is a major source of dermal type I procollagen in human scalp. *J Dermatol Sci,* 68**,** 194-7.

OH, J. W., KLOEPPER, J., LANGAN, E. A., KIM, Y., YEO, J., KIM, M. J., HSI, T. C., ROSE, C., YOON, G. S., LEE, S. J., SEYKORA, J., KIM, J. C., SUNG, Y. K., KIM, M., PAUS, R. & PLIKUS, M. V. 2016. A Guide to Studying Human Hair Follicle Cycling In Vivo. *J Invest Dermatol,* 136**,** 34-44.

OH, W. J., RISHI, V., OROSZ, A., GERDES, M. J. & VINSON, C. 2007. Inhibition of CCAAT/enhancer binding protein family DNA binding in mouse epidermis prevents and regresses papillomas. *Cancer Res,* 67**,** 1867-76.

OKANO, M., BELL, D. W., HABER, D. A. & LI, E. 1999. DNA methyltransferases Dnmt3a and Dnmt3b are essential for de novo methylation and mammalian development. *Cell,* 99**,** 247-57.

OLIVERA-MARTINEZ, I., VIALLET, J. P., MICHON, F., PEARTON, D. J. & DHOUAILLY, D. 2004. The different steps of skin formation in vertebrates. *Int J Dev Biol,* 48**,** 107-15.

ONDRUSOVA, L., VACHTENHEIM, J., REDA, J., ZAKOVA, P. & BENKOVA, K. 2013. MITF-independent pro-survival role of BRG1-containing SWI/SNF complex in melanoma cells. *PLoS One,* 8**,** e54110.

ORZECHOWSKA, B., PABIJAN, J., WILTOWSKA-ZUBER, J., ZEMLA, J. & LEKKA, M. 2018. Fibroblasts change spreading capability and mechanical properties in a direct interaction with keratinocytes in conditions mimicking wound healing. *J Biomech,* 74**,** 134-142.

OSHIMA, H., ROCHAT, A., KEDZIA, C., KOBAYASHI, K. & BARRANDON, Y. 2001. Morphogenesis and renewal of hair follicles from adult multipotent stem cells. *Cell,* 104**,** 233-45.

PANAMAROVA, M., COX, A., WICHER, K. B., BUTLER, R., BULGAKOVA, N., JEON, S., ROSEN, B., SEONG, R. H., SKARNES, W., CRABTREE, G. & ZERNICKA-GOETZ, M. 2016. The BAF chromatin remodelling complex is an epigenetic regulator of lineage specification in the early mouse embryo. *Development,* 143**,** 1271-83.

PANCHISION, D. M., PICKEL, J. M., STUDER, L., LEE, S. H., TURNER, P. A., HAZEL, T. G. & MCKAY, R. D. 2001. Sequential actions of BMP receptors control neural precursor cell production and fate. *Genes Dev,* 15**,** 2094-110.

PAULSEN, J., LIYAKAT ALI, T. M., NEKRASOV, M., DELBARRE, E., BAUDEMENT, M. O., KURSCHEID, S., TREMETHICK, D. & COLLAS, P. 2019. Long-range interactions between topologically associating domains shape the four-dimensional genome during differentiation. *Nat Genet,* 51**,** 835-843.

PAUS, R. & COTSARELIS, G. 1999. The biology of hair follicles. *N Engl J Med,* 341**,** 491-7.

PAUS, R., HASLAM, I. S., SHAROV, A. A. & BOTCHKAREV, V. A. 2013. Pathobiology of chemotherapy-induced hair loss. *Lancet Oncol,* 14**,** e50-9.

PERDIGOTO, C. N., VALDES, V. J., BARDOT, E. S. & EZHKOVA, E. 2014. Epigenetic Regulation of Epidermal Differentiation. *Cold Spring Harbor Perspectives in Medicine,* 4.

PHELAN, M. L., SIF, S., NARLIKAR, G. J. & KINGSTON, R. E. 1999. Reconstitution of a core chromatin remodeling complex from SWI/SNF subunits. *Mol Cell,* 3**,** 247-53.

PHILPOTT, M. P., SANDERS, D. A. & KEALEY, T. 1996. Whole hair follicle culture. *Dermatol Clin,* 14**,** 595-607.

PILCHER, B. K., WANG, M., QIN, X. J., PARKS, W. C., SENIOR, R. M. & WELGUS, H. G. 1999. Role of matrix metalloproteinases and their inhibition in cutaneous wound healing and allergic contact hypersensitivity. *Ann N Y Acad Sci,* 878**,** 12-24.

PLASARI, G., EDELMANN, S., HOGGER, F., DUSSERRE, Y., MERMOD, N. & CALABRESE, A. 2010. Nuclear factor I-C regulates TGF-{beta}-dependent hair follicle cycling. *J Biol Chem,* 285**,** 34115-25.

PLIKUS, M. V., GAY, D. L., TREFFEISEN, E., WANG, A., SUPAPANNACHART, R. J. & COTSARELIS, G. 2012. Epithelial stem cells and implications for wound repair. *Seminars in Cell & Developmental Biology,* 23**,** 946-953.

PLIKUS, M. V., GUERRERO-JUAREZ, C. F., TREFFEISEN, E. & GAY, D. L. 2015. Epigenetic control of skin and hair regeneration after wounding. *Exp Dermatol,* 24**,** 167-70.

PLYS, A. J., DAVIS, C. P., KIM, J., RIZKI, G., KEENEN, M. M., MARR, S. K. & KINGSTON, R. E. 2019. Phase separation of Polycomb-repressive complex 1 is governed by a charged disordered region of CBX2. *Genes Dev,* 33**,** 799-813.

POONPERM, R., TAKATA, H., HAMANO, T., MATSUDA, A., UCHIYAMA, S., HIRAOKA, Y. & FUKUI, K. 2015. Chromosome Scaffold is a Double-Stranded Assembly of Scaffold Proteins. *Sci Rep,* 5**,** 11916.

POULSON, N. D. & LECHLER, T. 2010. Robust control of mitotic spindle orientation in the developing epidermis. *J Cell Biol,* 191**,** 915-22.

POWELL, B. C., PASSMORE, E. A., NESCI, A. & DUNN, S. M. 1998. The Notch signalling pathway in hair growth. *Mech Dev,* 78**,** 189-92.

PUMMILA, M., FLINIAUX, I., JAATINEN, R., JAMES, M. J., LAURIKKALA, J., SCHNEIDER, P., THESLEFF, I. & MIKKOLA, M. L. 2007. Ectodysplasin has a dual role in ectodermal organogenesis: inhibition of Bmp activity and induction of Shh expression. *Development,* 134**,** 117-25.

PURBA, T. S., BRUNKEN, L., HAWKSHAW, N. J., PEAKE, M., HARDMAN, J. & PAUS, R. 2016. A primer for studying cell cycle dynamics of the human hair follicle. *Exp Dermatol,* 25**,** 663-8.

QADIR, M. I. & ANWER, F. 2019. Epigenetic Modification Related to Acetylation of Histone and Methylation of DNA as a Key Player in Immunological Disorders. *Crit Rev Eukaryot Gene Expr,* 29**,** 1-15.

RAAB, J. R., RUNGE, J. S., SPEAR, C. C. & MAGNUSON, T. 2017. Co-regulation of transcription by BRG1 and BRM, two mutually exclusive SWI/SNF ATPase subunits. *Epigenetics Chromatin,* 10**,** 62.

RAMOS-E-SILVA, M. & PIRMEZ, R. 2014. Red face revisited: Disorders of hair growth and the pilosebaceous unit. *Clin Dermatol,* 32**,** 784-99.

RAMOS, P. M. & MIOT, H. A. 2015. Female Pattern Hair Loss: a clinical and pathophysiological review. *An Bras Dermatol,* 90**,** 529-43.

RAY, S. & LECHLER, T. 2011. Regulation of asymmetric cell division in the epidermis. *Cell Div,* 6**,** 12.

REIK, W. 2007. Stability and flexibility of epigenetic gene regulation in mammalian development. *Nature,* 447**,** 425-32.

REINKE, J. M. & SORG, H. 2012. Wound repair and regeneration. *Eur Surg Res,* 49**,** 35-43.

RENDINA, R., STRANGI, A., AVALLONE, B. & GIORDANO, E. 2010. Bap170, a subunit of the Drosophila PBAP chromatin remodeling complex, negatively regulates the EGFR signaling. *Genetics,* 186**,** 167-81.

RENDL, M., POLAK, L. & FUCHS, E. 2008. BMP signaling in dermal papilla cells is required for their hair follicle-inductive properties. *Genes Dev,* 22**,** 543-57.

REYES, J. C., BARRA, J., MUCHARDT, C., CAMUS, A., BABINET, C. & YANIV, M. 1998. Altered control of cellular proliferation in the absence of mammalian brahma (SNF2alpha). *EMBO J,* 17**,** 6979-91.

RHEE, H., POLAK, L. & FUCHS, E. 2006. Lhx2 maintains stem cell character in hair follicles. *Science,* 312**,** 1946-9.

RICHARDSON, G. D., BAZZI, H., FANTAUZZO, K. A., WATERS, J. M., CRAWFORD, H., HYND, P., CHRISTIANO, A. M. & JAHODA, C. A. 2009. KGF and EGF signalling block hair follicle induction and promote interfollicular epidermal fate in developing mouse skin. *Development,* 136**,** 2153-64.

RICHLY, H., ROCHA-VIEGAS, L., RIBEIRO, J. D., DEMAJO, S., GUNDEM, G., LOPEZ-BIGAS, N., NAKAGAWA, T., ROSPERT, S., ITO, T. & DI CROCE, L. 2010. Transcriptional activation of polycomb-repressed genes by ZRF1. *Nature,* 468**,** 1124-8.

RIISING, E. M., COMET, I., LEBLANC, B., WU, X., JOHANSEN, J. V. & HELIN, K. 2014. Gene silencing triggers polycomb repressive complex 2 recruitment to CpG islands genome wide. *Mol Cell,* 55**,** 347-60.

RISHI, V., BHATTACHARYA, P., CHATTERJEE, R., ROZENBERG, J., ZHAO, J., GLASS, K., FITZGERALD, P. & VINSON, C. 2010. CpG methylation of half-CRE sequences creates C/EBPalpha binding sites that activate some tissue-specific genes. *Proc Natl Acad Sci U S A,* 107**,** 20311-6.

RISHIKAYSH, P., DEV, K., DIAZ, D., QURESHI, W. M., FILIP, S. & MOKRY, J. 2014. Signaling involved in hair follicle morphogenesis and development. *Int J Mol Sci,* 15**,** 1647-70.

RITTIE, L. 2016. Cellular mechanisms of skin repair in humans and other mammals. *J Cell Commun Signal,* 10**,** 103-20.

RIVAS, M. P., AGUIAR, T. F. M., FERNANDES, G. R., CAIRES-JUNIOR, L. C., GOULART, E., TELLES-SILVA, K. A., CYPRIANO, M., DE TOLEDO, S. R. C., ROSENBERG, C., CARRARO, D. M., DA COSTA, C. M. L., DA CUNHA, I. W. & KREPISCHI, A. C. V. 2019. TET Upregulation Leads to 5-Hydroxymethylation Enrichment in Hepatoblastoma. *Front Genet,* 10**,** 553.

ROGNONI, E., GOMEZ, C., PISCO, A. O., RAWLINS, E. L., SIMONS, B. D., WATT, F. M. & DRISKELL, R. R. 2016. Inhibition of beta-catenin signalling in dermal fibroblasts enhances hair follicle regeneration during wound healing. *Development,* 143**,** 2522-35.

ROMANO, R. A., BIRKAYA, B. & SINHA, S. 2007. A functional enhancer of keratin14 is a direct transcriptional target of deltaNp63. *J Invest Dermatol,* 127**,** 1175-86.

ROMANO, R. A., ORTT, K., BIRKAYA, B., SMALLEY, K. & SINHA, S. 2009. An active role of the DeltaN isoform of p63 in regulating basal keratin genes K5 and K14 and directing epidermal cell fate. *PLoS One,* 4**,** e5623.

ROMANO, R. A., SMALLEY, K., LIU, S. & SINHA, S. 2010. Abnormal hair follicle development and altered cell fate of follicular keratinocytes in transgenic mice expressing DeltaNp63alpha. *Development,* 137**,** 1431-9.

ROMANO, R. A., SMALLEY, K., MAGRAW, C., SERNA, V. A., KURITA, T., RAGHAVAN, S. & SINHA, S. 2012. DeltaNp63 knockout mice reveal its indispensable role as a master regulator of epithelial development and differentiation. *Development,* 139**,** 772-82.

RONAN, J. L., WU, W. & CRABTREE, G. R. 2013. From neural development to cognition: unexpected roles for chromatin. *Nat Rev Genet,* 14**,** 347-59.

SAHA, A., WITTMEYER, J. & CAIRNS, B. R. 2006. Chromatin remodelling: the industrial revolution of DNA around histones. *Nat Rev Mol Cell Biol,* 7**,** 437-47.

SALADI, S. V., WONG, P. G., TRIVEDI, A. R., MARATHE, H. G., KEENEN, B., ARAS, S., LIEW, Z. Q., SETALURI, V. & DE LA SERNA, I. L. 2013. BRG1 promotes survival of UV-

irradiated melanoma cells by cooperating with MITF to activate the melanoma inhibitor of apoptosis gene. *Pigment Cell Melanoma Res,* 26**,** 377-91.

SAMEJIMA, K., SAMEJIMA, I., VAGNARELLI, P., OGAWA, H., VARGIU, G., KELLY, D. A., DE LIMA ALVES, F., KERR, A., GREEN, L. C., HUDSON, D. F., OHTA, S., COOKE, C. A., FARR, C. J., RAPPSILBER, J. & EARNSHAW, W. C. 2012. Mitotic chromosomes are compacted laterally by KIF4 and condensin and axially by topoisomerase IIalpha. *J Cell Biol,* 199**,** 755-70.

SAMUELOV, L., SPRECHER, E., SUGAWARA, K., SINGH, S. K., TOBIN, D. J., TSURUTA, D., BIRO, T., KLOEPPER, J. E. & PAUS, R. 2013. Topobiology of human pigmentation: P-cadherin selectively stimulates hair follicle melanogenesis. *J Invest Dermatol,* 133**,** 1591-600.

SANDILANDS, A., SUTHERLAND, C., IRVINE, A. D. & MCLEAN, W. H. 2009. Filaggrin in the frontline: role in skin barrier function and disease. *J Cell Sci,* 122**,** 1285-94.

SANYAL, A., BAU, D., MARTI-RENOM, M. A. & DEKKER, J. 2011. Chromatin globules: a common motif of higher order chromosome structure? *Curr Opin Cell Biol,* 23**,** 325-31.

SASAKI, G. H. 2019. Review of Human Hair Follicle Biology: Dynamics of Niches and Stem Cell Regulation for Possible Therapeutic Hair Stimulation for Plastic Surgeons. *Aesthetic Plast Surg,* 43**,** 253-266.

SASS, P. A., DABROWSKI, M., CHARZYNSKA, A. & SACHADYN, P. 2017. Transcriptomic responses to wounding: meta-analysis of gene expression microarray data. *BMC Genomics,* 18**,** 850.

SCHAFER, M. & WERNER, S. 2007. Transcriptional control of wound repair. *Annu Rev Cell Dev Biol,* 23**,** 69-92.

SCHLESSINGER, D. I. & BHIMJI, S. S. 2018. Embryology, Epidermis. *StatPearls.* Treasure Island (FL).

SCHMIDT-ULLRICH, R. & PAUS, R. 2005. Molecular principles of hair follicle induction and morphogenesis. *Bioessays,* 27**,** 247-61.

SCHMIDT-ULLRICH, R., TOBIN, D. J., LENHARD, D., SCHNEIDER, P., PAUS, R. & SCHEIDEREIT, C. 2006. NF-kappaB transmits Eda A1/EdaR signalling to activate Shh and cyclin D1 expression, and controls post-initiation hair placode down growth. *Development,* 133**,** 1045-57.

SCHNEIDER, M. R., SCHMIDT-ULLRICH, R. & PAUS, R. 2009. The hair follicle as a dynamic miniorgan. *Curr Biol,* 19**,** R132-42.

SELTMANN, K., ROTH, W., KROGER, C., LOSCHKE, F., LEDERER, M., HUTTELMAIER, S. & MAGIN, T. M. 2013. Keratins mediate localization of hemidesmosomes and repress cell motility. *J Invest Dermatol,* 133**,** 181-90.

SEN, G. L., REUTER, J. A., WEBSTER, D. E., ZHU, L. & KHAVARI, P. A. 2010. DNMT1 maintains progenitor function in self-renewing somatic tissue. *Nature,* 463**,** 563-7.

SEN, G. L., WEBSTER, D. E., BARRAGAN, D. I., CHANG, H. Y. & KHAVARI, P. A. 2008. Control of differentiation in a self-renewing mammalian tissue by the histone demethylase JMJD3. *Genes Dev,* 22**,** 1865-70.

SHAHLAEE, A. H., BRANDAL, S., LEE, Y. N., JIE, C. & TAKEMOTO, C. M. 2007. Distinct and shared transcriptomes are regulated by microphthalmia-associated transcription factor isoforms in mast cells. *J Immunol,* 178**,** 378-88.

SHAIN, A. H. & POLLACK, J. R. 2013. The spectrum of SWI/SNF mutations, ubiquitous in human cancers. *PLoS One,* 8**,** e55119.

SHANKS, N., GREEK, R. & GREEK, J. 2009. Are animal models predictive for humans? *Philos Ethics Humanit Med,* 4**,** 2.

SHAROV, A. A., SHAROVA, T. Y., MARDARYEV, A. N., TOMMASI DI VIGNANO, A., ATOYAN, R., WEINER, L., YANG, S., BRISSETTE, J. L., DOTTO, G. P. & BOTCHKAREV, V. A. 2006. Bone morphogenetic protein signaling regulates the size of hair follicles and modulates the expression of cell cycle-associated genes. *Proc Natl Acad Sci U S A,* 103**,** 18166-71.

SHAW, T. J. & MARTIN, P. 2009. Wound repair at a glance. *Journal of Cell Science,* 122**,** 3209-3213.

SIMON, J. A. & KINGSTON, R. E. 2009. Mechanisms of polycomb gene silencing: knowns and unknowns. *Nat Rev Mol Cell Biol,* 10**,** 697-708.

SIMPSON, C. L., PATEL, D. M. & GREEN, K. J. 2011. Deconstructing the skin: cytoarchitectural determinants of epidermal morphogenesis. *Nat Rev Mol Cell Biol,* 12**,** 565-80.

SINGLETON, M. R. & WIGLEY, D. B. 2002. Modularity and specialization in superfamily 1 and 2 helicases. *J Bacteriol,* 184**,** 1819-26.

SOARES, E. & ZHOU, H. 2018. Master regulatory role of p63 in epidermal development and disease. *Cell Mol Life Sci,* 75**,** 1179-1190.

SON, J., SHEN, S. S., MARGUERON, R. & REINBERG, D. 2013. Nucleosome-binding activities within JARID2 and EZH1 regulate the function of PRC2 on chromatin. *Genes Dev,* 27**,** 2663-77.

SONG, C. X., YI, C. Q. & HE, C. 2012. Mapping recently identified nucleotide variants in the genome and transcriptome. *Nature Biotechnology,* 30**,** 1107-1116.

SOTIROPOULOU, P. A. & BLANPAIN, C. 2012. Development and homeostasis of the skin epidermis. *Cold Spring Harb Perspect Biol,* 4**,** a008383.

ST-JACQUES, B., DASSULE, H. R., KARAVANOVA, I., BOTCHKAREV, V. A., LI, J., DANIELIAN, P. S., MCMAHON, J. A., LEWIS, P. M., PAUS, R. & MCMAHON, A. P. 1998. Sonic hedgehog signaling is essential for hair development. *Curr Biol,* 8**,** 1058-68.

STENN, K. S. & PAUS, R. 2001. Controls of hair follicle cycling. *Physiol Rev,* 81**,** 449-494.

STOJADINOVIC, O., ITO, M. & TOMIC-CANIC, M. 2011. Hair cycling and wound healing: to pluck or not to pluck? *J Invest Dermatol,* 131**,** 292-4.

STOJADINOVIC, O. & TOMIC-CANIC, M. 2013. Human ex vivo wound healing model. *Methods Mol Biol,* 1037**,** 255-64.

STROBECK, M. W., REISMAN, D. N., GUNAWARDENA, R. W., BETZ, B. L., ANGUS, S. P., KNUDSEN, K. E., KOWALIK, T. F., WEISSMAN, B. E. & KNUDSEN, E. S. 2002. Compensation of BRG-1 function by Brm: insight into the role of the core SWI-SNF subunits in retinoblastoma tumor suppressor signaling. *J Biol Chem,* 277**,** 4782-9.

SUDARSANAM, P. & WINSTON, F. 2000. The Swi/Snf family nucleosome-remodeling complexes and transcriptional control. *Trends Genet,* 16**,** 345-51.

SUH, J. L., BARNASH, K. D., ABRAMYAN, T. M., LI, F., THE, J., ENGELBERG, I. A., VEDADI, M., BROWN, P. J., KIREEV, D. B., ARROWSMITH, C. H., JAMES, L. I. & FRYE, S. V. 2019. Discovery of selective activators of PRC2 mutant EED-I363M. *Sci Rep,* 9**,** 6524.

SUN, X., HOTA, S. K., ZHOU, Y. Q., NOVAK, S., MIGUEL-PEREZ, D., CHRISTODOULOU, D., SEIDMAN, C. E., SEIDMAN, J. G., GREGORIO, C. C., HENKELMAN, R. M., ROSSANT, J. & BRUNEAU, B. G. 2018. Cardiac-enriched BAF chromatin-remodeling complex subunit Baf60c regulates gene expression programs essential for heart development and function. *Biol Open,* 7.

SUZUKI, M. M. & BIRD, A. 2008. DNA methylation landscapes: provocative insights from epigenomics. *Nat Rev Genet,* 9**,** 465-76.

SZERLONG, H., HINATA, K., VISWANATHAN, R., ERDJUMENT-BROMAGE, H., TEMPST, P. & CAIRNS, B. R. 2008. The HSA domain binds nuclear actin-related proteins to regulate chromatin-remodeling ATPases. *Nat Struct Mol Biol,* 15**,** 469-76.

TAHILIANI, M., KOH, K. P., SHEN, Y., PASTOR, W. A., BANDUKWALA, H., BRUDNO, Y., AGARWAL, S., IYER, L. M., LIU, D. R., ARAVIND, L. & RAO, A. 2009. Conversion of 5-methylcytosine to 5-hydroxymethylcytosine in mammalian DNA by MLL partner TET1. *Science,* 324**,** 930-5.

TAKEDA, K., TAKEUCHI, O., TSUJIMURA, T., ITAMI, S., ADACHI, O., KAWAI, T., SANJO, H., YOSHIKAWA, K., TERADA, N. & AKIRA, S. 1999. Limb and skin abnormalities in mice lacking IKKalpha. *Science,* 284**,** 313-6.

TAKEUCHI, J. K. & BRUNEAU, B. G. 2009. Directed transdifferentiation of mouse mesoderm to heart tissue by defined factors. *Nature,* 459**,** 708-11.

THARMALINGAM, S. & HAMPSON, D. R. 2016. The Calcium-Sensing Receptor and Integrins in Cellular Differentiation and Migration. *Front Physiol,* 7**,** 190.

THOMPSON, K. W., MARQUEZ, S. B., LU, L. & REISMAN, D. 2015. Induction of functional Brm protein from Brm knockout mice. *Oncoscience,* 2**,** 349-61.

TOTO, P. C., PURI, P. L. & ALBINI, S. 2016. SWI/SNF-directed stem cell lineage specification: dynamic composition regulates specific stages of skeletal myogenesis. *Cell Mol Life Sci,* 73**,** 3887-96.

TREICH, I. & CARLSON, M. 1997. Interaction of a Swi3 homolog with Sth1 provides evidence for a Swi/Snf-related complex with an essential function in Saccharomyces cerevisiae. *Mol Cell Biol,* 17**,** 1768-75.

TRUONG, A. B., KRETZ, M., RIDKY, T. W., KIMMEL, R. & KHAVARI, P. A. 2006. p63 regulates proliferation and differentiation of developmentally mature keratinocytes. *Genes Dev,* 20**,** 3185-97.

TU, C. L., CHANG, W. & BIKLE, D. D. 2007. The role of the calcium sensing receptor in regulating intracellular calcium handling in human epidermal keratinocytes. *J Invest Dermatol,* 127**,** 1074-83.

TU, C. L., CRUMRINE, D. A., MAN, M. Q., CHANG, W., ELALIEH, H., YOU, M., ELIAS, P. M. & BIKLE, D. D. 2012. Ablation of the calcium-sensing receptor in keratinocytes impairs epidermal differentiation and barrier function. *J Invest Dermatol,* 132**,** 2350-9.

UCCELLI, A., LARONI, A., BRUNDIN, L., CLANET, M., FERNANDEZ, O., NABAVI, S. M., MURARO, P. A., OLIVERI, R. S., RADUE, E. W., SELLNER, J., SOELBERG SORENSEN, P., SORMANI, M. P., WUERFEL, J. T., BATTAGLIA, M. A., FREEDMAN, M. S. & GROUP, M.

S. 2019. MEsenchymal StEm cells for Multiple Sclerosis (MESEMS): a randomized, double blind, cross-over phase I/II clinical trial with autologous mesenchymal stem cells for the therapy of multiple sclerosis. *Trials,* 20**,** 263.

VANBOKHOVEN, H., MELINO, G., CANDI, E. & DECLERCQ, W. 2011. p63, a story of mice and men. *J Invest Dermatol,* 131**,** 1196-207.

VERSTEEGE, I., SEVENET, N., LANGE, J., ROUSSEAU-MERCK, M. F., AMBROS, P., HANDGRETINGER, R., AURIAS, A. & DELATTRE, O. 1998. Truncating mutations of hSNF5/INI1 in aggressive paediatric cancer. *Nature,* 394**,** 203-6.

VIDAL, V. P., CHABOISSIER, M. C., LUTZKENDORF, S., COTSARELIS, G., MILL, P., HUI, C. C., ORTONNE, N., ORTONNE, J. P. & SCHEDL, A. 2005. Sox9 is essential for outer root sheath differentiation and the formation of the hair stem cell compartment. *Curr Biol,* 15**,** 1340-51.

WANG, Q., OH, J. W., LEE, H. L., DHAR, A., PENG, T., RAMOS, R., GUERRERO-JUAREZ, C. F., WANG, X., ZHAO, R., CAO, X., LE, J., FUENTES, M. A., JOCOY, S. C., ROSSI, A. R., VU, B., PHAM, K., WANG, X., MALI, N. M., PARK, J. M., CHOI, J. H., LEE, H., LEGRAND, J. M. D., KANDYBA, E., KIM, J. C., KIM, M., FOLEY, J., YU, Z., KOBIELAK, K., ANDERSEN, B., KHOSROTEHRANI, K., NIE, Q. & PLIKUS, M. V. 2017. A multi-scale model for hair follicles reveals heterogeneous domains driving rapid spatiotemporal hair growth patterning. *Elife,* 6.

WANG, W., XUE, Y., ZHOU, S., KUO, A., CAIRNS, B. R. & CRABTREE, G. R. 1996. Diversity and specialization of mammalian SWI/SNF complexes. *Genes Dev,* 10**,** 2117-30.

WANG, X. & KADARMIDEEN, H. N. 2019. An Epigenome-Wide DNA Methylation Map of Testis in Pigs for Study of Complex Traits. *Front Genet,* 10**,** 405.

WANG, X., PASOLLI, H. A., WILLIAMS, T. & FUCHS, E. 2008. AP-2 factors act in concert with Notch to orchestrate terminal differentiation in skin epidermis. *J Cell Biol,* 183**,** 37-48.

WANG, X., WANG, X., LIU, J., CAI, T., GUO, L., WANG, S., WANG, J., CAO, Y., GE, J., JIANG, Y., TREDGET, E. E., CAO, M. & WU, Y. 2016. Hair Follicle and Sebaceous Gland De Novo Regeneration With Cultured Epidermal Stem Cells and Skin-Derived Precursors. *Stem Cells Transl Med*.

WANG, Z., SCHONES, D. E. & ZHAO, K. 2009. Characterization of human epigenomes. *Curr Opin Genet Dev,* 19**,** 127-34.

WANG, Z., ZHAI, W., RICHARDSON, J. A., OLSON, E. N., MENESES, J. J., FIRPO, M. T., KANG, C., SKARNES, W. C. & TJIAN, R. 2004. Polybromo protein BAF180 functions in mammalian cardiac chamber maturation. *Genes Dev,* 18**,** 3106-16.

WASSEF, M., LUSCAN, A., AFLAKI, S., ZIELINSKI, D., JANSEN, P., BAYMAZ, H. I., BATTISTELLA, A., KERSOUANI, C., SERVANT, N., WALLACE, M. R., ROMERO, P., KOSMIDER, O., JUST, P. A., HIVELIN, M., JACQUES, S., VINCENT-SALOMON, A., VERMEULEN, M., VIDAUD, M., PASMANT, E. & MARGUERON, R. 2019. EZH1/2 function mostly within canonical PRC2 and exhibit proliferation-dependent redundancy that shapes mutational signatures in cancer. *Proc Natl Acad Sci U S A,* 116**,** 6075-6080.

WATERS, J. M., RICHARDSON, G. D. & JAHODA, C. A. 2007. Hair follicle stem cells. *Semin Cell Dev Biol,* 18**,** 245-54.

WAWERSIK, M. J., MAZZALUPO, S., NGUYEN, D. & COULOMBE, P. A. 2001. Increased levels of keratin 16 alter epithelialization potential of mouse skin keratinocytes in vivo and ex vivo. *Mol Biol Cell,* 12**,** 3439-50.

WEINER, L., HAN, R., SCICCHITANO, B. M., LI, J., HASEGAWA, K., GROSSI, M., LEE, D. & BRISSETTE, J. L. 2007. Dedicated epithelial recipient cells determine pigmentation patterns. *Cell,* 130**,** 932-42.

WEINHOUSE, C., TRUONG, L., MEYER, J. N. & ALLARD, P. 2018. Caenorhabditis elegans as an emerging model system in environmental epigenetics. *Environ Mol Mutagen,* 59**,** 560-575.

WESTGATE, G. E., GINGER, R. S. & GREEN, M. R. 2017. The biology and genetics of curly hair. *Exp Dermatol,* 26**,** 483-490.

WEYANDT, G. H., BAUER, B., BERENS, N., HAMM, H. & BROECKER, E. B. 2009. Split-skin grafting from the scalp: the hidden advantage. *Dermatol Surg,* 35**,** 1873-9.

WILSON, S. I., RYDSTROM, A., TRIMBORN, T., WILLERT, K., NUSSE, R., JESSELL, T. M. & EDLUND, T. 2001. The status of Wnt signalling regulates neural and epidermal fates in the chick embryo. *Nature,* 411**,** 325-30.

WONG, P. & COULOMBE, P. A. 2003. Loss of keratin 6 (K6) proteins reveals a function for intermediate filaments during wound repair. *J Cell Biol,* 163**,** 327-37.

WONG, S. Y. & REITER, J. F. 2011. Wounding mobilizes hair follicle stem cells to form tumors. *Proc Natl Acad Sci U S A,* 108**,** 4093-8.

WU, C. & MORRIS, J. R. 2001. Genes, genetics, and epigenetics: a correspondence. *Science,* 293**,** 1103-5.

WU, H. & ZHANG, Y. 2011a. Mechanisms and functions of Tet protein-mediated 5-methylcytosine oxidation. *Genes Dev,* 25**,** 2436-52.

WU, H. & ZHANG, Y. 2011b. Tet1 and 5-hydroxymethylation: a genome-wide view in mouse embryonic stem cells. *Cell Cycle,* 10**,** 2428-36.

WU, J. I., LESSARD, J. & CRABTREE, G. R. 2009. Understanding the words of chromatin regulation. *Cell,* 136**,** 200-6.

WU, P., ZHANG, Y., XING, Y., XU, W., GUO, H., DENG, F., MA, X. & LI, Y. 2019a. The balance of Bmp6 and Wnt10b regulates the telogen-anagen transition of hair follicles. *Cell Commun Signal,* 17**,** 16.

WU, Q., HEIDENREICH, D., ZHOU, S., ACKLOO, S., KRAMER, A., NAKKA, K., LIMA-FERNANDES, E., DEBLOIS, G., DUAN, S., VELLANKI, R. N., LI, F., VEDADI, M., DILWORTH, J., LUPIEN, M., BRENNAN, P. E., ARROWSMITH, C. H., MULLER, S., FEDOROV, O., FILIPPAKOPOULOS, P. & KNAPP, S. 2019b. A chemical toolbox for the study of bromodomains and epigenetic signaling. *Nat Commun,* 10**,** 1915.

WU, X., JOHANSEN, J. V. & HELIN, K. 2013. Fbxl10/Kdm2b recruits polycomb repressive complex 1 to CpG islands and regulates H2A ubiquitylation. *Mol Cell,* 49**,** 1134-46.

WURSTER, A. L. & PAZIN, M. J. 2008. BRG1-mediated chromatin remodeling regulates differentiation and gene expression of T helper cells. *Mol Cell Biol,* 28**,** 7274-85.

XIAO, Y. T., XIANG, L. X. & SHAO, J. Z. 2007. Bone morphogenetic protein. *Biochem Biophys Res Commun,* 362**,** 550-3.

XIONG, Y., LI, W., SHANG, C., CHEN, R. M., HAN, P., YANG, J., STANKUNAS, K., WU, B., PAN, M., ZHOU, B., LONGAKER, M. T. & CHANG, C. P. 2013. Brg1 governs a positive feedback circuit in the hair follicle for tissue regeneration and repair. *Dev Cell,* 25**,** 169-81.

XU, Y., WU, F., TAN, L., KONG, L., XIONG, L., DENG, J., BARBERA, A. J., ZHENG, L., ZHANG, H., HUANG, S., MIN, J., NICHOLSON, T., CHEN, T., XU, G., SHI, Y., ZHANG, K. & SHI, Y. G. 2011. Genome-wide regulation of 5hmC, 5mC, and gene expression by Tet1 hydroxylase in mouse embryonic stem cells. *Mol Cell,* 42**,** 451-64.

XUE, Y., CANMAN, J. C., LEE, C. S., NIE, Z., YANG, D., MORENO, G. T., YOUNG, M. K., SALMON, E. D. & WANG, W. 2000. The human SWI/SNF-B chromatin-remodeling complex is related to yeast rsc and localizes at kinetochores of mitotic chromosomes. *Proc Natl Acad Sci U S A,* 97**,** 13015-20.

YAMAGUCHI, Y., MORITA, A., MAEDA, A. & HEARING, V. J. 2009. Regulation of skin pigmentation and thickness by Dickkopf 1 (DKK1). *J Investig Dermatol Symp Proc,* 14**,** 73-5.

YAN, L., XIE, S., DU, Y. & QIAN, C. 2017. Structural Insights into BAF47 and BAF155 Complex Formation. *J Mol Biol,* 429**,** 1650-1660.

YAN, Z., CUI, K., MURRAY, D. M., LING, C., XUE, Y., GERSTEIN, A., PARSONS, R., ZHAO, K. & WANG, W. 2005. PBAF chromatin-remodeling complex requires a novel specificity subunit, BAF200, to regulate expression of selective interferon-responsive genes. *Genes Dev,* 19**,** 1662-7.

YANG, A., KAGHAD, M., WANG, Y., GILLETT, E., FLEMING, M. D., DOTSCH, V., ANDREWS, N. C., CAPUT, D. & MCKEON, F. 1998. p63, a p53 homolog at 3q27-29, encodes multiple products with transactivating, death-inducing, and dominant-negative activities. *Mol Cell,* 2**,** 305-16.

YANG, A., SCHWEITZER, R., SUN, D., KAGHAD, M., WALKER, N., BRONSON, R. T., TABIN, C., SHARPE, A., CAPUT, D., CRUM, C. & MCKEON, F. 1999. p63 is essential for regenerative proliferation in limb, craniofacial and epithelial development. *Nature,* 398**,** 714-8.

YANG, H., LIU, Y., BAI, F., ZHANG, J. Y., MA, S. H., LIU, J., XU, Z. D., ZHU, H. G., LING, Z. Q., YE, D., GUAN, K. L. & XIONG, Y. 2013. Tumor development is associated with decrease of TET gene expression and 5-methylcytosine hydroxylation. *Oncogene,* 32**,** 663-669.

YANG, H., WANG, H. & JAENISCH, R. 2014. Generating genetically modified mice using CRISPR/Cas-mediated genome engineering. *Nat Protoc,* 9**,** 1956-68.

YE, J., COULOURIS, G., ZARETSKAYA, I., CUTCUTACHE, I., ROZEN, S. & MADDEN, T. L. 2012. Primer-BLAST: a tool to design target-specific primers for polymerase chain reaction. *BMC Bioinformatics,* 13**,** 134.

YONEY, A., ETOC, F., RUZO, A., CARROLL, T., METZGER, J. J., MARTYN, I., LI, S., KIRST, C., SIGGIA, E. D. & BRIVANLOU, A. H. 2018. WNT signaling memory is required for ACTIVIN to function as a morphogen in human gastruloids. *Elife,* 7.

YOO, A. S., STAAHL, B. T., CHEN, L. & CRABTREE, G. R. 2009. MicroRNA-mediated switching of chromatin-remodelling complexes in neural development. *Nature,* 460**,** 642-6.

YOO, K. H. & HENNIGHAUSEN, L. 2012. EZH2 methyltransferase and H3K27 methylation in breast cancer. *Int J Biol Sci,* 8**,** 59-65.

YOSHIDA, Y., SOMA, T. & KISHIMOTO, J. 2019. Characterization of human dermal sheath cells reveals CD36-expressing perivascular cells associated with capillary blood vessel formation in hair follicles. *Biochem Biophys Res Commun*.

YOUSEF, H. & SHARMA, S. 2018. Anatomy, Skin (Integument), Epidermis. *StatPearls.* Treasure Island (FL).

YU, H., FANG, D., KUMAR, S. M., LI, L., NGUYEN, T. K., ACS, G., HERLYN, M. & XU, X. 2006a. Isolation of a novel population of multipotent adult stem cells from human hair follicles. *Am J Pathol,* 168**,** 1879-88.

YU, H., KUMAR, S. M., KOSSENKOV, A. V., SHOWE, L. & XU, X. 2010. Stem cells with neural crest characteristics derived from the bulge region of cultured human hair follicles. *J Invest Dermatol,* 130**,** 1227-36.

YU, Z., LIN, K. K., BHANDARI, A., SPENCER, J. A., XU, X., WANG, N., LU, Z., GILL, G. N., ROOP, D. R., WERTZ, P. & ANDERSEN, B. 2006b. The Grainyhead-like epithelial transactivator Get-1/Grhl3 regulates epidermal terminal differentiation and interacts functionally with LMO4. *Dev Biol,* 299**,** 122-36.

YURCHENCO, P. D. 2011. Basement membranes: cell scaffoldings and signaling platforms. *Cold Spring Harb Perspect Biol,* 3.

ZENG, L. & ZHOU, M. M. 2002. Bromodomain: an acetyl-lysine binding domain. *FEBS Lett,* 513**,** 124-8.

ZHANG, B., WANG, M., GONG, A., ZHANG, X., WU, X., ZHU, Y., SHI, H., WU, L., ZHU, W., QIAN, H. & XU, W. 2015. HucMSC-Exosome Mediated-Wnt4 Signaling Is Required for Cutaneous Wound Healing. *Stem Cells,* 33**,** 2158-68.

ZHANG, H., NAN, W., WANG, S., ZHANG, T., SI, H., WANG, D., YANG, F. & LI, G. 2016. Epidermal growth factor promotes proliferation of dermal papilla cells via Notch signaling pathway. *Biochimie,* 127**,** 10-8.

ZHANG, W., CHRONIS, C., CHEN, X., ZHANG, H., SPALINSKAS, R., PARDO, M., CHEN, L., WU, G., ZHU, Z., YU, Y., YU, L., CHOUDHARY, J., NICHOLS, J., PARAST, M. M., GREBER, B., SAHLEN, P. & PLATH, K. 2019. The BAF and PRC2 Complex Subunits Dpf2 and Eed Antagonistically Converge on Tbx3 to Control ESC Differentiation. *Cell Stem Cell,* 24**,** 138-152 e8.

ZHANG, Y., ANDL, T., YANG, S. H., TETA, M., LIU, F., SEYKORA, J. T., TOBIAS, J. W., PICCOLO, S., SCHMIDT-ULLRICH, R., NAGY, A., TAKETO, M. M., DLUGOSZ, A. A. & MILLAR, S. E. 2008. Activation of beta-catenin signaling programs embryonic epidermis to hair follicle fate. *Development,* 135**,** 2161-72.

ZHEN, C. Y., DUC, H. N., KOKOTOVIC, M., PHIEL, C. J. & REN, X. 2014. Cbx2 stably associates with mitotic chromosomes via a PRC2- or PRC1-independent mechanism and is needed for recruiting PRC1 complex to mitotic chromosomes. *Mol Biol Cell,* 25**,** 3726-39.

ZHONG, X., DESILVA, T., LIN, L., BODINE, P., BHAT, R. A., PRESMAN, E., POCAS, J., STAHL, M. & KRIZ, R. 2007. Regulation of secreted Frizzled-related protein-1 by heparin. *J Biol Chem,* 282**,** 20523-33.

ZHU, A. S., LI, A., RATLIFF, T. S., MELSOM, M. & GARZA, L. A. 2017. After Skin Wounding, Noncoding dsRNA Coordinates Prostaglandins and Wnts to Promote Regeneration. *J Invest Dermatol,* 137**,** 1562-1568.

ZHU, X. J., LIU, Y., DAI, Z. M., ZHANG, X., YANG, X., LI, Y., QIU, M., FU, J., HSU, W., CHEN, Y. & ZHANG, Z. 2014. BMP-FGF signaling axis mediates Wnt-induced epidermal stratification in developing mammalian skin. *PLoS Genet,* 10**,** e1004687.

ZOMER, H. D. & TRENTIN, A. G. 2018. Skin wound healing in humans and mice: Challenges in translational research. *J Dermatol Sci,* 90**,** 3-12.

8. Supplementary data

8.1 Enrichment of GO terms of genes after SMARAC4 siRNA treatment in 0 hours after scratching

8.1.1 Enrichment of biological process related GO terms of downregulated genes after SMARAC4 siRNA treatment in 0 hours after scratching

GO Term (Biological Process)	Number of Genes	P-Value
GO:0006351~transcription, DNA-templated	831	1.28E-12
GO:0015031~protein transport	199	5.95E-10
GO:0000122~negative regulation of transcription from RNA polymerase II promoter	323	5.15E-08
GO:0098609~cell-cell adhesion	139	6.98E-08
GO:0045893~positive regulation of transcription, DNA-templated	240	7.59E-08
GO:0006355~regulation of transcription, DNA-templated	616	1.09E-06
GO:0030036~actin cytoskeleton organization	73	1.96E-06
GO:0006357~regulation of transcription from RNA polymerase II promoter	202	3.69E-06
GO:0045944~positive regulation of transcription from RNA polymerase II promoter	409	1.29E-05
GO:0016192~vesicle-mediated transport	79	3.25E-05
GO:0006888~ER to Golgi vesicle-mediated transport	82	4.33E-05
GO:0000289~nuclear-transcribed mRNA poly(A) tail shortening	22	4.96E-05
GO:0006886~intracellular protein transport	113	6.71E-05
GO:0016569~covalent chromatin modification	61	7.27E-05
GO:0008285~negative regulation of cell proliferation	177	8.07E-05
GO:0008544~epidermis development	48	0.000119
GO:0032922~circadian regulation of gene expression	35	0.000143
GO:0043044~ATP-dependent chromatin remodeling	18	0.000178
GO:0016055~Wnt signaling pathway	91	0.000181
GO:0030148~sphingolipid biosynthetic process	30	0.000321
GO:0048010~vascular endothelial growth factor receptor signaling pathway	41	0.000327
GO:0018105~peptidyl-serine phosphorylation	64	0.000341
GO:0061025~membrane fusion	28	0.00036
GO:0045892~negative regulation of transcription, DNA-templated	213	0.000399
GO:0007050~cell cycle arrest	70	0.000543
GO:0043066~negative regulation of apoptotic process	195	0.000554
GO:0022617~extracellular matrix disassembly	42	0.000628
GO:0007173~epidermal growth factor receptor signaling pathway	33	0.000652
GO:0007030~Golgi organization	41	0.000691
GO:0001525~angiogenesis	103	0.000726
GO:0042795~snRNA transcription from RNA polymerase II promoter	39	0.000835
GO:0048013~ephrin receptor signaling pathway	46	0.000837
GO:0031175~neuron projection development	52	0.00085
GO:0043001~Golgi to plasma membrane protein transport	19	0.000866
GO:0035329~hippo signaling	19	0.000866
GO:0034976~response to endoplasmic reticulum stress	41	0.000981
GO:0042147~retrograde transport, endosome to Golgi	38	0.001313
GO:0006396~RNA processing	50	0.001389
GO:0051092~positive regulation of NF-kappaB transcription factor activity	65	0.001454
GO:0000398~mRNA splicing, via spliceosome	101	0.001513
GO:0006366~transcription from RNA polymerase II promoter	214	0.001593
GO:0008380~RNA splicing	78	0.001907
GO:0036498~IRE1-mediated unfolded protein response	33	0.00213
GO:0010467~gene expression	28	0.002311
GO:0016575~histone deacetylation	27	0.002526
GO:0070555~response to interleukin-1	21	0.002564
GO:0030032~lamellipodium assembly	20	0.002728
GO:0006470~protein dephosphorylation	61	0.002729
GO:0006974~cellular response to DNA damage stimulus	94	0.002835
GO:0030216~keratinocyte differentiation	40	0.002859

GO Term (Biological Process)	Number of Genes	P-Value
GO:0007264~small GTPase mediated signal transduction	109	0.002866
GO:0016925~protein sumoylation	57	0.003222
GO:0006897~endocytosis	66	0.003237
GO:0070536~protein K63-linked deubiquitination	16	0.003255
GO:0017148~negative regulation of translation	32	0.003355
GO:0042752~regulation of circadian rhythm	28	0.003436
GO:0018107~peptidyl-threonine phosphorylation	23	0.00356
GO:0006446~regulation of translational initiation	22	0.003863
GO:0001933~negative regulation of protein phosphorylation	33	0.004257
GO:0043161~proteasome-mediated ubiquitin-dependent protein catabolic process	91	0.004383
GO:0055114~oxidation-reduction process	240	0.00469
GO:0051865~protein autoubiquitination	28	0.004989
GO:0007266~Rho protein signal transduction	28	0.004989
GO:0048280~vesicle fusion with Golgi apparatus	9	0.005046
GO:0051272~positive regulation of cellular component movement	9	0.005046
GO:0031398~positive regulation of protein ubiquitination	34	0.005287
GO:0030336~negative regulation of cell migration	47	0.005459
GO:0006468~protein phosphorylation	188	0.005489
GO:0031424~keratinization	27	0.005508
GO:0032211~negative regulation of telomere maintenance via telomerase	10	0.005891
GO:0031581~hemidesmosome assembly	10	0.005891
GO:0043065~positive regulation of apoptotic process	128	0.006063
GO:0010839~negative regulation of keratinocyte proliferation	11	0.006358
GO:1901673~regulation of mitotic spindle assembly	11	0.006358
GO:0016241~regulation of macroautophagy	25	0.00671
GO:0006915~apoptotic process	229	0.006966
GO:0071364~cellular response to epidermal growth factor stimulus	20	0.007159
GO:0016337~single organismal cell-cell adhesion	49	0.007177
GO:0016032~viral process	127	0.007441
GO:0007005~mitochondrion organization	39	0.007444
GO:0036258~multivesicular body assembly	19	0.007801
GO:0060271~cilium morphogenesis	63	0.00792
GO:0018279~protein N-linked glycosylation via asparagine	23	0.008167
GO:0000209~protein polyubiquitination	82	0.008186
GO:0006397~mRNA processing	80	0.008284
GO:0070936~protein K48-linked ubiquitination	26	0.008698
GO:0001701~in utero embryonic development	83	0.008814
GO:0048208~COPII vesicle coating	32	0.008821
GO:0001666~response to hypoxia	77	0.00915
GO:0006413~translational initiation	63	0.009572
GO:2001235~positive regulation of apoptotic signaling pathway	16	0.009933
GO:0016567~protein ubiquitination	149	0.010049
GO:0030574~collagen catabolic process	33	0.010601
GO:0043154~negative regulation of cysteine-type endopeptidase activity involved in apoptotic process	35	0.011297
GO:0035562~negative regulation of chromatin binding	8	0.011635
GO:0006596~polyamine biosynthetic process	8	0.011635
GO:0001889~liver development	37	0.011891
GO:0035556~intracellular signal transduction	165	0.012204
GO:0048568~embryonic organ development	12	0.012675
GO:0051764~actin crosslink formation	9	0.01278

GO Term (Biological Process)	Number of Genes	P-Value
GO:0061045~negative regulation of wound healing	9	0.01278
GO:0090161~Golgi ribbon formation	9	0.01278
GO:0034067~protein localization to Golgi apparatus	9	0.01278
GO:0045669~positive regulation of osteoblast differentiation	31	0.013095
GO:0030433~ER-associated ubiquitin-dependent protein catabolic process	31	0.013095
GO:0032897~negative regulation of viral transcription	10	0.013169
GO:1901796~regulation of signal transduction by p53 class mediator	57	0.013954
GO:0006457~protein folding	79	0.014507
GO:0010033~response to organic substance	17	0.014522
GO:0010977~negative regulation of neuron projection development	24	0.01503
GO:0060348~bone development	23	0.016715
GO:0051091~positive regulation of sequence-specific DNA binding transcription factor activity	49	0.016862
GO:0045444~fat cell differentiation	36	0.016913
GO:0042787~protein ubiquitination involved in ubiquitin-dependent protein catabolic process	68	0.017184
GO:0032956~regulation of actin cytoskeleton organization	25	0.018551
GO:0039702~viral budding via host ESCRT complex	14	0.018997
GO:0050821~protein stabilization	61	0.019572
GO:0019058~viral life cycle	18	0.019811
GO:0031667~response to nutrient levels	18	0.019811
GO:0032880~regulation of protein localization	27	0.020078
GO:0030512~negative regulation of transforming growth factor beta receptor signaling pathway	32	0.020094
GO:0032436~positive regulation of proteasomal ubiquitin-dependent protein catabolic process	32	0.020094
GO:0016477~cell migration	75	0.020322
GO:0006461~protein complex assembly	53	0.020325
GO:0001892~embryonic placenta development	13	0.020645
GO:0008542~visual learning	24	0.020667
GO:0034446~substrate adhesion-dependent cell spreading	21	0.020701
GO:0051056~regulation of small GTPase mediated signal transduction	60	0.021415
GO:0071549~cellular response to dexamethasone stimulus	17	0.021955
GO:0000920~cell separation after cytokinesis	12	0.022319
GO:0018149~peptide cross-linking	26	0.022369
GO:0006896~Golgi to vacuole transport	6	0.023004
GO:0044794~positive regulation by host of viral process	6	0.023004
GO:0043966~histone H3 acetylation	23	0.023037
GO:0030177~positive regulation of Wnt signaling pathway	20	0.023052
GO:0001843~neural tube closure	37	0.024213
GO:0035987~endodermal cell differentiation	16	0.024324
GO:0045579~positive regulation of B cell differentiation	10	0.02543
GO:2000353~positive regulation of endothelial cell apoptotic process	10	0.02543
GO:0045787~positive regulation of cell cycle	19	0.025684
GO:0043588~skin development	19	0.025684
GO:0030521~androgen receptor signaling pathway	22	0.025695
GO:0030335~positive regulation of cell migration	79	0.025772
GO:0031659~positive regulation of cyclin-dependent protein serine/threonine kinase activity involved in G1/S transition of mitotic cell cycle	7	0.026184
GO:0001945~lymph vessel development	7	0.026184
GO:0051247~positive regulation of protein metabolic process	7	0.026184
GO:0046825~regulation of protein export from nucleus	7	0.026184
GO:0033146~regulation of intracellular estrogen receptor signaling pathway	7	0.026184
GO:0034329~cell junction assembly	9	0.02656
GO:0048024~regulation of mRNA splicing, via spliceosome	9	0.02656

GO Term (Biological Process)	Number of Genes	P-Value
GO:0035518~histone H2A monoubiquitination	9	0.02656
GO:0071985~multivesicular body sorting pathway	9	0.02656
GO:0043123~positive regulation of I-kappaB kinase/NF-kappaB signaling	70	0.026681
GO:0022604~regulation of cell morphogenesis	15	0.026937
GO:0060674~placenta blood vessel development	8	0.027008
GO:0010038~response to metal ion	8	0.027008
GO:0032060~bleb assembly	8	0.027008
GO:0010761~fibroblast migration	8	0.027008
GO:0006464~cellular protein modification process	48	0.02714
GO:0006914~autophagy	59	0.027562
GO:0000186~activation of MAPKK activity	24	0.027814
GO:0016239~positive regulation of macroautophagy	14	0.02981
GO:0008286~insulin receptor signaling pathway	37	0.030031
GO:0060070~canonical Wnt signaling pathway	39	0.030198
GO:0023014~signal transduction by protein phosphorylation	23	0.031045
GO:0007507~heart development	78	0.031895
GO:0002474~antigen processing and presentation of peptide antigen via MHC class I	17	0.031932
GO:0090004~positive regulation of establishment of protein localization to plasma membrane	17	0.031932
GO:0007080~mitotic metaphase plate congression	20	0.032032
GO:0061077~chaperone-mediated protein folding	20	0.032032
GO:0070534~protein K63-linked ubiquitination	20	0.032032
GO:0006367~transcription initiation from RNA polymerase II promoter	66	0.032252
GO:0016197~endosomal transport	32	0.032455
GO:0000226~microtubule cytoskeleton organization	34	0.032937
GO:0032402~melanosome transport	13	0.032955
GO:0045861~negative regulation of proteolysis	13	0.032955
GO:0043085~positive regulation of catalytic activity	38	0.033367
GO:0006368~transcription elongation from RNA polymerase II promoter	40	0.033371
GO:0048511~rhythmic process	27	0.034276
GO:0008283~cell proliferation	147	0.034528
GO:0007566~embryo implantation	22	0.034675
GO:0045931~positive regulation of mitotic cell cycle	16	0.035635
GO:0016601~Rac protein signal transduction	12	0.036377
GO:0045926~negative regulation of growth	12	0.036377
GO:0006998~nuclear envelope organization	12	0.036377
GO:0042098~T cell proliferation	12	0.036377
GO:0045862~positive regulation of proteolysis	12	0.036377
GO:0009267~cellular response to starvation	24	0.036691
GO:0051028~mRNA transport	24	0.036691
GO:0008360~regulation of cell shape	61	0.036718
GO:0007420~brain development	80	0.040008
GO:0006370~7-methylguanosine mRNA capping	18	0.040059
GO:2000811~negative regulation of anoikis	11	0.040061
GO:0050775~positive regulation of dendrite morphogenesis	11	0.040061
GO:0030033~microvillus assembly	11	0.040061
GO:0006890~retrograde vesicle-mediated transport, Golgi to ER	38	0.040628
GO:0045454~cell redox homeostasis	36	0.040745
GO:0010506~regulation of autophagy	25	0.042584
GO:2001237~negative regulation of extrinsic apoptotic signaling pathway	20	0.043364
GO:0000470~maturation of LSU-rRNA	10	0.043964

GO Term (Biological Process)	Number of Genes	P-Value
GO:0036503~ERAD pathway	10	0.043964
GO:0007249~I-kappaB kinase/NF-kappaB signaling	29	0.044459
GO:0031146~SCF-dependent proteasomal ubiquitin-dependent protein catabolic process	14	0.044459
GO:0030099~myeloid cell differentiation	14	0.044459
GO:0043967~histone H4 acetylation	17	0.044861
GO:0030100~regulation of endocytosis	17	0.044861
GO:0032781~positive regulation of ATPase activity	17	0.044861
GO:0033138~positive regulation of peptidyl-serine phosphorylation	33	0.045062
GO:0008284~positive regulation of cell proliferation	183	0.045226
GO:1904837~beta-catenin-TCF complex assembly	22	0.045784
GO:0031623~receptor internalization	22	0.045784
GO:0060644~mammary gland epithelial cell differentiation	9	0.047984
GO:0046628~positive regulation of insulin receptor signaling pathway	9	0.047984
GO:0048268~clathrin coat assembly	9	0.047984
GO:0003016~respiratory system process	9	0.047984
GO:0007212~dopamine receptor signaling pathway	9	0.047984
GO:0051492~regulation of stress fiber assembly	9	0.047984
GO:0045197~establishment or maintenance of epithelial cell apical/basal polarity	9	0.047984
GO:0006352~DNA-templated transcription, initiation	19	0.04856
GO:0010842~retina layer formation	13	0.049705
GO:0006509~membrane protein ectodomain proteolysis	13	0.049705

8.1.2 Enrichment of molecular function related GO terms of downregulated genes after SMARAC4 siRNA treatment in 0 hours after scratching

GO Term (Molecular Function)	Number of Genes	P-Value
GO:0005515~protein binding	3651	4.22E-70
GO:0044822~poly(A) RNA binding	567	1.89E-26
GO:0098641~cadherin binding involved in cell-cell adhesion	155	3.42E-10
GO:0003676~nucleic acid binding	427	7.82E-08
GO:0046872~metal ion binding	838	1.38E-07
GO:0008270~zinc ion binding	492	6.16E-07
GO:0003677~DNA binding	682	1.02E-06
GO:0003713~transcription coactivator activity	125	1.31E-06
GO:0048365~Rac GTPase binding	29	8.39E-06
GO:0019904~protein domain specific binding	105	9.08E-06
GO:0003714~transcription corepressor activity	102	1.58E-05
GO:0016874~ligase activity	128	4.45E-05
GO:0003700~transcription factor activity, sequence-specific DNA binding	398	4.76E-05
GO:0016740~transferase activity	54	5.23E-05
GO:0035091~phosphatidylinositol binding	49	5.4E-05
GO:0008565~protein transporter activity	43	5.59E-05
GO:0046332~SMAD binding	29	6.63E-05
GO:0004842~ubiquitin-protein transferase activity	150	0.000109
GO:0001103~RNA polymerase II repressing transcription factor binding	20	0.000222
GO:0044212~transcription regulatory region DNA binding	101	0.000297
GO:0042803~protein homodimerization activity	302	0.000424
GO:0042802~identical protein binding	308	0.000609
GO:0043130~ubiquitin binding	43	0.000613
GO:0016301~kinase activity	110	0.000906
GO:0003723~RNA binding	229	0.001046
GO:0002020~protease binding	52	0.001224
GO:0003779~actin binding	124	0.001236
GO:0004386~helicase activity	45	0.001358
GO:0003682~chromatin binding	168	0.001367
GO:0019901~protein kinase binding	162	0.00145
GO:0003924~GTPase activity	106	0.001539
GO:0019899~enzyme binding	145	0.001575
GO:0047485~protein N-terminus binding	49	0.002856
GO:0035064~methylated histone binding	30	0.002987
GO:0005521~lamin binding	12	0.003082
GO:0008134~transcription factor binding	124	0.003096
GO:0017124~SH3 domain binding	58	0.003143
GO:0030374~ligand-dependent nuclear receptor transcription coactivator activity	29	0.003281
GO:0030674~protein binding, bridging	40	0.004079
GO:0032266~phosphatidylinositol-3-phosphate binding	20	0.004686
GO:0042974~retinoic acid receptor binding	10	0.006025
GO:0051787~misfolded protein binding	10	0.006025
GO:0051015~actin filament binding	62	0.006311
GO:0004709~MAP kinase kinase kinase activity	15	0.006349
GO:0008022~protein C-terminus binding	82	0.006391
GO:0032403~protein complex binding	91	0.00777
GO:0008013~beta-catenin binding	41	0.008306
GO:0003743~translation initiation factor activity	32	0.009251
GO:0000978~RNA polymerase II core promoter proximal region sequence-specific DNA binding	148	0.009648
GO:0004674~protein serine/threonine kinase activity	156	0.009692

GO Term (Molecular Function)	Number of Genes	P-Value
GO:0005524~ATP binding	571	0.010263
GO:0003712~transcription cofactor activity	36	0.010698
GO:0045296~cadherin binding	15	0.010992
GO:0001047~core promoter binding	33	0.011117
GO:0051087~chaperone binding	40	0.011785
GO:0031748~D1 dopamine receptor binding	8	0.011848
GO:0000287~magnesium ion binding	89	0.012374
GO:0031625~ubiquitin protein ligase binding	121	0.012878
GO:0051010~microtubule plus-end binding	9	0.013035
GO:0017160~Ral GTPase binding	10	0.013452
GO:0043024~ribosomal small subunit binding	10	0.013452
GO:0005484~SNAP receptor activity	22	0.013606
GO:0018024~histone-lysine N-methyltransferase activity	22	0.013606
GO:0004702~receptor signaling protein serine/threonine kinase activity	28	0.014033
GO:0061630~ubiquitin protein ligase activity	82	0.014159
GO:0008017~microtubule binding	90	0.015175
GO:0048306~calcium-dependent protein binding	30	0.015207
GO:0001106~RNA polymerase II transcription corepressor activity	16	0.016387
GO:0003824~catalytic activity	82	0.016406
GO:0004843~thiol-dependent ubiquitin-specific protease activity	39	0.016533
GO:0009055~electron carrier activity	43	0.017292
GO:0004871~signal transducer activity	88	0.017797
GO:0019003~GDP binding	28	0.018777
GO:0019902~phosphatase binding	24	0.021432
GO:0001671~ATPase activator activity	12	0.022839
GO:0030145~manganese ion binding	26	0.023231
GO:0001104~RNA polymerase II transcription cofactor activity	20	0.023803
GO:0051721~protein phosphatase 2A binding	16	0.025005
GO:0005178~integrin binding	48	0.028607
GO:0000149~SNARE binding	24	0.028805
GO:0004407~histone deacetylase activity	21	0.029615
GO:0080025~phosphatidylinositol-3,5-bisphosphate binding	14	0.030555
GO:0000166~nucleotide binding	141	0.031506
GO:0070273~phosphatidylinositol-4-phosphate binding	13	0.03373
GO:0016922~ligand-dependent nuclear receptor binding	13	0.03373
GO:0005525~GTP binding	154	0.035726
GO:0046875~ephrin receptor binding	15	0.040792
GO:0051020~GTPase binding	15	0.040792
GO:0042826~histone deacetylase binding	46	0.041036
GO:0071889~14-3-3 protein binding	14	0.045512
GO:0001948~glycoprotein binding	31	0.046623
GO:0019900~kinase binding	35	0.046899
GO:0070628~proteasome binding	9	0.048816
GO:0003697~single-stranded DNA binding	42	0.049976

8.1.3 Enrichment of cellular components related GO terms of downregulated genes after SMARAC4 siRNA treatment in 0 hours after scratching

GO Term (Cellular component)	Number of Genes	P-Value
GO:0005737~cytoplasm	2175	1.02E-35
GO:0005829~cytosol	1454	4.96E-34
GO:0005654~nucleoplasm	1232	3.48E-30
GO:0005634~nucleus	2183	2.25E-25
GO:0016020~membrane	970	9.25E-23
GO:0005925~focal adhesion	215	2.38E-16
GO:0005794~Golgi apparatus	403	1.15E-13
GO:0005783~endoplasmic reticulum	376	7.93E-11
GO:0005913~cell-cell adherens junction	169	9.51E-11
GO:0070062~extracellular exosome	1122	3.09E-10
GO:0043231~intracellular membrane-bounded organelle	264	5.52E-10
GO:0015629~actin cytoskeleton	118	6.31E-09
GO:0048471~perinuclear region of cytoplasm	281	3.48E-08
GO:0000139~Golgi membrane	266	1.46E-07
GO:0005622~intracellular	549	2.33E-07
GO:0017053~transcriptional repressor complex	37	3.2E-06
GO:0005739~mitochondrion	538	4.9E-06
GO:0005769~early endosome	112	1.11E-05
GO:0043234~protein complex	185	1.52E-05
GO:0031965~nuclear membrane	111	2E-05
GO:0031901~early endosome membrane	63	2.56E-05
GO:0005789~endoplasmic reticulum membrane	356	2.99E-05
GO:0005730~nucleolus	354	3.11E-05
GO:0016605~PML body	54	6.34E-05
GO:0016607~nuclear speck	97	8.55E-05
GO:0005813~centrosome	186	9.98E-05
GO:0031012~extracellular matrix	133	0.000246
GO:0030027~lamellipodium	78	0.000304
GO:0010494~cytoplasmic stress granule	24	0.000332
GO:0030134~ER to Golgi transport vesicle	19	0.000347
GO:0031410~cytoplasmic vesicle	108	0.000361
GO:0005759~mitochondrial matrix	144	0.000403
GO:0005856~cytoskeleton	160	0.000613
GO:0031519~PcG protein complex	19	0.000704
GO:0030014~CCR4-NOT complex	13	0.00119
GO:0030904~retromer complex	16	0.001405
GO:0005793~endoplasmic reticulum-Golgi intermediate compartment	37	0.00151
GO:0005819~spindle	59	0.001783
GO:0030529~intracellular ribonucleoprotein complex	65	0.001904
GO:0001533~cornified envelope	27	0.001979
GO:0016604~nuclear body	21	0.002085
GO:0005768~endosome	100	0.002295
GO:0015630~microtubule cytoskeleton	65	0.002378
GO:0005911~cell-cell junction	79	0.002406
GO:0010008~endosome membrane	84	0.002589
GO:0005884~actin filament	35	0.002625
GO:0042470~melanosome	50	0.002855
GO:0005815~microtubule organizing center	71	0.002972
GO:0000118~histone deacetylase complex	22	0.003139
GO:0001725~stress fiber	30	0.003182

GO Term (Cellular component)	Number of Genes	P-Value
GO:0045111~intermediate filament cytoskeleton	29	0.003539
GO:0031982~vesicle	60	0.004945
GO:0030057~desmosome	16	0.004989
GO:0071564~npBAF complex	10	0.005247
GO:0030659~cytoplasmic vesicle membrane	59	0.005482
GO:0000785~chromatin	44	0.005483
GO:0035098~ESC/E(Z) complex	12	0.005739
GO:0005795~Golgi stack	20	0.005946
GO:0030133~transport vesicle	46	0.007182
GO:0005938~cell cortex	57	0.008255
GO:0005776~autophagosome	33	0.008298
GO:0019005~SCF ubiquitin ligase complex	27	0.008824
GO:0031902~late endosome membrane	48	0.00913
GO:0035097~histone methyltransferase complex	15	0.009211
GO:0005604~basement membrane	39	0.009494
GO:0030496~midbody	59	0.009948
GO:0005874~microtubule	129	0.009982
GO:0031258~lamellipodium membrane	13	0.010592
GO:0031201~SNARE complex	28	0.01084
GO:0019898~extrinsic component of membrane	40	0.010871
GO:0035371~microtubule plus-end	12	0.011187
GO:0071013~catalytic step 2 spliceosome	44	0.011207
GO:0070971~endoplasmic reticulum exit site	10	0.011808
GO:0016580~Sin3 complex	10	0.011808
GO:0055038~recycling endosome membrane	24	0.012377
GO:0001726~ruffle	43	0.012477
GO:0005802~trans-Golgi network	61	0.0141
GO:0030426~growth cone	53	0.015042
GO:0002102~podosome	15	0.015121
GO:0000159~protein phosphatase type 2A complex	13	0.018201
GO:0032587~ruffle membrane	39	0.019192
GO:0005694~chromosome	48	0.020646
GO:0005635~nuclear envelope	69	0.020776
GO:0034045~pre-autophagosomal structure membrane	11	0.021447
GO:0005875~microtubule associated complex	19	0.021938
GO:0005774~vacuolar membrane	10	0.022951
GO:0045335~phagocytic vesicle	21	0.024303
GO:0000776~kinetochore	38	0.026463
GO:0045121~membrane raft	86	0.028901
GO:0030670~phagocytic vesicle membrane	29	0.029024
GO:0030667~secretory granule membrane	13	0.029246
GO:0005801~cis-Golgi network	22	0.029367
GO:0033116~endoplasmic reticulum-Golgi intermediate compartment membrane	31	0.029405
GO:0016592~mediator complex	19	0.030788
GO:0016363~nuclear matrix	44	0.03096
GO:0005643~nuclear pore	34	0.03297
GO:0016327~apicolateral plasma membrane	11	0.036104

GO Term (Cellular component)	Number of Genes	P-Value
GO:0005788~endoplasmic reticulum lumen	80	0.036485
GO:0030424~axon	91	0.039796
GO:0012505~endomembrane system	50	0.04042
GO:0005770~late endosome	53	0.041729
GO:0005777~peroxisome	46	0.042816
GO:0005771~multivesicular body	13	0.044397
GO:0035145~exon-exon junction complex	13	0.044397
GO:0032580~Golgi cisterna membrane	35	0.044495
GO:0042612~MHC class I protein complex	8	0.047906
GO:0031252~cell leading edge	20	0.049572

8.1.4 Enrichment of biological process related GO terms of upregulated genes after SMARAC4 siRNA treatment in 0 hours after scratching

GO Term (biological process)	Number of Genes	P-Value
GO:0043303~mast cell degranulation	4	0.000123
GO:0007268~chemical synaptic transmission	7	0.010989
GO:0032762~mast cell cytokine production	2	0.015424
GO:0016339~calcium-dependent cell-cell adhesion via plasma membrane cell adhesion molecules	3	0.019713
GO:0007186~G-protein coupled receptor signaling pathway	14	0.022059
GO:0033693~neurofilament bundle assembly	2	0.023047
GO:0007411~axon guidance	5	0.035134
GO:0002551~mast cell chemotaxis	2	0.038119
GO:0030011~maintenance of cell polarity	2	0.038119
GO:0007218~neuropeptide signaling pathway	4	0.043682
GO:0071376~cellular response to corticotropin-releasing hormone stimulus	2	0.045568
GO:0050885~neuromuscular process controlling balance	3	0.04934

8.1.5 Enrichment of molecular function related GO terms of upregulated genes after SMARAC4 siRNA treatment in 0 hours after scratching

GO Term (Molecular Function)	Number of Genes	P-Value
GO:0005523~tropomyosin binding	3	0.004965
GO:0031005~filamin binding	3	0.004965
GO:0004930~G-protein coupled receptor activity	13	0.008204
GO:0042923~neuropeptide binding	3	0.010062
GO:0043565~sequence-specific DNA binding	10	0.017973
GO:0008201~heparin binding	5	0.034405
GO:0032947~protein complex scaffold	3	0.037415
GO:0035473~lipase binding	2	0.04499

8.1.6 Enrichment of cellular component related GO terms of upregulated genes after SMARAC4 siRNA treatment in 0 hours after scratching

GO Term (Molecular Function)	Number of Genes	P-Value
GO:0042629~mast cell granule	4	0.000567
GO:0005886~plasma membrane	44	0.023226
GO:0005887~integral component of plasma membrane	19	0.028431

8.2 Enrichment of GO terms of genes after SMARAC4 siRNA treatment in 24 hours after scratching

8.2.1 Enrichment of biological process related GO terms of downregulated genes after SMARAC4 siRNA treatment in 24 hours after scratching

GO Term (Biological Process)	Number of Genes	P-Value
GO:0045893~positive regulation of transcription, DNA-templated	65	5.76E-06
GO:0008544~epidermis development	19	2.03E-05
GO:0071222~cellular response to lipopolysaccharide	21	0.000109
GO:0016477~cell migration	26	0.000416
GO:0001525~angiogenesis	31	0.000456
GO:0045944~positive regulation of transcription from RNA polymerase II promoter	96	0.0008
GO:0032755~positive regulation of interleukin-6 production	11	0.000935
GO:0050728~negative regulation of inflammatory response	15	0.001109
GO:0009611~response to wounding	13	0.001288
GO:0007155~cell adhesion	51	0.001331
GO:0032760~positive regulation of tumor necrosis factor production	11	0.001336
GO:0045672~positive regulation of osteoclast differentiation	7	0.001455
GO:0010628~positive regulation of gene expression	33	0.001584
GO:0006357~regulation of transcription from RNA polymerase II promoter	49	0.00166
GO:0008284~positive regulation of cell proliferation	51	0.001822
GO:0086091~regulation of heart rate by cardiac conduction	9	0.002475
GO:0001890~placenta development	9	0.002475
GO:0001822~kidney development	15	0.002561
GO:0042026~protein refolding	6	0.002813
GO:0001938~positive regulation of endothelial cell proliferation	13	0.002886
GO:0000122~negative regulation of transcription from RNA polymerase II promoter	71	0.003488
GO:0006954~inflammatory response	42	0.003842
GO:0007010~cytoskeleton organization	22	0.004429
GO:0001666~response to hypoxia	23	0.004612
GO:0042493~response to drug	35	0.004881
GO:0032496~response to lipopolysaccharide	22	0.005488
GO:0009408~response to heat	10	0.005626
GO:0008584~male gonad development	15	0.00584
GO:0060612~adipose tissue development	7	0.006609
GO:0010718~positive regulation of epithelial to mesenchymal transition	8	0.007053
GO:0032693~negative regulation of interleukin-10 production	5	0.007605
GO:1990440~positive regulation of transcription from RNA polymerase II promoter in response to endoplasmic reticulum stress	5	0.007605
GO:0006986~response to unfolded protein	9	0.008027
GO:0034080~CENP-A containing nucleosome assembly	9	0.009269
GO:0001558~regulation of cell growth	13	0.009722
GO:0032736~positive regulation of interleukin-13 production	4	0.009774
GO:0009615~response to virus	16	0.009972
GO:0002526~acute inflammatory response	5	0.010382
GO:0030198~extracellular matrix organization	24	0.010728
GO:0060070~canonical Wnt signaling pathway	13	0.012898
GO:0006468~protein phosphorylation	46	0.013185
GO:0071549~cellular response to dexamethasone stimulus	7	0.013948

GO Term (Biological Process)	Number of Genes	P-Value
GO:2001258~negative regulation of cation channel activity	3	0.01411
GO:0060596~mammary placode formation	3	0.01411
GO:0072539~T-helper 17 cell differentiation	3	0.01411
GO:0044597~daunorubicin metabolic process	4	0.014829
GO:0045630~positive regulation of T-helper 2 cell differentiation	4	0.014829
GO:0044598~doxorubicin metabolic process	4	0.014829
GO:0048671~negative regulation of collateral sprouting	4	0.014829
GO:0007275~multicellular organism development	51	0.015245
GO:0001501~skeletal system development	18	0.015658
GO:0009267~cellular response to starvation	9	0.0157
GO:0007411~axon guidance	20	0.016076
GO:0001954~positive regulation of cell-matrix adhesion	6	0.016367
GO:0032922~circadian regulation of gene expression	10	0.017185
GO:0009617~response to bacterium	6	0.019733
GO:0055114~oxidation-reduction process	56	0.020647
GO:0060452~positive regulation of cardiac muscle contraction	4	0.021096
GO:0007565~female pregnancy	13	0.02156
GO:0086002~cardiac muscle cell action potential involved in contraction	5	0.02233
GO:0030308~negative regulation of cell growth	16	0.02245
GO:0007160~cell-matrix adhesion	13	0.023344
GO:0090314~positive regulation of protein targeting to membrane	6	0.023523
GO:0007165~signal transduction	100	0.023815
GO:0071300~cellular response to retinoic acid	11	0.023853
GO:0050900~leukocyte migration	16	0.023996
GO:0051092~positive regulation of NF-kappaB transcription factor activity	17	0.024287
GO:0043491~protein kinase B signaling	7	0.025632
GO:0097191~extrinsic apoptotic signaling pathway	8	0.025766
GO:0071395~cellular response to jasmonic acid stimulus	3	0.026909
GO:0006651~diacylglycerol biosynthetic process	3	0.026909
GO:0070370~cellular heat acclimation	3	0.026909
GO:0006564~L-serine biosynthetic process	3	0.026909
GO:0042523~positive regulation of tyrosine phosphorylation of Stat5 protein	5	0.027615
GO:0070542~response to fatty acid	5	0.027615
GO:0060749~mammary gland alveolus development	5	0.027615
GO:0008344~adult locomotory behavior	9	0.027637
GO:0050715~positive regulation of cytokine secretion	6	0.027751
GO:0070365~hepatocyte differentiation	4	0.028588
GO:0019732~antifungal humoral response	4	0.028588
GO:0014823~response to activity	8	0.028973
GO:0007219~Notch signaling pathway	15	0.030755
GO:0045444~fat cell differentiation	11	0.030968
GO:0031668~cellular response to extracellular stimulus	5	0.033583
GO:0001889~liver development	11	0.03364
GO:0030182~neuron differentiation	13	0.033922
GO:0030574~collagen catabolic process	10	0.034081
GO:0000187~activation of MAPK activity	14	0.03698
GO:0050829~defense response to Gram-negative bacterium	9	0.037227
GO:0009312~oligosaccharide biosynthetic process	4	0.037296

GO Term (biological process)	Number of Genes	P-Value
GO:0030517~negative regulation of axon extension	4	0.037296
GO:0090051~negative regulation of cell migration involved in sprouting angiogenesis	4	0.037296
GO:0010941~regulation of cell death	4	0.037296
GO:0042592~homeostatic process	4	0.037296
GO:0051024~positive regulation of immunoglobulin secretion	4	0.037296
GO:0060021~palate development	11	0.03946
GO:0022617~extracellular matrix disassembly	11	0.03946
GO:0016055~Wnt signaling pathway	21	0.039708
GO:0030325~adrenal gland development	5	0.040242
GO:0007263~nitric oxide mediated signal transduction	5	0.040242
GO:0043011~myeloid dendritic cell differentiation	5	0.040242
GO:0019221~cytokine-mediated signaling pathway	16	0.041693
GO:0032869~cellular response to insulin stimulus	11	0.042615
GO:0086011~membrane repolarization during action potential	3	0.042776
GO:0051135~positive regulation of NK T cell activation	3	0.042776
GO:0045578~negative regulation of B cell differentiation	3	0.042776
GO:2000352~negative regulation of endothelial cell apoptotic process	6	0.043193
GO:0021983~pituitary gland development	6	0.043193
GO:0060306~regulation of membrane repolarization	4	0.047193
GO:0036499~PERK-mediated unfolded protein response	4	0.047193
GO:0060707~trophoblast giant cell differentiation	4	0.047193
GO:2000505~regulation of energy homeostasis	4	0.047193
GO:0010468~regulation of gene expression	13	0.047536
GO:0018107~peptidyl-threonine phosphorylation	7	0.047565
GO:0042517~positive regulation of tyrosine phosphorylation of Stat3 protein	7	0.047565
GO:0043542~endothelial cell migration	6	0.049285
GO:0048662~negative regulation of smooth muscle cell proliferation	6	0.049285
GO:0006629~lipid metabolic process	18	0.049689

8.2.2 Enrichment of molecular function related GO terms of downregulated genes after SMARAC4 siRNA treatment in 24 hours after scratching

GO Term (Molecular Function)	Number of Genes	P-Value
GO:0000978~RNA polymerase II core promoter proximal region sequence-specific DNA binding	51	1.73E-06
GO:0001077~transcriptional activator activity, RNA polymerase II core promoter proximal region sequence-specific binding	34	0.000111
GO:0008201~heparin binding	25	0.000323
GO:0043565~sequence-specific DNA binding	58	0.000461
GO:0001078~transcriptional repressor activity, RNA polymerase II core promoter proximal region sequence-specific binding	19	0.000684
GO:0004623~phospholipase A2 activity	9	0.001047
GO:0005125~cytokine activity	25	0.001293
GO:0045236~CXCR chemokine receptor binding	5	0.002272
GO:0005102~receptor binding	40	0.003186
GO:0005520~insulin-like growth factor binding	6	0.00665
GO:0003700~transcription factor activity, sequence-specific DNA binding	88	0.007603
GO:0009055~electron carrier activity	14	0.009752
GO:0004713~protein tyrosine kinase activity	18	0.0116
GO:0005509~calcium ion binding	67	0.013446
GO:0047718~indanol dehydrogenase activity	3	0.014035
GO:0000254~C-4 methylsterol oxidase activity	3	0.014035
GO:0016655~oxidoreductase activity, acting on NAD(P)H, quinone or similar compound as acceptor	4	0.014718
GO:0001085~RNA polymerase II transcription factor binding	9	0.015464
GO:0001530~lipopolysaccharide binding	6	0.016189
GO:0097110~scaffold protein binding	9	0.017451
GO:0008083~growth factor activity	20	0.018759
GO:0004672~protein kinase activity	37	0.019032
GO:0000982~transcription factor activity, RNA polymerase II core promoter proximal region sequence-specific binding	6	0.019522
GO:0000977~RNA polymerase II regulatory region sequence-specific DNA binding	24	0.020007
GO:0002162~dystroglycan binding	4	0.020941
GO:0005200~structural constituent of cytoskeleton	15	0.021428
GO:0003714~transcription corepressor activity	23	0.027563
GO:0046875~ephrin receptor binding	6	0.0321
GO:0030295~protein kinase activator activity	6	0.0321
GO:0005112~Notch binding	5	0.033289
GO:0050786~RAGE receptor binding	4	0.037034
GO:0042056~chemoattractant activity	6	0.037197
GO:0004879~RNA polymerase II transcription factor activity, ligand-activated sequence-specific DNA binding	7	0.03732
GO:0005109~frizzled binding	7	0.03732
GO:0004527~exonuclease activity	5	0.039896
GO:0016491~oxidoreductase activity	22	0.041294
GO:0008142~oxysterol binding	3	0.042558
GO:0047499~calcium-independent phospholipase A2 activity	3	0.042558
GO:0044212~transcription regulatory region DNA binding	23	0.043652
GO:0000976~transcription regulatory region sequence-specific DNA binding	9	0.048181
GO:0005164~tumor necrosis factor receptor binding	6	0.048802

8.2.3 Enrichment of cellular component related GO terms of downregulated genes after SMARAC4 siRNA treatment in 24 hours after scratching

GO Term (Cellular component)	Number of Genes	P-Value
GO:0005615~extracellular space	150	1.1E-08
GO:0005576~extracellular region	161	2.83E-06
GO:0005578~proteinaceous extracellular matrix	36	0.000282
GO:0030018~Z disc	18	0.003574
GO:0070062~extracellular exosome	19	0.005418
GO:0031012~extracellular matrix	34	0.005695
GO:0043005~neuron projection	27	0.015744
GO:0005856~cytoskeleton	38	0.019631
GO:0072562~blood microparticle	19	0.020211
GO:0005622~intracellular	113	0.024393
GO:0009986~cell surface	51	0.028271
GO:0046658~anchored component of plasma membrane	6	0.043004
GO:0031224~intrinsic component of membrane	4	0.047047
GO:0043197~dendritic spine	13	0.047197

8.2.4 Enrichment of biological process related GO terms of upregulated genes after SMARAC4 siRNA treatment in 24 hours after scratching

GO Term (biological process)	Number of Genes	P-Value
GO:0000398~mRNA splicing, via spliceosome	18	0.000206
GO:2000679~positive regulation of transcription regulatory region DNA binding	5	0.000679
GO:0008334~histone mRNA metabolic process	4	0.004114
GO:1900158~negative regulation of bone mineralization involved in bone maturation	3	0.004632
GO:0042273~ribosomal large subunit biogenesis	5	0.005027
GO:0008380~RNA splicing	12	0.007801
GO:0048705~skeletal system morphogenesis	5	0.012231
GO:0051170~nuclear import	4	0.013453
GO:0045926~negative regulation of growth	4	0.015645
GO:0071294~cellular response to zinc ion	4	0.015645
GO:0010544~negative regulation of platelet activation	3	0.020048
GO:0006396~RNA processing	8	0.02031
GO:0000027~ribosomal large subunit assembly	4	0.020597
GO:0030509~BMP signaling pathway	7	0.020715
GO:0048704~embryonic skeletal system morphogenesis	5	0.023976
GO:0044320~cellular response to leptin stimulus	3	0.025297
GO:0006369~termination of RNA polymerase II transcription	6	0.034842
GO:0014068~positive regulation of phosphatidylinositol 3-kinase signaling	6	0.036902
GO:0001775~cell activation	3	0.037233
GO:0030183~B cell differentiation	6	0.039035
GO:0006400~tRNA modification	4	0.040005
GO:0006364~rRNA processing	12	0.04198
GO:0000387~spliceosomal snRNP assembly	4	0.043892
GO:0032355~response to estradiol	7	0.044581
GO:0010467~gene expression	5	0.046595
GO:0030148~sphingolipid biosynthetic process	5	0.046595
GO:0045892~negative regulation of transcription, DNA-templated	22	0.047224

8.2.5 Enrichment of molecular function related GO terms of upregulated genes after SMARAC4 siRNA treatment in 24 hours after scratching

GO Term (Molecular Function)	Number of Genes	P-Value
GO:0044822~poly(A) RNA binding	66	3.28E-08
GO:0003723~RNA binding	32	0.000206
GO:0003729~mRNA binding	12	0.000852
GO:0008134~transcription factor binding	15	0.032134

8.2.6 Enrichment of cellular component related GO terms of upregulated genes after SMARAC4 siRNA treatment in 24 hours after scratching

GO Term (Cellular Component)	Number of Genes	P-Value
GO:0030687~preribosome, large subunit precursor	6	0.001177
GO:0005685~U1 snRNP	5	0.001718
GO:0030529~intracellular ribonucleoprotein complex	11	0.005158
GO:0034715~pICln-Sm protein complex	3	0.011004
GO:0030054~cell junction	23	0.011074
GO:0005730~nucleolus	37	0.011197
GO:0034719~SMN-Sm protein complex	4	0.011237
GO:0030285~integral component of synaptic vesicle membrane	3	0.019788
GO:0005687~U4 snRNP	3	0.036764
GO:0005887~integral component of plasma membrane	52	0.040434
GO:0019013~viral nucleocapsid	4	0.043149
GO:0034709~methylosome	3	0.04331
GO:0071013~catalytic step 2 spliceosome	7	0.045355

8.3 Enrichment of GO terms of genes after control siRNA treatment in 24 hours after scratching

8.3.1 Enrichment of biological process related GO terms of downregulated genes after control siRNA treatment in 24 hours after scratching

GO Term (Biological Process)	Number of Genes	P-Value
GO:0006364~rRNA processing	85	4.57E-19
GO:0070125~mitochondrial translational elongation	40	5.04E-12
GO:0000398~mRNA splicing, via spliceosome	73	1.31E-11
GO:0070126~mitochondrial translational termination	39	3.85E-11
GO:0051301~cell division	96	6.08E-10
GO:0007067~mitotic nuclear division	72	8.25E-09
GO:0032981~mitochondrial respiratory chain complex I assembly	25	3.89E-06
GO:0006400~tRNA modification	15	6.02E-06
GO:0006397~mRNA processing	50	6.48E-06
GO:0006120~mitochondrial electron transport, NADH to ubiquinone	21	7.25E-06
GO:0006396~RNA processing	32	1.19E-05
GO:0042273~ribosomal large subunit biogenesis	14	1.25E-05
GO:0032543~mitochondrial translation	17	1.65E-05
GO:0010467~gene expression	20	2.06E-05
GO:0008283~cell proliferation	83	3.79E-05
GO:0016925~protein sumoylation	35	4.33E-05
GO:0006413~translational initiation	39	4.94E-05
GO:0000086~G2/M transition of mitotic cell cycle	39	4.94E-05
GO:0000387~spliceosomal snRNP assembly	14	5.86E-05
GO:0031581~hemidesmosome assembly	9	5.9E-05
GO:0008380~RNA splicing	44	9.53E-05
GO:0008033~tRNA processing	16	0.00011
GO:0007062~sister chromatid cohesion	31	0.000114
GO:0045926~negative regulation of growth	11	0.000114
GO:0006406~mRNA export from nucleus	30	0.00016
GO:0006369~termination of RNA polymerase II transcription	22	0.000193
GO:0007077~mitotic nuclear envelope disassembly	17	0.000294
GO:0006409~tRNA export from nucleus	14	0.000307
GO:0051170~nuclear import	10	0.000418
GO:0006412~translation	58	0.000468
GO:0071294~cellular response to zinc ion	10	0.000692
GO:0035987~endodermal cell differentiation	12	0.000863
GO:0006086~acetyl-CoA biosynthetic process from pyruvate	6	0.001081
GO:0042254~ribosome biogenesis	14	0.001155
GO:0070911~global genome nucleotide-excision repair	13	0.001213
GO:0000462~maturation of SSU-rRNA from tricistronic rRNA transcript (SSU-rRNA, 5.8S rRNA, LSU-rRNA)	13	0.001213
GO:0031124~mRNA 3'-end processing	17	0.001465
GO:0007080~mitotic metaphase plate congression	14	0.001545
GO:0098609~cell-cell adhesion	59	0.001562
GO:0031145~anaphase-promoting complex-dependent catabolic process	23	0.001694
GO:0050821~protein stabilization	34	0.001944
GO:0009113~purine nucleobase biosynthetic process	5	0.002017
GO:0030198~extracellular matrix organization	45	0.002099
GO:0006626~protein targeting to mitochondrion	13	0.002222
GO:0006362~transcription elongation from RNA polymerase I promoter	12	0.002376
GO:0072321~chaperone-mediated protein transport	6	0.002535
GO:0034475~U4 snRNA 3'-end processing	6	0.002535

GO Term (biological process)	Number of Genes	P-Value
GO:0061179~negative regulation of insulin secretion involved in cellular response to glucose stimulus	6	0.002535
GO:0000447~endonucleolytic cleavage in ITS1 to separate SSU-rRNA from 5.8S rRNA and LSU-rRNA from tricistronic rRNA transcript (SSU-rRNA, 5.8S rRNA, LSU-rRNA)	6	0.002535
GO:0006122~mitochondrial electron transport, ubiquinol to cytochrome c	8	0.003097
GO:1904874~positive regulation of telomerase RNA localization to Cajal body	8	0.003097
GO:0006363~termination of RNA polymerase I transcription	12	0.003202
GO:0006281~DNA repair	51	0.003568
GO:0030574~collagen catabolic process	19	0.003822
GO:0006446~regulation of translational initiation	13	0.003828
GO:0006457~protein folding	41	0.003923
GO:0010510~regulation of acetyl-CoA biosynthetic process from pyruvate	7	0.004062
GO:0006405~RNA export from nucleus	17	0.004323
GO:0007051~spindle organization	8	0.004817
GO:1904851~positive regulation of establishment of protein localization to telomere	6	0.005018
GO:0000463~maturation of LSU-rRNA from tricistronic rRNA transcript (SSU-rRNA, 5.8S rRNA, LSU-rRNA)	6	0.005018
GO:0034427~nuclear-transcribed mRNA catabolic process, exonucleolytic, 3'-5'	6	0.005018
GO:0007094~mitotic spindle assembly checkpoint	9	0.005032
GO:0075733~intracellular transport of virus	16	0.005037
GO:0006260~DNA replication	36	0.005119
GO:0019083~viral transcription	28	0.005226
GO:0006189~'de novo' IMP biosynthetic process	5	0.005347
GO:0006415~translational termination	5	0.005347
GO:0042255~ribosome assembly	5	0.005347
GO:0051437~positive regulation of ubiquitin-protein ligase activity involved in regulation of mitotic cell cycle transition	21	0.005442
GO:0006361~transcription initiation from RNA polymerase I promoter	12	0.005539
GO:0010827~regulation of glucose transport	12	0.005539
GO:0051726~regulation of cell cycle	30	0.006146
GO:0000281~mitotic cytokinesis	11	0.006151
GO:0006099~tricarboxylic acid cycle	11	0.006151
GO:0043488~regulation of mRNA stability	26	0.006408
GO:0000460~maturation of 5.8S rRNA	7	0.006617
GO:0009168~purine ribonucleoside monophosphate biosynthetic process	7	0.006617
GO:0055093~response to hyperoxia	8	0.007167
GO:0000910~cytokinesis	15	0.007179
GO:0042787~protein ubiquitination involved in ubiquitin-dependent protein catabolic process	35	0.007403
GO:0045727~positive regulation of translation	16	0.007431
GO:0007059~chromosome segregation	19	0.007608
GO:0045773~positive regulation of axon extension	11	0.008039
GO:0006511~ubiquitin-dependent protein catabolic process	40	0.0082
GO:0010501~RNA secondary structure unwinding	14	0.008381
GO:0021762~substantia nigra development	15	0.008728

GO Term (biological process)	Number of Genes	P-Value
GO:0035999~tetrahydrofolate interconversion	6	0.008835
GO:0006418~tRNA aminoacylation for protein translation	13	0.009763
GO:0030705~cytoskeleton-dependent intracellular transport	8	0.010269
GO:0018149~peptide cross-linking	15	0.010528
GO:0019919~peptidyl-arginine methylation, to asymmetrical-dimethyl arginine	5	0.011034
GO:0022617~extracellular matrix disassembly	20	0.011761
GO:0051436~negative regulation of ubiquitin-protein ligase activity involved in mitotic cell cycle	19	0.012081
GO:0051439~regulation of ubiquitin-protein ligase activity involved in mitotic cell cycle	9	0.013072
GO:0061024~membrane organization	11	0.013114
GO:0001525~angiogenesis	46	0.014251
GO:0043486~histone exchange	6	0.014268
GO:0000470~maturation of LSU-rRNA	7	0.014875
GO:0006301~postreplication repair	7	0.014875
GO:0006513~protein monoubiquitination	10	0.01507
GO:0007517~muscle organ development	22	0.016206
GO:0034446~substrate adhesion-dependent cell spreading	12	0.017231
GO:0051592~response to calcium ion	16	0.017442
GO:0045892~negative regulation of transcription, DNA-templated	91	0.018781
GO:0006294~nucleotide-excision repair, preincision complex assembly	10	0.019083
GO:0043928~exonucleolytic nuclear-transcribed mRNA catabolic process involved in deadenylation-dependent decay	10	0.019083
GO:0006541~glutamine metabolic process	8	0.019202
GO:1904871~positive regulation of protein localization to Cajal body	5	0.019533
GO:0000467~exonucleolytic trimming to generate mature 3'-end of 5.8S rRNA from tricistronic rRNA transcript (SSU-rRNA, 5.8S rRNA, LSU-rRNA)	5	0.019533
GO:0034551~mitochondrial respiratory chain complex III assembly	5	0.019533
GO:0051315~attachment of mitotic spindle microtubules to kinetochore	5	0.019533
GO:0016032~viral process	58	0.020081
GO:0000082~G1/S transition of mitotic cell cycle	24	0.020755
GO:0042274~ribosomal small subunit biogenesis	7	0.02091
GO:0006605~protein targeting	12	0.020913
GO:0008334~histone mRNA metabolic process	6	0.021558
GO:0031000~response to caffeine	6	0.021558
GO:0006164~purine nucleotide biosynthetic process	6	0.021558
GO:0048024~regulation of mRNA splicing, via spliceosome	6	0.021558
GO:0060315~negative regulation of ryanodine-sensitive calcium-release channel activity	6	0.021558
GO:0000070~mitotic sister chromatid segregation	9	0.022062
GO:0015914~phospholipid transport	9	0.022062
GO:0007052~mitotic spindle organization	10	0.023817
GO:0071038~nuclear polyadenylation-dependent tRNA catabolic process	4	0.024806
GO:0042773~ATP synthesis coupled electron transport	4	0.024806
GO:1902035~positive regulation of hematopoietic stem cell proliferation	4	0.024806
GO:0071051~polyadenylation-dependent snoRNA 3'-end processing	4	0.024806
GO:1902808~positive regulation of cell cycle G1/S phase transition	4	0.024806
GO:0051262~protein tetramerization	12	0.025142

GO Term (biological process)	Number of Genes	P-Value
GO:0006293~nucleotide-excision repair, preincision complex stabilization	8	0.025252
GO:0048025~negative regulation of mRNA splicing, via spliceosome	8	0.025252
GO:0000209~protein polyubiquitination	38	0.025644
GO:0000245~spliceosomal complex assembly	9	0.02789
GO:0007173~epidermal growth factor receptor signaling pathway	15	0.028083
GO:0016571~histone methylation	7	0.028405
GO:0010259~multicellular organism aging	7	0.028405
GO:0071276~cellular response to cadmium ion	7	0.028405
GO:0007017~microtubule-based process	11	0.029933
GO:0001522~pseudouridine synthesis	6	0.030895
GO:0006195~purine nucleotide catabolic process	6	0.030895
GO:0007049~cell cycle	43	0.032991
GO:0051496~positive regulation of stress fiber assembly	12	0.035397
GO:0032212~positive regulation of telomere maintenance via telomerase	10	0.035674
GO:0008544~epidermis development	20	0.03622
GO:0000184~nuclear-transcribed mRNA catabolic process, nonsense-mediated decay	26	0.036951
GO:0006606~protein import into nucleus	15	0.037132
GO:0070266~necroptotic process	7	0.037473
GO:0045807~positive regulation of endocytosis	7	0.037473
GO:0046655~folic acid metabolic process	7	0.037473
GO:0006888~ER to Golgi vesicle-mediated transport	33	0.038381
GO:0032436~positive regulation of proteasomal ubiquitin-dependent protein catabolic process	16	0.040289
GO:0006479~protein methylation	8	0.04098
GO:0006295~nucleotide-excision repair, DNA incision, 3'-to lesion	8	0.04098
GO:0001731~formation of translation preinitiation complex	8	0.04098
GO:0030155~regulation of cell adhesion	12	0.041495
GO:0036498~IRE1-mediated unfolded protein response	15	0.042363
GO:0007064~mitotic sister chromatid cohesion	6	0.042413
GO:0031929~TOR signaling	6	0.042413
GO:0030490~maturation of SSU-rRNA	6	0.042413
GO:0033683~nucleotide-excision repair, DNA incision	11	0.042452
GO:0000381~regulation of alternative mRNA splicing, via spliceosome	11	0.042452
GO:0006378~mRNA polyadenylation	9	0.042554
GO:0043161~proteasome-mediated ubiquitin-dependent protein catabolic process	40	0.042819
GO:0007018~microtubule-based movement	19	0.042869
GO:0009060~aerobic respiration	10	0.042898
GO:0046134~pyrimidine nucleoside biosynthetic process	4	0.044265
GO:0006207~'de novo' pyrimidine nucleobase biosynthetic process	4	0.044265
GO:0000055~ribosomal large subunit export from nucleus	4	0.044265
GO:0038063~collagen-activated tyrosine kinase receptor signaling pathway	4	0.044265
GO:0071035~nuclear polyadenylation-dependent rRNA catabolic process	4	0.044265
GO:0006999~nuclear pore organization	4	0.044265

GO Term (biological process)	Number of Genes	P-Value
GO:0070585~protein localization to mitochondrion	4	0.044265
GO:0000480~endonucleolytic cleavage in 5'-ETS of tricistronic rRNA transcript (SSU-rRNA, 5.8S rRNA, LSU-rRNA)	4	0.044265
GO:0009396~folic acid-containing compound biosynthetic process	4	0.044265
GO:0031115~negative regulation of microtubule polymerization	5	0.046017
GO:0033762~response to glucagon	5	0.046017
GO:0006890~retrograde vesicle-mediated transport, Golgi to ER	19	0.047695
GO:0008543~fibroblast growth factor receptor signaling pathway	19	0.047695
GO:0000226~microtubule cytoskeleton organization	17	0.048341

8.3.2 Enrichment of molecular function related GO terms of downregulated genes after control siRNA treatment in 24 hours after scratching

GO Term (Molecular Function)	Number of Genes	P-Value
GO:0044822~poly(A) RNA binding	365	1.53E-55
GO:0005515~protein binding	1501	4.57E-23
GO:0003723~RNA binding	153	2.66E-16
GO:0003729~mRNA binding	40	1.61E-06
GO:0008137~NADH dehydrogenase (ubiquinone) activity	21	4.58E-06
GO:0019843~rRNA binding	18	1.73E-05
GO:0003735~structural constituent of ribosome	57	1.8E-05
GO:0000166~nucleotide binding	80	2.68E-05
GO:0030515~snoRNA binding	11	0.000315
GO:0098641~cadherin binding involved in cell-cell adhesion	65	0.000343
GO:0000049~tRNA binding	18	0.000587
GO:0003743~translation initiation factor activity	20	0.000745
GO:0004004~ATP-dependent RNA helicase activity	20	0.001737
GO:0034604~pyruvate dehydrogenase (NAD+) activity	6	0.002474
GO:0047485~protein N-terminus binding	26	0.002573
GO:0017069~snRNA binding	6	0.004901
GO:0034511~U3 snoRNA binding	5	0.005242
GO:0043024~ribosomal small subunit binding	7	0.006444
GO:0008143~poly(A) binding	7	0.006444
GO:0051537~2 iron, 2 sulfur cluster binding	10	0.006473
GO:0003924~GTPase activity	49	0.007838
GO:0005068~transmembrane receptor protein tyrosine kinase adaptor activity	6	0.008636
GO:0008017~microtubule binding	44	0.009935
GO:1990247~N6-methyladenosine-containing RNA binding	5	0.010825
GO:0035242~protein-arginine omega-N asymmetric methyltransferase activity	5	0.010825
GO:1990446~U1 snRNP binding	5	0.010825
GO:0016788~hydrolase activity, acting on ester bonds	8	0.013849
GO:0003899~DNA-directed RNA polymerase activity	12	0.016603
GO:0001054~RNA polymerase I activity	6	0.0211
GO:1990050~phosphatidic acid transporter activity	4	0.024447
GO:0001094~TFIID-class transcription factor binding	4	0.024447
GO:0032357~oxidized purine DNA binding	4	0.024447
GO:0003697~single-stranded DNA binding	22	0.024578
GO:0008565~protein transporter activity	18	0.027125
GO:0008168~methyltransferase activity	22	0.027448
GO:0004812~aminoacyl-tRNA ligase activity	7	0.027739
GO:0017091~AU-rich element binding	7	0.027739
GO:0008574~ATP-dependent microtubule motor activity, plus-end-directed	7	0.027739
GO:0070628~proteasome binding	6	0.03026
GO:0047144~2-acylglycerol-3-phosphate O-acyltransferase activity	5	0.030596
GO:0016274~protein-arginine N-methyltransferase activity	5	0.030596
GO:0003676~nucleic acid binding	165	0.032201

GO Term (Molecular Function)	Number of Genes	P-Value
GO:0009055~electron carrier activity	21	0.032501
GO:0004177~aminopeptidase activity	9	0.033741
GO:0043539~protein serine/threonine kinase activator activity	7	0.036619
GO:0001056~RNA polymerase III activity	7	0.036619
GO:0004843~thiol-dependent ubiquitin-specific protease activity	19	0.036697
GO:0004532~exoribonuclease activity	6	0.041568
GO:0030544~Hsp70 protein binding	10	0.041654
GO:0005524~ATP binding	242	0.041679
GO:0052858~peptidyl-lysine N-acetyltransferase activity, acting on acetyl phosphate as donor	4	0.043651
GO:0016614~oxidoreductase activity, acting on CH-OH group of donors	4	0.043651
GO:0019899~enzyme binding	61	0.044273
GO:0005092~GDP-dissociation inhibitor activity	5	0.045236
GO:0002161~aminoacyl-tRNA editing activity	5	0.045236
GO:0003841~1-acylglycerol-3-phosphate O-acyltransferase activity	7	0.047129

8.3.3 Enrichment of cellular component related GO terms of downregulated genes after control siRNA treatment in 24 hours after scratching

GO Term (Cellular component)	Number of Genes	P-Value
GO:0005654~nucleoplasm	603	8.05E-31
GO:0005730~nucleolus	249	2.88E-30
GO:0005739~mitochondrion	304	2.06E-18
GO:0005743~mitochondrial inner membrane	131	4.5E-17
GO:0005829~cytosol	625	8.25E-16
GO:0005634~nucleus	947	2.69E-15
GO:0005737~cytoplasm	908	8.12E-14
GO:0030529~intracellular ribonucleoprotein complex	52	1.52E-11
GO:0016020~membrane	415	2.37E-10
GO:0030496~midbody	45	1.13E-08
GO:0032040~small-subunit processome	20	3.37E-08
GO:0071013~catalytic step 2 spliceosome	35	5.49E-08
GO:0005840~ribosome	50	3.05E-07
GO:0005762~mitochondrial large ribosomal subunit	22	7.53E-07
GO:0019013~viral nucleocapsid	16	1.2E-06
GO:0071011~precatalytic spliceosome	15	1.35E-06
GO:0031012~extracellular matrix	73	2.71E-06
GO:0005694~chromosome	34	5.74E-06
GO:0005759~mitochondrial matrix	77	8.68E-06
GO:0005819~spindle	37	8.91E-06
GO:0005813~centrosome	94	1.42E-05
GO:0005747~mitochondrial respiratory chain complex I	20	2.1E-05
GO:0034719~SMN-Sm protein complex	11	2.59E-05
GO:0000776~kinetochore	27	3.62E-05
GO:0000777~condensed chromosome kinetochore	28	5.04E-05
GO:0005925~focal adhesion	85	6.59E-05
GO:0005604~basement membrane	26	6.61E-05
GO:0005689~U12-type spliceosomal complex	13	9.69E-05
GO:0070469~respiratory chain	11	0.000163
GO:0005643~nuclear pore	23	0.000311
GO:0005587~collagen type IV trimer	6	0.000314
GO:0043209~myelin sheath	39	0.000321
GO:0030687~preribosome, large subunit precursor	13	0.000343
GO:0070062~extracellular exosome	462	0.000359
GO:0034709~methylosome	8	0.000494
GO:0005913~cell-cell adherens junction	68	0.000926
GO:0005763~mitochondrial small ribosomal subunit	11	0.001462
GO:0030426~growth cone	30	0.001549
GO:0042719~mitochondrial intermembrane space protein transporter complex	5	0.001845
GO:0005871~kinesin complex	17	0.002266
GO:0000176~nuclear exosome (RNase complex)	8	0.002708
GO:0015630~microtubule cytoskeleton	33	0.002972
GO:0005758~mitochondrial intermembrane space	21	0.003006
GO:0005680~anaphase-promoting complex	10	0.003007
GO:0005874~microtubule	63	0.003708
GO:0016607~nuclear speck	44	0.003917

GO Term (Cellular component)	Number of Genes	P-Value
GO:0000178~exosome (RNase complex)	8	0.004225
GO:0016363~nuclear matrix	25	0.004339
GO:0005686~U2 snRNP	9	0.004358
GO:0070761~pre-snoRNP complex	5	0.004907
GO:0031428~box C/D snoRNP complex	5	0.004907
GO:0001650~fibrillar center	5	0.004907
GO:0034715~pICln-Sm protein complex	5	0.004907
GO:0000922~spindle pole	27	0.005192
GO:0005635~nuclear envelope	36	0.005438
GO:0022627~cytosolic small ribosomal subunit	15	0.005857
GO:0005732~small nucleolar ribonucleoprotein complex	7	0.005897
GO:0070971~endoplasmic reticulum exit site	7	0.005897
GO:0000177~cytoplasmic exosome (RNase complex)	7	0.005897
GO:0005736~DNA-directed RNA polymerase I complex	7	0.005897
GO:0031965~nuclear membrane	48	0.00607
GO:0034399~nuclear periphery	9	0.00617
GO:0005741~mitochondrial outer membrane	34	0.00618
GO:0030532~small nuclear ribonucleoprotein complex	8	0.006306
GO:0005876~spindle microtubule	14	0.006919
GO:0031080~nuclear pore outer ring	6	0.008001
GO:0005788~endoplasmic reticulum lumen	41	0.008332
GO:0042645~mitochondrial nucleoid	14	0.008483
GO:0015934~large ribosomal subunit	7	0.009085
GO:0000942~condensed nuclear chromosome outer kinetochore	4	0.010421
GO:0070545~PeBoW complex	4	0.010421
GO:0005681~spliceosomal complex	23	0.012038
GO:0000775~chromosome, centromeric region	16	0.012201
GO:0051233~spindle midzone	8	0.012608
GO:0030686~90S preribosome	6	0.012959
GO:0005605~basal lamina	7	0.013336
GO:0001726~ruffle	22	0.014413
GO:0000940~condensed chromosome outer kinetochore	5	0.018032
GO:0036464~cytoplasmic ribonucleoprotein granule	9	0.019407
GO:0005753~mitochondrial proton-transporting ATP synthase complex	8	0.022491
GO:0005697~telomerase holoenzyme complex	8	0.022491
GO:0097526~spliceosomal tri-snRNP complex	4	0.023285
GO:0008622~epsilon DNA polymerase complex	4	0.023285
GO:0001533~cornified envelope	13	0.025186
GO:0031527~filopodium membrane	7	0.02562
GO:0010494~cytoplasmic stress granule	11	0.025938
GO:0005793~endoplasmic reticulum-Golgi intermediate compartment	17	0.027995
GO:0032797~SMN complex	6	0.028227
GO:0005750~mitochondrial respiratory chain complex III	6	0.028227
GO:0042405~nuclear inclusion body	6	0.028227
GO:0005744~mitochondrial inner membrane presequence translocase complex	5	0.028833
GO:0005832~chaperonin-containing T-complex	5	0.028833

GO Term (Cellular component)	Number of Genes	P-Value
GO:0016581~NuRD complex	7	0.033899
GO:0016604~nuclear body	10	0.037736
GO:0005761~mitochondrial ribosome	9	0.037775
GO:0045254~pyruvate dehydrogenase complex	4	0.041663
GO:0042382~paraspeckles	4	0.041663
GO:0005742~mitochondrial outer membrane translocase complex	5	0.042722
GO:0005685~U1 snRNP	7	0.043725
GO:0005666~DNA-directed RNA polymerase III complex	7	0.043725

8.3.4 Enrichment of biological process related GO terms of upregulated genes after control siRNA treatment in 24 hours after scratching

GO Term (biological process)	Number of Genes	P-Value
GO:0000122~negative regulation of transcription from RNA polymerase II promoter	97	5.01E-07
GO:0045893~positive regulation of transcription, DNA-templated	74	1.28E-06
GO:0045944~positive regulation of transcription from RNA polymerase II promoter	120	2.97E-06
GO:0030335~positive regulation of cell migration	35	3.75E-06
GO:0006935~chemotaxis	25	3.38E-05
GO:0042026~protein refolding	8	7.72E-05
GO:0006986~response to unfolded protein	13	7.9E-05
GO:0060395~SMAD protein signal transduction	16	8.81E-05
GO:0006954~inflammatory response	53	9.86E-05
GO:0043065~positive regulation of apoptotic process	44	0.000147
GO:0060326~cell chemotaxis	16	0.000156
GO:0008285~negative regulation of cell proliferation	54	0.000164
GO:0042127~regulation of cell proliferation	31	0.000169
GO:0071407~cellular response to organic cyclic compound	15	0.000188
GO:0006366~transcription from RNA polymerase II promoter	65	0.000274
GO:0050918~positive chemotaxis	11	0.00031
GO:0009408~response to heat	13	0.000317
GO:0050830~defense response to Gram-positive bacterium	18	0.00037
GO:0045892~negative regulation of transcription, DNA-templated	63	0.000384
GO:0035556~intracellular signal transduction	53	0.000461
GO:0043401~steroid hormone mediated signaling pathway	14	0.000477
GO:0070372~regulation of ERK1 and ERK2 cascade	9	0.000534
GO:0030522~intracellular receptor signaling pathway	11	0.000639
GO:0007565~female pregnancy	18	0.000648
GO:0051607~defense response to virus	27	0.000697
GO:0032200~telomere organization	9	0.000949
GO:0009267~cellular response to starvation	12	0.001016
GO:0010941~regulation of cell death	6	0.00102
GO:0006357~regulation of transcription from RNA polymerase II promoter	55	0.001231
GO:0060337~type I interferon signaling pathway	14	0.001512
GO:0071222~cellular response to lipopolysaccharide	20	0.001613
GO:0031668~cellular response to extracellular stimulus	7	0.00213
GO:0034605~cellular response to heat	10	0.002158
GO:0021952~central nervous system projection neuron axonogenesis	5	0.002237
GO:0034097~response to cytokine	12	0.002433
GO:0007179~transforming growth factor beta receptor signaling pathway	17	0.002563
GO:0006468~protein phosphorylation	55	0.00261
GO:0006351~transcription, DNA-templated	191	0.002648
GO:0030509~BMP signaling pathway	15	0.002685
GO:0009615~response to virus	19	0.002873
GO:0006335~DNA replication-dependent nucleosome assembly	9	0.003135
GO:0032570~response to progesterone	10	0.003179
GO:0032760~positive regulation of tumor necrosis factor production	11	0.003613
GO:1904262~negative regulation of TORC1 signaling	5	0.003771
GO:0043280~positive regulation of cysteine-type endopeptidase activity involved in apoptotic process	10	0.003815

GO Term (biological process)	Number of Genes	P-Value
GO:0048545~response to steroid hormone	7	0.003869
GO:0070098~chemokine-mediated signaling pathway	14	0.003963
GO:0032436~positive regulation of proteasomal ubiquitin-dependent protein catabolic process	13	0.004533
GO:0051726~regulation of cell cycle	20	0.004728
GO:0043547~positive regulation of GTPase activity	64	0.004931
GO:0045599~negative regulation of fat cell differentiation	10	0.005381
GO:0018108~peptidyl-tyrosine phosphorylation	23	0.005453
GO:0006955~immune response	50	0.005584
GO:0090084~negative regulation of inclusion body assembly	5	0.005887
GO:0060070~canonical Wnt signaling pathway	15	0.006115
GO:0044267~cellular protein metabolic process	19	0.006149
GO:0090023~positive regulation of neutrophil chemotaxis	7	0.006484
GO:0007568~aging	24	0.00667
GO:0042981~regulation of apoptotic process	29	0.006749
GO:0009409~response to cold	9	0.006771
GO:0071549~cellular response to dexamethasone stimulus	8	0.006914
GO:0048662~negative regulation of smooth muscle cell proliferation	8	0.006914
GO:0070374~positive regulation of ERK1 and ERK2 cascade	25	0.006938
GO:0042493~response to drug	38	0.00743
GO:0009749~response to glucose	13	0.007474
GO:0048661~positive regulation of smooth muscle cell proliferation	12	0.007656
GO:0000183~chromatin silencing at rDNA	9	0.008043
GO:0060213~positive regulation of nuclear-transcribed mRNA poly(A) tail shortening	5	0.008668
GO:0060968~regulation of gene silencing	5	0.008668
GO:0006950~response to stress	12	0.00868
GO:0001649~osteoblast differentiation	17	0.008722
GO:0051092~positive regulation of NF-kappaB transcription factor activity	20	0.010016
GO:0045766~positive regulation of angiogenesis	18	0.010361
GO:0007275~multicellular organism development	58	0.010596
GO:0009611~response to wounding	12	0.011041
GO:0000187~activation of MAPK activity	17	0.011374
GO:0010628~positive regulation of gene expression	33	0.011572
GO:0006915~apoptotic process	62	0.011807
GO:0045779~negative regulation of bone resorption	5	0.012186
GO:0060707~trophoblast giant cell differentiation	5	0.012186
GO:1990440~positive regulation of transcription from RNA polymerase II promoter in response to endoplasmic reticulum stress	5	0.012186
GO:0007267~cell-cell signaling	32	0.012922
GO:0051384~response to glucocorticoid	12	0.013865
GO:0046330~positive regulation of JNK cascade	12	0.013865
GO:0002043~blood vessel endothelial cell proliferation involved in sprouting angiogenesis	4	0.014183
GO:0070059~intrinsic apoptotic signaling pathway in response to endoplasmic reticulum stress	8	0.01429
GO:0010718~positive regulation of epithelial to mesenchymal transition	8	0.01429
GO:0006887~exocytosis	14	0.014794
GO:0007254~JNK cascade	10	0.01497

GO Term (biological process)	Number of Genes	P-Value
GO:0032757~positive regulation of interleukin-8 production	7	0.015184
GO:0070373~negative regulation of ERK1 and ERK2 cascade	11	0.016344
GO:0048246~macrophage chemotaxis	5	0.016499
GO:0030308~negative regulation of cell growth	18	0.016708
GO:0045814~negative regulation of gene expression, epigenetic	10	0.016992
GO:0002548~monocyte chemotaxis	9	0.017232
GO:0051290~protein heterotetramerization	9	0.017232
GO:0009636~response to toxic substance	14	0.017825
GO:0007050~cell cycle arrest	20	0.017969
GO:0009612~response to mechanical stimulus	11	0.018307
GO:0042326~negative regulation of phosphorylation	6	0.018638
GO:1902895~positive regulation of pri-miRNA transcription from RNA polymerase II promoter	6	0.018638
GO:0050679~positive regulation of epithelial cell proliferation	11	0.020437
GO:0043433~negative regulation of sequence-specific DNA binding transcription factor activity	11	0.020437
GO:0045669~positive regulation of osteoblast differentiation	11	0.020437
GO:0050702~interleukin-1 beta secretion	4	0.021351
GO:1904706~negative regulation of vascular smooth muscle cell proliferation	4	0.021351
GO:0032731~positive regulation of interleukin-1 beta production	4	0.021351
GO:0021983~pituitary gland development	7	0.021664
GO:0043392~negative regulation of DNA binding	7	0.021664
GO:0090200~positive regulation of release of cytochrome c from mitochondria	7	0.021664
GO:0006977~DNA damage response, signal transduction by p53 class mediator resulting in cell cycle arrest	11	0.025229
GO:0032755~positive regulation of interleukin-6 production	9	0.025457
GO:0045746~negative regulation of Notch signaling pathway	7	0.025512
GO:0051898~negative regulation of protein kinase B signaling	8	0.026054
GO:0050727~regulation of inflammatory response	11	0.027906
GO:0007165~signal transduction	112	0.02968
GO:0071773~cellular response to BMP stimulus	7	0.029789
GO:0034504~protein localization to nucleus	7	0.029789
GO:0001568~blood vessel development	8	0.029795
GO:0001657~ureteric bud development	8	0.029795
GO:0060452~positive regulation of cardiac muscle contraction	4	0.030141
GO:0006688~glycosphingolipid biosynthetic process	4	0.030141
GO:0042448~progesterone metabolic process	4	0.030141
GO:0030036~actin cytoskeleton organization	18	0.031398
GO:0031100~organ regeneration	9	0.032259
GO:0051781~positive regulation of cell division	9	0.032259
GO:0071230~cellular response to amino acid stimulus	9	0.032259
GO:0043507~positive regulation of JUN kinase activity	7	0.03451
GO:0071726~cellular response to diacyl bacterial lipopeptide	3	0.03473
GO:0032286~central nervous system myelin maintenance	3	0.03473
GO:0070370~cellular heat acclimation	3	0.03473
GO:0043276~anoikis	3	0.03473
GO:1901031~regulation of response to reactive oxygen species	3	0.03473
GO:0038124~toll-like receptor TLR6:TLR2 signaling pathway	3	0.03473

GO Term (biological process)	Number of Genes	P-Value
GO:0016477~cell migration	22	0.035758
GO:0046777~protein autophosphorylation	22	0.035758
GO:0006367~transcription initiation from RNA polymerase II promoter	20	0.035998
GO:0006959~humoral immune response	10	0.037031
GO:0007399~nervous system development	33	0.03714
GO:0045071~negative regulation of viral genome replication	8	0.038323
GO:0016042~lipid catabolic process	13	0.038813
GO:0007264~small GTPase mediated signal transduction	29	0.039008
GO:0051602~response to electrical stimulus	6	0.039168
GO:0007596~blood coagulation	23	0.039378
GO:0031663~lipopolysaccharide-mediated signaling pathway	7	0.039687
GO:0060021~palate development	12	0.039901
GO:0051533~positive regulation of NFAT protein import into nucleus	4	0.040536
GO:0022407~regulation of cell-cell adhesion	4	0.040536
GO:0032525~somite rostral/caudal axis specification	4	0.040536
GO:0009948~anterior/posterior axis specification	5	0.042494
GO:0007169~transmembrane receptor protein tyrosine kinase signaling pathway	14	0.043411
GO:0043491~protein kinase B signaling	7	0.045331

8.3.5 Enrichment of molecular function related GO terms of upregulated genes after control siRNA treatment in 24 hours after scratching

GO Term (Molecular Function)	Number of Genes	P-Value
GO:0000978~RNA polymerase II core promoter proximal region sequence-specific DNA binding	62	2.33E-08
GO:0003700~transcription factor activity, sequence-specific DNA binding	128	3.69E-08
GO:0004879~RNA polymerase II transcription factor activity, ligand-activated sequence-specific DNA binding	13	1.73E-05
GO:0001077~transcriptional activator activity, RNA polymerase II core promoter proximal region sequence-specific binding	40	1.96E-05
GO:0043565~sequence-specific DNA binding	70	4.07E-05
GO:0044212~transcription regulatory region DNA binding	35	0.000131
GO:0005515~protein binding	787	0.000135
GO:0042056~chemoattractant activity	10	0.000197
GO:0000982~transcription factor activity, RNA polymerase II core promoter proximal region sequence-specific binding	9	0.000322
GO:0001078~transcriptional repressor activity, RNA polymerase II core promoter proximal region sequence-specific binding	21	0.000648
GO:0005102~receptor binding	48	0.000663
GO:0008083~growth factor activity	27	0.000711
GO:0003714~transcription corepressor activity	31	0.001169
GO:0008201~heparin binding	26	0.001318
GO:0003707~steroid hormone receptor activity	13	0.001663
GO:0001228~transcriptional activator activity, RNA polymerase II transcription regulatory region sequence-specific binding	18	0.001727
GO:0005520~insulin-like growth factor binding	7	0.002364
GO:0008009~chemokine activity	11	0.005714
GO:0000976~transcription regulatory region sequence-specific DNA binding	12	0.006847
GO:0046982~protein heterodimerization activity	54	0.009165
GO:0004861~cyclin-dependent protein serine/threonine kinase inhibitor activity	5	0.009312
GO:0008134~transcription factor binding	36	0.010088
GO:0046983~protein dimerization activity	22	0.010957
GO:0005057~receptor signaling protein activity	9	0.014507
GO:0005125~cytokine activity	24	0.017528
GO:0019706~protein-cysteine S-palmitoyltransferase activity	7	0.019972
GO:0042393~histone binding	18	0.021512
GO:0031730~CCR5 chemokine receptor binding	4	0.022548
GO:0004713~protein tyrosine kinase activity	19	0.024047
GO:0005161~platelet-derived growth factor receptor binding	5	0.029594
GO:0003677~DNA binding	159	0.031271
GO:0004715~non-membrane spanning protein tyrosine kinase activity	9	0.031921
GO:0000977~RNA polymerase II regulatory region sequence-specific DNA binding	26	0.034572
GO:0016807~cysteine-type carboxypeptidase activity	3	0.036087
GO:0017147~Wnt-protein binding	7	0.037604
GO:0004623~phospholipase A2 activity	7	0.037604
GO:0016301~kinase activity	29	0.038801

GO Term (Molecular Function)	Number of Genes	P-Value
GO:0000979~RNA polymerase II core promoter sequence-specific DNA binding	10	0.041356
GO:0000900~translation repressor activity, nucleic acid binding	4	0.042701
GO:0008270~zinc ion binding	113	0.045953
GO:0017137~Rab GTPase binding	18	0.047354
GO:0005178~integrin binding	15	0.047826

8.3.6 Enrichment of cellular component related GO terms of upregulated genes after control siRNA treatment in 24 hours after scratching

GO Term (Cellular Component)	Number of Genes	P-Value
GO:0005622~intracellular	148	1.86E-05
GO:0005667~transcription factor complex	33	5.16E-05
GO:0016323~basolateral plasma membrane	30	0.00019
GO:0005615~extracellular space	141	0.00045
GO:0005923~bicellular tight junction	19	0.003326
GO:0000786~nucleosome	16	0.00688
GO:0016324~apical plasma membrane	36	0.008761
GO:0005737~cytoplasm	454	0.009998
GO:0005576~extracellular region	153	0.011178
GO:0048471~perinuclear region of cytoplasm	66	0.012307
GO:0005634~nucleus	468	0.013286
GO:0031234~extrinsic component of cytoplasmic side of plasma membrane	12	0.017318
GO:0000790~nuclear chromatin	25	0.018467
GO:0046658~anchored component of plasma membrane	7	0.020314
GO:0014731~spectrin-associated cytoskeleton	4	0.020536
GO:0000788~nuclear nucleosome	9	0.020782
GO:0042629~mast cell granule	6	0.021627
GO:0016328~lateral plasma membrane	10	0.022315
GO:0000228~nuclear chromosome	10	0.022315
GO:0072562~blood microparticle	20	0.031764
GO:0005938~cell cortex	17	0.033591
GO:0042567~insulin-like growth factor ternary complex	3	0.033792
GO:0061700~GATOR2 complex	4	0.039055